



CYCLOTRIVERATRYLENE AND PORPHYRIN SCAFFOLDS FOR MOLECULAR RECOGNITION AND SELF-ASSEMBLY

Berta Camafort Blanco

Dipòsit Legal: T 677-2015

ADVERTIMENT. L'accés als continguts d'aquesta tesi doctoral i la seva utilització ha de respectar els drets de la persona autora. Pot ser utilitzada per a consulta o estudi personal, així com en activitats o materials d'investigació i docència en els termes establerts a l'art. 32 del Text Refós de la Llei de Propietat Intel·lectual (RDL 1/1996). Per altres utilitzacions es requereix l'autorització prèvia i expressa de la persona autora. En qualsevol cas, en la utilització dels seus continguts caldrà indicar de forma clara el nom i cognoms de la persona autora i el títol de la tesi doctoral. No s'autoritza la seva reproducció o altres formes d'explotació efectuades amb finalitats de lucre ni la seva comunicació pública des d'un lloc aliè al servei TDX. Tampoc s'autoritza la presentació del seu contingut en una finestra o marc aliè a TDX (framing). Aquesta reserva de drets afecta tant als continguts de la tesi com als seus resums i índexs.

ADVERTENCIA. El acceso a los contenidos de esta tesis doctoral y su utilización debe respetar los derechos de la persona autora. Puede ser utilizada para consulta o estudio personal, así como en actividades o materiales de investigación y docencia en los términos establecidos en el art. 32 del Texto Refundido de la Ley de Propiedad Intelectual (RDL 1/1996). Para otros usos se requiere la autorización previa y expresa de la persona autora. En cualquier caso, en la utilización de sus contenidos se deberá indicar de forma clara el nombre y apellidos de la persona autora y el título de la tesis doctoral. No se autoriza su reproducción u otras formas de explotación efectuadas con fines lucrativos ni su comunicación pública desde un sitio ajeno al servicio TDR. Tampoco se autoriza la presentación de su contenido en una ventana o marco ajeno a TDR (framing). Esta reserva de derechos afecta tanto al contenido de la tesis como a sus resúmenes e índices.

WARNING. Access to the contents of this doctoral thesis and its use must respect the rights of the author. It can be used for reference or private study, as well as research and learning activities or materials in the terms established by the 32nd article of the Spanish Consolidated Copyright Act (RDL 1/1996). Express and previous authorization of the author is required for any other uses. In any case, when using its content, full name of the author and title of the thesis must be clearly indicated. Reproduction or other forms of for profit use or public communication from outside TDX service is not allowed. Presentation of its content in a window or frame external to TDX (framing) is not authorized either. These rights affect both the content of the thesis and its abstracts and indexes.



CYCLOTRIVERATRYLENE AND PORPHYRIN SCAFFOLDS FOR MOLECULAR RECOGNITION AND SELF-ASSEMBLY

Berta Camafort Blanco

Dipòsit Legal: T 677-2015

ADVERTIMENT. L'accés als continguts d'aquesta tesi doctoral i la seva utilització ha de respectar els drets de la persona autora. Pot ser utilitzada per a consulta o estudi personal, així com en activitats o materials d'investigació i docència en els termes establerts a l'art. 32 del Text Refós de la Llei de Propietat Intel·lectual (RDL 1/1996). Per altres utilitzacions es requereix l'autorització prèvia i expressa de la persona autora. En qualsevol cas, en la utilització dels seus continguts caldrà indicar de forma clara el nom i cognoms de la persona autora i el títol de la tesi doctoral. No s'autoritza la seva reproducció o altres formes d'explotació efectuades amb finalitats de lucre ni la seva comunicació pública des d'un lloc aliè al servei TDX. Tampoc s'autoritza la presentació del seu contingut en una finestra o marc aliè a TDX (framing). Aquesta reserva de drets afecta tant als continguts de la tesi com als seus resums i índexs.

ADVERTENCIA. El acceso a los contenidos de esta tesis doctoral y su utilización debe respetar los derechos de la persona autora. Puede ser utilizada para consulta o estudio personal, así como en actividades o materiales de investigación y docencia en los términos establecidos en el art. 32 del Texto Refundido de la Ley de Propiedad Intelectual (RDL 1/1996). Para otros usos se requiere la autorización previa y expresa de la persona autora. En cualquier caso, en la utilización de sus contenidos se deberá indicar de forma clara el nombre y apellidos de la persona autora y el título de la tesis doctoral. No se autoriza su reproducción u otras formas de explotación efectuadas con fines lucrativos ni su comunicación pública desde un sitio ajeno al servicio TDR. Tampoco se autoriza la presentación de su contenido en una ventana o marco ajeno a TDR (framing). Esta reserva de derechos afecta tanto al contenido de la tesis como a sus resúmenes e índices.

WARNING. Access to the contents of this doctoral thesis and its use must respect the rights of the author. It can be used for reference or private study, as well as research and learning activities or materials in the terms established by the 32nd article of the Spanish Consolidated Copyright Act (RDL 1/1996). Express and previous authorization of the author is required for any other uses. In any case, when using its content, full name of the author and title of the thesis must be clearly indicated. Reproduction or other forms of for profit use or public communication from outside TDX service is not allowed. Presentation of its content in a window or frame external to TDX (framing) is not authorized either. These rights affect both the content of the thesis and its abstracts and indexes.

UNIVERSITAT ROVIRA I VIRGILI

CYCLOTRIVERATRYLENE AND PORPHYRIN SCAFFOLDS FOR MOLECULAR RECOGNITION AND SELF-ASSEMBLY

Berta Camafort Blanco

Dipòsit Legal: T 677-2015

UNIVERSITAT ROVIRA I VIRGILI

CYCLOTRIVERATRYLENE AND PORPHYRIN SCAFFOLDS FOR MOLECULAR RECOGNITION AND SELF-ASSEMBLY

Berta Camafort Blanco

Dipòsit Legal: T 677-2015

Berta Camafort Blanco

**Cyclotrimeratrylene and Porphyrin Scaffolds for
Molecular Recognition and Self-Assembly**

PhD Thesis

Supervised by Prof. Javier de Mendoza

Institut Català d'Investigació Química (ICIQ)



UNIVERSITAT ROVIRA I VIRGILI

Tarragona

2015

UNIVERSITAT ROVIRA I VIRGILI

CYCLOTRIVERATRYLENE AND PORPHYRIN SCAFFOLDS FOR MOLECULAR RECOGNITION AND SELF-ASSEMBLY

Berta Camafort Blanco

Dipòsit Legal: T 677-2015

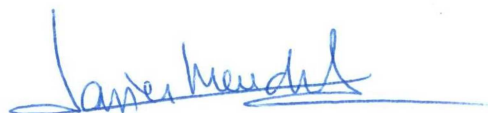


Av. Països Catalans, 16
43007 Tarragona
Tel. 977 920 218
Fax. 977 920 225

FAIG CONSTAR que aquest treball, titulat "Cyclotrimeratrylene and Porphyrin Scaffolds for Molecular Recognition and Self-Assembly", que presenta Berta Camafort Blanco per a l'obtenció del títol de Doctor, ha estat realitzat sota la meua direcció a l'Institut Català d'Investigació Química i que aconsegueix els requeriments per poder optar a Menció Internacional.

Tarragona, 15 de desembre de 2014

El director de la tesi doctoral



Prof. Javier de Mendoza Sans

UNIVERSITAT ROVIRA I VIRGILI

CYCLOTRIVERATRYLENE AND PORPHYRIN SCAFFOLDS FOR MOLECULAR RECOGNITION AND SELF-ASSEMBLY

Berta Camafort Blanco

Dipòsit Legal: T 677-2015

Agraïments

Durant aquests anys, són moltes les persones que han estat al meu costat i m'han ajudat a arribar fins aquí. Primer de tot voldria agrair al Prof. Javier de Mendoza per aquesta gran oportunitat, pels seus consells i sobretot per la confiança i la llibertat que m'ha donat tot aquest temps.

I would like to thank Prof. Dirk Guldi for giving me the opportunity to work in his group and for his advices.

A tots els companys que han passat pel grup, al Gerald, a la Caterina, la Elisa, el Yong, la Alla, el Matt, l'Augustin, La Sara S., la Laura, el Qixun, el Jin per totes les hores compartides. A les secretàries: la Núria i l'Aurora per l'ajuda administrativa. Als tècnics del grup: a l'Aritz pels seus consells i a la Eva per les seves opinions i per aguantar i compartir els meus gustos musicals al laboratori.

M'emporto un record especial d'aquells amb els que he compartit molt més que les hores a vitrina, el Timm i l'Ondrej pel seu sentit de l'humor. A la Sarita, per la seva amistat, les discussions científiques, els consells, el recolzament i per ser una persona tan autèntica. Al Philipp amb qui no només he compartit el doctorat, sinó que també he compartit el pis i les factures, per la seva amistat i la seva tranquil·litat. I a tots aquells companys de l'ICIQ i de Tarragona que han esdevingut quelcom més que això: A la Caye, la Gizem, l'Antonio, l'Asraa, el Jaume, el Marc, la Carla, l'Anna, el Pep, l'Uri i l'Andrea els vull agrair totes les hores, els dinars al Delta, el sopars, els caps de setmana a Albarca, els cine fòrums i tot el que queda per venir. A la Núria, amb qui ha estat un plaer esmorzar tots aquests anys.

Finalment vull agrair als que des de fora m'han seguit animant i m'han fet més fàcil el camí. A Ana que a pesar de la distància, cuando nos vemos parece como si el tiempo no hubiera pasado. A l'Anaïs i l'Alba, per cuidar-me, a l'Emma per ser l'Emma, a la Vero, per ser tant autèntica, al C. Team (la Elena, la Merche, la Rubi, la Mireia i la Laura) a la Irene, a la Mimi, la Iru i al Pepelu per totes les hores que hem passat al teatre, al Queimada, cantant o menjant pollastre a l'ast al terrat. Però sobretot a la Laura, sempre a un cop de telèfon o de cotxe, per estar allà "pa lo bueno y pa lo malo" y por todas las risas que nos pegamos.

Molt especialment li vull agrair al Robert, I would like to thank him for his love, his patience, his advices and for all his time and dedication, for making me happy.

I finalment als meus pares, que sempre han confiat en mi, pel seu recolzament, pel seu amor i per la seva sinceritat. Sense ells res d'això hagués estat possible. I al Miquel, que és un exemple a seguir, el que més li agraeixo és que sempre em tregui una rialla quan sóc a casa.

A la meva àvia

UNIVERSITAT ROVIRA I VIRGILI

CYCLOTRIVERATRYLENE AND PORPHYRIN SCAFFOLDS FOR MOLECULAR RECOGNITION AND SELF-ASSEMBLY

Berta Camafort Blanco

Dipòsit Legal: T 677-2015

List of Abbreviations and Acronyms

Ac	Acetyl
ACN	Acetonitrile
APCI	Atmospheric-Pressure Chemical Ionization
aq.	Aqueous
Ar	Aromatic, Aryl
a.u.	Absorbance Units
Bn	Benzyl
Boc	<i>tert</i> -Butoxycarbonyl
Bu	Butyl
CD	Circular Dichroism
CDI	1,1'-Carbonyldiimidazole
CNO	Carbon Nano Onions
CNT	Carbon Nanotubes
conc.	Concentrated
COSY	Correlation Spectroscopy
CTC	Cyclotricatechylene
CTG	Cyclotriguaiacylene
CTV	Cyclotrimeratrylene
CTTV	Cyclotetraveratrylene
DCB	1,2-Dichlorobenzene
DCM	Dichloromethane
DDQ	2,3-Dichloro-5,6-dicyano-1,4-benzoquinone
DFT	Density Functional Theory
DME	1,2-dimethoxyethane
DMF	Dimethylformamide
DMSO	Dimethylsulfoxide
DOBOB	3,4,5,-tris(<i>p-n</i> -dodecyloxybenzyloxy)benzoyloxy
DOSY	Diffusion Ordered Spectroscopy

DPPA	Diphenylphosphoryl azide
DSC	Differential Scanning Calorimetry
<i>et al.</i>	Et Alii
ES	Electrospray
ESI-MS	Electrospray Ionization Mass Spectrometry
Et	Ethyl
EtOH	Ethanol
ex-TTF	Extended Tetrathiafulvalene
GPC	Gel Permeation Chromatography
h	Hour
H-bonding	Hydrogen Bonding
Hex	Hexyl
HIV	Human Immunodeficiency Virus
HMBC	Heteronuclear Multiple Bond Correlation
HMQC	Heteronuclear Multiple Quantum Correlation
HPLC	High Performance Liquid Chromatography
HPLC-ms	High Performance Liquid Chromatography-Mass Spectroscopy
HRMS	High Resolution Mass Spectrometry
HSQC	Heteronuclear Single Quantum Correlation
IPR	Isolated Pentagon Rule
<i>i</i>-Pr	Isopropyl
IR	Infrared
ITC	Isothermal Titration Calorimetry
K_{ass}	Association Constant
M	Metal
MALDI-TOF	Matrix Assisted Laser Desorption/Ionization- Time of Fly
Me	Methyl
MeOH	Methanol
min	Minute

Mp	Melting point
MRI	Magnetic Resonance Imaging
MW	Microwave
n-BuLi	<i>n</i> -Butyl lithium
NCFs	Metal-Nitride Cluster Fullerenes
n.d.	Non Determined
NMR	Nuclear Magnetic Resonance
NOESY	Nuclear Overhauser Effect Spectroscopy
PEG	Polyethylene glycol
PET	Polyethylene terephthalate
Ph	Phenyl
POM	Polarized optical microscopy
PPh₃	Triphenylphosphine
PyC₆₀	Pyridine-Functionalized Fullerene
Py-HCl	Pyridine Hydrochloride
SPS	Solvent purification system
r.t.	Room temperature
SAM	Self-Assembled Monolayer
SWCNT	Single Wall Carbon Nanotubes
TCE	Tetrachloroethane
TFA	Trifluoroacetic Acid
THF	Tetrahydrofuran
TLC	Thin layer chromatography
TMEDA	Tetramethylethylenediamine
TMS	Tetramethylsilane
TPFPP	Tetrapentafluorophenyl Porphyrin
TPP	Tetra-Phenyl Porphyrin
UPy	Ureidopyrimidinone
UV-Vis	Ultraviolet-visible
w	Working

UNIVERSITAT ROVIRA I VIRGILI

CYCLOTRIVERATRYLENE AND PORPHYRIN SCAFFOLDS FOR MOLECULAR RECOGNITION AND SELF-ASSEMBLY

Berta Camafort Blanco

Dipòsit Legal: T 677-2015

Table of Contents

PART I: Porphyrin-Based Trimeric Receptors for Recognition of Fullerene Guests

Chapter 1: Introduction.....	1
1.1 Fullerenes as Target Guests.....	5
1.1.1 Introduction.....	5
1.1.2 Fullerene Properties and Applications	9
1.1.3 Supramolecular Receptors for Fullerenes	12
1.2 Cyclotrimeratrylene-Based Receptors	15
1.2.1 Introduction.....	15
1.2.2 CTV Host-Guest Inclusion Complexes	17
1.3 Porphyrin-Based Receptors	29
1.3.1 Introduction.....	29
1.3.2 Porphyrin-Based Fullerene Receptors	36
1.4 Template Directed Synthesis	57
1.4.1 Introduction.....	57

1.4.2	Template Directed Synthesis of Porphyrin Cycles	57
General Objectives: Part I		63
Chapter 2: Flexible Receptor: CTV-Based Acyclic Porphyrin Tripod		67
2.1	Design and Aim of the Project	69
2.2	Synthesis and Characterization	71
2.1.1	Synthesis of CTV-Porphyrin Host 1	71
2.1.2	Characterization of CTV-Porphyrin Host 1	76
2.3	Results and Discussion	80
2.3.1	Binding Studies of the CTV-Porphyrin Tripod with Fullerenes and Other Carbon Materials	81
2.3.2	Summary and Discussion	97
2.4	Conclusions	99
Chapter 3: Preorganized Receptor I: Cyclic Porphyrin Trimer		101
3.1	Design and Aim of the Project	103
3.2	Synthesis and Characterization	105
3.2.1	Synthesis of Cyclic Porphyrin Trimer 2	105
3.2.2	Characterization of Cyclic Porphyrin Trimer 2	114

3.3	Results and Discussion	117
3.3.1	Binding Studies of Porphyrin Trimer 2 with Fullerenes	117
3.3.2	Summary and Discussion.....	117
3.4	Conclusions	125
	Chapter 4: Preorganized Receptor II: Flexible Cyclic Porphyrin Trimer	127
4.1	Design and Aim of the Project	129
4.2	Synthesis and Characterization	130
4.2.1	Synthesis of Cyclic Porphyrin Trimer 3.....	130
4.2.2	Characterization of Cyclic Porphyrin Trimer 3.....	131
4.3	Results and Discussion	132
4.3.1	Binding Studies of Porphyrin Trimer 3 with Fullerenes	132
4.3.2	Summary and Discussion.....	138
4.4	Conclusions	139
	Chapter 5: Preorganized Receptor III: Sterically Unhindered Cyclic Porphyrin Trimer	141
5.1	Design and Aim of the Project	143
5.2	Synthesis and Characterization	144
5.2.1	Synthesis of Cyclic Porphyrin Trimer 4.....	144

5.2.2	Synthesis of Cyclic Porphyrin Trimer 5.....	147
5.2.3	Characterization of Cyclic Porphyrin Trimer 5	151
5.3	Results and Discussion	152
5.3.1	Binding Studies of Porphyrin Trimer 5 with Fullerenes	152
5.3.2	Preliminary Binding Studies of Porphyrin Trimer 5 with Other Carbon Materials	158
5.3.3	Summary and Discussion.....	161
5.4	Conclusions	163
Chapter 6: Preorganized Receptor IV: Enlarged Cyclic Porphyrin Trimer for Giant Carbon Nano Onions. Preliminary Studies		165
6.1	Design and Aim of the Project	167
6.2	Synthesis and Characterization	170
6.2.1	Synthesis of Cyclic Porphyrin Trimer 6.....	170
6.2.2	Synthesis of Cyclic Porphyrin Trimer 7	174
6.2.3	Characterization of Cyclic Porphyrin Trimer 7	183
6.3	Results and Discussion	185
6.3.1	Preliminary Complexation Studies of Porphyrin Trimer 7 with a Bucky Onion Mixture Solution	185

6.3.2	Summary and Discussion.....	186
6.4	Conclusions	186
Chapter 7: Experimental Part I		187
7.1	General Information and Instrumentation	189
7.2	Synthetic Procedures	191
7.2.1	Flexible Receptor: CTV-Based Acyclic Porphyrin Tripod	191
7.2.2	Preorganized Receptor I: Cyclic Porphyrin Trimer	199
7.2.3	Preorganized Receptor II: Flexible Cyclic Porphyrin Trimer	206
7.2.4	Preorganized Receptor III: Sterically Unhindered Cyclic Porphyrin Trimer	208
7.2.5	Preorganized Receptor IV: Enlarged Cyclic Porphyrin Trimer	215
 PART II: CTV-Based Self-Assembled Columnar Structures		
Chapter 8: Introduction.....		231
8.1	CTV-Based Self-Assembled Columnar Structures	233
8.2	Pyramidal Liquid Crystals	234
8.2.1	Introducing Chirality into the CTV-Based Pyramidal Aggregates ...	237

8.2.2	Hydrogen Bonding Promoted Columnar Twisting	242
8.3	Amplification of Chirality on Supramolecular Aggregates	243
General Objectives: Part II		247
Chapter 9: CTV-Based Pyramidic Monomers for Chiral Columnar Aggregates		249
9.1	Design and Aim of the Project	251
9.2	Synthesis and Characterization	252
9.2.1	Synthesis of CTV Monomer 35. Route (a).....	253
9.2.2	Synthesis of CTV Monomer 35. Route (b).....	264
9.2.3	Synthesis of CTV Monomer 35: Route (c).....	272
9.3	Summary and Discussion	273
9.4	Conclusions	275
Chapter 10: CTV-Based Pyramidic Monomers for Chiral Columnar Aggregates II		277
10.1	Design and Aim of the Project	279
10.2	Synthesis and Characterization	280
10.2.1	Synthesis of CTV Monomer 36.....	280
10.2.2	Target Molecule 36 Characterization	285

10.3	Results and Discussion	287
10.3.1	Self-Assembly, Chiral Amplification and Mesomorphic Behavior. Preliminary Studies	287
10.3.2	Summary and Discussion	294
10.4	Conclusions	296
	Chapter 11: Experimental Part II	297
11.1	General Information and Instrumentation	299
11.2	Synthetic Procedures	301
11.2.1	CTV-based Pyramidic Monomers for Chiral Columnar Aggregates	301
11.2.2	CTV-Based Pyramidic Monomers for Chiral Columnar Aggregates II	310
	General Conclusions	319

UNIVERSITAT ROVIRA I VIRGILI

CYCLOTRIVERATRYLENE AND PORPHYRIN SCAFFOLDS FOR MOLECULAR RECOGNITION AND SELF-ASSEMBLY

Berta Camafort Blanco

Dipòsit Legal: T 677-2015

Part I: Porphyrin-Based Trimeric Receptors for Recognition of Fullerene Guests

UNIVERSITAT ROVIRA I VIRGILI

CYCLOTRIVERATRYLENE AND PORPHYRIN SCAFFOLDS FOR MOLECULAR RECOGNITION AND SELF-ASSEMBLY

Berta Camafort Blanco

Dipòsit Legal: T 677-2015

Chapter 1: Introduction

UNIVERSITAT ROVIRA I VIRGILI

CYCLOTRIVERATRYLENE AND PORPHYRIN SCAFFOLDS FOR MOLECULAR RECOGNITION AND SELF-ASSEMBLY

Berta Camafort Blanco

Dipòsit Legal: T 677-2015

1.1 Fullerenes as Target Guests

1.1.1 Introduction

Pure carbon can exist in different forms or allotropes. The most common and thermodynamically stable form of carbon is α -graphite followed by the diamond allotrope. Fullerenes are the third form among the carbon allotropes.¹

Fullerenes were discovered in 1985 by Kroto, Kurl and Smalley *et al.*² for what they were awarded with the Nobel Prize in Chemistry in 1996. In 1990, Kratschmer and Hoffmann³ developed the first yielding method for the preparation of fullerenes, consisting on graphite vaporization under helium atmosphere. Along with the carbon soot (amorphous carbon form) the major fullerenes C₆₀ and C₇₀ together with minor higher homologues (>C₇₀) were identified. Fullerenes were later found to exist naturally in cosmic dust⁴ as well as in geological formations on Earth, although only in the ppm-range.⁵

¹ (a) Hirsh, A.; Brettreich, M. *Fullerenes: Chemistry and Reactions*, Wiley-VCH, Weinheim, **2005**.
(b) Kroto, H. W.; Allaf, A. W.; Balm, S. P. *Chem. Rev.* **1991**, *91*, 1213.

² Kroto, H. W.; Heath, J. R.; O'Brein, S. C.; Curl, R. F.; Smalley, R. E. *Nature* **1985**, *318*, 162.

³ (a) Kratschmer, W.; Lamb, L. D.; Hoffman, D. R. *Nature* 1990, 347, 354.

⁴ (a) Henning, H.; Salama, F.; *Science* **1998**, *282*, 2204. (b) Ehrenfreund P.; Foing, B. H.; *Science* **2010**, *329*, 1159.

⁵ (a) Busek, P. R.; Tsipursky, S. J.; Hettich, R. *Science* **1992**, *257*, 215. (b) Heymann, D.; Chibante, L. P. F.; Brooks, R. R.; Wolbach, W. S.; Smalley R. E. *Science* **1994**, *265*, 645. (c) Becker, L.; Bada, J. L.; Winans, R. E.; Hunt, J. E.; Bunch, T. E.; French, B. M. *Science* **1994**, *265*, 642.

1. Introduction

Fullerenes Structure

Fullerenes are assembled from fused pentagons and hexagons. The pentagons which are absent in the flat infinite graphite lattices, provide curvature to this carbon allotrope giving it its spheroidal shape. According to Euler's theorem, each fullerene contains $2x(10+M)$ carbon where M is the number of hexagons. Twelve pentagons are required for the closure of any carbon fullerene structure. The smallest fullerene that fulfills this theorem is the dodecahedral C_{20} composed exclusively by 12 pentagons.

Nevertheless, fulfillment of the "isolated pentagon rule" (IPR) according to which all pentagons should be completely separated from each other by hexagons is required for the formation of stable cages.

The smallest fullerene that fulfills the IPR rule is composed by 60 carbons. Buckminsterfullerene⁶ (C_{60}) is formed by 12 pentagons and 20 hexagons that fold into the closed ball-shaped molecule. The shape of the Buckminsterfullerene is that of a truncated icosahedron (Figure 1.1) what provides C_{60} with high symmetry, being 120 the number of symmetry operations that can map the molecule onto itself. C_{60} is the most abundant fullerene found in carbon soot.

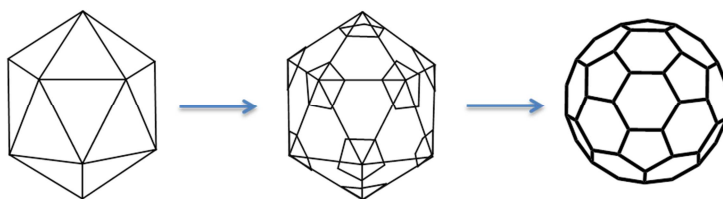


Figure 1.1 Icosahedron, truncated icosahedron, and schematic representation of ball-shaped Bukminsterfullerene C_{60} .

⁶ Buckminsterfullerene C_{60} was named after the architect Richard Buckminster Fuller, who created Montreal's dome in 1967 with the same shape as the carbon cluster.

1. Introduction

The rugby-ball shaped C_{70} , composed of 25 hexagons, is the second most abundant fullerene found in carbon soot. The 10 extra carbons of C_{70} are placed in the center of the fullerene throughout its equatorial belt, enlarging the fullerene and giving its ellipsoidal shape (Figure 1.2). The C_{60} / C_{70} relative ratio obtained after toluene extraction of the carbon soot is 85:15.⁷

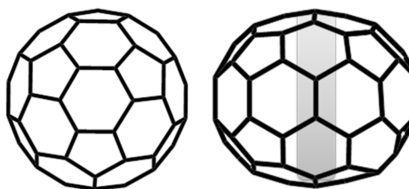


Figure 1.2 Schematic representation of C_{60} and C_{70} . The equatorial belt of C_{70} is highlighted.

Higher Fullerenes

Along with the major fullerenes C_{60} and C_{70} , minor higher fullerenes ($>C_{70}$) are obtained within the carbon soot extracts in a total amount of 3% to 4% by weight.⁸ Some of these higher fullerenes have been isolated and studied in detail.

Among fullerenes, C_{84} is the third most abundant member of the family, after C_{60} and C_{70} .^{8a, 9} Although, a total of 24 isomers of C_{84} have been predicted by calculations

⁷ Ajje, H.; Alvarez, M. M.; Anz, S. J.; Beck, R. D.; Diederich, F.; Fostiropoulos, K.; Huffman, D. R.; Krätschmer, W.; Rubin, Y.; Shriver, K. E.; Sensharma, D.; Whetten, R. L.; *J. Phys. Chem.* **1990**, *94*, 8630.

⁸ (a) Diederich, F.; Ettl, R.; Rubin, Y.; Whetten, R. L.; Beck, R.; Álvarez, M.; Anz, S. J.; Sensharma, D.; Wuld, F.; Khemani K. C.; Koch, A. *Science*, **1991**, *252*, 548. (b) Diederich, F.; Whetten, R. L. *Acc. Chem, Res.* **1992**, *25*, 119.

⁹ (a) Diederich, F.; Ettl, R.; Rubin, Y.; Whetten, R. L.; Beck, R.; Álvarez, M.; Anz, S. J.; Sensharma, D.; Wuld, F.; Khemani K. C.; Koch, A. *Science*, **1991**, *252*, 548. (b) Diederich, F.; Whetten, R. L. *Acc. Chem, Res.* **1992**, *25*, 119.

1. Introduction

obeying the IPR rule¹⁰, the two major isomer, D_2 and D_{2d} , are those mostly studied in detail.¹¹

In general, the chemistry, physical properties and applications of the higher fullerenes compared to C_{60} and C_{70} have been poorly due to the limited accessibility and high cost of their isolation.

Endohedral Fullerenes

Fullerenes that contain additional atoms, ions, or clusters trapped within the hollow sphere are known as endohedral fullerenes.¹² The existence of endohedral fullerenes was first reported in 1985. Smalley *et al.*¹³ reported the formation of $La@C_{60}$ after laser vaporization of lanthanum-impregnated low-density graphite. The endohedral fullerene was detected by means of mass spectrometry. Later in 1999, $Sc_3N@C_{80}$ and the trimetallic nitride family of cluster endofullerenes ($M_3N@C_{2n}$, $n = 34 - 42$) was discovered and reported by Stevenson *et al.*¹⁴. They reported that the small presence

¹⁰ (a) Manolopoulos, D. E.; Fowler, P.W. *J. Chem. Phys.*, **1992**, *96*, 7603. (b) Khamatgalimov, A. R.; Kovalenko, V. I.; *Int. J. Quantum. Chem.* **2012**, *112*, 1055.

¹¹ (a) Hawkins, J. M.; Nambu M.; Meyer, A. *J. Am. Chem. Soc.*, **1994**, *116*, 7642. (b) Crassous, J.; Rivera, J.; Fender, N. S.; Shu, L. H.; Echegoyen, L.; Thilgen, C.; Herrmann A.; Diederich, F.; *Angew. Chem., Int. Ed.*, **1999**, *38*, 1613. (c) Wakahara, T.; Han, A. H.; Niino, Y.; Maeda, Y.; Akasaka, T.; Suzuki, T.; Yamamoto, K.; Kako, M.; Nakadaira, Y.; Kobayashi K.; Nagase, S. *J. Mater. Chem.*, **2002**, *12*, 2061. (d) Darwish, A. D.; Martsinovich, N.; Taylor, R. *Org. Biomol. Chem.*, **2004**, *2*, 1364.

¹² (a) Bethune, D. S.; Johnson, R. D.; Salem, J. R.; de Vries, M. S.; Yannoni, C. S. *Nature* **1993**, *366*, 123. (b) Popov, A. A.; Yang, S.; Dunsch, L. *Chem. Rev.* **2013**, *113*, 5989. (b) Cerón, M. R.; Li, F.-F.; Echegoyen, A. *J. Phys. Org. Chem.* **2014**, *27*, 258.

¹³ Heath, J. R.; O'Brien, S. C.; Zhang, Q.; Liu, Y.; Curl, R. F.; Kroto, H. W.; Tittel, F. K.; Smalley, R. E. *J. Am. Chem. Soc.* **1985**, *107*, 7779.

¹⁴ Stevenson, S.; Rice, G.; Glass, T.; Harich, K.; Cromer, F.; Jordan, M. R.; Craft, J.; Hadju, E.; Bible, R.; Olmstead, M. M.; Maitra, K.; Fisher, A. J.; Balch, A. L.; Dorn, H. C. *Nature* **1999**, *401*, 55.

1. Introduction

of nitrogen gas, that was accidentally introduced through an air leak into the arc-burning reactor, was required during vaporization of metal-oxides-containing graphite for the metal-nitride cluster fullerenes (NCFs) to be obtained.

The $\text{Sc}_3\text{N@C}_{80}$ endohedral fullerene (Figure 1.3) is the most abundant endohedral fullerene and the third most abundant synthesized fullerene, after C_{60} and C_{70} , yielding up to 5 % of the soot extract.¹²

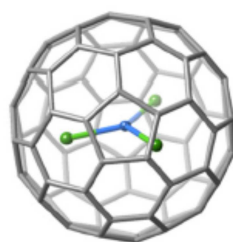


Figure 1.3 $\text{Sc}_3\text{N@C}_{80}$ Scandium metal clusters inside the icosahedral C_{80} cage.^{12c}

1.1.2 Fullerene Properties and Applications

Fullerenes derivatives are promising candidates for applications in many fields such as materials or medical sciences.

Pharmaceutical Applications of Fullerenes

Fullerenes exhibit interesting biological activities and several pharmaceutical applications have been reported in the last years.^{12b, 15} For instance, fullerene

¹⁵ Da Ros, T.; Prato, M. *Chem. Commun.* **1999**, 663.

1. Introduction

derivatives have shown to target the HIV-1 protease enzyme.¹⁶ The spheroidal fullerene derivatives fit into the hydrophobic cavity of the enzyme active site inhibiting its activity. Photoinduced cytotoxicity and antitumoral activity has been also reported for fullerene derivatives. Fullerenes are able to generate cytotoxic singlet oxygen by energy transfer from the metastable fullerene triplet excited-state to molecular oxygen upon irradiation with light. For instance, C₆₀-PEG fullerene derivative was reported to selectively induce tumor necrosis when irradiated with light without affecting the healthy tissue.¹⁷ Endohedral fullerene Gd@C₈₀(OH)₂₂ nanoparticles have been also reported to exhibit antitumor activity against mice H22 hepatoma.¹⁸

The potential applications of endohedral metallofullerenes in medical imaging diagnostics and tracing procedures have been widely reported. For instance, several metallofullerenes have been reported as magnetic resonance imaging (MRI)¹⁹ and X-ray²⁰ contrast agents as well as radiotracers²¹ for the imaging of diseased organs and targeting cancerous tumors. In this way, the radioactive metal is embedded inside

¹⁶ (a) Friedman, S. H.; DeCamp, D. L.; Sijbesma, R. P.; Srdanov, G.; Wudl, F.; Kenyon, G. L. *J. Am. Chem. Soc.* **1993**, *115*, 6506. (b) Friedman, S. H.; Ganapathi, P. S.; Rubin, Y.; Kenyon, G. L. *J. Med. Chem.* **1998**, *41*, 2424.

¹⁷ Tabata, Y.; Murakami, Y.; Ikada, Y. *Jpn. J. Cancer Res.* **1997**, *88*, 1108.

¹⁸ Chen, C. Y.; Xing, G. M.; Wang, J. X.; Zhao, Y. L.; Li, B.; Tang, J.; Jia, G.; Wang, T. C.; Sun, J.; Xing, L.; Yuan, H.; Gao, Y. X.; Meng, H.; Chen, Z.; Zhao, F.; Chai, Z. F.; Fang, X. H. *Nano Lett.* **2005**, *5*, 2050.

¹⁹ (a) Sitharaman, B.; Wilson, L. J. *J. Biomed. Nanotechnol.* **2007**, *3*, 342. (b) Anilkumar, P.; Lu, F.; Cao, L.; Luo, P. G.; Liu, J.-H.; Sahu, S.; Tackett, K. N. II; Wang, Y.; Sun, Y.-P. *Curr. Med. Chem.* **2011**, *18*, 2045. (c) Zhang, J.; Liu, K. M.; Xing, G. M.; Ren, T. X.; Wang, S. K. *J. Radioanal. Nucl. Chem.* **2007**, *272*, 605.

²⁰ Iezzi, E. B.; Duchamp, J. C.; Fletcher, K. R.; Glass, T. E.; Dorn, H. C. *Nano Lett.* **2002**, *2*, 1187.

²¹ (a) Cagle, D. W.; Kennel, S. J.; Mirzadeh, S.; Alford, J. M. and Wilson, L. J., *Proc. Natl. Acad. Sci. USA* **1993**, *96*, 5182. (b) Kobayashi, K.; Kuwano, M.; Sueki, K.; Kikuchi, K.; Achiba, Y.; Nakahara, H.; Kananishi, N.; Watanabe, M.; Tomura, K. *J. Radioanal. Nucl. Chem.* **1995**, *192*, 81.

1. Introduction

the carbon material that provides it with lower toxicity and extra resistance to metabolism.

Fullerene Applications in Materials Science

Due to their unique chemical, electronic and photophysical properties, fullerenes and other carbon nanomaterials such as carbon nanotubes (CNT) have been widely reported in the field of materials science and nanotech engineering.

Fullerene derivatives and endohedral fullerenes exhibit very interesting properties such as electronic absorption bands expanding throughout the entire UV-Vis spectrum, a strong electron-acceptor character (being C₆₀ able to accept up to six electrons) and small reorganization energy. These characteristics make them very interesting building blocks for the study of energy transport and electron and charge transfer processes.²²

Many molecular architectures have been reported bearing fullerenes and endohedral fullerenes as electron acceptors linked either covalently or non-covalently to electron-donor species such as porphyrins that are able to undergo photoinduced electron transfer (PET) and perform highly efficient conversion of the harvested light into the high-energy state of the charge separation. These constructs have been widely reported as photosynthetic antenna or reaction center for the construction of artificial photosynthetic devices.²²

Other applications in the field of material science have been described. To give some examples, fullerene derivatives have been reported in applications as lubricants,²³

²² (a) Imahori, H.; Sakata, Y. *Eur. J. Org. Chem.* **1999**, 2445. (b) Guldi, D. M.; Imahori, H. *J. Porphyrins Phthalocyanines*, **2004**, *8*, 976. (c) Guldi, D. M.; *Pure Appl. Chem.* **2003**, *8*, 1069. (d) Imhori, H.; Fukuzumi, S. *Adv. Funct. Mater.* **2004**, *14*, 525. (e) Guldi, D. M. *Chem. Soc. Rev.* **2002**, *31*, 22.

²³ Zhmud, B.; Pasalskiy, B. *Lubricants*, **2013**, *1*, 95.

1. Introduction

composites in well-organized materials such as polymers and thin films²⁴ or superconductors when doped with alkali metals.^{12b}

However, despite of a useful scope, the access to fullerenes is challenging. Apart from the limited occurrence, its low solubility in water and in organic solvents is the reason for cost-intensive purification and isolation methods. Furthermore, the low access to the fullerenes is the main factor restricting the development of the applications.

To overcome these challenges, strategies based on supramolecular complexation of fullerene targets with appropriate receptors have been developed.

1.1.3 Supramolecular Receptors for Fullerenes

The spherical shape and the electron deficient nature of the fullerenes restrict the types of non-covalent forces that can be used to stabilize the interactions within host-guest inclusion complex. Several fullerene receptors have been reported targeting both their electronic properties and unusual shapes.²⁵

The first receptors designed for the encapsulation of fullerenes were described in 1992 by Ringsdorf *et al.*²⁶ They reported two azacrown-based receptors functionalized with long alkyl chains that formed a lipophilic cavity able to form 1:1 inclusion complexes with both C₆₀ with C₇₀ (Figure 1.4).

²⁴ Prato, M. *J. Mater. Chem.* **1997**, *7*, 1097.

²⁵ (a) Diederich, F.; Gómez-López, M. *Chem. Soc. Rev.* **1999**, *28*, 263. (b) Komatsu, N. *J. Incl. Phenom. Macrocycl. Chem.* **2008**, *61*, 195. (c) Canevet, D.; Pérez, E. M.; Martín, N. *Angew. Chem. Int. Ed.* **2011**, *50*, 9248.

²⁶ Diederich, F.; Effing, J.; Jonas, U.; Jullien, L.; Plesnivý, T.; Ringsdorf, H.; Thilgen, C.; Weinstein, D. *Angew. Chem. Int. Ed. Engl.* **1992**, *31*, 1599.

1. Introduction

Also in 1992, Wennerström *et al.*²⁷ reported the formation of a 2:1 γ -cyclodextrin/ C_{60} inclusion complex that allowed water solubilization and selective extraction of C_{60} from a C_{60}/C_{70} mixture (Figure 1.4).



Figure 1.4 First reported fullerene receptors: γ -cyclodextrin and azacrown-based receptor.^{26, 27}

Since these first fullerene receptors were reported, a huge effort has been put into the preparation of molecular hosts able to form inclusion complexes with C_{60} , C_{70} , higher fullerenes and other carbon materials. In attempts to target the curved electron deficient surface of the carbon nanomaterials, receptors have been functionalized with concave and/or electron rich moieties. For instance, calixarene⁻²⁸, cyclotrimeratrylene (CTV)⁻²⁹, π -extended tetrathiafulvalene (exTTF)⁻³⁰ and porphyrin-based³¹ receptors

²⁷ Andersson, K.; Nilson, K.; Sundahl, M.; Westman, G.; Wennerström, O. *Chem. Commun.* **1992**, 604.

²⁸ (a) Atwood, J. L.; Koutsantonis, G. A.; Raston, C. L. *Nature*, **1994**, 368,229. (b) Suzuki, T.; Nakashima, K.; Shinkai, S. *Chem. Lett.* **1994**, 669. (c) Atwood, J. L.; Barbour, L. J.; Raston, C. L.; Sudria, I. B. N. *Angew. Chem. Int. Ed.* **1998**, 37, 981. (d) Haino, T.; Yanase, M.; Fukazawa, Y. *Angew. Chem. Int. Ed.* **1997**, 36, 259 (e) Haino, T.; Yanase, M.; Fukazawa, Y. *Angew. Chem. Int. Ed.* **1998**, 37, 997.

²⁹ See chapter 1.2

³⁰ (a) Pérez, E. M., Martín, N. *Pure Appl. Chem.* **2010**, 82, 523. (b) Pérez, E. M., Sánchez, L.; Fernández, N.; Martín, N. *J. Am. Chem. Soc.* **2006**, 128, 7172. (c) Canevet, D.; Gallego, M.; Isla, H.; de Juan, A.; Pérez, E. M.; Martín, N. *J. Am. Chem. Soc.* **2011**, 133, 3184. (d) Grimm, B.; Santos, J.; Illescas, B. M.; Muñoz, A.; Guldí, D. M.; Martín, N. *J. Am. Chem. Soc.* **2010**, 132, 17387.

³¹ See chapter 1.3

1. Introduction

have been widely reported. CTV- and porphyrin-based receptors play a special role in this work and are discussed in detail in the next chapters of the introduction.

Receptors for Higher Fullerenes and Endohedral Fullerenes

Most of the separation methods based on supramolecular complexation of the fullerenes target the major fullerenes C₆₀ and C₇₀. Only a few examples of molecular hosts that target higher fullerenes or endohedral fullerenes have been reported. One of example of such receptor is the double calix[5]arene container reported by Fukazawa *et al.*³² The *syn* isomer of the double calix[5]arene container was able to selectively extract higher fullerenes, especially C₉₄ and C₉₆, from fullerene mixtures. Increment of the temperature above 100 °C induced a receptor conformation change that led to the liberation of the extracted fullerenes. More examples of receptors targeting high fullerenes and endohedral fullerenes are discussed in detail in the next chapters of the introduction.

³² Haino, T.; Fukunaga, C.; Fukazawa, Y. *Org. Lett.* **2006**, *8*, 3545.

1.2 Cyclotrivenatrylene-Based Receptors

1.2.1 Introduction

Cyclotrivenatrylene (CTV) (I) is a cyclic trimer of veratrole (II). In its preferred crown conformation, the three aryl rings point toward the same direction, what confers the CTV (I) with a cone shape and a superficial molecular cavity which is capable of reversible binding of guest molecules in a non-covalent manner. Thus, CTV derivatives are suitable for host-guest interactions and self-assembly.³³

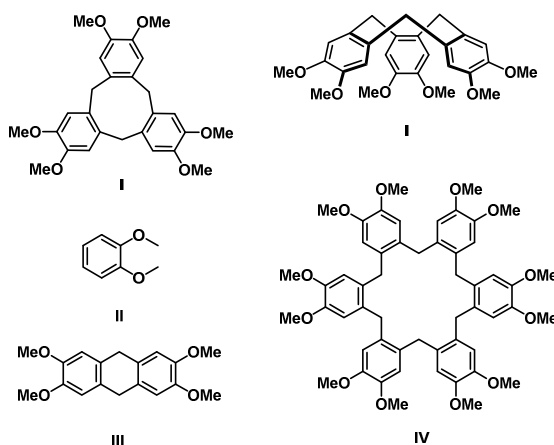


Figure 1.5 Structures I-IV.

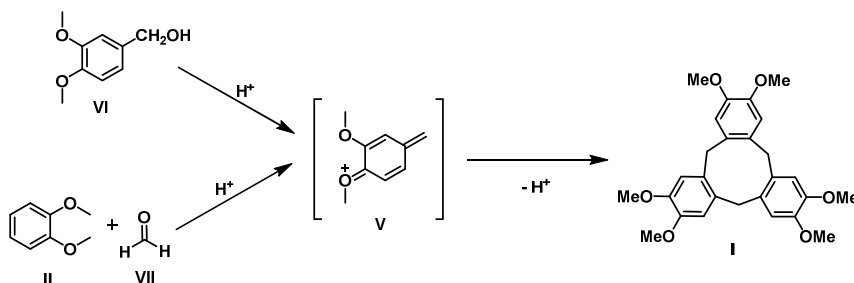
³³ (a) Hardie, M. J. "Cyclotrivenatrylene and Cryptophanes" in: *Supramolecular Chemistry: from Molecules to Nanomaterials*, Vol. 3, P. A. Gale, J. W. Steed (eds.), J. Wiley & Sons, Chichester, 2012, 895. (b) Steed, J. W.; Atwood, J. L. *Supramolecular Chemistry*, Wiley, Chichester, **2009**. (c) Collet A. *Tetrahedron* **1987**, *43*, 5725. (d) Hardie, M. J. *Chem. Soc. Rev.* **2010**, *39*, 516.

1. Introduction

CTV was first synthesized by Gertrude Robinson in 1915 but wrongly formulated as the 2,3,6,7-tetramethoxy-9,10-dihydroanthracene (**III**). Later in 1950s, the CTV was reassigned as the hexamer **IV**, although it took until the work of Lindsey, Erdtman *et al.* and Goldup *et al.* in the 1960s that the trimeric structure **I** was established, based on molecular weight determination, mass and NMR spectroscopy analysis and re-examination of the earlier X-ray data.^{33a, 33c}

1.2.1.1 Synthesis of Cyclotrimeratrylene

Cyclotrimeratrylene can be synthesized in *ca.* 70 % yield by self-condensation of the veratryl cation (**V**) (Scheme 1.1), which is produced under strong dehydrating acidic conditions from either veratryl alcohol (**VI**) or from veratrole (**II**) and formaldehyde (**VII**).^{33a, 33c, 34}



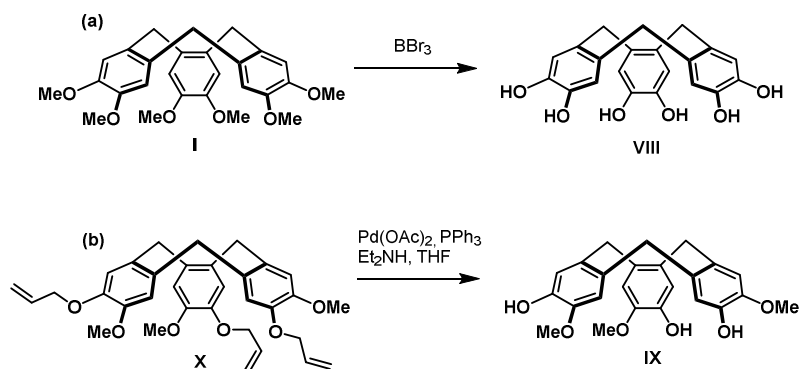
Scheme 1.1 Synthesis of Cyclotrimeratrylene (**I**).

³⁴ Typical conditions for the condensation of veratrole alcohol are 60 % perchloric acid (yield 60 %), trifluoroacetic acid in chloroform (yield 19 %), sulfuric acid in hot acetic acid (yield 87%) or BF₃ etherate in benzene (45 %); Recently milder alternative conditions using catalytic levels of Sc(OTf)₃ in acetonitrile have been reported by Brotin *et al.* (yield 44 %). See ref. 33

1.2.1.2 Synthesis of Extended Cavities

CTV cavities can be extended and functionalized by appending side-arms to the CTV upper rim, making them better suited for host-guest interactions.

There are two different approaches to prepare extended cavities: either condensation of the corresponding 3,4-substituted benzyl alcohols or substitution reaction of the CTV analogues CTC (**VIII**) or CTG (**IX**) with alkyl halides or acid chlorides to give the ether- and ester-linked side-arms, respectively. CTV analogues cyclotricatechylene (CTC, **VIII**) and cyclotriguaiacylene (CTG, **IX**) are readily accessible from demethylation of CTV (**I**) or deallylation of **X**, respectively.^{33a, 33c}



Scheme 1.2 Synthesis of CTV analogues CTC (**VIII**) and CTG (**IX**).

1.2.2 CTV Host-Guest Inclusion Complexes

1.2.2.1 Inclusion Chemistry of CTV

CTV (**I**) is known to form inclusion complexes with ions, small neutral molecules, such as organic solvents, and large spherical guests, such as fullerene and *o*-carborane.

1. Introduction

In the case of CTV-fullerene inclusion complexes, the intra-cavity host-guest complexes are held together by non-covalent interactions. Both electronic and shape complementarities stabilize the complex: the electron rich CTV aryl rings, consequence of the electron-donating effect of the methoxy groups, complement the electron-deficient nature of fullerene. Furthermore, the curvature and symmetry match favor complex stabilization.³³

In the early 1990s, Atwood and co-workers³⁵ first described the formation of the so-called ball-and-socket complex between CTV and C₆₀ (Figure 1.6).

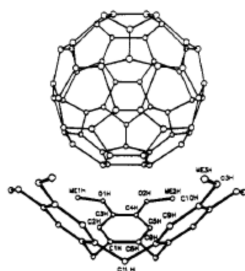


Figure 1.6 Ball-and-socket crystal structure.^{35a}

These ball-and-socket nanostructures can exist as discrete monomeric species, aggregates and polymeric infinite arrays. One of the first examples of such networks was reported in 1999 by Hardie *et al.*³⁶ Complexation of C₆₀ in toluene resulted in two different CTV/C₆₀ polymeric structures, the 1:1 phase (C₆₀)(CTV), where each CTV has a C₆₀ associated within the cavity, and the 1.5:1 fullerene rich phase (C₆₀)_{1.5}(CTV) with half of the fullerenes outside the CTV cavity (Figure 1.7).

³⁵ (a) Steed, J. W.; Junk, P. C.; Atwood J. L. *J. Am. Chem. Soc.* **1994**, *116*, 10346. (b) Atwood, J. L.; Barnes, M. J.; Gardiner, M. G.; Raston, C. L. *Chem Commun.* **1996**, *342*, 1449.

³⁶ Hardie, M. J.; Raston, C. L. *Chem. Commun.* **1999**, 1153

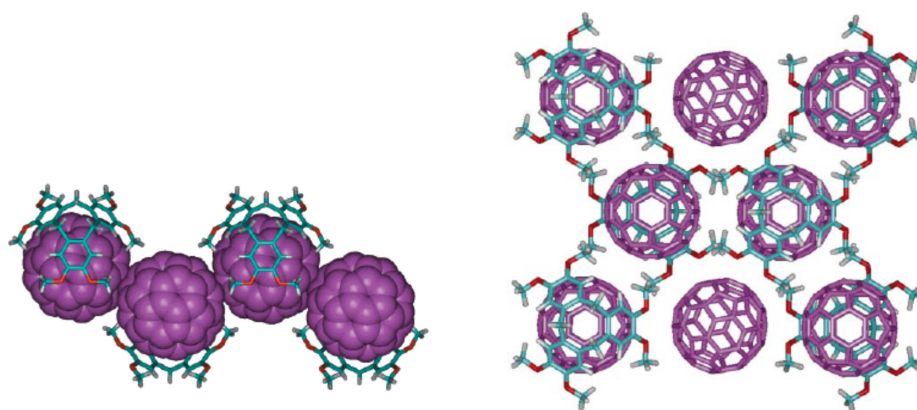


Figure 1.7 X-ray structure of $(C_{60})(CTV)$. Crystal packing of $(C_{60})_{1.5}(CTV) \cdot C_7H_6$

1.2.2.2 CTV-Based Hosts for Discrete C_{60} Inclusion and its Applications

Several solid-state as well as solution complexes have been characterized and reported as fullerene hosts since the ball-and-socket complex was first described. These molecular receptors are capable of fullerene recognition for potential applications. The fullerene binding abilities of CTVs have been exploited in order to purify and solubilize as well as to incorporate them into well-organized systems such as liquid crystals or solid surfaces. Here some remarkable examples are highlighted.

Fullerene-Containing Liquid Crystals

Nierengarten *et al.* reported CTV derivative **XI** surrounded by long alkyl chains that is able to self-assemble into host-guest complexes with C_{60} . The CTV/ C_{60} inclusion complex (Figure 1.8) exhibits liquid crystalline behavior at room temperature. X-ray diffraction patterns confirmed that such mesophases correspond to a nematic phase

1. Introduction

which irreversibly changed to a cubic phase when heating above 70 °C. This process was confirmed by differential scanning calorimetry (DSC).³⁷

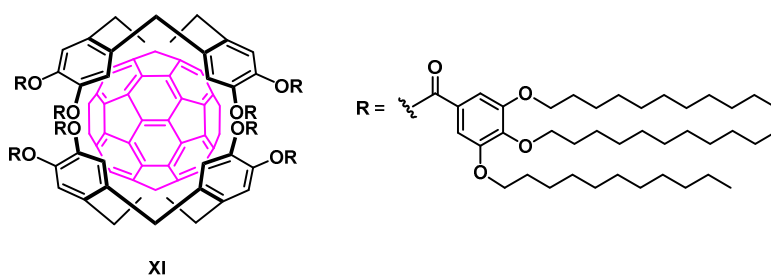


Figure 1.8 CTV-based C₆₀ containing-liquid crystal **XI**.

Inclusion of C₆₀ was evidenced by both UV-Vis titration and X-ray spectroscopy. In diluted solution the CTV derivative forms 1:1 complexes with an association constant of 230 M⁻¹ in benzene whereas the stoichiometry of the host-guest complex in the solid state was found to be 2:1.

Incorporation of Fullerenes into Surfaces

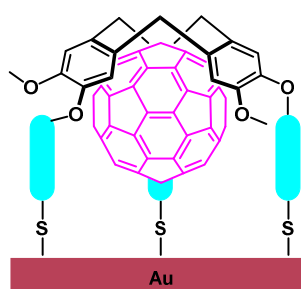
Thin films of fullerene-based materials exhibit interesting characteristics such as superconductivity, nonlinear optics and biological activity. Classical approaches based on covalent attachment of C₆₀ on surfaces partially destroy the electron delocalization of the fullerenes. Furthermore, covalent attachment allows fullerene aggregation which can also affect their electronic properties.

De Mendoza, Echegoyen *et al.*³⁸ reported in 2005 a supramolecular system that incorporates C₆₀ into surfaces based on the thio-derived CTV **XII** that can be anchored

³⁷ (a) Felder, D.; Heinrich, B.; Guillon, D.; Nicoud, J.-F.; Nierengarten, J.-F. *Chem. Eur. J.* **2000**, *6*, 3501. (b) Felder, D.; Guillon, D.; Nierengarten, J.-F. *Mater. Sci. Eng. C*, **2001**, *18*, 161

1. Introduction

on gold surfaces. The C_{60} is encapsulated by the CTV forming self-assembled monolayers (SAMs). This receptor maintains the electron properties of the fullerenes. At the same time it inhibits the C_{60} aggregation (Figure 1.9).



XII

Figure 1.9 Schematic representation of CTV-based SAMs XII.

Solubilization of Fullerenes in Aqueous Media

Fullerenes exhibit interesting biological activities due to their unique shape and electronic characteristics. Several biological and pharmaceutical applications have been reported over the last years. Unfortunately, the inherent lack of solubility of fullerenes in aqueous media limits its application. The fullerene binding abilities of CTV can be exploited in order to solubilize fullerenes in aqueous solutions.

³⁸ Zhang, S.; Palkar, A.; Fragoso, A.; Prados, P.; de Mendoza, J.; Echegoyen, L. *Chem. Mater.* **2005**, *17*, 2063

1. Introduction

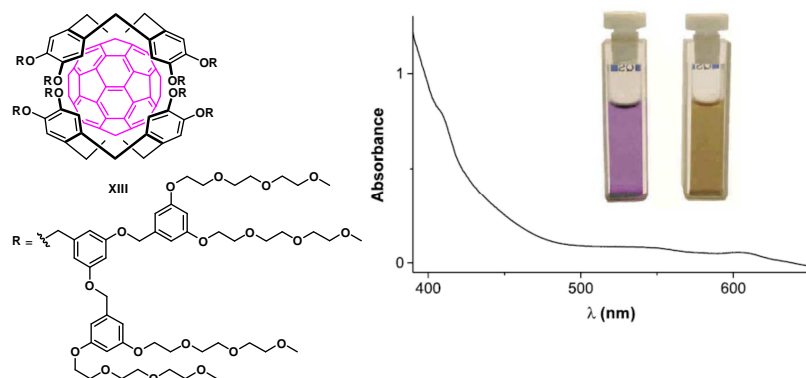


Figure 1.10 a) Water soluble functionalized CTV **XIII**. b) Absorption spectra of $[C_{60}(\mathbf{XIII})_2]$ in water. Inset: solution of C_{60} in benzene (left) and the brown solution of $[C_{60}(\mathbf{XIII})_2]$ in water (right).

Nierengarten *et al.* reported the synthesis of an extended CTV derivative functionalized with peripheral triethyleneglycol chains **XIII** able to form water soluble supramolecular complexes with C_{60} .³⁹ The association with the fullerene was evidenced by UV-Vis spectroscopy and the association constant calculated in benzene ($K_{\text{ass}} = 190 \text{ M}^{-1}$). The water soluble CTV host forms 1:1 complexes in solution whereas, after slow evaporation, 2:1 host-guest complexes were obtained in the solid state. The complex was soluble in water and methanol, and the solubilization of the complex in water was monitored by UV-Vis absorption (Figure 1.10).

More recently in 2011 Han *et al.* reported glucose and lactose functionalized CTV derivatives **XIV** and **XV** which are able to form water-soluble 1:1 supramolecular complexes with C_{60} .⁴⁰

³⁹ Rio, Y.; Nierengarten J.-F. *Tetrahedron Lett.*, **2002**, 43, 4321.

⁴⁰ Yang, F.; Chen, Q.; Cheng, Q.-Y.; Yan, C.-G.; Han, B.-H. *J. Org. Chem.* **2012**, 77, 971.

1. Introduction

Complex formation was evidenced by UV-Vis and fluorescence spectroscopy. The association constants were quantified by fluorescence titration in toluene-DMSO ($K_{\text{ass}}(\text{C}_{60}@\text{XIV}) = 1.38 \times 10^5 \text{ M}^{-1}$; $K_{\text{ass}}(\text{C}_{60}@\text{XV}) = 5.09 \times 10^4 \text{ M}^{-1}$).

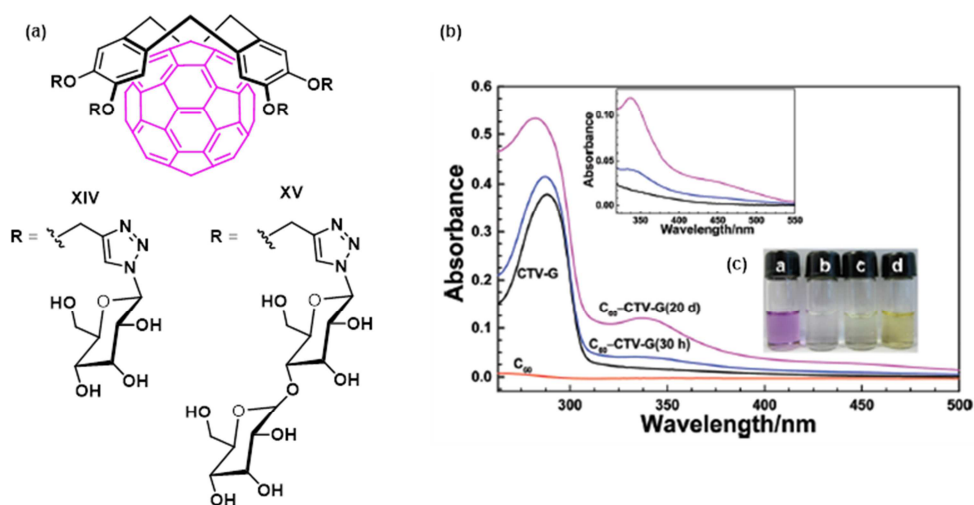


Figure 1.11 (a) Water soluble glucose and lactose functionalized CTVs **XIV** and **XV**. (b) Absorption spectra of aqueous C₆₀@**XIV** and **XIV** solution, and C₆₀ in water. (c) C₆₀ in various solvents: a. C₆₀ in toluene; b. C₆₀ in water after centrifugation; c. **XIV** in water; d. C₆₀@**XIV** in water after centrifugation.

The sugar moieties extended the CTV host cavity, enhancing the planar conformation of the CTV and the binding ability of the host.

The higher steric effect of the lactose functionalized receptor **XV** reduced the cavity size available for fullerene encapsulation which resulted in a lower binding ability than for the glucose substituted host **XIV** and therefore in a weaker association. Nevertheless, the association constant for the lactose functionalized CTV is still among the higher CTV based receptor values reported to date.

1. Introduction

The introduction of sugar moieties to a CTV platform not only extended the cavity enhancing the binding ability but also provided the complex with good solubility in water.

The solubility of the glucose functionalized CTV **XIV** complex with C₆₀ in water was monitored by UV-Vis spectroscopy and compared with the solubility of the free guest and free hosts solutions as seen in Figure 1.11.

CTV-Based Cages for Fullerene Purification.

In 2007, de Mendoza *et al.* reported a chromatography-free methodology for C₇₀ and C₈₄ purification based on its selective complexation by a CTV derivative featuring 2-ureido-4-[1H]-pyrimidinone (UPy) moieties **XVI** that reversibly self-assemble into a dimeric capsule.⁴¹ The UPy moieties contain quadruple self-complementary DDAA (D = donor, A = acceptor) hydrogen bonding sequences that result in a strong dimerization in apolar media. The resulting spherical host forms 2:1 inclusion complex with fullerenes with a high selectivity for C₈₄ and C₇₀.

The high association constants were determined by UV-Vis titrations and isothermal titration calorimetry (ITC) in tetrachloroethane (TCE) ($K_{\text{ass}}(\text{C}_{60}) = 2 \times 10^3 \text{ M}^{-1}$; $K_{\text{ass}}(\text{C}_{70}) = 4 \times 10^4 \text{ M}^{-1}$, $K_{\text{ass}}(\text{C}_{84}) = 4 \times 10^5 \text{ M}^{-1}$). These results are in fully agreement with the DFT calculations that also predicted a lower energy for the interaction with C₈₄ rather than for C₇₀ or C₆₀.

C₇₀ and C₈₄ were efficiently selectively purified from crude soot or fullerite mixtures by simple solid-liquid extractions. 85 % of C₇₀ was recovered after one single extraction directly from fullerite and was isolated after only two runs with a purity of 97 %. C₈₄

⁴¹ (a) Huerta, E.; Metselaar, G. A.; Fragoso, A.; Santos, E.; Bo, C.; de Mendoza, J. *Angew. Chem. Int. Ed.* **2007**, *46*, 202. (b) Huerta, E.; Cequier, E.; de Mendoza, J. *Chem. Commun.* **2007**, 5016.

1. Introduction

could be enriched up to 76 % after one single extraction and isolated with an 85 % purity. Addition of TFA disrupted the H-Bonding dimer promoting the precipitation of the encapsulated fullerene what allowed the recovery of both the fullerene and the capsule.

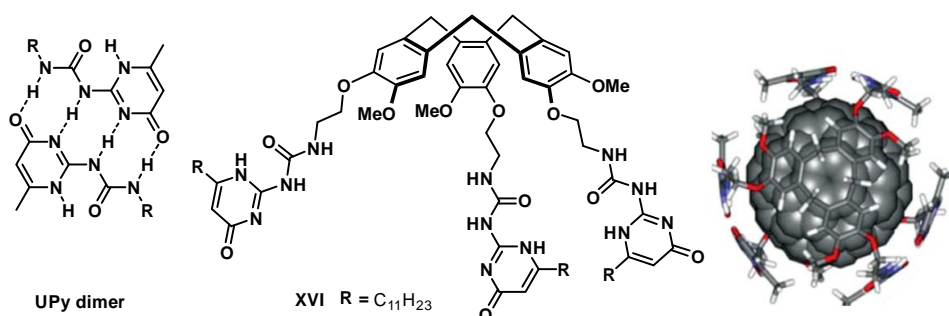


Figure 1.12 2-Ureido-4-[1H]-pyrimidinone (UPy) dimer, UPy functionalized CTV **XVI**. Top view of the DFT-calculated molecular structure of the C₈₄@**XVI** capsule.⁴¹

De Mendoza *et al.* established the first reported chromatographic-free procedure for the selective encapsulation and purification of C₇₀ and C₈₄. Moreover, they also reported that the selectivity toward these fullerenes can be tuned by modifying the receptor/fullerite ratio. For instance, selectivity toward C₈₄ was maximized at low receptor/fullerite ratios whereas high receptor/fullerite ratios improve the selectivity towards C₇₀.

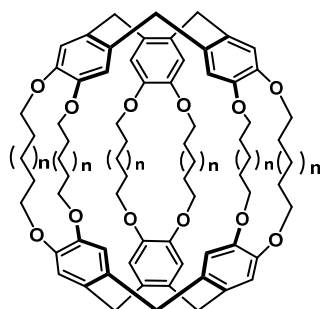
Recently Chiu *et al.* reported the synthesis and characterization of a CTV based hemicarcerand **XVII** able to selectively sequester C₇₀ from a fullerene extract.⁴²

The C₇₀@**XVII** complex can be isolated by chromatography with very high-purity (>99%) and a total amount of C₇₀ recovery of 72 % after guest release. Association

⁴² Li, M.-J.; Huang, C.-H.; Lai, C.-C.; Chiu, S.-H. *Org Lett*, **2012**, *14*, 6146.

1. Introduction

with C_{60} was not strong enough to isolate the complex. Nevertheless, the association was evidenced by $^1\text{H-NMR}$ spectroscopy.



XVII $n=8$

Figure 1.13 CTV based hemicarcerand **XVII**.

The association with both C_{60} and C_{70} was monitored and quantified by means of $^1\text{H-NMR}$ spectroscopy. The $C_{70}@XVII$ association constant was quantified from the dissociation equilibrium in TCE ($K_{\text{ass}}(C_{70}@XVII) = 4,2 \times 10^3 \text{ M}^{-1}$) after it was isolated by column chromatography. The $C_{60}@XVII$ association constant was calculated from $^1\text{H-NMR}$ titration in TCE ($K_{\text{ass}}(C_{60}@XVII) = 500 \text{ M}^{-1}$).

After isolation of the $C_{70}@XVII$ complex, the fullerene was released by heating the sample at 303 K and precipitation of the cage in toluene and the molecular cage was recovered and recycled.

CTV-Based Receptors featuring other Fullerene-Selective Recognition Motifs.

The combination of more than one fullerene recognition motif in the same molecular host has also been reported in the literature.

1. Introduction

In 2010, de Mendoza, Martín *et al.* reported a CTV based host combined with three π -extended tetrathiafulvalenes (exTTF) moieties **XVIII**.⁴³ The curvature and the aromaticity of the exTTF make them suitable candidates for fullerene recognition. In this case, the combination of these two concave recognition fragments results in a very effective association with both C₆₀ and C₇₀.

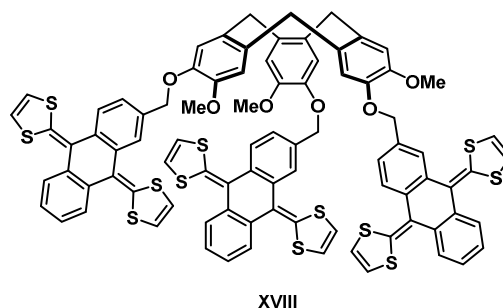


Figure 1.14 exTTF-CTV host **XVIII**

The association with C₆₀ was confirmed by ¹H-NMR, ¹³C-NMR and UV-Vis spectroscopy and the association constants with both fullerenes were calculated from absorption titration in chlorobenzene ($K_{\text{ass}}(\text{C}_{60}) = 2 \times 10^5 \text{ M}^{-1}$; $K_{\text{ass}}(\text{C}_{70}) = 2 \times 10^6 \text{ M}^{-1}$). These associations are the highest ever reported for CTV based receptors and comparable to the bis-porphyrin dimers reported by Aida *et al.*⁴⁴, with exception of the RhMe and IrMe metallated hosts.

More recently, Yanney and Sygula synthesized a CTV-based molecular clip functionalized with three corannulene moieties **XIX**.⁴⁵ They combined two concave aromatic fullerene recognition motifs, the CTV and the pendant corannulene-scaffolds.

⁴³ Huerta, E.; Isla, H.; Pérez, E. M.; Bo, C.; Martín, N.; de Mendoza, J. *J. Am. Chem. Soc.* **2010**, *132*, 5351.

⁴⁴ See chapter 1.3.

⁴⁵ Yanney, M.; Sygula, A. *Tetrahedron Lett.* **2013**, *54*, 2604.

1. Introduction

$^1\text{H-NMR}$ titration experiment in toluene suggested the formation of a 1:1 complex with association constants of $1.5 \cdot 10^3 \text{ M}^{-1}$ and $1.2 \cdot 10^3 \text{ M}^{-1}$ for C_{60} and C_{70} , respectively.

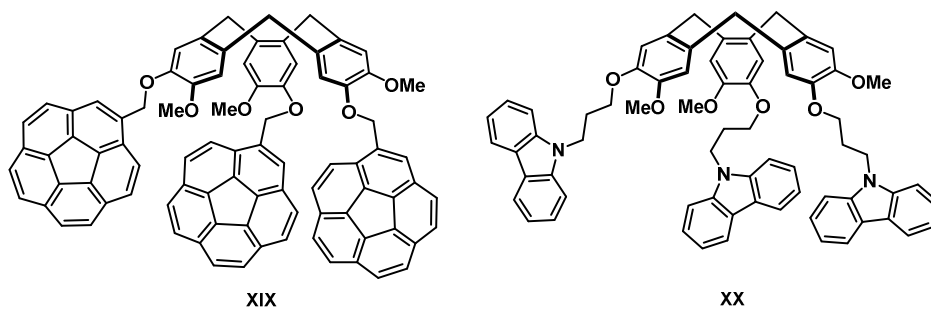


Figure 1.15 Corannulene and carbazole functionalized CTV hosts **XIX** and **XX**.

In 2013, Shuang *et al.* reported the synthesis of a CTV-based clip bearing three carbazole **XX** units able to form 1:1 complexes with C_{60} in solution.⁴⁶ They combined the CTV scaffold with electron-rich aromatic carbazoles, well known for their fullerene recognition ability. The association was studied by UV-Vis and fluorescence spectroscopy and quantified from fluorescence titration in DCM ($K_{\text{ass}} = 5 \times 10^4 \text{ M}^{-1}$)

⁴⁶ Wu, H.; Zhang, C.; Li, L.; Chao, J.; Han, Y.; Dong, C.; Guo, Y.; Shuang, S. *Talanta* **2013**, *106*, 454.

1.3 Porphyrin-Based Receptors

1.3.1 Introduction.

Porphyrins are tetrapyrrole macrocycles. The pyrrole units are connected through a methyne carbon known as *meso*-carbon what allows electronic conjugation of the 18 π -electrons throughout the inner porphyrin ring. Porphyrins are therefore highly conjugated aromatic compounds and consequently they feature rigid and planar geometry, high stability and intense coloration.⁴⁷

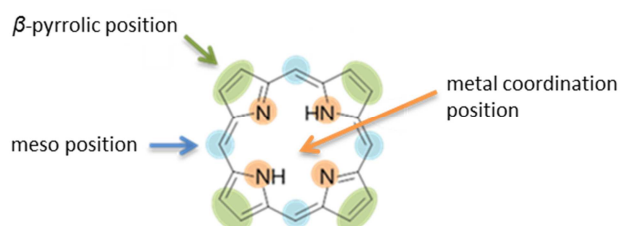


Figure 1.16 Porphyrin positions available for functionalization.

Porphyrins have three positions available for functionalization. The *meso* and β -pyrrolic positions can be covalently modified to synthesize expanded porphyrin systems with a wide variety of functional groups. Furthermore, porphyrin characteristics can be tuned by metal coordination of the inner N-H protons (Figure 1.16).

⁴⁷ (a) Sessler, J. L.; Karnas, E.; Sedenberg, E. "Porphyrins and Expanded Porphyrins as Receptors" in: *Supramolecular Chemistry: from Molecules to Nanomaterials*, Vol. 3, P. A. Gale, J. W. Steed (eds.), J. Wiley & Sons, Chichester, **2012**, 1045. (b) Boyd, P. D. W. *Acc. Chem. Res.* **2005**, *38*, 235. (c) Tashiro, K.; Aida, T. *Chem. Soc. Rev.* **2007**, *36*, 189. (d) Guldi, D. M. *Chem. Soc. Rev.* **2002**, *31*, 22. (e) Komatsu, N. *J. Incl. Phenom. Macrocycl. Chem.* **2008**, *61*, 195. (f) Mironov, A. F. *Macroheterocycles* **2011**, *3*, 186.

1. Introduction

1.3.1.1 Porphyrin-Based Hosts and their Inclusion Complex Characterization.

UV-Vis and Fluorescence Spectroscopy.

Porphyrins feature intense electronic absorption and have a very characteristic electronic spectrum. The $\pi\text{-}\pi^*$ transition from the ground state to the second excited singlet state translates into an intense band between 380 and 420 nm, known as the *Soret* band, as seen in Figure 1.17.^{47a, 47b}

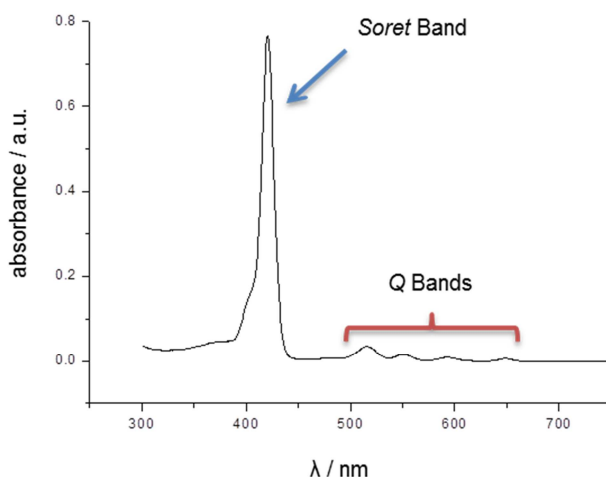


Figure 1.17 Typical absorption spectrum of a free-base porphyrin

In metal-free porphyrins, another set of weaker four bands, known as Q bands, are observed between 480 and 700 nm (Figure 1.17). These bands correspond to the $\pi\text{-}\pi^*$ transitions from the ground state to the first excited state. Higher symmetry systems such as diprotonated or metallated porphyrins only show two Q-bands.

Any electronic perturbation, such as covalent or supramolecular modifications of the porphyrin, is translated into a change in its absorption spectrum. Synthetic modification and non-covalent guest inclusion can therefore be monitored by UV-Vis spectroscopy.

1. Introduction

Upon interaction with the guest, the absorption intensity is typically quenched and/or bands are shifted.

Free-base and the majority of metalloporphyrins also exhibit strong fluorescence emission following photoexcitation. Upon close interaction with a guest the fluorescence emission is quenched. Furthermore, fluorescence spectroscopy is a direct detection technique and therefore very sensitive. For all these reasons, both UV-Vis and fluorescence spectroscopies are widely used to monitor and quantify the interactions between porphyrins and guest molecules.

NMR Spectroscopy.

¹H-NMR spectroscopy is an excellent technique to characterize porphyrin-guest interactions providing information of the inclusion complex geometry.

In a porphyrin ¹H-NMR spectrum, the *meso* and β -pyrrolic protons typically are downshielded by the diamagnetic ring current and shifted downfield while the shielded inner N-H protons are shifted upfield. Any electronic perturbation induced by guest inclusion will be reflected in the spectra. The shifting of the proton signals as function of guest addition can be monitored and the association quantified.

In the case of porphyrin-fullerene interactions, ¹³C-NMR is also widely used to characterize the complex. The signals corresponding to those fullerene carbons having a closer interaction with the porphyrin would exhibit a more significant shift.^{47a, 48}

⁴⁸ Sun, D.; Tham, F. S.; Reed, C. A.; Chaker, L.; Burgess, M.; Boyd, P. D. W. *J. Am. Chem. Soc.* **2000**, *122*, 10704.

1. Introduction

1.3.1.2 Host-Guest Chemistry of Porphyrins and Fullerenes.

Porphyrins are large electron-rich molecules and therefore good electron donors. This makes them suitable receptors for electron-deficient species such as nanocarbon materials like fullerenes or carbon nanotubes (CNT).⁴⁷

These porphyrin-fullerene complexes are held together by non covalent interactions such as van der Waals, donor-acceptor and charge-transfer interactions between the flat π -surface of the porphyrin and the curved π -surface of the fullerene.^{47d, 47f}

A large number of porphyrin-based receptors for fullerenes have been reported in the literature since such interaction was first described in 1993. Meyerhoff *et al.* reported a C₇₀ selective porphyrin functionalized silica able to separate C₆₀ and C₇₀.⁴⁹ The higher selectivity for C₇₀ over C₆₀ ($\alpha \approx 4.8$)⁵⁰ was attributed to the π - π^* interactions between the porphyrin units and the large surface area available in C₇₀. For this reason, longer retention times are achieved as the fullerene is bigger. One year later, they also reported the use of the porphyrin functionalized silica for the isolation of La@C₈₂ endohedral fullerene.⁵¹

Later in 1997, Boyd, Reed *et al.* reported the crystal structure of a covalently linked porphyrin-C₆₀ conjugate **XXI** showing close (2.75 Å) porphyrin-fullerene intermolecular interactions (Figure 1.18). This was the first report on such unexpectedly short distances between a porphyrin and a fullerene.⁵²

⁴⁹ Kibbey, C. E.; Savina, M. R.; Pareeghian, B. K.; Francis, A. H.; Meyerhoff, M. E. *Anal. Chem.* **1993**, *95*, 3717.

⁵⁰ Where α = selectivity factor of C₇₀ over C₆₀.

⁵¹ Xiao, J.; Savina, M. R.; Martin, G. B.; Francis, A. H.; Meyerhoff, M. E. *J. Am. Chem. Soc.* **1994**, *116*, 9341.

⁵² Sun, Y.; Drovetskaya, T.; Bolskar, R. D.; Bau, R.; Boyd, P. D. W.; Reed, C. A.; *J. Org. Chem.* **1997**, *62*, 3642.

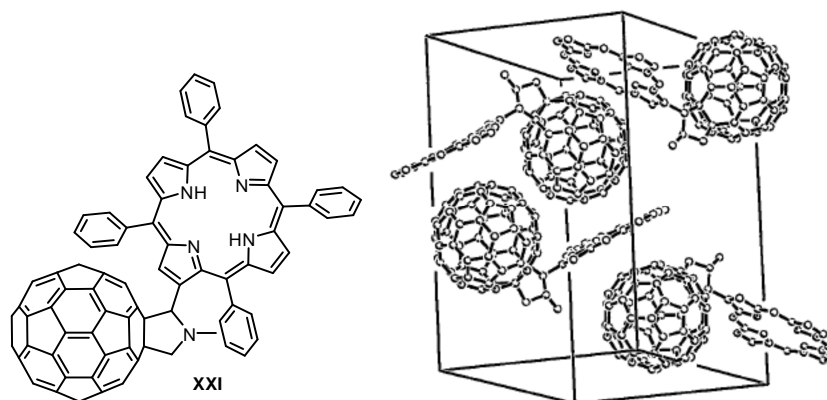


Figure 1.18 Pyrrolidine-linked TPP-C60 conjugate **XXI**. Unit cell packing of **XXI** in the crystal structure.⁵²

In 1999, the first solid state structures of non-covalent linked fullerene porphyrin complexes were independently published by Boyd *et al.* and Olmstead, Balch and co-workers.^{53, 54}

Both reported supramolecular co-crystals of porphyrins and fullerenes (Figure 1.19). In both cases, very short porphyrin-fullerene distances were observed (2.7-3.0 Å), shorter than ordinary van der Waals (3.0-3.5 Å), fullerene-fullerene (*ca.* 3.2 Å), porphyrin-porphyrin (> 3.2 Å), porphyrin-arene, and fullerene/arene distances (typically 3.0-3.5 Å), and shorter than arene-arene distances, such as the spacing between graphene layers in graphite (3.3-3.5 Å).^{47b}

⁵³ Boyd, P. D. W.; Hodgson, M. C.; Rickard, C. E. F.; Oliver, A. G.; Chaker, L.; Brothers, P. J.; Bolska, R. D.; Tham, F. S.; Reed, C. A. *J. Am. Chem. Soc.* **1999**, *121*, 10487.

⁵⁴ Olmstead, M. M.; Costa, D. A.; Maitra, K.; Noll, B. C.; Phillips, S. L.; Van Calcar, P. M.; Balch, A. L.; *J. Am. Chem. Soc.* **1999**, *121*, 7090.

1. Introduction

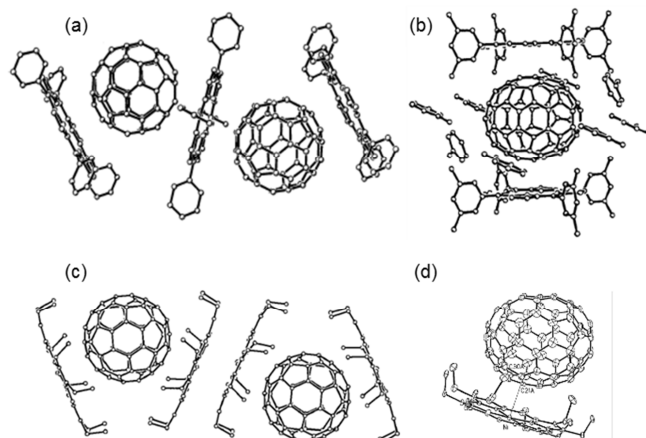


Figure 1.19 Supramolecular co-crystals of porphyrins and fullerenes: (a) $\text{H}_2\text{TPP}\cdot\text{C}_{60}\cdot\text{toluene}$ chain (from ref. 6). (b) Molecular packing diagram for $\text{H}_2\text{T}_{3,5}\text{-dimethylPP}\cdot\text{C}_{70}\cdot 4$ toluene (from ref. 6). (c) Helical chain of $\text{C}_{60}\cdot 2\text{Co}^{\text{II}}(\text{OEP})\cdot\text{CHCl}_3$.⁵³ (d) Porphyrin-fullerene unit of $\text{C}_{70}\cdot\text{Ni}^{\text{II}}(\text{OEP})\cdot\text{C}_6\text{H}_6\cdot\text{CHCl}_3$.⁵³

The supramolecular fullerene-mono-porphyrin interactions observed in the solid state also persist in solution. However, these interactions are often too weak to be detected or quantified.

Boyd *et al.* also reported UV-Vis studies in toluene that shown no interaction between porphyrins and C_{60} , suggesting that either the association was too weak to be observed or that no interaction at all happened in solution. However, small but significant upfield shifts were observed both in $^1\text{H-NMR}$ and $^{13}\text{C-NMR}$ spectra of the porphyrins and C_{60} indicating complexation.

General Characteristics of Porphyrin-Fullerene Interaction

Reported solid state structures of the co-crystals with C_{60} and C_{70} indicate that fullerenes face the electropositive center of the porphyrin with their electron rich carbons. C_{60} approaches the porphyrin with the 6:6 ring-juncture C-C bond while C_{70} typically approaches the porphyrin with the intersection of the three fused six-member

1. Introduction

rings in the equatorial belt in what is known as the “side-on” manner. This maximizes the interaction between the porphyrin and the fullerene surfaces due to the greater π - π contact area available from the less curved region of the fullerene for interaction. This observation has been confirmed in solution by ^{13}C -NMR spectroscopy, since carbons in the equatorial belt are more influenced by the porphyrin and therefore “suffer” a bigger upfield shift.^{47b, 47e, 48, 53}

The “side-on” orientation is the most common way for C_{70} to interact with the porphyrins and it has been widely documented in the literature. However, some exceptions have been reported where the C_{70} approaches the porphyrin in an “end-on” manner due to steric or electronic reasons.

In *meso*-substituted mono-porphyrins bearing bulky substituents, the steric hindrance does not allow a “side-on” orientation, forcing the “end-on” orientation instead.⁵⁵

In some cases the π - π interactions are not the dominant factor in C_{70} /porphyrin interactions. For example, in the Ni-metallated bis-porphyrins reported by Komatsu *et al.*,⁵⁶ they proposed an electrostatic interaction between the electron-negative 6-6 juncture of the fullerene and the electron-positive center of the porphyrins, as the driving force for the interaction. In the iridium-metallated bis-porphyrin receptor reported by Aida *et al.*,⁵⁷ the Ir-bond interaction is the dominant factor, forcing the fullerene to approach the porphyrin center in an “end-on” manner.

Most porphyrin-based receptors show stronger affinity to C_{70} than to C_{60} . This is related to the fullerene bigger size and its larger π surface available to interact with the

⁵⁵ (a) Jung, S.; Shin, S. K. *Mass Spectrom. Lett.* **2011**, *2*, 49-52. (b) Jung, S.; Seo, J.; Shin, S. K. *J. Phys. Chem. A* **2010**, *114*, 11376-11385.

⁵⁶ Bhattacharya, S.; Hashimoto, M.; Fujimoto, A.; Kimura, T.; Unob, H.; Komatsu, N. *Spectrochim. Acta, Part A* **2008**, *70*, 416.

⁵⁷ Yanagisawa, M.; Tashiro, K.; Yamasaki, M.; Aida, T. *J. Am. Chem. Soc.* **2007**, *129*, 11912.

1. Introduction

porphyrin. The bigger the fullerene is and the higher its available π -surface, the stronger is the interaction.

1.3.2 Porphyrin-Based Fullerene Receptors

Since the supramolecular recognition element between the flat π -surface of porphyrins and the curved π -surface of fullerenes was identified, several porphyrin-based fullerene receptors have been synthesized and reported. Basically, these receptors can be classified in two different groups: acyclic receptors, where the porphyrins are linked from one side via a rigid scaffold, such as porphyrin tweezers, and porphyrin tripods or cyclic-type receptors such as cyclic dimers or trimers.

1.3.2.1 Bis-Porphyrin Receptors

Acyclic Bis-Porphyrin Receptors

When designing an acyclic porphyrin receptor, the choice of the scaffold and spacers that hold the porphyrin units is essential. The aim of those scaffolds and linkers is to pre-organize the porphyrin units around the fullerene, simulating those geometries found in the crystal structure. The nature and geometry of the scaffold and spacers is determinant on the receptor ability for fullerene recognition which can be further modified by changing the substitution pattern on the porphyrin periphery or by the choice of the central metal ion.

Porphyrin tweezers linked through metal coordination, hydrogen bond pre-organized scaffolds or macrocyclic central cores have been reported. Here we have summarized some of the more representative examples.

The first examples of acyclic porphyrin hosts ever reported were the palladium coordination mediated bis-porphyrin jaw receptors **2-3** reported by Boyd *et al.* in 2000 (Figure 1.20).⁴⁸

1. Introduction

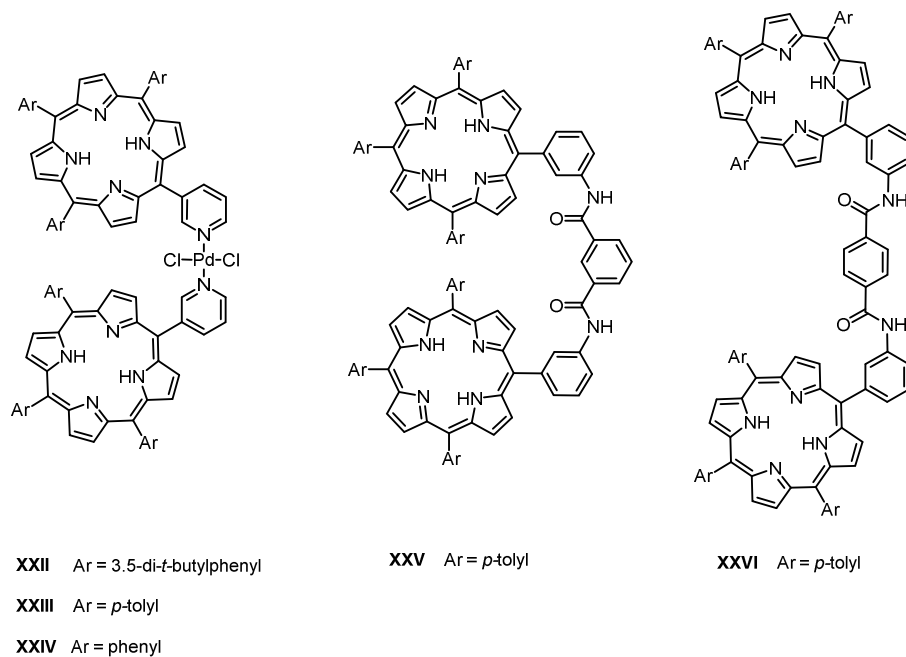


Figure 1.20 Jaws porphyrin hosts **XXII-XXVI**.^{48, 57}

Later in 2002, the same group reported three additional covalently linked analogues (**XXIV-XXVI**) and compared the recognition ability of the whole series (Figure 1.20).⁵⁸ The less strained structure of free base porphyrin Pd-mediated receptor **XXIV** was able to pre-organize the porphyrins in a more suitable manner around the fullerene C₆₀ as seen in the optimized structure (Figure 1.21). Therefore **XXIV** displayed a stronger association with the fullerene than **XXV-XXVI**. MALDI spectrometry experiment of Cu-metallated host **XXIV** showed evidences of strong binding with C₈₄ indicating that such interaction would be favored over C₇₀ and C₆₀.

⁵⁸ Sun, D.; Tham, F. S.; Reed, C. A.; Chaker, L.; Boyd, P. D. W. *J. Am. Chem. Soc.* **2002**, *124*, 6604.

1. Introduction

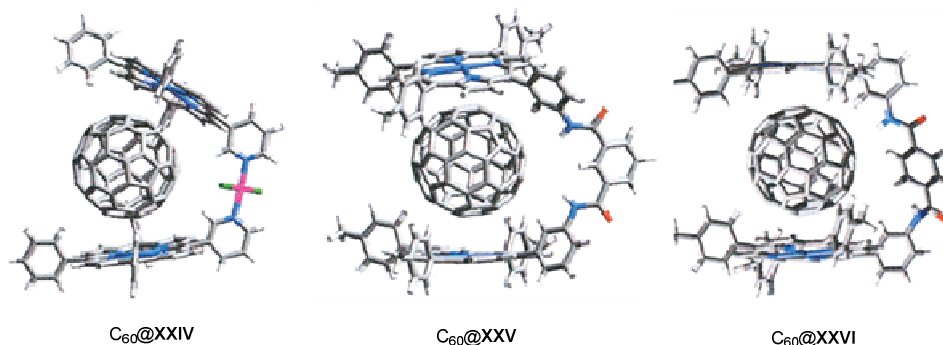


Figure 1.21 Jaws porphyrin- C_{60} inclusion complexes $C_{60}@XXIV$ - $C_{60}@XXVI$ (calculated structures).⁵⁷

The aggregation with C_{60} and C_{70} was characterized by MALDI mass spectrometry, UV-Vis absorption, fluorescence emission, 1H -NMR and ^{13}C -NMR spectroscopy. Receptor **XXII**, bearing *t*-butyl-substituted porphyrins, was found to be a better receptor than *p*-tolyl-substituted **XXIII**. The calculated association constant for receptor **XXII** with C_{60} ($K_{\text{ass}} = 5.2 \times 10^3 \text{ M}^{-1}$) was about two times higher than those reported for mono-porphyrins. The covalently linked receptor **XXV** was able to interact with fullerene but with much weaker association. The structure of receptor **XXVI** was too strained to be able to pre-organize the porphyrins around the C_{60} and failed to interact with the fullerene.

In 2005 Li *et al.* reported two bis-porphyrin molecular tweezers whose cavity was pre-organized and stabilized by intramolecular hydrogen bond interactions, making the receptor suitable for fullerene encapsulation (Figure 1.22).⁵⁹ The encapsulation of both C_{60} and C_{70} was proven by 1H -NMR and ^{13}C -NMR, UV-Vis and fluorescence spectroscopy and the association constants calculated from UV-Vis titrations in toluene ($K_{\text{ass}}(C_{60}@XXVII) = 1.0 \times 10^5 \text{ M}^{-1}$; $K_{\text{ass}}(C_{60}@XXVIII) = 2.7 \times 10^4 \text{ M}^{-1}$). These

⁵⁹ Wu, Z.-Q.; Shao, X.-B.; Li, C.; Hou, J.-L.; Wang, K.; Jiang, X.-K.; Li, Z.-T. *J. Am. Chem. Soc.* **2005**, *127*, 17460.

1. Introduction

association constants are almost ten times higher than those of the Pd coordination mediated receptor previously reported. As expected, C₇₀ yielded higher association constants, with K_{ass} values between 9.8×10^5 and $1.1 \times 10^6 \text{ M}^{-1}$.

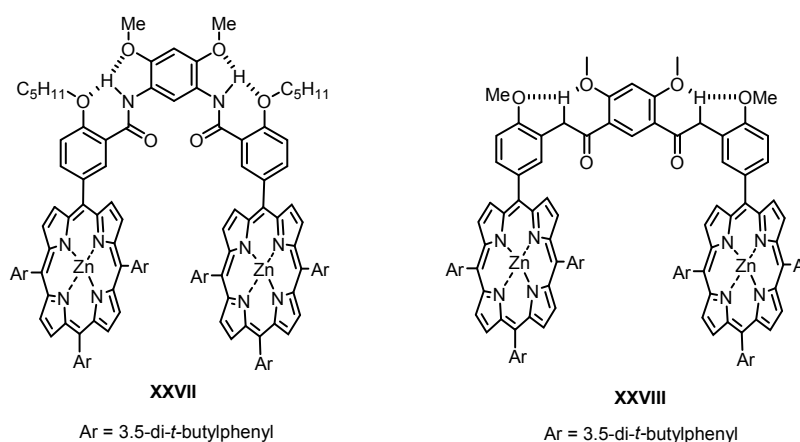


Figure 1.22 Hydrogen bond pre-organized bis-porphyrin molecular tweezers **XXVII-XXVIII**.⁵⁸

The rigidity of the U-shaped receptor and consequently the preorganization of the porphyrins was found to be a key factor for the association. In a control experiment the addition of a small amount of a polar competitive solvent (10% methanol) led to a partial disruption of the hydrogen bonds and a reduction of the receptor preorganization. The association constant K_{ass} consequently dropped to $2.3 \times 10^3 \text{ M}^{-1}$ (in 9:1 chloroform / methanol), that is pronouncedly smaller than that of the complex obtained in chloroform

Calix[4]arenes have also been reported as central scaffolds for bis-porphyrin tweezers because of their ability to appropriately orient the porphyrin units at the required geometry and distances to encapsulate fullerenes. The number of porphyrin sites, the substituents on the upper rim, the nature and size of the linkers as well as the substituents on the porphyrin periphery can strongly affect the fullerene complex formation.

1. Introduction

In 2006, Boyd *et al.* reported a systematic study of the effect of linkers and the peripheral porphyrin substituents on the fullerene complexation ability of calixarene-based bis-porphyrin tweezers.⁶⁰

The association with C₆₀ and C₇₀ was evidenced by MALDI spectrometry, ¹H-NMR, ¹³C-NMR, UV-Vis absorption and fluorescence emission spectroscopies. Stoichiometry was assigned via ¹³C-NMR spectroscopy as well as electrospray ionization mass spectrometry (ESI-MS) and the association constants were calculated by UV-Vis, fluorescence and ¹H-NMR titrations in toluene.

Receptors bearing three different spacers were studied featuring an ester-like linker (**XXIV**), and two different amide-like linkers (**XXX** and **XXXI**) (Figure 1.23). Receptor attached by an amide linker with a single methylene carbon **11** proved to be better suitable for fullerene encapsulation, as the spacer seems to have the appropriate distance to accommodate the porphyrin units around the fullerene without being too flexible ($K_{\text{ass}}(\text{C}_{60}@\text{XXXI}) = 8.7 \times 10^3 \text{ M}^{-1}$, $K_{\text{ass}}(\text{C}_{70}@\text{XXXI}) = 3.9 \times 10^4 \text{ M}^{-1}$ in toluene). These associations were found to be almost three times higher than those for **9** and **XXX**. Receptor **XXXI** bearing *p*-tolyl-substituted porphyrins also leads to a nearly double association constant than its phenyl-substituted analogue **XXXII** ($K_{\text{ass}}(\text{C}_{60}@\text{XXXII}) = 4.9 \times 10^3 \text{ M}^{-1}$) reported previously by Lhoták *et al.* in 2004 (Figure 1.23).⁶¹

To gain more insight into the effect of porphyrin periphery substituents they synthesized another three analogues of **XXXI** bearing different substituents (**XXXIII-XXXV**). As expected from the previous observed trend, the di-*t*-butylphenylporphyrin receptor **XXXIII** showed better association values with both C₆₀

⁶⁰ Hosseini, A.; Taylor, S.; Accorsi, G.; Armaroli, N.; Reed, C. A.; Boyd, P. D. W.; *J. Am. Chem. Soc.* **2006**, *128*, 15903.

⁶¹ Dudič, M.; Lhoták, P.; Stibor, I.; Petříčková, H.; Lang, K. *New J. Chem.* **2004**, *28*, 85.

1. Introduction

and C_{70} ($K_{\text{ass}} = 2.6 \times 10^4$ and $2.3 \times 10^5 \text{ M}^{-1}$ in toluene), up to six times higher than those of *p*-tolyl-substituted receptor **XXXXI**. Moreover they studied the effect of the central metal ion on the association and found that the free base porphyrin tweezer was the best receptor.

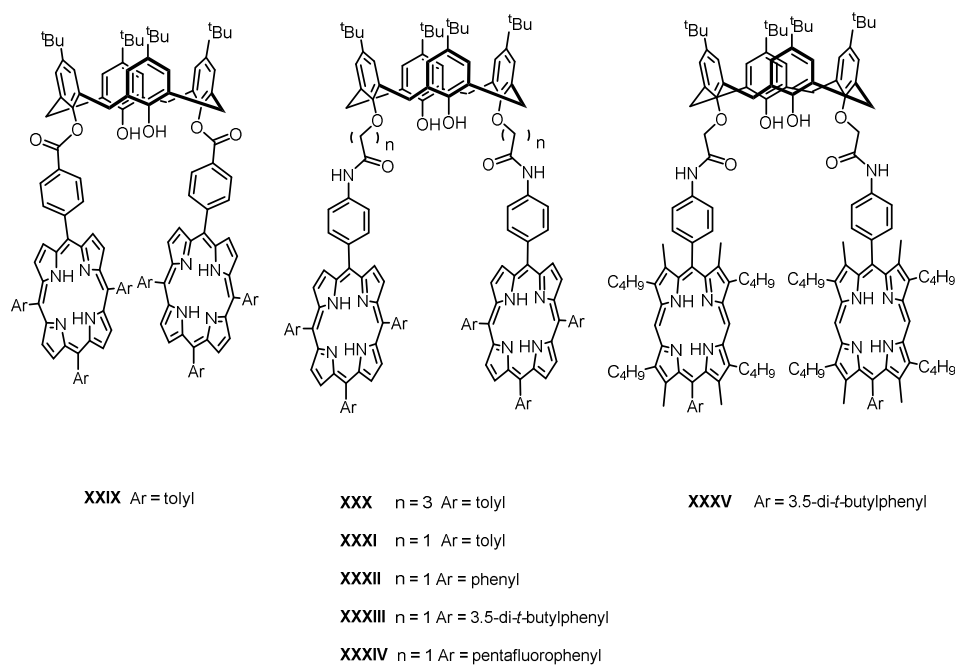


Figure 1.23 Calixarene-linked bis-porphyrin hosts **XXIX-XXXV**.^{59, 60}

The association constant of pentafluorophenyl-substituted host **XXXIV** was slightly lower than that for the *p*-tolyl-substituted receptor **XXXI**. For the octaalkylporphyrin receptor **XXXV**, the association constant was much lower ($K_{\text{ass}} = 2.6 \times 10^3 \text{ M}^{-1}$), which was attributed to the lack of aromatic substituents, thus reducing the interaction with the porphyrin and allowing also face-to-face porphyrin stacking to directly compete with the fullerene encapsulation process.

1. Introduction

Cyclic Bis-Porphyrin Receptors

Among the various receptors for fullerenes, cyclic bis-porphyrin hosts possess one of the highest affinities ever reported. The complexation ability of these porphyrin dimers can be easily tuned by modifying the porphyrin substituents, the length and flexibility of the spacers and the central metal ion.

In 1999, Aida *et al.*⁶² reported face-to-face zinc-porphyrin cyclic dimers **Zn-XXXVI** and **Zn-XXXVII** (Figure 1.24). Host **Zn-XXXVII** is able to form very stable complexes with fullerenes that are isolable by column chromatography. Such strong interaction was also evidenced by ESI-MS, UV-Vis absorption, ¹H-NMR and ¹³C-NMR spectroscopies. The bathochromic shift of the *Soret* band was observed when performing UV-Vis titration of **Zn-XXXVII** with C₆₀ suggesting an electronic interaction between the receptor and the fullerene. The calculated association constant ($K_{\text{ass}} = 6.7 \times 10^5 \text{ M}^{-1}$ in benzene) was the highest association constant ever reported at its publication date.

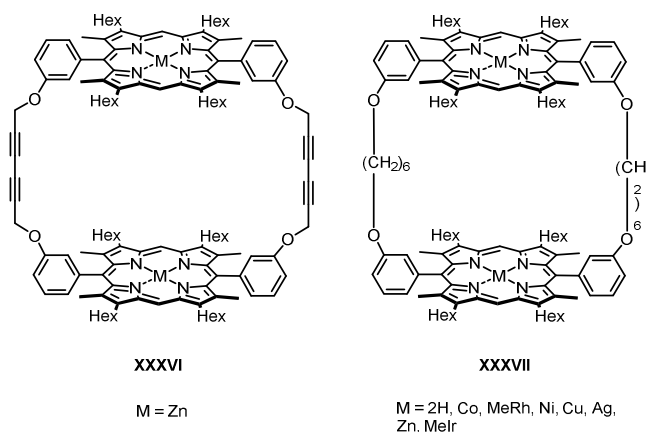


Figure 1.24 Cyclic porphyrin-based hosts **XXXVI-XXXVII**.^{57, 62, 63}

⁶² Tashiro, K.; Aida, T.; Zheng, J.-Y.; Kinbara, K.; Saigo, K.; Sakamoto, S.; Yamaguchi, K. *J. Am. Chem. Soc.* **1999**, *121*, 9477.

1. Introduction

Due to the spacer flexibility, free host **Zn-XXXVII** exists as a mixture of conformational isomers in solution what translates into complex $^1\text{H-NMR}$ and $^{13}\text{C-NMR}$ spectra. Upon addition of C_{60} , spectra are simplified, indicating inclusion complex formation.

Interestingly, the cyclic dimer precursor **XXXVI**, featuring rigid diacetylene linkers between the porphyrins units, did not show any sign of complexation with fullerenes. Conformational flexibility of the linkers seems to be essential for the porphyrin dimer to be able to adapt to the fullerene.

Later in 2001, Aida *et al.*⁶³ reported the crystal structure of the ethylpyrrole-substituted cyclic dimer complex with C_{60} @**XXXVIII** (Figure 1.25).

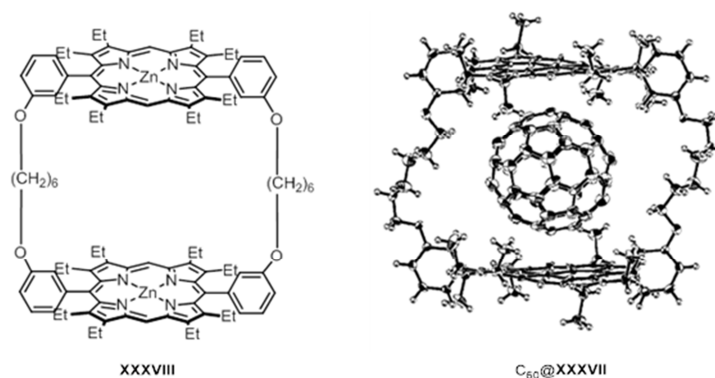


Figure 1.25 Cyclic porphyrin-based hosts **XXXVIII**. Crystal structure of C_{60} @**XXXVIII**.^[Error! Marcador no definido.]

In the X-ray structure, the hexamethylene linkers are folded to adjust the porphyrin-porphyrin distance, thus maximizing the interaction between their π -electronic systems. The porphyrin-fullerene distances ($< 2.765 \text{ \AA}$) confirm the presence of π interactions.

⁶³ Zheng, J.-Y.; Tashiro, K.; Hirabayashi, Y.; Kinbara, K.; Saigo, K.; Aida, T.; Sakamoto, S.; Yamaguchi, K. *Angew. Chem. Int. Ed.* **2001**, *40*, 1857.

1. Introduction

In this same article, Aida *et al.*⁶³ studied the role of the central metal ion on the receptor affinity towards the fullerenes. They performed a UV-Vis titration of differently metallated cyclic receptors **M-XXXVII** (Figure 1. 24) with C₆₀ and C₇₀ and reported that the affinity of free base host for fullerenes was comparable if not stronger than that found for the Zn-metallated analogue. Furthermore, receptor metallated with group 10 and 11 metal ions (M = Ni, Cu, Ag) resulted in lower association constants. On the other hand group 9 (Co and RhMe) metallated host display a much larger affinity toward fullerenes. In particular rhodium metallated host exhibited extremely high affinity towards C₆₀ and C₇₀. The association constant K_{ass} for rhodium metallated host **RhMe-XXXVII** with C₆₀ was $2.5 \times 10^7 \text{ M}^{-1}$ in benzene. Association with C₇₀ was too high to be accurately calculated by UV-Vis spectroscopy and was estimated to be about 10^8 M^{-1} , two orders of magnitude higher than the calculated value for the Zn-metallated analogue.

A variable temperature ¹³C-NMR experiment also evidenced the extremely low dissociation of the RhMe-porphyrin fullerene complex, which was attributed to the strong bond forming interaction between the metal and the carbon material for second row metals.

Later in 2007, Aida *et al.* reported an iridium metallated host **IrMe-XXXVII** (Figure 1.24) that displays even higher association constants with fullerenes,⁵⁸ too large to be calculated in benzene, so they were calculated in 1,2-dichlorobenzene (DCB) instead, where the fullerenes are better solvated. The association constant ($K_{\text{ass}} = 1.3 \times 10^8 \text{ M}^{-1}$ in DCB) is almost three orders of magnitude higher than the calculated for the RhMe metallated receptor in the same solvent ($K_{\text{ass}} = 3.4 \times 10^5 \text{ M}^{-1}$). The affinity to iridium-metallated porphyrins for fullerenes is so strong that even iridium metallated porphyrin monomers can strongly interact with C₆₀ in solution.

This exceptionally high attraction of iridium porphyrins is the consequence of the strong bond-forming interactions between the metal and the carbon nanomaterial. The interaction is so strong that even deformation of C₆₀ takes place. Moreover, in iridium-

1. Introduction

porphyrin complexes with C_{70} , the fullerene does not approach the porphyrin center in the common “side-on” manner, what would maximize the π - π host-guest interactions, but interacts instead in an “end-on” orientation, maximizing the metal-fullerene interactions.

To approach the selective extraction of higher fullerenes ($\geq C_{76}$), Aida *et al.* synthesized three new porphyrin dimers bearing dodecyloxy *beta*-substituted porphyrin and linkers of different sizes (**XXXIXa-XXXIXc**, Figure 1.26), and compared their high fullerene extraction ability and selectivity together with the previously reported host **Zn-XXXVII**.⁶⁴

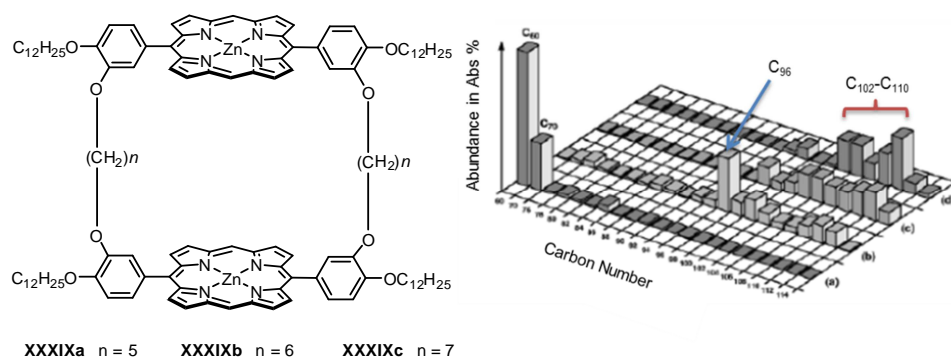


Figure 1.26 Cyclic porphyrin-based hosts **XXXIXa-XXXIXc**. Abundances (Abs %) of C_{60} - C_{114} of fullerene mixtures (a) prior extraction (b) after first- (c) after second- (d) after third-stage extraction. Estimated by HPLC.⁶⁴

Even though dimer **Zn-XXXVII** shows stronger association with C_{96} than the dodecyloxy *beta*-substituted porphyrin dimer **XXXIXb**, its high affinity for C_{60} and C_{70} drops the selectivity for C_{96} . Selectivities for higher fullerenes ($\geq C_{76}$) were enhanced from 10% to 68%, whereas C_{96} was only enriched from 0.4% to 6%. On the other hand, the dodecyloxy *beta*-substituted porphyrin receptor **XXXIXb** was able to increase the total amount of higher fullerenes up to 93%, enhancing the C_{96} ratio from 0.4% to

⁶⁴ Shoji, Y.; Tashiro, K.; Aida, T. *J. Am. Chem. Soc.* **2004**, *126*, 6570.

1. Introduction

36% after one extraction cycle. Two more extractions afforded very rare higher fullerenes (C_{102} - C_{110}), with an enrichment from <0.1 % to 82 % (abundances of fullerene mixtures, prior and after different extraction cycles, are shown in Figure 1.26).

Dodecyloxy *beta*-substituted porphyrin dimers bearing C_5 and C_7 alkyldene linkers, which are connecting the porphyrin units **XXXIXa** and **XXXIXc**, also extract negligible amounts of C_{60} and C_{70} . Unfortunately when extracting with receptor **XXXIXa**, endowed with shorter linkers the total content of higher fullerenes ($\geq C_{76}$) increases only to 74% and C_{96} is only enriched up to 10%. A receptor bearing longer spacers, such as **XXXIXc**, enhances the total amount of higher fullerenes up to 97% but unfortunately, due to their large sizes, higher fullerenes are already encapsulated within the cavity on the first extraction cycle, which reduces the C_{96} selectivity within the first cycle to an enrichment of only 25%.

In 2006 and 2007, Aida *et al.* reported an asymmetric porphyrin dimer bearing a rhodium-metallated porphyrin and a C_1 -symmetric *N*-methylporphyrin **XL** (Figure 1.27).

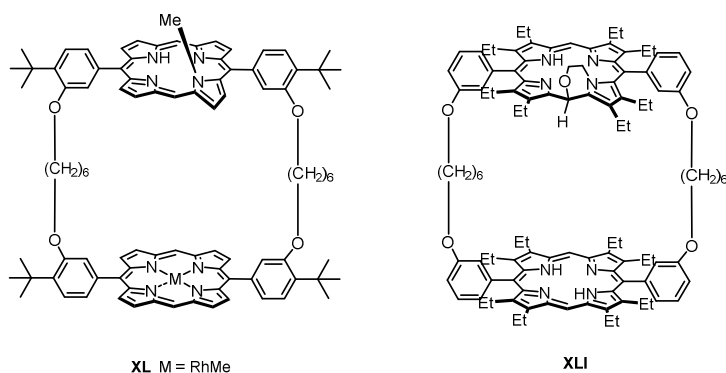


Figure 1.27 Asymmetric cyclic porphyrin-based dimers **XL** and **XLI**.⁶⁶

1. Introduction

Porphyrin dimer **XL** was able to discriminate C_{76} enantiomers and to assign its enantiomeric purity by $^1\text{H-NMR}$.⁶⁵ Unfortunately, the dimer was not enantioselective in the guest binding.

Later in 2010, Aida *et al.* reported a π -electronic cyclic host bearing a highly π -basic and asymmetrically distorted N -substituted porphyrin subunit **XLI** (Figure 1.27), that was able to enantioselectively incorporate C_{76} in its cavity.⁶⁶ After enantioselective extraction of the chiral C_{76} from racemic mixture, the isolated complex was found to be CD-active and the ee was enriched up to 7% in one single extraction.

In 2011, Ballester *et al.* reported a Zn-porphyrin cyclic dimer **XLII** bearing flexible linkers and its unsaturated precursor **XLIII** (Figure 1.28).⁶⁷ They studied the complexation behavior with C_{60} and C_{70} , both in the solid state and in, by means of X-ray crystallography, $^1\text{H-NMR}$, UV-Vis and fluorescence spectroscopies.

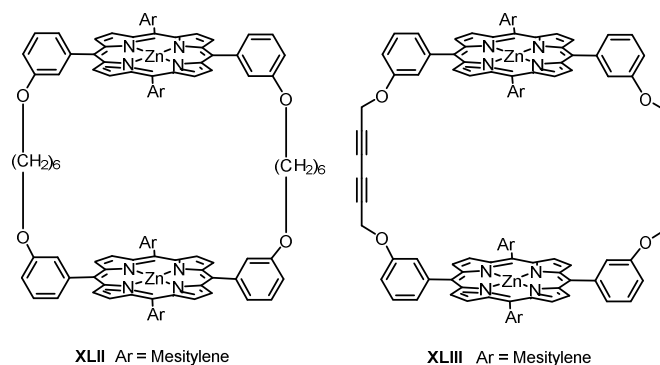


Figure 1.28 Porphyrin-based cyclic dimer **XLII** and its unsaturated precursor **XLIII**.⁶⁷

⁶⁵ (a) Shoji, Y.; Tashiro, K.; Aida, T.; *J. Am. Chem. Soc.* **2006**, *128*, 10690. (b) Shoji, Y.; Tashiro, K.; Aida, T. *Chirality* **2008**, *20*, 420.

⁶⁶ Shoji, Y.; Tashiro, K.; Aida, T. *J. Am. Chem. Soc.* **2010**, *132*, 5928.

⁶⁷ Hernández-Eguía, L. P.; Escudero-Adán, E. C.; Pintre, I. C.; Ventura, B.; Flamigni, L.; Ballester, P. *Chem. Eur. J.* **2011**, *17*, 14564.

1. Introduction

The porphyrin dimer **XLIII** bearing unsaturated six-carbon linkers is not able to encapsulate C_{60} but forms 1:1 inclusion complexes with C_{70} , adopting a scoop-like conformation (Figure 1.29). On the contrary, receptor **XLII**, bearing flexible saturated linkers, forms clamshell-like solid state inclusion complexes with both C_{60} and C_{70} ($C_{70}@XLII$ solid state structure is shown in Figure 1.29).

As expected, the receptors bearing flexible linkers are able to adapt and interact better with the fullerenes in the solid state. This is also observed in solution, and flexible receptor **XLII** was able to encapsulate both fullerenes, as evidenced by a modest bathochromic shift and a decrease in intensity of the *Soret* band. UV-Vis and fluorescence titration experiments evidenced the existence of strong π - π interactions between the cyclic bis-porphyrin receptor and the fullerenes.

UV-Vis titration of the unsaturated receptor **XLIII** with C_{70} showed only a negligible decrease of the *Soret* band, whereas addition of C_{60} to **XLIII** resulted in no change to either the absorption or the emission spectrum, neither in toluene nor in dichloromethane.

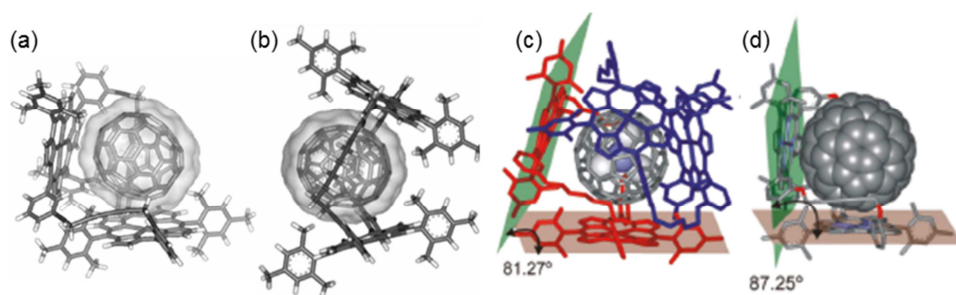


Figure 1.29 Solid State structures of $C_{70}@XLII$, $C_{70}@XLIII$, $Sc_3N@C_{80}@XLII$, $Sc_3N@C_{80}@XLIII$.^{67, 68}

Association constants were calculated by means of absorption and fluorescence emission techniques, and were found to be on the range of $10^4 \times M^{-1}$ in toluene except

1. Introduction

for C_{60} @**23**, whose K_{ass} was estimated to be lower than 10^3 M^{-1} . $^1\text{H-NMR}$ titration experiments are in agreement with these results.

Again in 2011, they reported complexation of $\text{Sc}_3\text{N}@C_{80}$ endohedral fullerene by **XLII** and **XLIII**.⁶⁸ The rigid receptor **XLIII** adopts a scoop-like conformation when forming a 1:1 inclusion complex in the solid state with $\text{Sc}_3\text{N}@C_{80}$ with a short separation of 2.961 Å (Figure 1.29). This suggests the existence of strong π - π interactions between the porphyrins and the endohedral fullerene. The flexible receptor **XLII** also adopts a scoop-like conformation forms 2:1 capsule-type complex with $\text{Sc}_3\text{N}@C_{80}$ in the solid state (Figure 1.29).

Solution studies indicate the exclusive formation of 1:1 inclusion complexes between the cyclic receptors and the endohedral fullerene. UV-Vis and fluorescence titration experiments confirmed the existence of strong π - π interactions between $\text{Sc}_3\text{N}@C_{80}$ and the flexible bis-porphyrin dimer **XLII**. Association constants were calculated for the flexible receptor **XLII** ($K_{\text{ass}} = 2.3\text{-}2.9 \times 10^5 \text{ M}^{-1}$ in toluene). This association is one order of magnitude larger than that found for the C_{70} complex. The larger available π surface of the endohedral fullerene and electronic polarization seem to be the the main reasons for such increase in association.

1.3.2.2 Trimeric Porphyrin Receptors

3:1 Coordination geometries in the solid state were reported for the first time by Boyd *et al.* and Olmstead *et al.* in 2006.⁶⁹ Both described the complexation of C_{60} by three tetrapentafluorophenyl porphyrin (TPFPP **XLIV**) units with distances close to the range found on monoporphyrin-fullerene crystal structures (Figure 1.30).

⁶⁸ Hernández-Eguía, L. P.; Escudero-Adán, E. C.; Pinzón, J. R.; Echegoyen, L.; Ballester, P.; *J. Org. Chem.* **2011**, *76*, 3258.

⁶⁹ (a) Hosseini, A.; Hodgson, M. C.; Tham, F. S.; Reed, C. A.; Boyd, P. D. W. *Cryst. Growth. Des.* **2006**, *6*, 397. (b) Olmstead, M. M.; Nurco, D. J. *Cryst. Growth. Des.* **2006**, *6*, 109.

1. Introduction

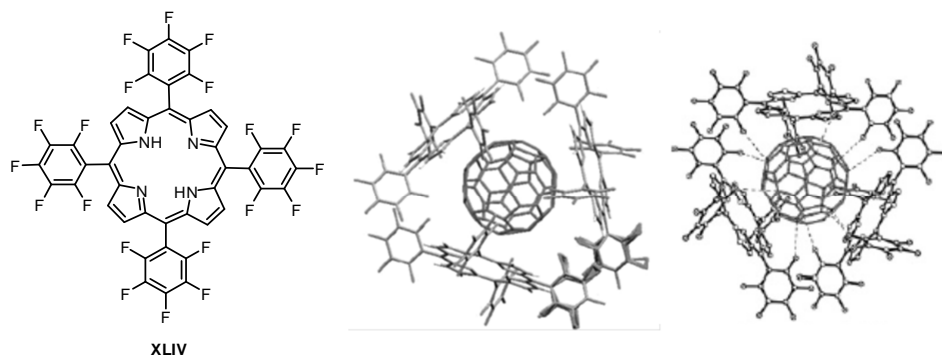


Figure 1.30 Tetrapentafluorophenyl porphyrin **XLIV**. Solid state prismatic arrangements of the H₂TPFPP **XLIV** molecules around C₆₀.⁶⁹

These suggested that trimeric porphyrin receptors should be able to accommodate the three porphyrin subunits around the fullerenes as observed in the solid state. This third porphyrin subunit, moreover, could have an extra positive influence on binding to the fullerenes.

Two different types of trimeric porphyrin hosts have been reported to date, namely acyclic porphyrin tripods and cyclic porphyrin trimers.

Acyclic Porphyrin Trimers

In 2008, Sanders *et al.* reported two tripodal porphyrin hosts (**XLVa** and **XLVb**, Figure 1.31) bearing rigid linkers. They studied their complexation behavior with C₆₀ both in the solid state and in solution by means of X-ray crystallography and ¹H-NMR and fluorescence spectroscopies.⁷⁰

⁷⁰ Tong, L. H.; Wietor, J.-L.; Clegg, W.; Raithby, P. R.; Pascu, S. I.; Sanders, J. K. M. *Chem. Eur J.* **2008**, *14*, 3035.

1. Introduction

The solid state structures reveal close fullerene-porphyrin contacts in both cases. In the crystal structure of $C_{60}@XLVb$ two of the porphyrin arms act as a tweezer with one C_{60} while the third arm interacts with a second guest molecule (Figure 1.31). In the crystal structure $C_{60}@XLVa$, the arms of the tripod are too short for the receptor to be able to accommodate a fullerene between two porphyrins and instead each C_{60} is surrounded by porphyrins from different hosts. These complexation behaviors result in formation of supramolecular networks. In solution, the entropic penalty to form these supramolecular structures is too large and only weak complexes are formed ($K_{ass} \approx 10^3 M^{-1}$ and $10^2 M^{-1}$ at 300K in toluene).

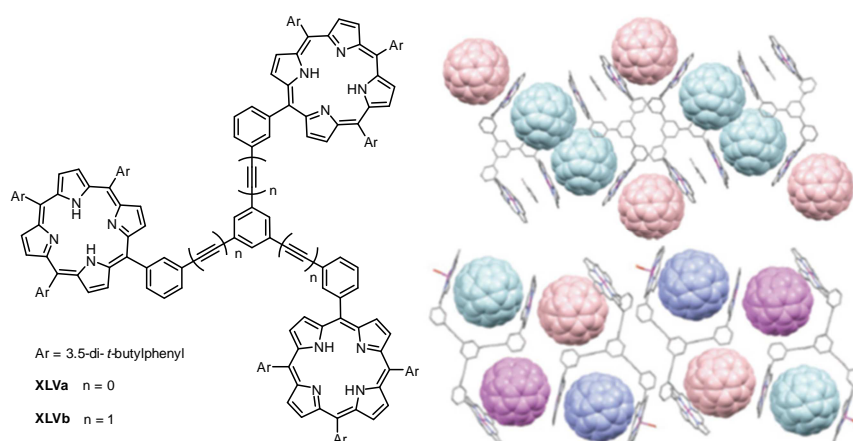


Figure 1.31 Tripodal porphyrin hosts **XLVa** and **XLVb**. Crystal packing diagram of **XLVa**. Crystal packing diagram of **XLVb**.⁷⁰

In 2010, Fukuzumi *et al.* reported another porphyrin-based tripod **XLVI** bearing flexible linkers able to encapsulate pyridine-functionalized fullerene (PyC_{60}) (Figure 1.32).⁷¹ The 1:1 complex is stabilized by π - π interactions as well as coordination between the zinc and the pyridine moiety. The association was evidenced by UV-Vis and 1H -NMR

⁷¹ Takai, A.; Chkounda, M.; Eggenspieler, A.; Gros, C. P.; Lachkar, M.; Barbe, J.-M.; Fukuzumi, S. *J. Am. Chem. Soc.* **2010**, *132*, 4477.

1. Introduction

spectroscopies and quantified by UV-Vis ($K_{\text{ass}} = 9.4 \times 10^4 \text{ M}^{-1}$ in DCB at 298K), as well as fluorescence titration ($K_{\text{ass}} = 5.5 \times 10^4 \text{ M}^{-1}$ in DCB at 298K).

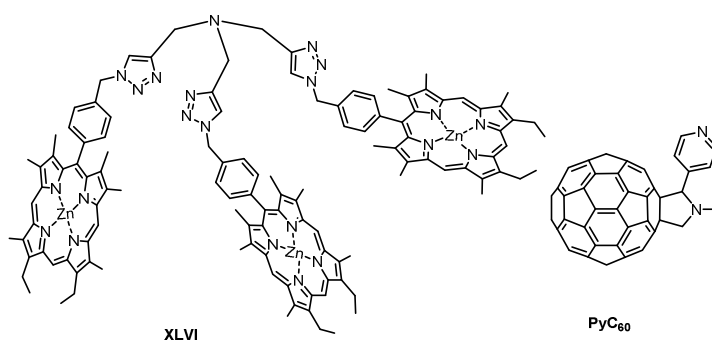


Figure 1.32 Porphyrin-based tripod **XLVI**.⁷¹ Pyridine-functionalized fullerene (PyC₆₀).

Recently in 2014, Zheng *et al.* reported a tweezer-like porphyrin tripod **XLVII** bearing three urea moieties (Figure 1.33).⁷² These ureas are able to pre-organize through directional intramolecular hydrogen bonds promoting the formation of a rigid cone-shape cavity and stabilize the fullerene complex.

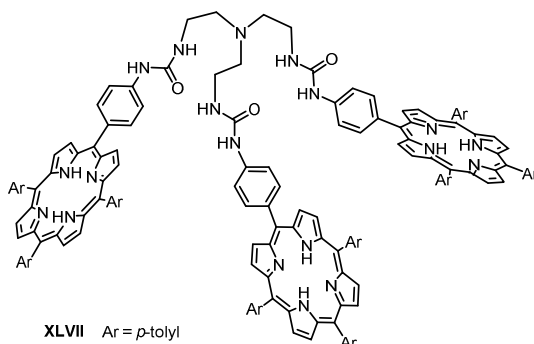


Figure 1.33 Tweezer-like porphyrin tripod **XLVII**.⁷³

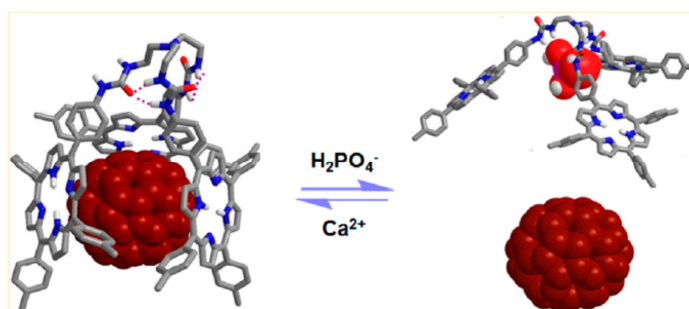
⁷² Fang, X.; Zhu, Y.-Z.; Zheng, J.-Y. *J. Org. Chem.* **2014**, *79*, 1184.

1. Introduction

Encapsulations of C_{60} and C_{70} were evidenced by a red shift in the electronic absorption band and the association constants were quantified from UV-Vis titration experiments in toluene [$K_{\text{ass}}(C_{60}) = 1.5 \times 10^5 \text{ M}^{-1}$; $K_{\text{ass}}(C_{70}) = 1.8 \times 10^7 \text{ M}^{-1}$].

Control experiments with mono- and bis-porphyrin host analogues certify that preorganization of the host by intramolecular hydrogen bonding was essential to successfully encapsulate fullerenes, showing no interaction with either C_{60} or C_{70} . A thiourea analogue tripod was also unable to interact with the fullerenes. Thiourea moieties, unlike their urea version, are not able to form such strong hydrogen bonds with each other and consequently the cavity was not pre-organized.

The strong urea affinity for oxoanions was exploited to modify the cavity size by ion-controlled reversible association-dissociation of the complex using a H_2PO_4^- - Ca^{2+} system as shown in Scheme 1.3.



Scheme 1.3 Model representation of the ion-controlled on-off switch of the C_{60} @**XLVII** complex using a H_2PO_4^- - Ca^{2+} feeding system. ⁷²

When H_2PO_4^- , as the tetrabutylammonium salt, was introduced to the host-guest complex solution, the oxoanion strongly interacted with the urea moieties making the complex lose its preorganization and release the fullerene. Later Ca^{2+} , as calcium perchlorate, was introduced which caused CaH_2PO_4 precipitation and rebuilding of the complex. These ion-controlled inclusion experiments were monitored by fluorescence

1. Introduction

emission. The reversible association-dissociation process can be repeated several times by alternately feeding H_2PO_4^- and Ca^{2+} .

Finally Zheng and Zhu *et al.* reported the use of host **XLVII** on the selective extraction of C_{70} from fullerite mixtures. Starting from 2:1 mixtures of $\text{C}_{60}/\text{C}_{70}$, the C_{70} ratio was enriched up to 87% after one cycle and simultaneously C_{60} abundance was increased up to 96%. Only one extra cycle gave a C_{70} enrichment of 95%. Starting from a commercially available fullerene extract, a 94% purity of C_{70} was obtained after only two cycles.

Cyclic Porphyrin Trimers

In 2010, Anderson *et al.* reported macrocycle **XLVIII**, the first cyclic porphyrin trimer, which forms 1:1 complexes with a wide range of fullerenes displaying extremely high associations which were quantified by means of UV-Vis spectroscopy and fluorescence emission (Figure 1.34).⁷³

The zinc cyclic trimer binds C_{60} slightly better than the zinc cyclic dimers such as **Zn-XLVII** reported by Aida *et al.*, evidencing a small cooperative effect on C_{60} binding ($K_{\text{ass}} = 2 \times 10^6 \text{ M}^{-1}$ in toluene; $K_{\text{ass}} = 2.1 \times 10^7 \text{ M}^{-1}$ in cyclohexane). However this effect becomes much more important the bigger the fullerene is. The association constant with C_{70} was found to be $1 \times 10^8 \text{ M}^{-1}$ in toluene, which is much higher than the values reported previously.

The association with larger fullerenes such as C_{86} and $\text{La}@\text{C}_{82}$ endohedral fullerene is so strong that the constants could not be measured by fluorescence titrations (which means that $K_{\text{ass}} > 10^9 \text{ M}^{-1}$ in toluene). These extremely high associations are the consequence of the high pre-organization of the receptor together with the close

⁷³ Gil-Ramírez, G.; Karlen, S. D.; Shundo, A.; Porfyrakis, K.; Ito, Y.; Briggs, G. A. D.; Morton, J. J. L.; Anderson, H. L. *Org. Lett.* **2010**, *12*, 3544.

1. Introduction

distances between the porphyrin units and the fullerene. Unlike other highly pre-organized receptors such as **XXXVI** and **XLIII** the short linkers of this trimer allow strong interaction with the fullerenes despite their low flexibility.

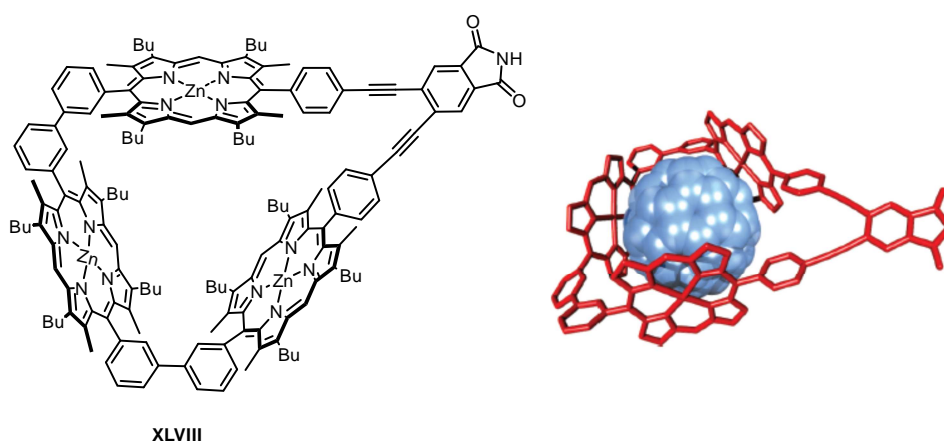


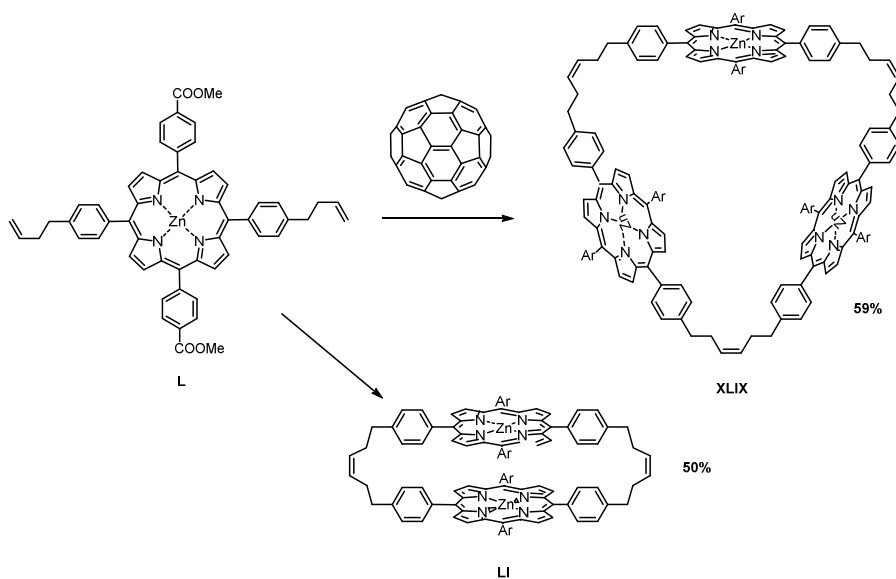
Figure 1.34 Cyclic porphyrin trimer **XLVIII**. Calculated structure of the C_{60} @**XLVIII** inclusion complex.⁷³

In 2011, Langford *et al.* reported the first fullerene-templated porphyrin receptor **XLIX**.⁷⁴ They used C_{60} and C_{70} as templates to pre-organize the mono-porphyrin **L** subunits around the fullerenes and later covalently linked to the porphyrins through olefin metathesis.

In absence of C_{60} , porphyrin dimer **LI** was obtained as major product in a 50% yield whereas the trimer was only isolated as a by-product in a 9% yield. In the presence of the template, the trimer was obtained as the major product in a 59% yield, as shown in Scheme 1.4.

⁷⁴ Mulholland, A. R.; Woodward, C. P.; Langford, S. J. *Chem. Commun.* **2011**, 47, 1494.

1. Introduction



Scheme 1.4 Template-directed synthesis of cyclic porphyrin trimer **29**. Synthesis of cyclic porphyrin dimer **31**.⁷⁴

However, the low preorganization and the big cavity size of the resulting porphyrin trimer **XLIX** lead to a very low association with the fullerenes. In toluene the interaction was too weak to be detected either by UV-Vis or fluorescence spectroscopy. UV-Vis titration in chloroform showed slight bathochromic shift and intensity quenching of the *Soret* band. The calculated association constant ($K_{\text{ass}} = 2.7 \times 10^3 \text{ M}^{-1}$) is much lower than those reported previously for other porphyrin-based cyclic receptors.

1.4 Template-Directed Chemistry

Template chemistry is a synthetic strategy based on the molecular recognition of the reactive species by an external molecule, known as template. The template recognizes and self-assembles the molecular components around its binding sites pre-organizing them into a particular geometry. In this way, they can be covalently linked into complex molecules that are not readily accessible by classical synthetic methods or that have the potential to assemble in a variety of ways.⁷⁵

The template induces the reaction to proceed toward an otherwise thermodynamically or kinetically non-preferred product minimizing the formation of side products.

1.4.1 Template Directed Synthesis of Porphyrin Cycles

Template directed synthesis has shown to be an efficient strategy for the preparation of porphyrin cycles as widely reported in the literature. Typically, templates bearing pyridine moieties are used for such matter. The porphyrin ligands are functionalized with terminal alkynes that can be covalently linked through cross coupling reactions.^{76, 77}

The coupling of functionalized mono-porphyrins or porphyrin arrays in the absence of a template typically leads to the formation of linear porphyrin oligomers. Template directed synthesis reduces the formation of the linear arrays and promotes the formation of the porphyrin cycle that fits the number of binding sites of the template (Scheme 1.5).

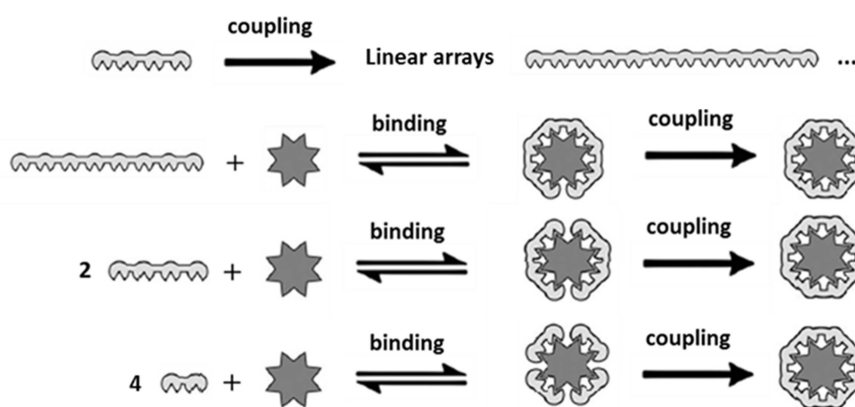
⁷⁵ Anderson, S.; Anderson, H. L.; Sanders, J. K. M. *Acc. Chem. Res.* **1993**, 26, 469.

⁷⁶ Yu; L. Lindsey, J. S. *J. Org. Chem.* **2001**, 66, 7402.

⁷⁷ Hoffmann, M. ; Wilson, C. J.; Odell, B.; Anderson, H. L. *Angew. Chem. Int. Ed.*, **2007**, 46, 3122

1. Introduction

For instance, the coupling of porphyrin dimers, tetramers or octamers in the absence of a template would lead to the formation of porphyrin linear oligomers, whereas the addition of a template bearing eight pyridine moieties would promote the formation of the eight membered cycle in all three cases (Scheme 1.5).

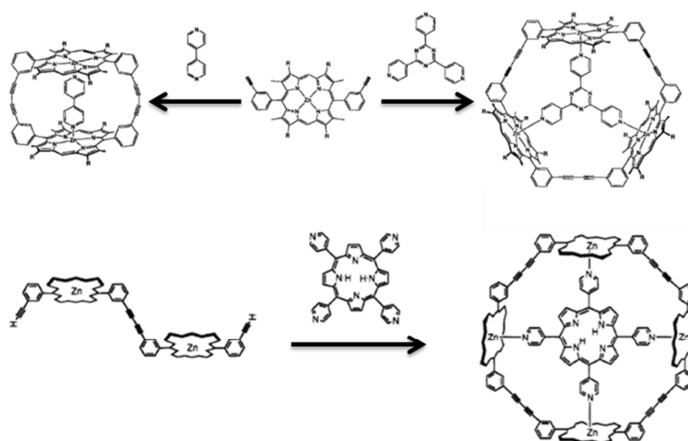


Scheme 1.5 Template directed synthesis.⁷⁷

The first examples of porphyrin cycles synthesis using template directed strategies were described in the early 1990s. Sanders *et al.* reported the template directed synthesis of small porphyrin rings. The number of porphyrin units of the final porphyrin ring was controlled by selection of the adequate template (Scheme 1.6).⁷⁸

⁷⁸ (a) Anderson, H. L.; Sanders, J. K. M. *J. Chem. Soc. Chem. Commun.* **1989**, 1714.
(b) Anderson, H. L.; Sanders, J. K. M. *Angew. Chem Int. Ed. Engl.*, **1990**, 29, 1400.

1. Introduction



Scheme 1.6 Template directed synthesis of dimeric, trimeric and tetrameric porphyrin rings.^{78, 75}

Recently, Anderson *et al.* reported the template directed synthesis of big porphyrin macrocycles, such as an eight membered ring and a twelve membered ring (Figure 1.35).^{77, 79}

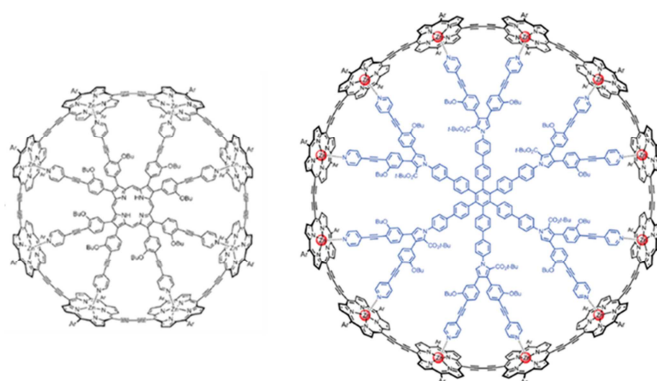


Figure 1.35 Eight and twelve membered porphyrin rings.^{77, 79}

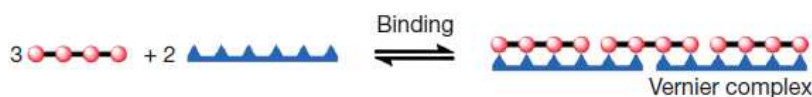
⁷⁹ O'Sullivan, M. C.; Sprafke, J. K.; Kondratuk, D. V.; Rinfray, C.; Claridge, T. D. W.; Saywell, A.; Blunt, M. O.; O'Shea, J. N.; Beton, P. H.; Malfois M.; Anderson, H. L. *Nature*, **2011**, 469, 72.

1. Introduction

The preparation of such large porphyrin macrocycles required the synthesis of large templates which implies a huge synthetic effort. The synthesis of those templates is often more challenging than the porphyrin ring synthesis itself. To overcome this defiance, Anderson *et al.* reported the application of the *Vernier* template strategy to the synthesis of large macrocycles.

Vernier Template Directed Synthesis

In the *Vernier* strategy, the molecular components containing a different number (n and m) of complementary binding sites, separated by the same distance, interact with each other forming an assembly of length = $n \times m$. Within this strategy, small templates can be used to direct the assembly of small ligands into relatively large complexes. Vernier templating allows simple templates to be used to direct the formation of complex targets (Scheme 1.7).^{79, 80, 81}



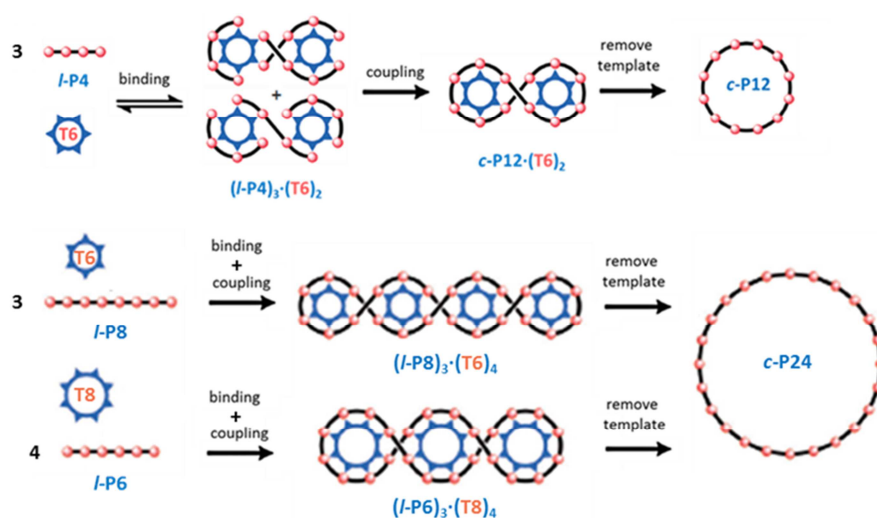
Scheme 1.7 Vernier template directed synthesis.⁷⁹

⁸⁰ Hunter, C. A.; Tomas, S. *J. Am. Chem. Soc.*, **2006**, *128*, 8975.

⁸¹ Lindsey, J. S. *New J. Chem.*, **1991**, *15*, 153.

1. Introduction

Anderson *et al.* reported the synthesis of large twelve and twenty-four membered porphyrin rings by combination of relatively short linear porphyrin arrays and considerably small templates (Scheme 1.8).^{79, 82}



Scheme 1.8 Vernier template directed synthesis of a twelve and twenty-four membered porphyrin macrocycles.^{79, 82}

⁸² Kondratuk, D. V.; Perdigao, L. M. A.; O'Sullivan, M. C.; Svatek, S.; Smith, G.; O'Shea, J. N.; Beton, P. H.; Anderson, H. L. *Angew. Chem. Int. Ed.*, **2012**, *51*, 6696.

1. Introduction

General Objectives: Part I

The aim of this first part of the thesis deals with the preparation of porphyrin-based trimeric (acyclic and cyclic) receptors able to form host-guest inclusion complexes with a wide range of fullerenes. Such receptors have been specially designed to promote the encapsulation of big fullerenes such as C_{84} , $Sc_3N@C_{80}$ and other carbon materials such as SWCNT or giant carbon *nano onions* (CNOs). The host-guest interactions have been studied by means of by 1H -NMR, UV-Vis absorption and fluorescence emission spectroscopic techniques as well as mass spectrometry.

In chapter 2, the synthesis, characterization and complex behavior of porphyrin-based tweezer-like receptor **1** will be described. Since CTV-porphyrin **1** is a flexible host whose cavity size can vary adapting to the size requirements of the guest, CTV-porphyrin **1** is expected to form host-guest inclusion complexes with a wide range of fullerenes showing the greater affinity the bigger the fullerene is.

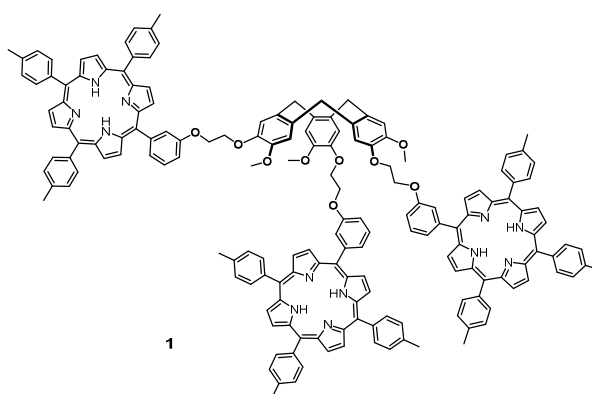


Figure 1.37 CTV-Porphyrin receptor **1**.

In chapter 3, the synthesis, characterization and complexation behavior of the rigid cyclic porphyrin trimer **2** is described. Cyclic porphyrin receptors have shown to be successful approaches towards the formation of fullerene inclusion complexes and the

General Objectives: Part I

flexibility of the spacers that connect the porphyrin subunits is a key aspect of the encapsulation process. Porphyrin trimer **2** is expected to encapsulate preferably big fullerenes while avoiding inclusion of the major components of the carbon soot (C_{60} and C_{70}). The synthesis, characterization and complex behavior of the flexible cyclic porphyrin trimer **3** will be described in chapter 4 in order to evaluate the effect of the spacer's flexibility on the receptor performance. Receptor **3** is a flexible version of trimer **2**. Receptor flexibility is expected to allow the porphyrin units to adapt to the fullerenes leading to a more successful encapsulation.

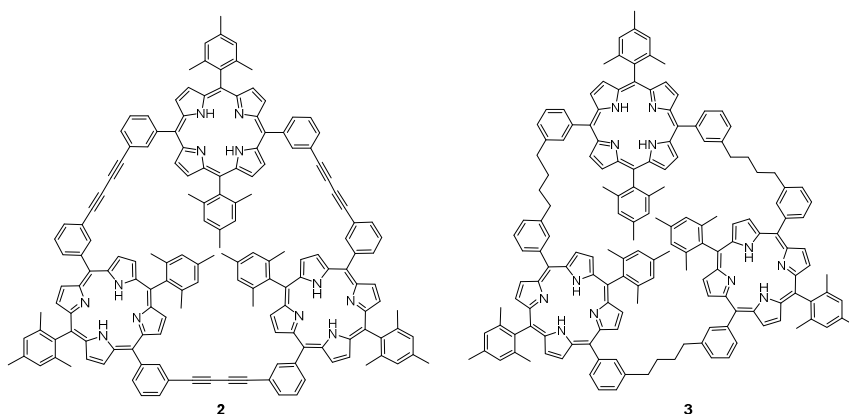


Figure 1.38 Cyclic porphyrin trimer **2** and flexible cyclic porphyrin trimer analogue **3**.

As well as the spacer's flexibility, the effect of bulky *meso*-substituents on the porphyrin units will be discussed in chapter 5. Two different cyclic porphyrin-based receptors **4** and **5** bearing sterically unhindered *meso*-substituents were designed to facilitate the encapsulation of big fullerenes. The synthetic attempts, characterization and complexation behavior of the unhindered cyclic porphyrin trimers **4** and **5** will be described in this chapter.

The aim of chapter 6 is the preparation of giant porphyrin cyclic receptor that could potentially encapsulate $C_{60}@C_{240}$ and eventually achieve separation of $C_{60}@C_{240}$ from a *bucky onion* mixture.

General Objectives: Part I

**Chapter 2: Flexible Receptor: A CTV-Based
Acyclic Porphyrin Tripod**

2. Flexible Receptor: A CTV-Based Acyclic Porphyrin Tripod

2.1 Design and Aim of the Project

The aim of this project is the preparation of a porphyrin-based tweezer-like receptor able to form host-guest inclusion complexes with a wide range of fullerenes. In an attempt to prepare such receptor a porphyrin tripod bearing a cyclotrimeratrylene (CTV) scaffold as central core and three pendant porphyrin units was designed.

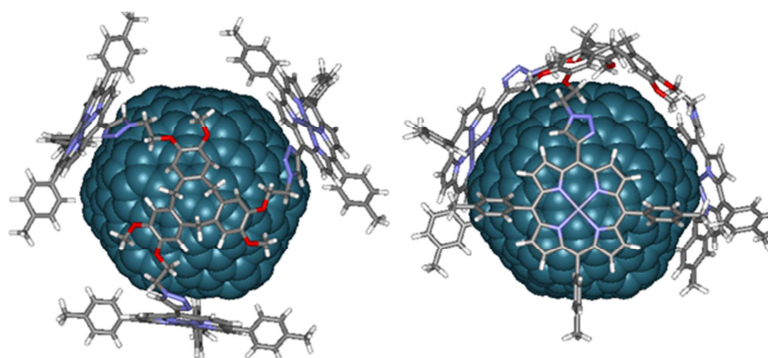


Figure 2.1 Top and side view images of an optimized structure of a CTV-Porphyrin target type receptor complex with $C_{60}@C_{240}$ bucky onion.

This molecular host is expected to preferably form inclusion complexes with giant fullerenes, such as the so-far never isolated $C_{60}@C_{240}$ double fullerene (a fullerene inside a fullerene, called a *bucky onion*) (Figure 2.1).⁸³ The encapsulation,

⁸³ (a) Sano, N.; Wang, H.; Chhowalla, H.; Alexandrou, I.; Amaratunga, G. A. J. *Nature*, **2001**, 414, 506. (b) Rettenbacher, A. S.; Elliott, B.; Hudson, J. S.; Amirkhanian, A.; Echegoyen L. *Chem. Eur. J.* **2006**, 12, 376. (c) Palkar, A.; Melin, F.; Cardona, C. M.; Elliott, B.; Naskar, A. K.; Edie, D. D.; Kumbhar, A.; Echegoyen, L. *Chem. Asian J.* **2007**, 2, 625. (d) López-Urías, F.; Terrones, M.; Terrones, H. *Chem. Phys. Lett.* **2003**, 381, 683. (e) Palkar, A.; Kumbhar, A.; Athans, A. J.; Echegoyen, L. *Chem. Mater.* **2008**, 20, 1685.

2. Flexible Receptor: A CTV-Based Acyclic Porphyrin Tripod

solubilization and isolation of non-functionalized *bucky onions* have never been reported in the literature so far. Only the encapsulation of pyridyl-functionalized carbon nano onions by zinc tetra-phenyl porphyrins (ZnTPP) was reported in 2008 by Echegoyen *et al.*^{83e}

In the designed molecular receptor two fullerene recognition motifs, the CTV and the porphyrins, are combined and connected through short alkyl-spacers (Figure 2.2). The interaction between a flexible CTV-based porphyrin tripod and the fullerenes would be both electronically and geometrically stabilized. The CTV scaffold is known to show good curvature and symmetry match with fullerenes, favoring complex stabilization. Moreover, both the CTV and the porphyrins are good electron donors that complement the electron-deficient nature of fullerenes and other electron-poor carbon materials.

Receptor **1** is a flexible host whose cavity size can vary adapting to the size requirements of the guest, making it a suitable receptor for a wide range of fullerene sizes and expected to display enhanced affinity for the larger fullerene targets.

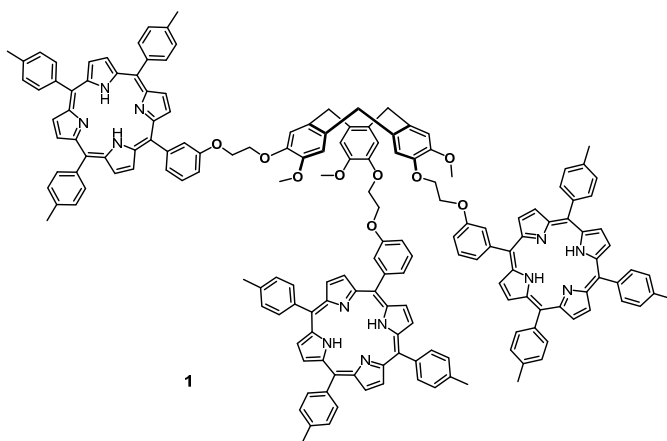


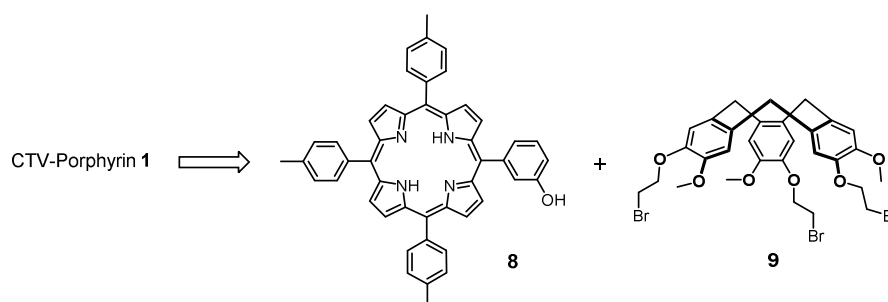
Figure 2.2 CTV-Porphyrin receptor 1

2. Flexible Receptor: A CTV-Based Acyclic Porphyrin Tripod

2.2 Synthesis and Characterization

2.2.1 Synthesis of CTV-Porphyrin Host 1

The CTV-porphyrin host **1** can be prepared through alkylation of the phenol porphyrin **8** and a CTV-bromide building block **9** (Scheme 2.1).



Scheme 2.1 Retrosynthesis of receptor **1**. Final step.

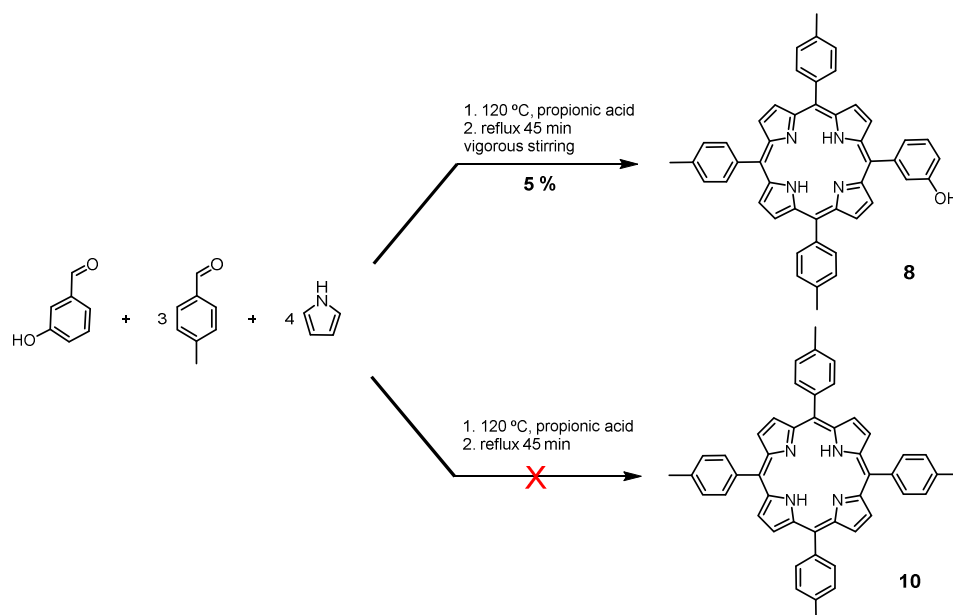
Synthesis of the Porphyrin Building Block

The synthesis of tripod **1** started with the preparation of its building blocks **8** and **9**. An initial attempt to prepare the porphyrin component **8** following a synthetic procedure reported by Johnstone, Yamaguchi and Gunter⁸⁴ did not succeed, since the direct acid-catalyzed condensation of four pyrrole equivalents with one equivalent of 3-hydroxybenzaldehyde and three equivalents of 4-tolualdehyde resulted in the exclusive isolation of the symmetric porphyrin **10**. No traces of **8** were detected (Scheme 2.2).

⁸⁴ Johnstone, K. D.; Yamaguchi, K.; Gunter, M. J. *Org. Biomol. Chem.*, **2005**, 3, 3008

2. Flexible Receptor: A CTV-Based Acyclic Porphyrin Tripod

Once the pyrrole was added, the condensation reaction took place quickly and the kinetically trapped product, the symmetric porphyrin **10**, was the only product formed. To promote the formation of the minor porphyrin **8**, external conditions play a crucial role, such as vigorous stirring to ensure a good distribution of the aldehydes.



Scheme 2.2 Synthetic attempts of phenol porphyrin building block **8**.

Under vigorous stirring, the target porphyrin was obtained in a 5 % yield, comparable to the yield reported in the literature (6 %).⁸⁴ The reaction was protected from light to avoid the formation of linear polymerization products (Scheme 2.2). The desired A₃B-porphyrin **8** was isolated from the major product **10** by column chromatography (CHCl₃).

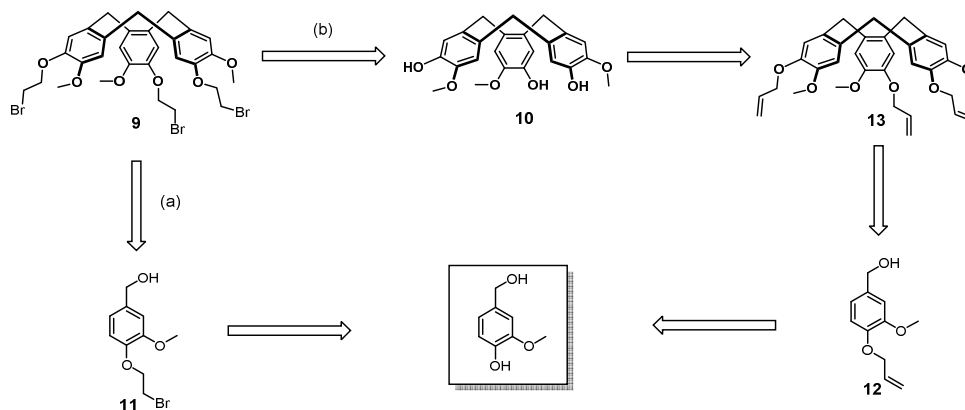
Synthesis of the CTV-Bromide Building Block

Two different synthetic routes were selected to prepare CTV-bromide building block **9**. The synthesis can be approached either by alkylation of vanillyl alcohol with

2. Flexible Receptor: A CTV-Based Acyclic Porphyrin Tripod

1,2-dibromoethane and further acid catalyzed condensation to obtain the desired CTV-bromide **9** in a two steps reaction [route (a), Scheme 2.3] or starting with the synthesis of triphenol **10** followed by alkylation with 1,2-dibromoethane to give **9** in four steps [route (b), Scheme 2.3].

The benefits of the first synthetic strategy are the avoidance of the extra protection and deprotection steps required for the synthesis of compound **10** and, more importantly, the alkylation with 1,2-dibromoethane is performed on the vanillyl alcohol that has only one reaction site, avoiding the formation of partially alkylated products. On the contrary, the alternative synthetic pathway (b) involves alkylation of **10** leading to mono- and bis-alkylated side products that would difficult the isolation of the target CTV-bromide **9**. The main advantage of the second synthetic route is the versatility of intermediate **10** as building block.

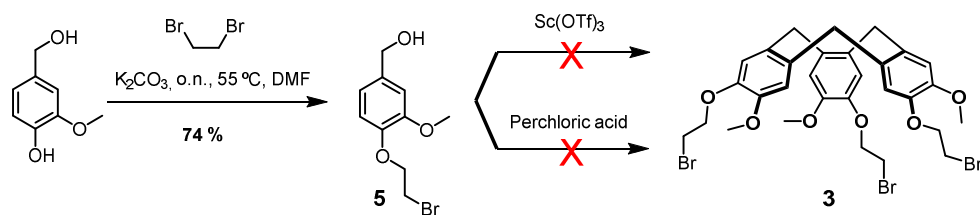


Scheme 2.3 Retrosynthetic routes (a) and (b) for CTV-bromide building block **9**.

In efforts to synthesize the desired CTV-bromide building block through the two step synthetic route (a), the vanillyl alcohol was successfully alkylated with dibromoethane in the presence of potassium carbonate in dimethylformamide (DMF) with good yields (Scheme 2.4). Unfortunately, attempts to trimerize the vanillyl alcohol **11** by acid

2. Flexible Receptor: A CTV-Based Acyclic Porphyrin Tripod

catalyzed condensation with either $\text{Sc}(\text{OTf})_3$ or perchloric acid failed, starting material being exclusively recovered.

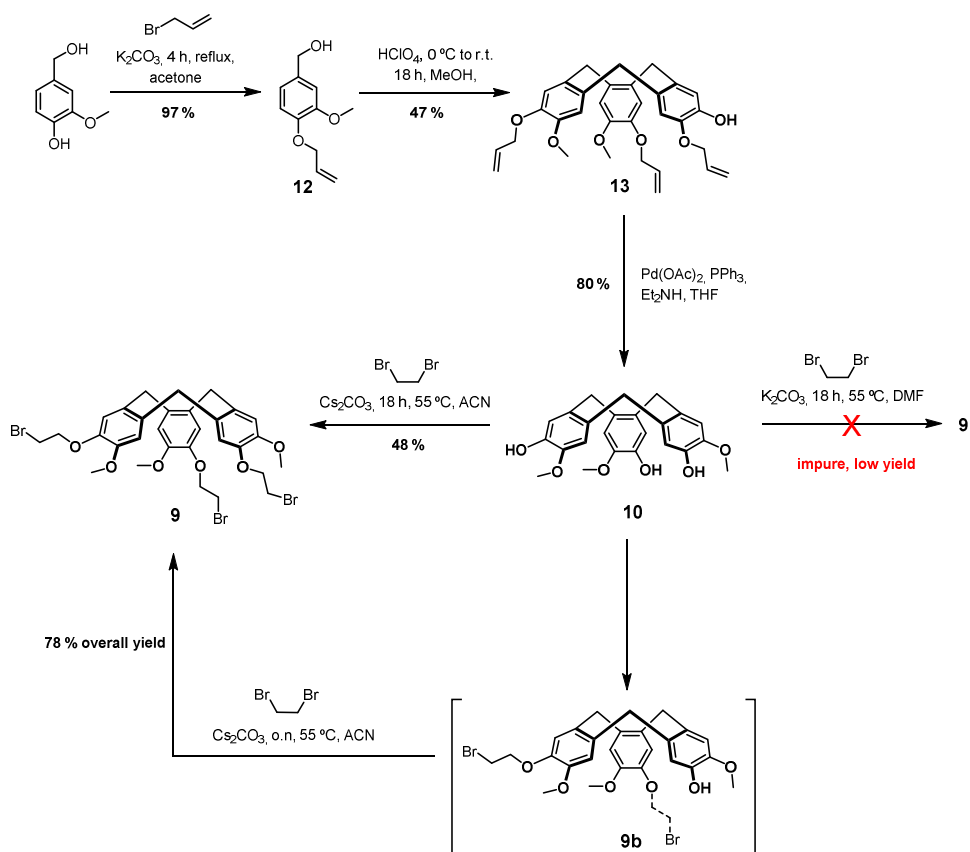


Scheme 2.4 Synthesis attempt of CTV-bromide building block 3.

The CTV-bromide building block **9** was finally synthesized through the four step synthesis route (b) in overall good yield. The commercially available vanillyl alcohol was successfully alkylated with allyl bromide in the presence of potassium carbonate in DMF to give the 4-(allyloxy)-vanillyl alcohol **12** in good yield (89 %). Acid catalyzed condensation of the protected vanillyl alcohol gave the desired tris(allyloxy)-substituted CTV triphenol **13** in good yields. This compound was then deprotected in the presence of palladium acetate, triphenylphosphine and diethylamine in tetrahydrofuran (THF) under microwave (MW) irradiation, to produce compound **10** in good yield (Scheme 2.5).

The triphenol **10** was then alkylated with dibromoethane to give the building block CTV-bromide **9**. When potassium carbonate was used as alkylating agent, very low yield and impure crude was obtained. On the contrary, the use of cesium carbonate in acetonitrile (ACN) improved the yield and purity significantly. The desired CTV-bromide **9** was initially obtained in moderate yield together with the mono- and dialkyl-derivatives **9b**. The partially alkylated CTVs were subjected again to the same reaction conditions, causing the final yield to improve up to 78 % after two alkylations (Scheme 2.5).

2. Flexible Receptor: A CTV-Based Acyclic Porphyrin Tripod

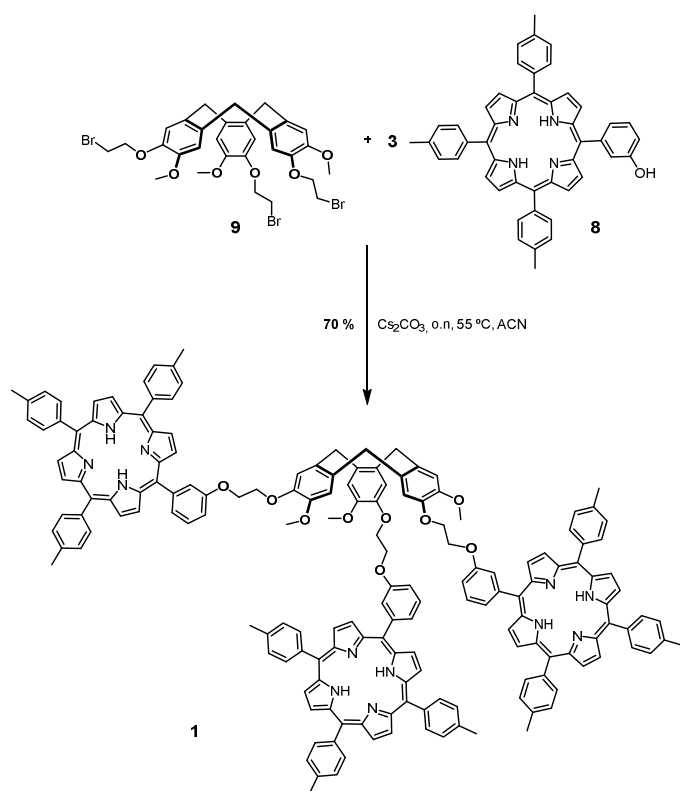


Scheme 2.5 Synthesis of CTV-bromide building block **9**.

Synthesis of the Target CTV-Porphyrin Host **1**

The reaction of three equivalents of porphyrin **8** with one equivalent of CTV-bromide **9** using CsCO_3 as base in ACN/DMF (to ensure the solubility of both the building blocks and the product) gave the target CTV-based porphyrin tripod **1** in good yields (Scheme 2.6). The desired CTV-porphyrin receptor **1** was purified by column chromatography (cyclohexane / CHCl_3 6:4).

2. Flexible Receptor: A CTV-Based Acyclic Porphyrin Tripod



Scheme 2.6 Synthesis of CTV-porphyrin host 1.

2.2.2 Characterization of CTV-Porphyrin Host 1

Receptor 1 was characterized by $^1\text{H-NMR}$ and mass spectrometry. In the $^1\text{H-NMR}$ spectrum (Figure 2.3), all significant protons could be identified.

2. Flexible Receptor: A CTV-Based Acyclic Porphyrin Tripod

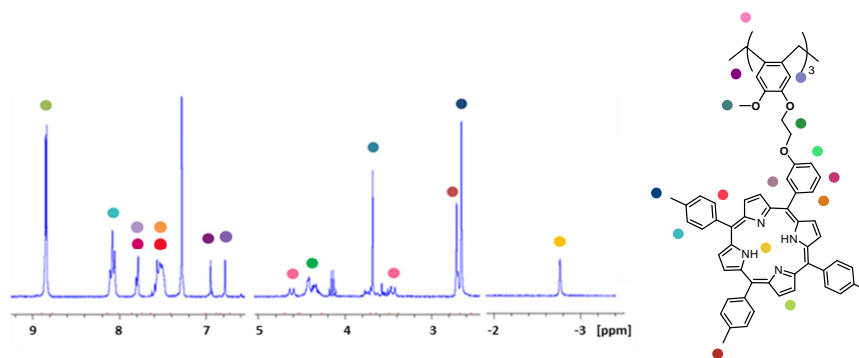


Figure 2.3 $^1\text{H-NMR}$ spectrum of CTV-porphyrin **1** in CDCl_3 .

The $^1\text{H-NMR}$ spectrum of CTV receptor **1** was recorded in toluene as a reference for fullerene complexation experiments (Figure 2.4). In this solvent the β -pyrrolic protons appear as a singlet at 9 ppm integrating 24 protons. The singlet at 3.3 ppm corresponding to the methoxy protons appears overlapped with the doublet corresponding to the methylene bridge protons. The rest of the $^1\text{H-NMR}$ spectrum is comparable to that obtained in CDCl_3 .

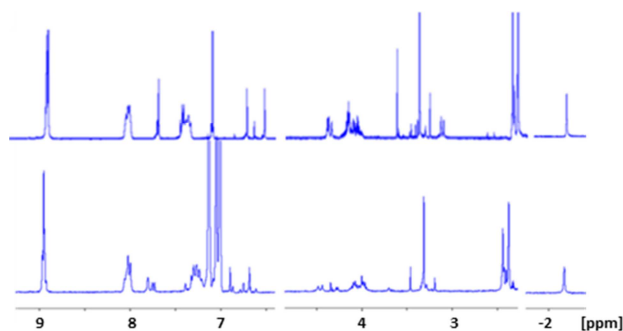


Figure 2.4 $^1\text{H-NMR}$ spectra of CTV-porphyrin **1** in CDCl_3 (upper trace) and toluene (lower trace).

Mass analysis of receptor **1** was performed by means of MM-ES+APCI and MALDI-TOF spectrometry (Figure 2.5). In MM-ES+APCI the molecular mass is double protonated. (Free receptor mass/ z^+ : 1253.0, calculated mass/ z^+ : 1253.0). In MALDI-

2. Flexible Receptor: A CTV-Based Acyclic Porphyrin Tripod

TOF both the M^+ and the MH^{2+} masses are observed, the isotopic pattern corresponding to a mixture of both. (Free receptor mass/ z^+ : 2505.0127, calculated mass/ z^+ : 2505.0743).

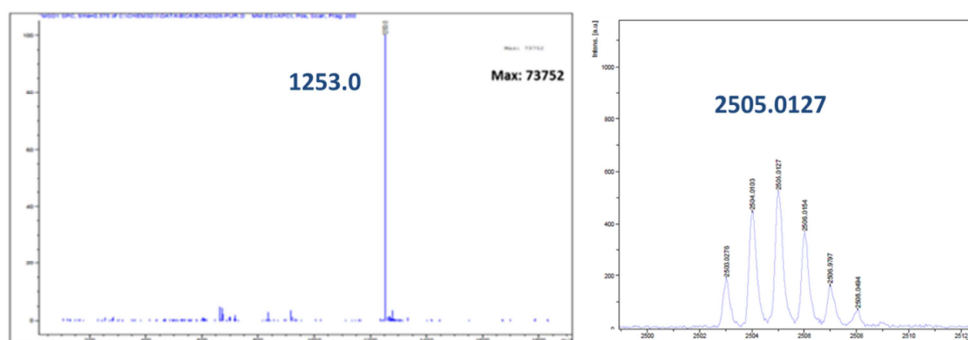


Figure 2.5 MM ES+APCI and MALDI-TOF mass spectra of the CTV-porphyrin 1.

High Temperature CTV-Porphyrin $^1\text{H-NMR}$ Studies

$^1\text{H-NMR}$ spectra at different temperatures were recorded to gain more insight into the spatial disposition of the receptor. High temperature spectra were recorded in tetrachloroethane (TCE) (between 298-398 K) (Figure 2.6). Upon increasing the temperature, the β -pyrrolic signals collapse into one broad singlet. This indicates that at high temperatures, the non-equivalent aromatic β -pyrrolic protons cannot be distinguished at the NMR time scale due to the fast turning of the porphyrin units. Downfield shift and broadening of the pyrrole N-H signal are also observed.

CTV-based derivatives are known to stack on top of each other forming columnar aggregates. Such stacking would translate into chemical shifting of the aromatic protons of the CTV and the porphyrin units due to the closer interaction. Upon increasing the temperature an inverse effect should be observed as the aggregates would be destabilized. Nevertheless no chemical shifts of either the aromatic CTV or

2. Flexible Receptor: A CTV-Based Acyclic Porphyrin Tripod

porphyrin protons were observed upon increasing the temperature, indicating the lack of interaction between the CTV-porphyrin **1** molecules.

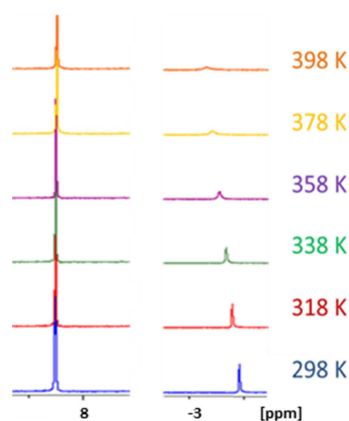


Figure 2.6 CTV-porphyrin **1** high temperature $^1\text{H-NMR}$ studies in TCE.

Low Temperature CTV-Porphyrin $^1\text{H-NMR}$ Studies

$^1\text{H-NMR}$ spectra of receptor **1** were also recorded at low temperature in CDCl_3 (in the range 213-298 K); selected regions are shown in Figure 2.7. At low temperature the movement of the pendant porphyrins is restricted and the non-equivalent protons can be easily identified. The sharp β -pyrrolic protons signals broaden and eventually collapse into one single broad signal at 253 K. After further cooling, the β -pyrrolic broad signal splits and simultaneously the two β -pyrrolic signals get sharper as they separate from each other.

2. Flexible Receptor: A CTV-Based Acyclic Porphyrin Tripod

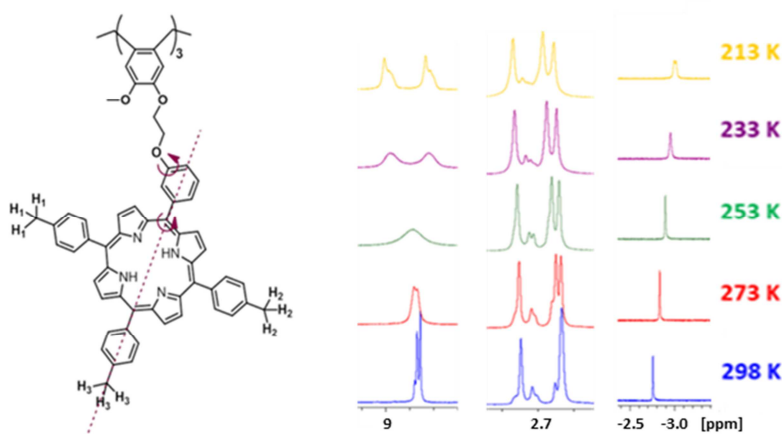


Figure 2.7 CTV-porphyrin **1** low temperature ¹H-NMR studies in CDCl₃.

Typically at room temperature two methyl proton signals are observed, corresponding to the methyl protons of the *p*-tolyl group in *trans* to the phenol (porphyrin position 15, H³, Figure 2.7) and the methyl protons of the *p*-tolyl group in *cis* to the phenol (porphyrin positions 10 and 20, H¹ and H², Figure 2.7) with a relative ratio of 1:2, respectively. Upon decreasing the temperature, the H¹ and H² singlet splits into two signals. At 233 K, for instance, three sets of sharp singlets integrating 9 protons each are identified. Moreover, upfield shift of the N-H signals is observed upon decreasing the temperature. At 213 K two N-H singlets can be identified.

2.3 Results and Discussion

The CTV-porphyrin **1** is a flexible host whose cavity size can vary adapting to the size requirements of the guest. For this reason, it is expected to form host-guest inclusion complexes with a wide range of fullerenes showing the greater affinity the bigger the fullerene is.

2. Flexible Receptor: A CTV-Based Acyclic Porphyrin Tripod

2.3.1 Binding Studies of the CTV-Porphyrin Tripod with Fullerenes and Other Carbon Materials

Inclusion complex formation was studied for C_{60} , C_{70} , C_{84} , Sc_3NC_{80} , and with complex fullerene mixtures (fullerite) as well. For pure fullerene samples, the interaction was monitored and quantified by UV-Vis absorption and fluorescence emission spectroscopic techniques, 1H -NMR spectroscopy and mass spectrometry. Preliminary complexation studies were performed with a sample provided by Prof. L. Echegoyen containing a *bucky onions* mixture. The interaction was monitored and evaluated by UV-Vis absorption and 1H -NMR spectroscopy.

Binding Studies of the CTV-Porphyrin Tripod 1 with C_{60}

Starting with the smaller and most abundant fullerene, the encapsulation of C_{60} was studied by UV-Vis absorption and fluorescence emission spectroscopy (Figure 2.8). No changes were observed in either the absorption or the emission spectra of the receptor upon addition of the fullerene, probably because C_{60} is too small to fill the receptor cavity at the employed 10^{-6} M concentration.

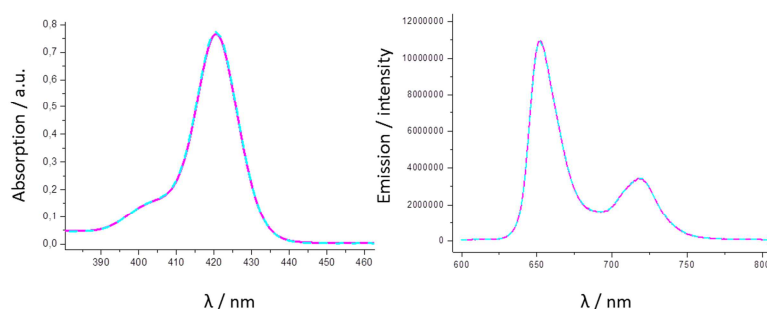


Figure 2.8 UV-Vis and fluorescence emission complexation experiments with C_{60} . Free receptor **1** (purple line); **1** + 6.5 eq. C_{60} (blue dashed line). $[1] = 1.0 \times 10^{-6}$ M.

2. Flexible Receptor: A CTV-Based Acyclic Porphyrin Tripod

Similarly, no changes were observed on the $^1\text{H-NMR}$ spectrum of the host upon addition of 1 equivalent of C_{60} to a 10^{-4} M solution of the receptor in toluene (Figure 2.9).

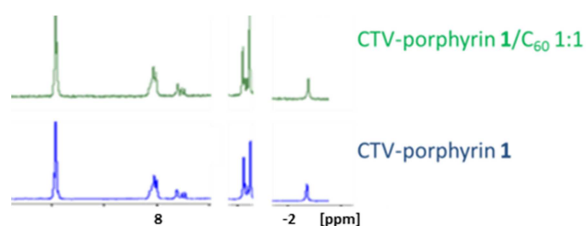


Figure 2.9 Selected regions of the free receptor **1** and **1/C₆₀** 1:1 mixture $^1\text{H-NMR}$ spectra in toluene (10^{-4} M).

However, mass analysis of the 1:1.5 mixture of receptor **1** and C_{60} evidenced formation of a 1:1 complex with the fullerene at this concentration (Figure 2.10). Both the masses of the free host and the 1:1 complex were identified. The masses appear double protonated (free receptor mass/z^+ : 1253.2, calculated mass/z^+ : 1253.0; Complex mass/z^+ : 1612.8, calculated mass/z^+ : 1613.0).

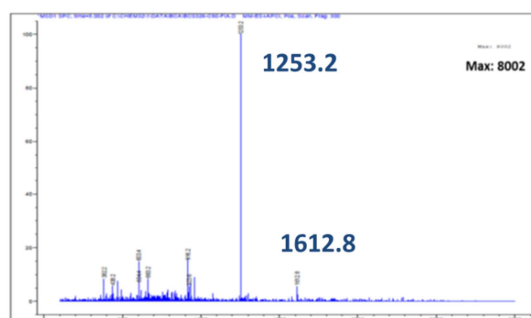


Figure 2.10 MM-ES+APCI spectrum of the 1:1.5 CTV-porphyrin **1/C₆₀** mixture.

Although receptor **1** is expected to form 1:1 inclusion complexes with the fullerenes, several 2:3 stoichiometries for the inclusion complex could be as well form between the flexible porphyrin tripod and the fullerene guest. In this way, two receptor units

2. Flexible Receptor: A CTV-Based Acyclic Porphyrin Tripod

would be involved in the encapsulation of three guests as reported previously for porphyrin based tripod described by Sanders *et al.*⁷⁰ (Schematic examples are shown in Figure 2.11). No signal corresponding to any 2:3 complex was observed in the MM-ES+APCI mass spectrum, suggesting the exclusive formation of a 1:1 complex (Figure 2.10).

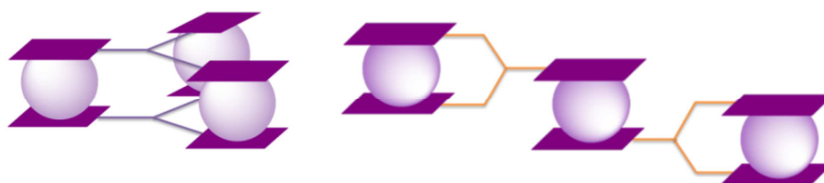


Figure 2.11 Schematic representation of 2:3 CTV-porphyrin 1 / fullerene inclusion complexes.

The ¹H-NMR spectrum was then recorded at a higher concentration (Figure 2.12). To avoid problems such as precipitation and/or aggregation, the concentration of C₆₀ was kept constant at 10⁻³ M whereas the concentration of the receptor was adjusted to achieve fullerene ratios of 0.5, 1 and 1.5. The changes on the ¹H-NMR spectra of the receptor upon increasing the ratio of fullerene were recorded. Both the β-pyrrolic and the N-H protons of the porphyrin units split into two signals which can be assigned as the free and the complexed host.

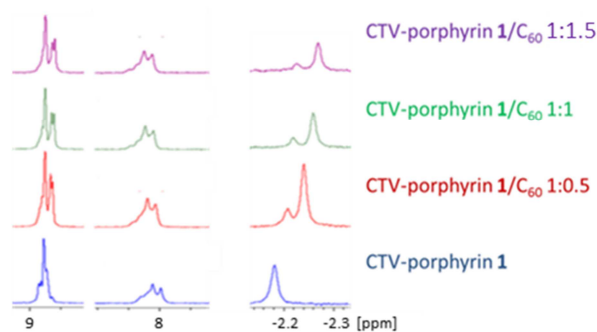


Figure 2.12 Selected regions of the ¹H-NMR spectra of the free receptor **1** and 1:0.5, 1:1 and 1:1.5 mixtures of 1/C₆₀ in toluene (10⁻³ M).

2. Flexible Receptor: A CTV-Based Acyclic Porphyrin Tripod

Binding Studies of the CTV-Porphyrin Tripod with C₇₀

As for C₆₀, the formation of an inclusion complex with C₇₀ was initially monitored and quantified by means of UV-Vis absorption and fluorescence emission spectroscopic techniques.

In the UV-Vis absorption titration experiment both quenching of the *Soret* band and appearance of a new band at 437 nm evidenced interaction with the fullerene and formation of an inclusion complex. An isosbestic point was observed at 438 nm. No shifting of the *Soret* band was observed (Figure 2.13). The association was quantified from the nonlinear fitting of both the quenching of the *Soret* band and the increment in absorption of the new complex band formed to a 1:1 complexation model ($K_{\text{ass}} = 2.0 \times 10^4 \text{ M}^{-1}$ and $1.3 \times 10^4 \text{ M}^{-1}$ respectively).

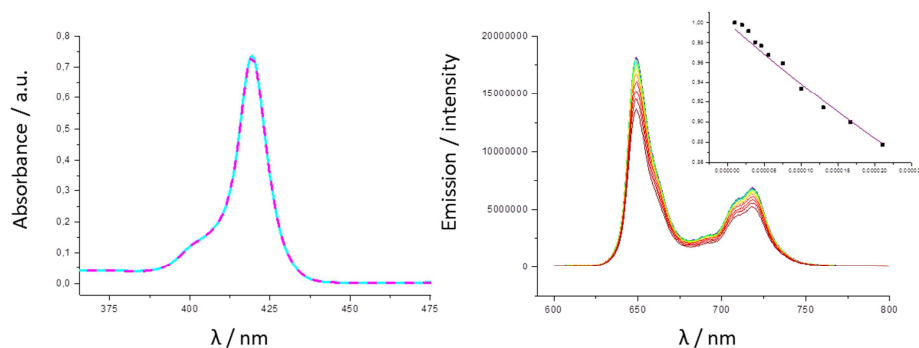


Figure 2.13 Absorption and fluorescence emission titration experiments of receptor **1** with C₇₀. [CTV-porphyrin **1**] = $1.0 \times 10^{-6} \text{ M}$; C₇₀ working concentration ($[\text{C}_{70}]_w$) = $5.0 \times 10^{-5} \text{ M}$; Final host/guest ratio added = 1:20; insets: UV-visible titration data (change in absorbance at 420 and 435 nm; left) and fluorescence emission titration data (change in intensity at 653 nm; right) for the binding of CTV-porphyrin **1** with C₇₀ in toluene fitted to the theoretical binding curves for a simple 1:1 complexation model.

In the fluorescence emission titration experiment, quenching of the emission upon addition of the guest also evidenced interaction (Figure 2.13). The association was quantified from the nonlinear fitting of the emission titration data to a 1:1 complexation

2. Flexible Receptor: A CTV-Based Acyclic Porphyrin Tripod

model ($K_{\text{ass}} = 3.3 \times 10^4 \text{ M}^{-1}$). The association constant was in agreement with the one calculated from the UV-Vis absorption data.

A Job's plot was recorded to establish the stoichiometry of the inclusion complex (Figure 2.14). Job's plot is a method of continuous variation that involves a series of isomolar solutions of the two reactants. The total molar concentration of the two binding reactants is held constant, but their mole fractions are varied. Then an observable value proportional to the complex formation such as the absorbance activity is plotted against the mole fractions of these two components. The maximum (or minimum) on the plot corresponds to the stoichiometry of the two species. For stable complexes, the plot is a triangle whose vertex indicates the complex stoichiometry.⁸⁵

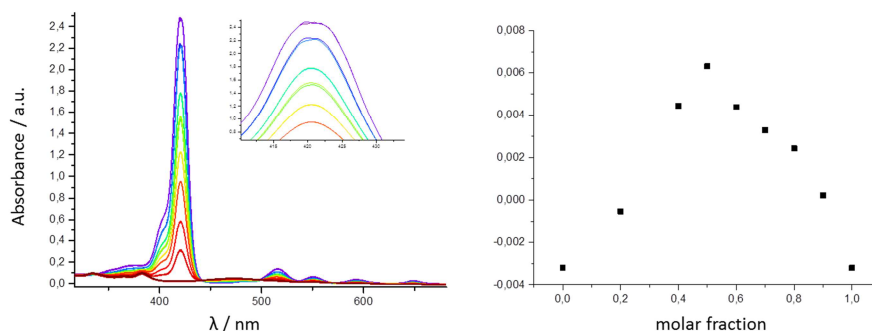


Figure 2.14 Job's plot of 1/C₇₀ complex: UV-Vis absorption spectra of the reactants absorbance and the mixed reactants absorbance upon changing the molar ratio; the absorbance measurements were recorded using a tandem cuvette (left). Plotting of the corrected absorbance at 435 nm vs. the C₇₀ mole fraction (right).

Although the difference in absorbance of the reactants and the complex mixture is very small, plotting of the measured absorbance (corrected for reactants absorbance) upon

⁸⁵ Hirose, K. in *Analytical Methods in Supramolecular Chemistry*, Wiley-VCH, Weinheim, **2005**

2. Flexible Receptor: A CTV-Based Acyclic Porphyrin Tripod

increasing the mole fraction of the fullerene clearly indicated the exclusive formation of a 1:1 complex.

The CTV-porphyrin receptor **1** was able to encapsulate C_{70} with an association constant in the range of 10^4 M^{-1} , whereas no interaction was observed for the smaller fullerene despite having a comparable diameter. This can be related to the additional carbons of C_{70} located around the central belt of the fullerene that enlarge the C_{70} giving it its typical rugby ball shape. The larger electron deficient area of C_{70} allows the fullerene to fit the inner space of the flexible receptor leaving the electron deficient belt centered with respect to the electron rich porphyrin units.

Binding Studies of the CTV-Porphyrin Tripod with C_{84}

The formation of inclusion complex with C_{84} was also studied by means of UV-Vis absorption and fluorescence emission spectroscopy, $^1\text{H-NMR}$ spectroscopy and mass spectrometry.

In the UV-Vis absorption titration experiment both quenching of the *Soret* band and appearance of a new band at 438 nm evidenced interaction with the fullerene and formation of the inclusion complex. An isosbestic point was observed at 431 nm. No shifting of the *Soret* band was observed (Figure 2.15). The association was quantified from the nonlinear fitting of both the quenching of the *Soret* band and the increment in absorption of the new complex band to a 1:1 complexation model ($K_{\text{ass}} = 9.2 \times 10^4 \text{ M}^{-1}$ and $1.0 \times 10^5 \text{ M}^{-1}$ respectively).

In the fluorescence emission titration experiment, quenching of the emission upon addition of the guest also evidenced interaction (Figure 2.15). The association was quantified from the nonlinear fitting of the emission titration data to a 1:1 complexation model ($K_{\text{ass}} = 2.5 \times 10^5 \text{ M}^{-1}$). The constant was found to be in agreement with those calculated from the UV-Vis absorption data.

2. Flexible Receptor: A CTV-Based Acyclic Porphyrin Tripod

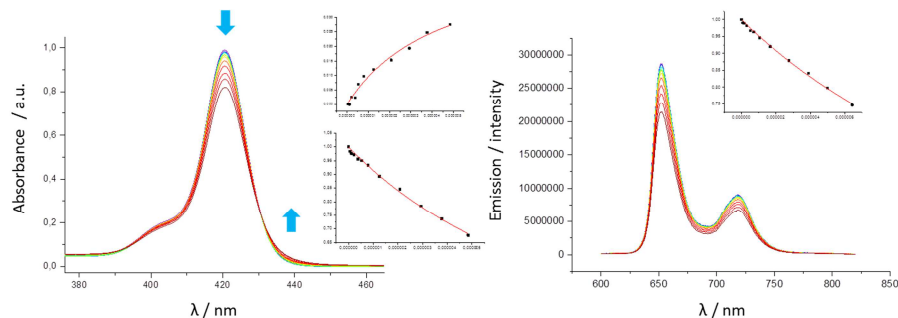


Figure 2.15 Absorption and fluorescence emission titration experiments of receptor **1** with C₈₄. [CTV-porphyrin **1**] = 1.0×10^{-6} M; [C₈₄]_w = 1.5×10^{-5} M; Final host/guest ratio added = 1:6.5; insets: UV-visible titration data (change in absorbance at 420 and 435 nm; left) and fluorescence emission titration data (change in intensity at 653 nm; right) for the binding of CTV-porphyrin **1** with C₈₄ in toluene fitted to the theoretical binding curves for a simple 1:1 complexation model.

A Job's plot to determine the stoichiometry of the inclusion complex was performed (Figure 2.16). The results unambiguously indicated the exclusive formation of a 1:1 complex with C₈₄.

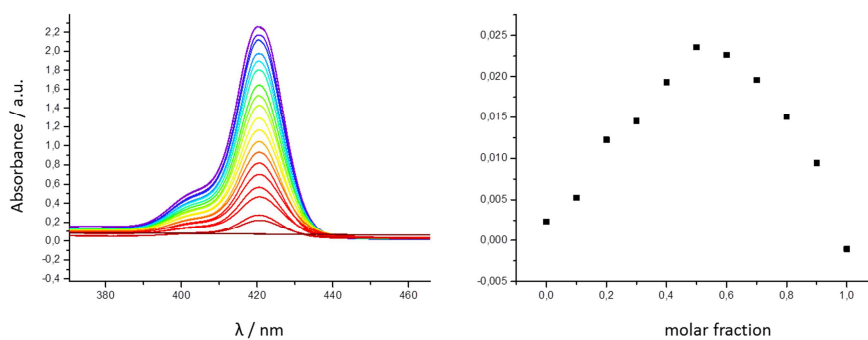


Figure 2.16 Job's plot of 1/C₈₄ complex: UV-Vis absorption spectra of the reactants absorbance and the mixed reactants absorbance upon changing the molar ratio; the absorbance measurements were recorded using a tandem cuvette (left). Plotting of the corrected absorbance at 437 nm versus the C₈₄ mole fraction (right).

2. Flexible Receptor: A CTV-Based Acyclic Porphyrin Tripod

A qualitative $^1\text{H-NMR}$ complexation study was performed with C_{84} to gain some insight into the $\text{C}_{84}@1$ host-guest interaction (Figure 2.17). Because of the low solubility of C_{84} , the concentration of C_{84} was kept constant at 5×10^{-5} M. Then, 2, 1 and 4 eq. of receptor **1** were added. Changes observed upon increasing the ratio of fullerene indicated interaction with the guest, in agreement with the UV-Vis and fluorescence emission titration experiments.

Upon increasing the ratio of C_{84} , both the β -pyrrolic protons and the N-H singlet split into two signals that correspond to the free and the complexed porphyrin host, as previously observed for C_{60} . The equilibrium between the free molecules and the complexed receptor is slow enough for the two species to be observed in the NMR time scale. The relative ratio between the free and the complexed host (1:3) can be determined from the integration of the N-H signals at the 1:1 mixture. This ratio does not change upon further addition of guest but the N-H signals of the complexed host porphyrin shifted upfield upon addition of more fullerene.

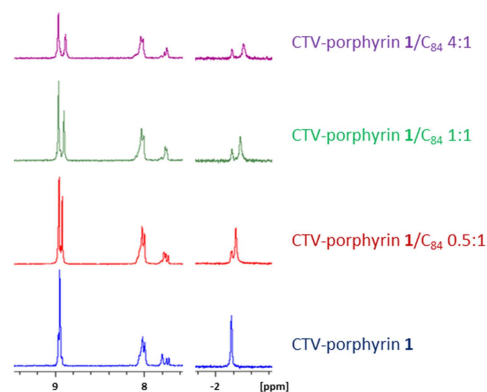


Figure 2.17 Selected regions of the $^1\text{H-NMR}$ spectra of the free receptor **1** and 0.5:1, 1:1 and 1:4 mixtures of **1**/ C_{84} in toluene $[\text{C}_{84}] = 5.0 \times 10^{-5}$ M.

Mass spectrometry of the higher concentrated solution of the porphyrin tripod **1** and C_{84} mixtures confirmed the formation of the 1:1 inclusion complex. Both the masses of the free guest and the 1:1 complex were observed. No mass corresponding to a 2:3

2. Flexible Receptor: A CTV-Based Acyclic Porphyrin Tripod

complex was observed. The masses appear double protonated (free receptor mass/z⁺: 1252.6, calculated mass/z⁺: 1253.0; Complex mass/z⁺: 1757.6, calculated mass/z⁺: 1757.0) (Figure 2.18).

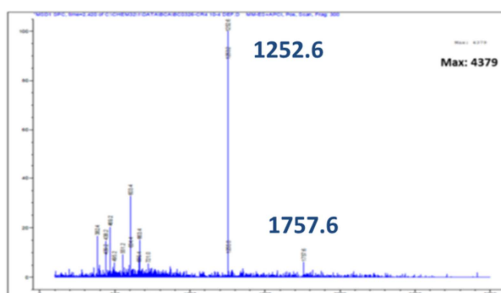


Figure 2.18 MM-ES+APCI spectra of the 1:1 CTV-porphyrin 1/C₈₄ mixtures.

To gain more insight into the stability of the complex, ¹H-NMR spectra of the CTV-porphyrin 1 / C₈₄ 1:0.5 mixture was monitored both at high temperature and upon addition of trifluoroacetic acid (TFA).

When increasing the temperature, the N-H signal corresponding to the free host and the 1:1 complex could be identified even at the highest temperature monitored (378 K). The relative integrals of the free host and complex signals were found to be stable up to 338 K (Figure 2.19).

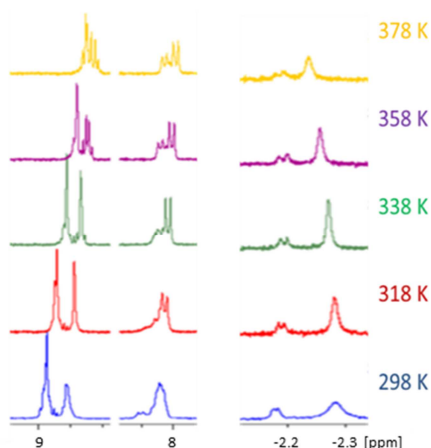


Figure 2.19 1/C₈₄ 1:0.5 mixture high temperature ¹H-NMR studies in TCE.

2. Flexible Receptor: A CTV-Based Acyclic Porphyrin Tripod

Finally the stability of the complex under acidic conditions was monitored by $^1\text{H-NMR}$ spectroscopy (Figure 2.20). The electron donating ability of the receptor is reduced in acidic conditions and consequently the complex stability should be also lower. Addition of 0.3 eq. of TFA to the 1:1 receptor $1/\text{C}_{84}$ mixture induced the free receptor/complex ratio to increase from 1:3 to 1:1. This experiment allowed the confirmation of the CTV-porphyrin/complex ratio assignment, since upon addition of TFA the integral that increased corresponds to the free receptor, as previously assigned.

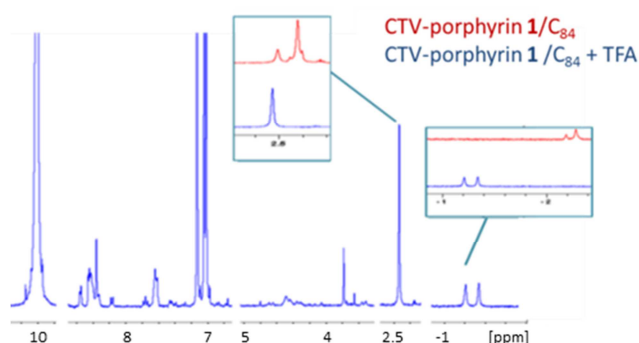


Figure 2.20. Selected regions of the $1/\text{C}_{84}$ 1:0.5 mixture $^1\text{H-NMR}$ spectra in toluene + 0.3 eq. TFA.

2D DOSY $^1\text{H-NMR}$ of the free receptor **1** and the 1:1 and 1:0.5 mixtures of receptor and C_{84} were recorded (Figure 2.21). Superposition of the spectra allowed to confirm the assignment of the free host and the complex signals. The signals corresponding to the free receptor **1** match perfectly whereas the complex signal shifts upfield upon addition of the fullerene. Also the complex diffusion was found to be slightly slower than the one for the free host as expected due to its bigger size. Nevertheless, the differences are too small to be taken in account.

2. Flexible Receptor: A CTV-Based Acyclic Porphyrin Tripod

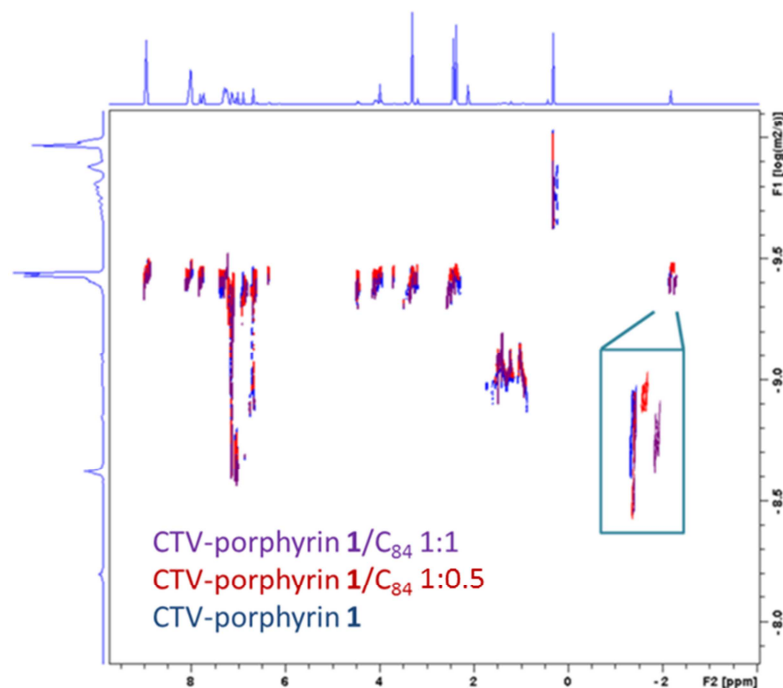


Figure 2.21. Superimposed DOSY ¹H-NMR spectra in toluene of CTV-porphyrin receptor 1 and 1:0.5 and 1:1 1/C₈₄ mixtures. [CTV-porphyrin 1] = 5 × 10⁻⁵ M

Binding Studies of the CTV-Porphyrin Tripod with Sc₃N@C₈₀

Regarding Sc₃N@C₈₀, complex formation was evidenced by both UV-Vis absorption and fluorescence emission titration experiments, revealing a high association.

In the UV-Vis absorption titration experiment, a significant quenching and a small red shift of the *Soret* band were observed. A new band appeared at 441 nm corresponding to the new complex formed. An isosbestic point was observed at 432 nm (Figure 2.22). The association was quantified from the nonlinear fitting of the absorption titration data to a 1:1 complexation model ($K_{\text{ass}} = 1.8 \times 10^5 \text{ M}^{-1}$ and $3.3 \times 10^4 \text{ M}^{-1}$).

2. Flexible Receptor: A CTV-Based Acyclic Porphyrin Tripod

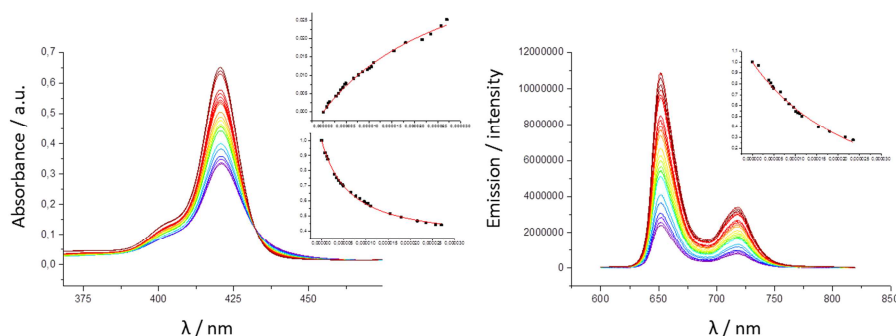


Figure 2.22 Absorption and fluorescence emission titration experiments of receptor **1** with $\text{Sc}_3\text{N}@C_{80}$. $[\text{CTV-porphyrin } \mathbf{1}] = 1.0 \times 10^{-6} \text{ M}$; $[\text{Sc}_3\text{N}@C_{80}]_w = 5.0 \times 10^{-5} \text{ M}$; Final host/guest ratio added = 1:27; insets: UV-visible titration data (change in absorbance at 420.5 and 441 nm; left) and fluorescence emission titration data (change in intensity at 651 nm; right) for the binding of CTV-porphyrin **1** with $\text{Sc}_3\text{N}@C_{80}$ in toluene fitted to the theoretical binding curves for a simple 1:1 complexation model. Inverse titration! Sc conc = $2.7 \times 10^{-5} \text{ M}$

In agreement with these results, a strong fluorescence emission intensity quenching was observed upon addition of $\text{Sc}_3\text{N}@C_{80}$ to the receptor solution. The association constant was calculated from the nonlinear fitting of the emission data for a 1:1 complexation model ($K_{\text{ass}} = 5.5 \times 10^4 \text{ M}^{-1}$). The calculated association was found to be in agreement with that calculated from the UV-Vis absorption titration experiment.

Preliminary Binding Studies of the CTV-Porphyrin Tripod with Fullerite

Finally, preliminary complexation studies were performed with commercially available fullerite (a commercial mixture of fullerenes).⁸⁶

The $^1\text{H-NMR}$ spectra of the CTV-porphyrin host was recorded in the presence of added fullerite (Figure 2.23). As in the previous experiments performed with C_{60} and

⁸⁶ The fullerite mixture employed from Sigma Aldrich typically contains 70-90% C_{60} , 10-30% C_{70} and less than 2% of high order fullerenes.

2. Flexible Receptor: A CTV-Based Acyclic Porphyrin Tripod

C_{84} , splitting of the β -pyrrolic and N-H protons was observed upon addition of the fullerenes mixture. The free receptor **1** / complex ratio was calculated from the N-H protons integrals and was found to be 1:4.

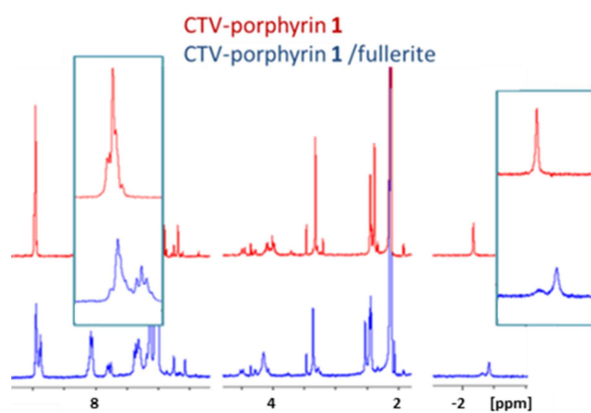


Figure 2.23 $^1\text{H-NMR}$ spectra selected regions of the spectra free receptor **1** and **1** / fullerite in toluene. $[\mathbf{1}] = 1.0 \times 10^{-3} \text{ M}$.

The mass spectrum of the CTV-Porphyrin **1** / fullerite mixture was recorded. In the spectrum, the masses of the free guest **1** and the 1:1 complexes with C_{60} , C_{70} and C_{84} are observed. The masses appear double protonated (Free receptor **1** mass/ z^+ : 1253.6, calculated mass/ z^+ : 1253.0; **1** / C_{60} complex mass/ z^+ : 1612.4 calculated mass/ z^+ : 1613.0; **1** / C_{70} complex mass/ z^+ : 1672.8, calculated mass/ z^+ : 1673.0); **1** / C_{84} complex mass/ z^+ : 1757.4, calculated mass/ z^+ : 1757.0) (Figure 2.24).

2. Flexible Receptor: A CTV-Based Acyclic Porphyrin Tripod

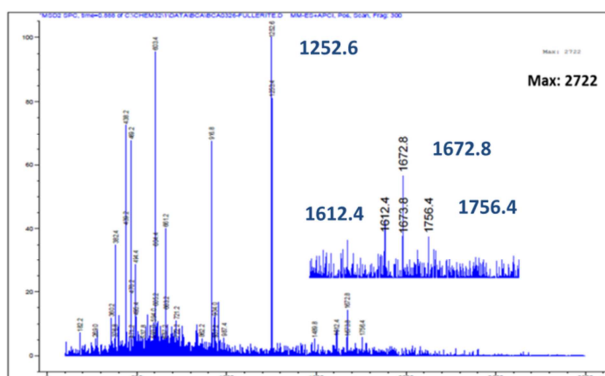


Figure 2.24 MM-ES+APCI spectrum of the 1:1 CTV-porphyrin 1 / fullerite mixture.

Preliminary Binding Studies of the CTV-Porphyrin Tripod with a *Bucky Onion* Mixture

Preliminary binding studies were performed with the *bucky onion* sample (a carbonaceous mixture containing undetermined amount of *bucky onions*). The nature, size and amount of the carbon nano onions (CNOs) of the sample are unknown although it is expected to contain $C_{60}@C_{240}$. CTV-Porphyrin 1 is specially designed to target $C_{60}@C_{240}$ *bucky onion*.

A preliminary complexation study with the *bucky onion* sample was performed in DMF. The interaction between the CTV-porphyrin receptor 1 and the CNO was studied by means of UV-Vis absorption spectroscopy.

Carbon onions such as $C_{60}@C_{240}$ *bucky onion* are extremely insoluble in all solvents. Attempts of complete solubilization in different solvents such as THF, toluene or DMF failed. Only partially solubilized suspensions in DMF were found to be stable enough for the UV-Vis titration experiments to be performed. To prepare the *bucky onion* suspension in DMF, the CNOs sample was sonicated in DMF for no more than 10 minutes at 20 °C (to avoid possible degradation of the carbon onions).

2. Flexible Receptor: A CTV-Based Acyclic Porphyrin Tripod

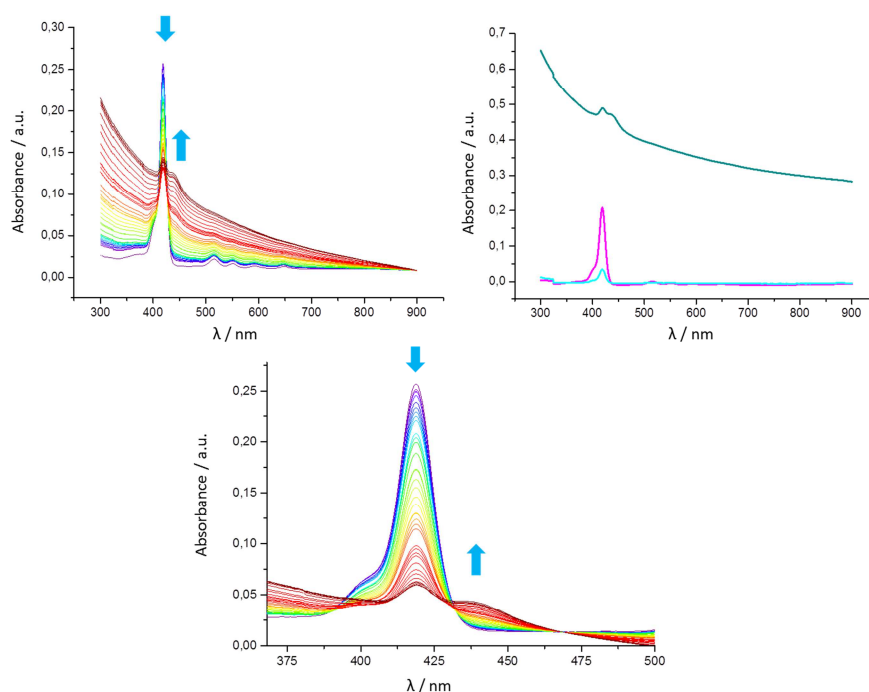


Figure 2.25 Absorption titration experiments of receptor **1** with CNOs [**1**] = 5.0×10^{-7} M; [CNOs]_w = 0.036 g/L; Up left: Changes observed on the absorption spectrum upon addition of the guest; spectra normalized at 900 nm. Down: Changes observed on the absorption spectrum upon addition of the guest; spectra normalized at 468.5 nm; Up right: absorption spectra of **1** (purple line), final **1** + CNOs mixture (dark blue line), final **1** + CNOs mixture after filtration (light blue line).

The changes on the receptor absorbance were monitored by UV-Vis spectroscopy upon addition of the *bucky onion* mixture. The concentration of the mixture was increased whereas the concentration of receptor **1** was kept constant. The strong quenching of the *Soret* band and appearance of the new band at 438 nm indicated interaction with the mixture and formation of inclusion complexes. An isosbestic point was observed at 431 nm (Figure 2.25).

2. Flexible Receptor: A CTV-Based Acyclic Porphyrin Tripod

Fluorescence emission titration experiment could not be performed. The scattering effect derived from the insolubilized *bucky onion* mixture would lead to a decrease of the detected light resulting in a false fluorescence response. For this reason quenching of the fluorescence emission intensity cannot be monitored as a direct measure of the interaction.

Preliminary complexation studies with the *bucky onion* sample were as well monitored by $^1\text{H-NMR}$ spectroscopy in toluene, TCE and DMF (Figure 2.26).

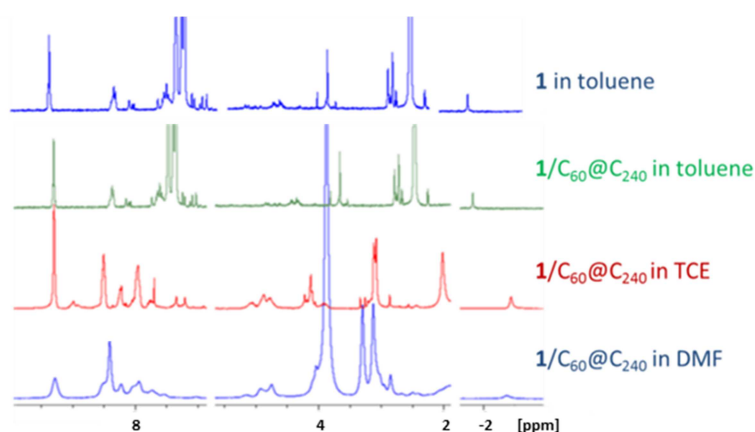


Figure 2.26 $^1\text{H-NMR}$ solvent study of CTV-porphyrin **1**/ $\text{C}_{60}@C_{240}$.

No changes on the $^1\text{H-NMR}$ spectrum of the receptor were observed in toluene, confirming the lack of interaction in that solvent. The $^1\text{H-NMR}$ spectrum was as well recorded in DMF and in TCE. In both solvents broadening of all the proton signals was observed, indicating that the complexation is improved in those solvents as the solubility of the carbon onion slightly increases. No splitting or shifting of the signals is observed. The *bucky onion* sample remains extremely insoluble even in the presence of the receptor.

2. Flexible Receptor: A CTV-Based Acyclic Porphyrin Tripod

2.3.2 Summary and Discussion

The receptor **1** flexibility allows the cavity to adapt to a wide variety of guests and was specially designed to form host-guest inclusion complexes with giant fullerenes as the so-far never isolated C₆₀@C₂₄₀.

Table 2.1 Summary of the receptor **1** complexation studies with the different carbon guests.

Entry	Guest	Binding	$K_{\text{ass}}^{\text{q}}$ [x 10 ⁻⁴ M ⁻¹]	$K_{\text{ass}}^{\text{a}}$ [x 10 ⁻⁴ M ⁻¹]	$K_{\text{ass}}^{\text{f}}$ [x 10 ⁻⁴ M ⁻¹]
1	C ₆₀	✓	n.d.	n.d.	n.d.
2	C ₇₀	✓	2.0	1.4	3.3
3	C ₈₄	✓	9.2	10	25
4	Sc ₃ N@C ₈₀	✓	18	3.3	5.5
4	Fullerite*	✓	-	-	-
5	<i>Bucky onion</i> *	✓	-	-	-

$K_{\text{ass}}^{\text{q}}$ = association constant calculated from the absorbance quenching data; $K_{\text{ass}}^{\text{a}}$ = association constant calculated from the absorbance increase data; $K_{\text{ass}}^{\text{f}}$ = association constant calculated from the fluorescence emission quenching data. *Preliminary complexation studies

The CTV-porphyrin receptor **1** was able to form 1:1 complexes with all the fullerene guests. As a general tendency, a bigger size of the carbon guest lead to a larger binding affinity. The largest quenching was observed for the complexation of the *bucky onion* sample. The results are summarized in Table 2.1.

2. Flexible Receptor: A CTV-Based Acyclic Porphyrin Tripod

No association was observed between the receptor and the C_{60} by absorption and emission titration experiments due to the weak binding. Nevertheless the association was qualitatively proved by $^1\text{H-NMR}$ spectroscopy and mass spectrometry at a higher concentration. On the contrary, the receptor was able to form inclusion complexes with C_{70} at a 10^{-6} M concentration despite of having a comparable diameter as C_{60} . The larger electron deficient area of C_{70} allows the fullerene to fit the inner space of the flexible receptor leaving the electron deficient belt centered with respect to the electron rich porphyrin units. Receptor **1** successfully formed inclusion complexes with C_{84} at 10^{-6} M. The calculated association constant was found to be an order of magnitude bigger than that for C_{70} .

The preferred supramolecular interaction between porphyrins and endohedral fullerenes over smaller empty fullerenes has been reported in the literature. As examples the porphyrin functionalized silica reported by Meyerhoff *et al.*⁵¹ or the porphyrin based cyclic dimers reported by Boyd *et al.*⁵⁸ and Ballester *et al.*⁶⁸ can be mentioned (see chapter 1.1).

In the case of CTV-Porphyrin host **1**, the association calculated from the titration experiments performed with $\text{ScN}_3@C_{80}$ endohedral fullerene diverges, depending on which spectroscopic method was employed for the calculations. If the *Soret* band quenching is taken as a reference, the quantified association was found to be in the range of the association with C_{84} and one order of magnitude larger than C_{70} , whereas $K_{\text{ass}}^{\text{a}}$ and $K_{\text{ass}}^{\text{f}}$ were found to lie between the C_{70} and C_{84} values.

Due to six electrons transferred from the cluster to the cage, $\text{ScN}_3@C_{80}$ could be formally treated as a positively charged cluster inside a negatively charged icosahedral carbon cage ($[\text{Sc}_3\text{N}]^{6+}@C_{80}^{6-}$). The planar $[\text{Sc}_3\text{N}]^{6+}$ cluster fits perfectly inside the icosahedral cage of C_{80} (I_h). No pyramidalization of the cage is reported in the literature.

For these reason it can be assumed that the presence of the cluster does not significantly alter the size of the cage but it does alter the electronic polarization of the

2. Flexible Receptor: A CTV-Based Acyclic Porphyrin Tripod

endohedral fullerene as compared to the empty cage. This fullerene electronic polarization could lead to an increase of the association between the CTV-porphyrin host **1** and $\text{ScN}_3@C_{80}$.⁸⁷

In preliminary complexation studies performed with commercially available fullerite mixture, both ¹H-NMR spectroscopy and mass spectrometry evidenced complex formation with the fullerenes of the mixture. The masses of the 1:1 receptor **1** complex with C_{60} , C_{70} and C_{84} were observed.

The preliminary complexation studies were performed with the *bucky onion* sample. Strong quenching of the receptor **1** *Soret* band during UV-Vis absorption titration experiment evidenced interaction between the receptor **1** and the CNOs.

2.4 Conclusions

The porphyrin based flexible tweezer-like receptor **1** bearing a CTV central core combines two different fullerene recognition motifs linked through flexible linkers what provides it with an expandable cavity. The receptor has been successfully synthesized and characterized.

The formation of inclusion complexes with C_{60} , C_{70} , C_{84} and $\text{Sc}_3\text{NC}_{80}$ was monitored by means of by UV-Vis absorption and fluorescence emission spectroscopic techniques, ¹H-NMR spectroscopy and mass spectrometry. Preliminary complexation experiments were performed with *bucky onion* sample and commercially available fullerite.

⁸⁷ (a) Stevenson, S.; Rice, G.; Glass, T.; Harich, K.; Cromer, F.; Jordan, M.R.; Craft, J.; Hajdu, E.; Bible, R.; Olmstead, M. M.; Maitra, K.; Fisher, A. J.; Balch, A. L.; Dorn, H. C. *Nature*, **1999**, *55*, 401. (b) Alvarez, L.; Pichler, T.; Georgi, P.; Schwieger, T.; Peisert, H.; Dunsch, L.; Hu, Z.; Knupfer, M.; Fink, J.; Bressler, P.; Mast, M.; Golden, M. S. *Phys. Rev. B*, **2002**, *66*, 035107. (c) Ceróna, M. R.; Lia F.-F.; Echegoyen, L. *J. Phys. Org. Chem.* **2014**, *27*, 258.

2. Flexible Receptor: A CTV-Based Acyclic Porphyrin Tripod

Receptor **1** was able to target a wide range of fullerene sizes. CTV-Porphyrin **1** successfully formed host-guest interactions with C_{60} , C_{70} , C_{84} and Sc_3NC_{80} . A clear trend is observed throughout the fullerenes. CTV-porphyrin receptor **1** show greater affinity the bigger the size of the fullerene is. In the case of C_{60} the interaction with the fullerene was only observed at high concentration (1.0×10^{-3} M).

The association constants for the encapsulation of C_{70} , C_{84} and Sc_3NC_{80} were quantified in toluene from both the UV-Vis absorption and the fluorescence emission titration experiments. The association with C_{70} was found to be on the range of 10^4 M⁻¹. The association with C_{84} was found to be seven times higher than that calculated for C_{70} .

The association values calculated from the UV-Vis absorption and fluorescence emission titration experiments with $ScN_3@C_{80}$ diverge up to more than one order of magnitude depending on the spectroscopic data the calculations are based on. It is not conclusive whether or not the association with C_{84} is preferred over the encapsulation of the endohedral fullerene. Nevertheless, the association with the nitride cluster fullerenes is at least double the association with C_{70} .

Mass spectrometry analysis of receptor **1** / fullerene mixtures indicate exclusive formation of 1:1 complex for C_{60} , C_{84} and C_{70} . Job's Plot experiments performed with both C_{70} and C_{84} confirmed the 1:1 stoichiometry for both complexes.

Preliminary complexation studies with the *bucky onion* sample indicated interaction with the CNOs.

**Chapter 3: Preorganized Receptor I: A Cyclic
Porphyrin Trimer**

3. Preorganized Receptor I: **Cyclic Porphyrin Trimer**

3.1 Design and Aim of the Project

Cyclic porphyrin receptors have shown to be successful approaches towards the formation of fullerene inclusion complexes.⁸⁸ The flexibility of the spacers that connect the porphyrin subunits is a key aspect of the encapsulation process. In general, spacer flexibility is required for the cyclic receptors to be able to encapsulate the fullerenes. Nevertheless, the rigid cyclic porphyrin trimer **XLVIII** described by Anderson *et al.*,⁷³ was able to form host-guest complexes with a wide range of fullerenes, including large carbon guests as C₉₆ with very high association constants.

In the attempt to prepare a preorganized porphyrin-based receptor able to encapsulate big fullerenes, while avoiding inclusion of the major components of the carbon soot (C₆₀ and C₇₀), porphyrin trimer **2**, connected through rigid acetylene linkers was designed (Figure 3.1). Energy-minimized structures of the designed receptor indicate that C₈₄ should best fit the inner space of the receptor.

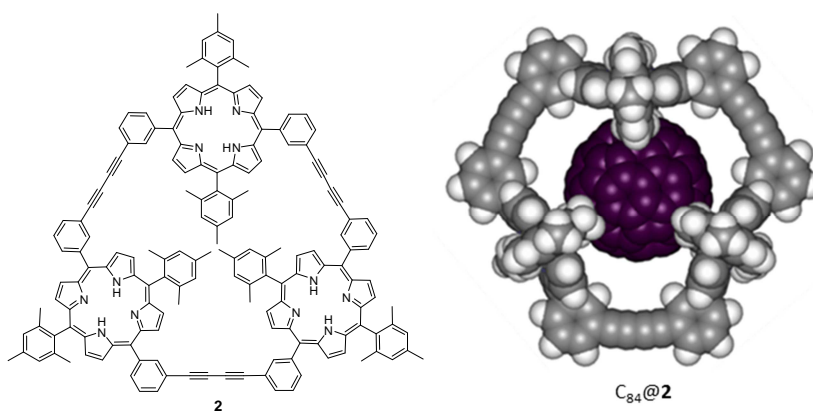


Figure 3.1 Cyclic porphyrin trimer **2**, Energy-minimized (SCIGRESS) structure of the C₈₄@**2** inclusion complex.

⁸⁸ See Chapter 1.3 and references therein.

3. Preorganized Receptor I: **Cyclic Porphyrin Trimer**

The target *trans*-A₂B₂-type porphyrin (5,15-porphyrin) monomer building block is functionalized with four *meso*-aryl substituents (Figure 3.2). Two of these substituents consist of 3-ethynylphenyl groups designed to connect the porphyrin units within the trimer **2**. The porphyrin units were also equipped with two mesityl-substituents.

Acetylene chemistry has been widely used in the synthesis of porphyrin cycles.^{88,89} Acetylenes are easily prepared and can be covalently linked through cross-coupling reactions providing rigidity to the final host and preorganization to the ligand. For instance, in the 3-ethynylphenyl *meso*-substituent, the terminal alkynes are directly attached to the *meta* position of the substituents, providing the porphyrin ligand with the right preorganization required for ring formation.

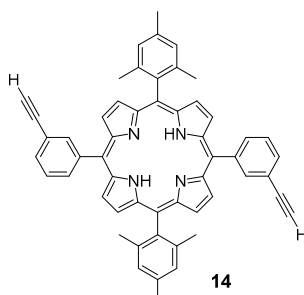


Figure 3.2 *trans*-A₂B₂-porphyrin building block **14**

Sterically unhindered 5-substituted dipyrromethanes are known to partially revert to its starting components under the lewis acid catalysis conditions required for the synthesis of *trans*-A₂B₂-porphyrins (5,15-porphyrin). This rearrangement of the dipyrromethanes is known as “scrambling”. During this process, the reverted starting components can rearrange with the added aldehyde leading to the formation of unwanted products such as the *cis*-A₂B₂-porphyrin (5,10-porphyrin), the unsymmetrical

⁸⁹ See Chapter 1.4 and references therein.

3. Preorganized Receptor I: **Cyclic Porphyrin Trimer**

A₃B-, the AB₃-porphyrins, etc.⁹⁰ The presence of sterically hindering substituents such as the mesityl group reduces the scrambling of the dipyrromethanes and minimizes the formation of unwanted products^{90, 67, 68}.

Moreover, the mesityl-substituted groups are expected to promote an increase in π -basicity of the porphyrin unit similar to that observed for pyrrole- β -substituted porphyrins. This would also induce the porphyrin units to adopt a shallow concave conformation as reported by Ballester *et al.*^{67, 68} Hence, the presence of mesityl *meso*-substituents would electronically and geometrically stabilize the supramolecular interactions with the fullerene guest.

Furthermore, the *orto* methyl groups of the mesity-substituents could also participate in additional CH- π interactions increasing the van der Waals contacts with the guest, as reported for both β -pyrrolic and mesityl *meso*-substituted porphyrin-based receptors.^{57, 67, 68, 91} Thus, improving the association with the fullerenes as also observed for tweezer-like porphyrin hosts bearing mesityl *meso*-substituents.^{60, 61}

3.2 Synthesis and Characterization

3.2.1 Synthesis of Cyclic Porphyrin Trimer 2

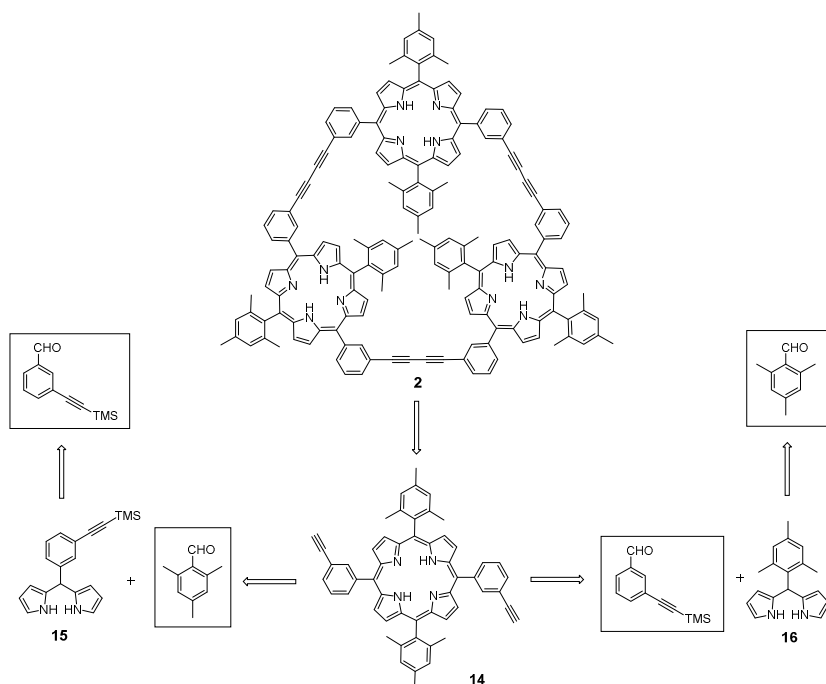
The target cyclic porphyrin trimer **2** can be approached through template-directed synthesis of the zinc-metallated porphyrin building block **Zn-14**. The *trans*-A₂B₂-porphyrin **14** can be readily prepared through condensation of either 5-substituted dipyrromethanes **15** or **16** with the correspondent aldehyde. The

⁹⁰ (a) Littler, B. J.; Ciringh, Y.; Lindsey, J. S. *J. Org. Chem.* **1999**, *64*, 2864. (b) Rao, P. D.; Dhanalekshmi, S.; Littler, B. J.; Lindsey J. S. *J. Org. Chem.* **2000**, *65*, 7323.

⁹¹ (a) Takahashi, O.; Kohno, Y.; Nishio, M. *Chem. Rev.* **2010**, *110*, 6049.

3. Preorganized Receptor I: **Cyclic Porphyrin Trimer**

dipyrromethanes are as well prepared through condensation of the aldehydes and two pyrroles (Scheme 3.1)



Scheme 3.1 Retrosynthetic routes towards the synthesis of cyclic porphyrin trimer **2**

Synthesis of Dipyrromethane Building Blocks

The synthesis of the cyclic porphyrin trimer started with the preparation of the dipyrromethane building blocks, which were synthesized through acid catalyzed condensation of two pyrrole units and the corresponding aldehyde. Two different conditions were screened for the preparation of dipyrromethanes. Higher yields were obtained by using TFA and a large excess of pyrrole [condition (a), Table 3.1], but these conditions, besides the large amount of pyrrole employed, required a tedious purification. A much easier access was achieved when three equivalents of pyrrole and aqueous HCl were used [conditions (b), Table 3.1]. Moreover, the isolated

3. Preorganized Receptor I: **Cyclic Porphyrin Trimer**

dipyrromethane showed a higher degree of purity than the compound synthesized following conditions (a). Hence, conditions (b) were used for the synthesis of dipyrromethanes reported unless otherwise specified.

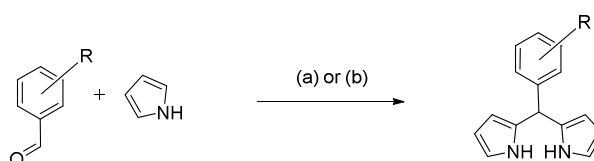


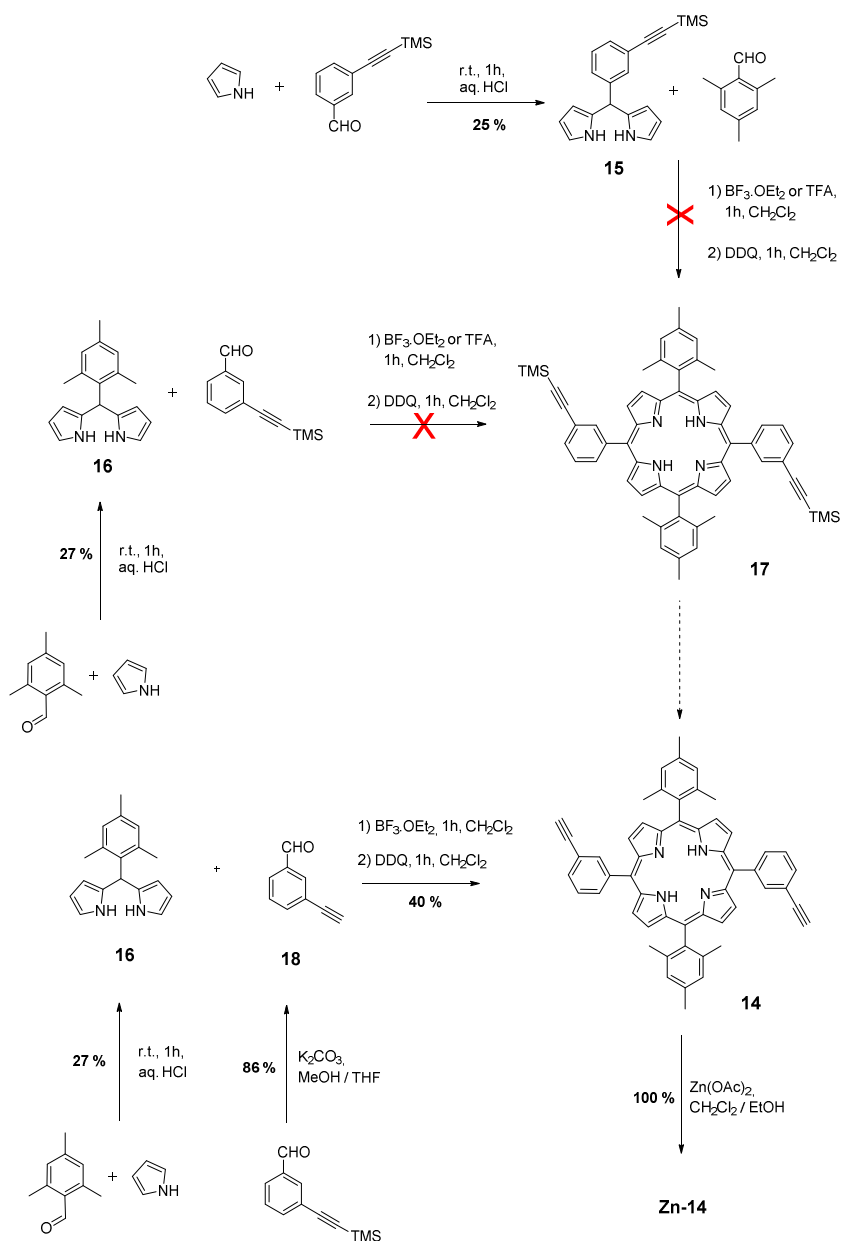
Table 3.1 Screening of reaction parameters for the general synthesis of dipyrromethanes.

	<i>Reagents</i>	<i>equiv. of Pyrrole</i>	<i>Temperature</i>	<i>Time</i>	<i>Yield</i>
(a)	TFA	25	r.t.	1 h	up to 40 %
(b)	aq. HCl	3	r.t.	3 h	up to 30 %

Synthesis of Zinc Metallated Porphyrin Building Block Zn-14

Attempts to prepare the TMS-protected porphyrin **17** starting from the commercially available TMS-protected 3-ethynylbenzaldehyde and the corresponding dipyrromethane **15** or **16** through acid catalyzed condensation with either TFA or BF₃ etherate followed by oxidation with DDQ failed (Scheme 3.2). Deprotection of the terminal alkyne was required for the porphyrin to be formed.

3. Preorganized Receptor I: Cyclic Porphyrin Trimer



Scheme 3.2 Synthetic attempts of free base porphyrin building block **14**. Synthesis of zinc-metallated ligand **Zn-14**.

3. Preorganized Receptor I: **Cyclic Porphyrin Trimer**

Deprotection of the commercially available 3-((trimethylsilyl)ethynyl)benzaldehyde with potassium carbonate yielded 3-ethynylbenzaldehyde **18** quantitatively. Acid catalyzed condensation of mesityl substituted dipyrromethane **16** and 3-ethynylbenzaldehyde **18** with BF_3 etherate followed by oxidation with DDQ gave the desired *trans*- A_2B_2 -porphyrin **14** in moderated yield. Besides, *cis*- A_2B_2 -porphyrin and A_3B -porphyrin were obtained as minor side products. The desired porphyrin was isolated by column chromatography (cyclohexane / CHCl_3 7:3). The porphyrin was then quantitatively metallated with zinc acetate in DCM/EtOH to give the metallated porphyrin ligand **Zn-14** (Scheme 3.2).

Template Directed Synthesis of Cyclic Porphyrin Trimer **2**

Template-assisted ring closure through homocoupling of the terminal alkynes was selected as synthetic approach for the preparation of the cyclic porphyrin trimer **2**. Commercially available 2,4,6-tri(4-pyridyl)-1,3,5-triazine **19** was used as the trimeric template.

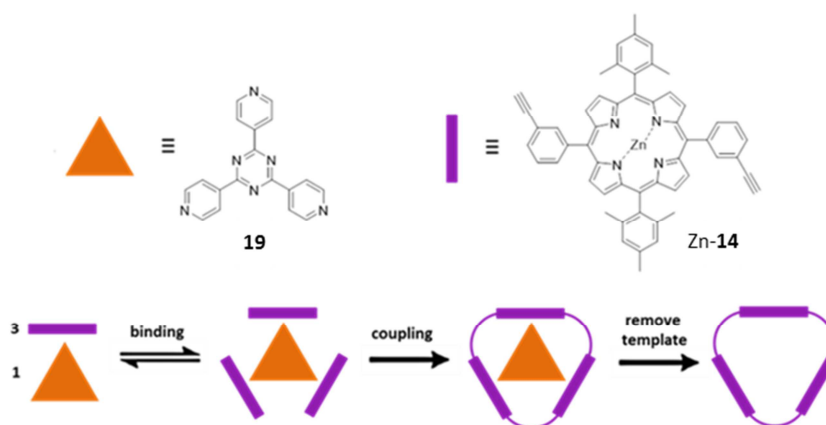


Figure 3.3 Schematic template-directed synthesis of porphyrin trimer.

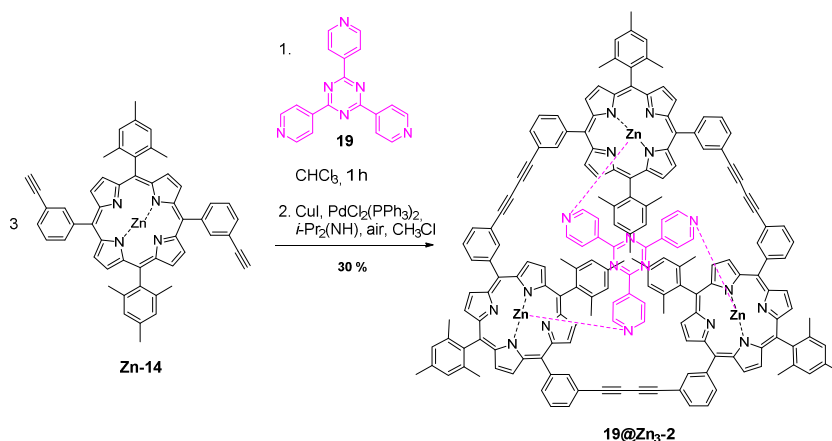
Although *Hay* coupling reaction represents the most important method for oxidative coupling to provide linear oligo- and polyacetylenes, these conditions were initially

3. Preorganized Receptor I: **Cyclic Porphyrin Trimer**

rejected because TMEDA is known to bind metallated porphyrins and can act as a template promoting the formation of porphyrin dimers.^{67, 68}

To avoid competition with dimer formation, *Sonogashira*-based conditions were used instead. Typically, the *Sonogashira* cross-coupling reaction is used for the formation of new C-C bonds starting from a terminal alkyne and an aryl or vinyl halide. Nevertheless, the presence of an oxidant agent leads to the formation of side products resulting from homocoupling of the acetylenes.

In this particular case, with no halide involved and in the presence of oxygen only the homocoupling products were obtained. The use of modified *Sonogashira* conditions for the homocoupling of terminal alkynes was already reported for the synthesis of giant porphyrin rings by Anderson *et al.*,^{89b-f} although in their case they used 1,4-benzoquinone as an oxidant agent.



Scheme 3.4 Template directed synthesis of the **19@Zn₃-2**

A 1:3 mixture of the template and the metallated porphyrin was sonicated for 2 h before addition of the catalyst. Coupling of the terminal alkynes by modified *Sonogashira* conditions gave the desired complex **19@Zn₃-2** in moderate yield

3. Preorganized Receptor I: **Cyclic Porphyrin Trimer**

(Scheme 3.4). The complex was purified by preparative TLC (cyclohexane / CHCl_3 7:3).

Unfortunately, even when using the trimeric template to preorganize the porphyrin units and promote the formation of the cyclic product, **19@Zn₃-2** was obtained only in a 30 % yield. Most of the porphyrin monomers still reacted within each other to form insoluble linear porphyrin arrays. Nevertheless, a template effect was unambiguously observed since coupling of the porphyrin monomers in the absence of template led only to traces of the desired trimer. Attempts to improve the final yield by increasing the template binding time did not succeed.

The porphyrin trimer complex **19@Zn₃-2** was characterized by $^1\text{H-NMR}$ spectroscopy and MM-ES+APCI and MALDI-TOF mass spectrometry.

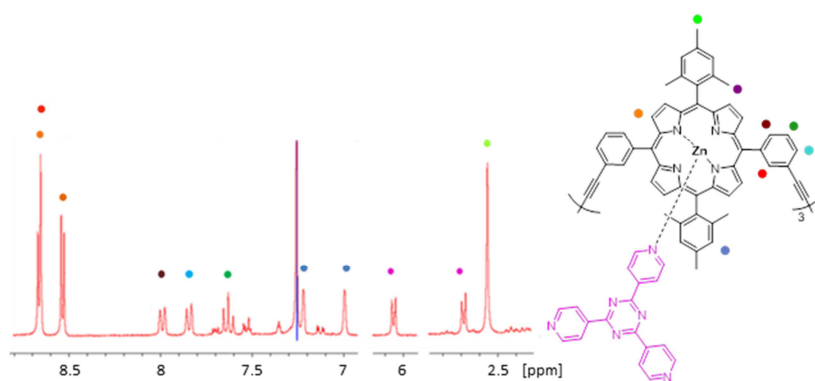


Figure 3.4 $^1\text{H-NMR}$ spectrum of **19@Zn₃-2** complex in CDCl_3

The $^1\text{H-NMR}$ spectrum of the complexed trimer is shown in Figure 3.4. In the spectrum, the typical peak corresponding to the proton in *ortho* to both the porphyrin and the terminal alkyne appears in this case considerably downfield shifted and overlapped with the β -pyrrolic proton signal at 8.7 ppm (red, Figure 3.4, typically found around 8.2 ppm). This is the only proton facing inside the trimer cavity and therefore is the most influenced by the presence of the template. The proton in *ortho* facing outside

3. Preorganized Receptor I: **Cyclic Porphyrin Trimer**

the cavity also appears upfield shifted in the presence of the template (brown, Figure 3.4). The pyridine protons of the template appear drastically upfield shifted at 2.7 and 6.0 ppm (pink, Figure 3.4, typically found around 8-9 ppm).

Mass analysis of the **20@Zn₃-2** complex was performed by means of both ESI+ and MALDI-TOF spectroscopic techniques (Figure 3.5). Only the free metallated host **Zn₃-2** mass (mass/z⁺: 2424,9) was observed in the MALDI spectrum. Surprisingly, both the free receptor **Zn₃-2** and the **19@Zn₃-2** complex were detected in the ESI+ analysis despite the reported difficulties⁹² for the detection of amine-Zn porphyrin complexes by mass spectrometry. Both single and double protonated mass peaks were detected, although the second appear to me much more intense (**19@Zn₃-2** mass/z⁺: 1212,9, calculated mass/z⁺: 1212,0; **Zn₃-2** mass/z⁺:1368,0, calculated mass/z⁺: 1367,9).

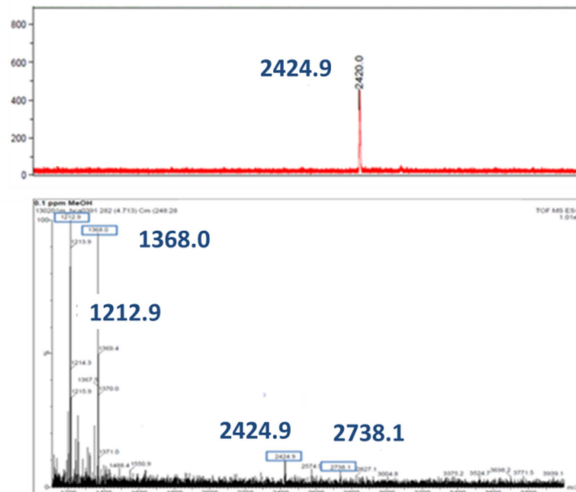
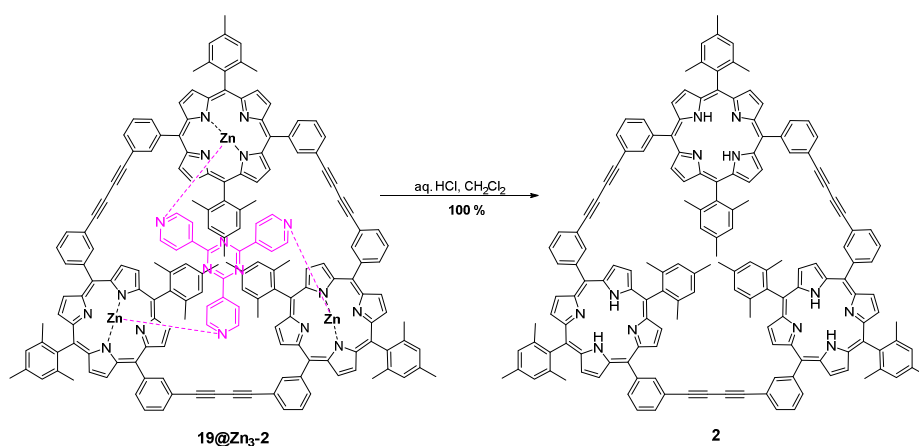


Figure 3.5 MALDI-TOF and ESI+ mass spectra of the **19@Zn₃-2** complex.

⁹² Ballester, P.; Costa, A.; Castilla, A. M.; Deyá, P. M.; Frontera, A.; Gomila, R. M.; Hunter, C. A. *Chem. Eur. J.* **2005**, *11*, 2196.

3. Preorganized Receptor I: Cyclic Porphyrin Trimer

Finally, the template was removed by protonation of the pyrrolic protons in acidic media. Addition of aq. HCl led to porphyrin's demetallation and template loss. Cyclic porphyrin trimer **2** was quantitatively demetallated (Scheme 3.5).



Scheme 3.5 Synthesis of the **2**: Template removal

Template removal process was monitored by ¹H-NMR. Upon addition of acid, the signals corresponding to the template **19** disappear (in pink, Figure 3.6). Simultaneously a new singlet corresponding to N-H protons of the free base porphyrins appears at -3 ppm (in orange).

Shifts of most of the aryl *meso*-substituents protons are observed upon releasing the template as consequence of the electronic environment changes after template loss. The protons that are facing inside the cavity are those more affected by the template loss. For instance, the proton in *ortho* to the porphyrin and the terminal alkyne shifts upfield from 8.7 to 8.2 ppm upon releasing the template (blue arrow, Figure 3.6), whereas the *ortho* proton to the porphyrin that faces out the cavity shifts downfield from 8.0 to 8.2 ppm (orange arrow, Figure 3.6). The β-pyrrolic protons (in green, Figure 3.6) shift towards each other. Finally, regarding the non-equivalent mesityl protons, the mesityl proton facing outside the cavity is not affected by the template loss whereas

3. Preorganized Receptor I: **Cyclic Porphyrin Trimer**

the one facing inside the cavity suffers a downfield shift from 7.0 to 7.2 ppm upon releasing the template.

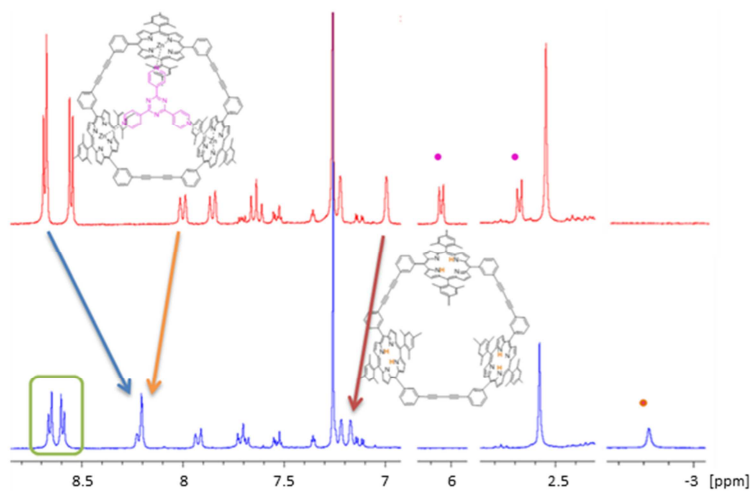


Figure 3.6 pH-directed template release process monitored by $^1\text{H-NMR}$.

3.2.2 Characterization of Cyclic Porphyrin Trimer 2

The porphyrin trimer **2** was characterized by both $^1\text{H-NMR}$ spectroscopy and both MM-ES+APCI and MALDI-TOF mass spectrometry. The $^1\text{H-NMR}$ spectrum the trimer **2** is shown in Figure 3.7.

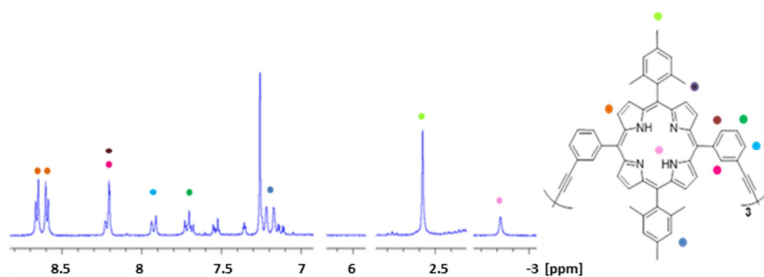


Figure 3.7 $^1\text{H-NMR}$ spectrum of the target cyclic porphyrin trimer **2** in CDCl_3

3. Preorganized Receptor I: **Cyclic Porphyrin Trimer**

Mass analysis of trimer **2** was performed by means of MM-ES+APCI and MALDI-TOF spectroscopic techniques (Figure 3.8). In the MM-ES+APCI experiment the mass appeared double protonated (trimer **2** mass/ z^+ : 1117.9, calculated mass/ z^+ : 1118.0). In the MALDI-TOF experiment the mass of the trimer is observed, and the isotopic pattern matches the theoretical distribution (trimer **2** mass/ z^+ : 2233.9790, calculated mass/ z^+ : 2233.9792)

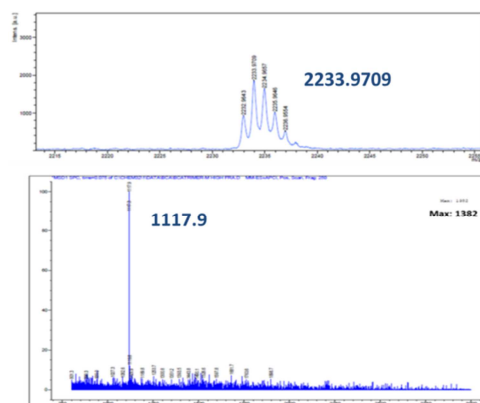


Figure 3.8 MALDI-TOF and MM-ES+APCI mass spectra of the target receptor **2**.

High Temperature Cyclic Porphyrin Trimer **2 $^1\text{H-NMR}$ Studies**

A high temperature $^1\text{H-NMR}$ experiment was performed to get a better insight into the geometry of the receptor **2** (Figure 3.9). At room temperature, the aromatic groups of the porphyrin *meso* positions are oriented perpendicular to the porphyrin plane as evidenced by two sets of signals observed for both the aromatic and the methyl protons. By increasing the temperature, the sharp singlets corresponding to the aromatic and the methyl protons get broader and eventually collapse into one broad signal at 378 K that gets sharper upon further heating, indicating that the rotation of the pendant groups is fast enough to prevent these protons to be differentiated in the $^1\text{H-NMR}$ spectrum.

3. Preorganized Receptor I: **Cyclic Porphyrin Trimer**

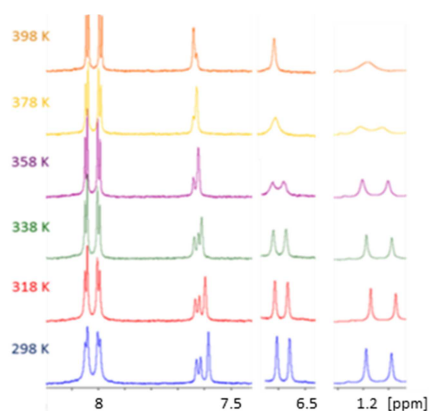


Figure 3.9 Cyclic trimer **2** high temperature $^1\text{H-NMR}$ studies in CDCl_3 .

Low Temperature Cyclic Porphyrin Trimer **2** $^1\text{H-NMR}$ Studies

$^1\text{H-NMR}$ spectra of porphyrin trimer **2** in CDCl_3 were recorded upon decreasing the temperature (298 \rightarrow 213K); selected regions are shown in Figure 3.10.

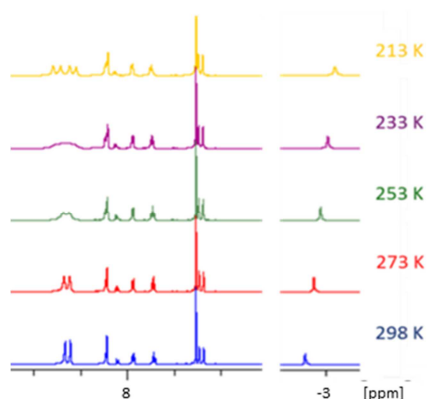


Figure 3.10 Cyclic porphyrin trimer **2** low temperature $^1\text{H-NMR}$ studies in CDCl_3 .

Upon decreasing the temperature, the sharp β -pyrrolic protons signals broaden and eventually collapse into one broad signal at 233 K. After further cooling, the β -pyrrolic

3. Preorganized Receptor I: **Cyclic Porphyrin Trimer**

broad signal further splits into two doublet signals at 213 K. An upfield shift of the N-H protons is also observed.

3.3 Results and Discussion

The cyclic porphyrin trimer **2** is a rigid host designed to form inclusion complexes with the fullerenes. Receptor **2** is expected to preferably form inclusion complexes with C_{84} which, according to molecular modeling, would best fit the inner space of the receptor.

3.3.1 Binding Studies of Porphyrin Trimer **2** with Fullerenes

UV-Vis absorption titration experiments as well as fluorescence emission titration experiments were performed with different fullerenes (C_{60} , C_{70} , C_{76} , C_{78} and C_{84}). The formation of host-guest inclusion complexes was monitored and the interaction quantified.

Binding Studies of Trimer **2 with C_{84}**

Despite receptor **2** was designed to preferably form inclusion complexes with C_{84} , no indication of complex formation was observed between the receptor and C_{84} . Both UV-Vis absorption and fluorescence emission titration experiments show no signs of interaction between trimer **2** and C_{84} (Figure 3.11).

3. Preorganized Receptor I: Cyclic Porphyrin Trimer

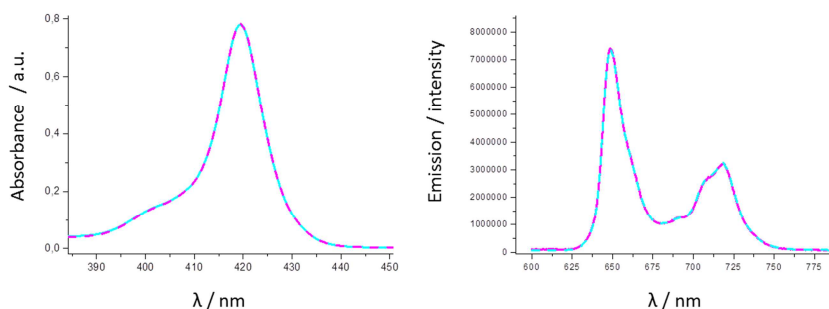


Figure 3.11 UV-Vis and fluorescence emission complexation experiments with C_{84} . Free receptor **2** (purple line); **2** + 21 eq. C_{84} (blue dashed line). $[2] = 1.0 \times 10^{-6}$ M.

In agreement to these results, no evidences of interaction between the cyclic porphyrin receptor and C_{84} were observed in the $^1\text{H-NMR}$ spectra at 10^{-4} M (Figure 3.12).

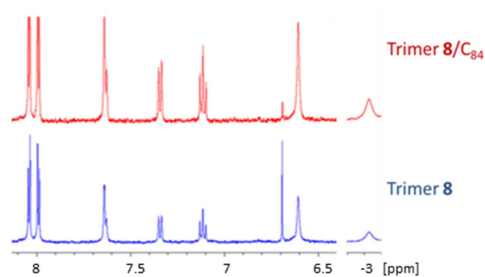


Figure 3.12 Selected regions of the $^1\text{H-NMR}$ spectra of the free receptor **2** and **2** / C_{84} 1:0.5 mixture in toluene.

To gain more insight into the inclusion complex formation ability of receptor **2**, complexation studies with C_{60} , C_{70} , C_{76} , C_{78} were also performed.

Binding studies of Trimer **2** with C_{60}

UV-Vis absorption and fluorescence emission titration experiments showed no evidences of inclusion complex formation with C_{60} as shown in Figure 3.13. No

3. Preorganized Receptor I: Cyclic Porphyrin Trimer

changes in either the absorption or the emission spectra evidenced the lack of interaction with the major fullerene.

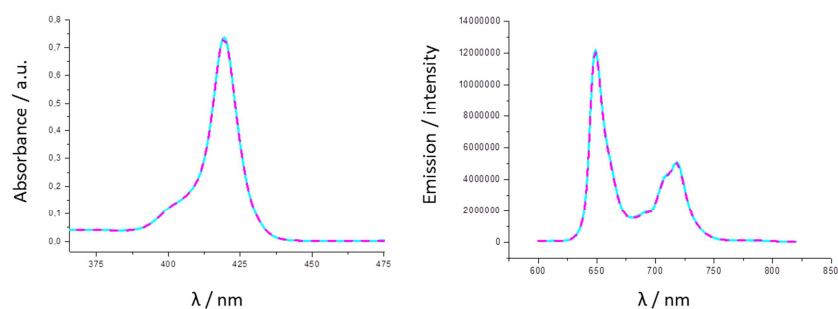


Figure 3.13 UV-Vis and fluorescence emission complexation experiments with C₆₀. Free receptor **2** (purple line); **2** + 14 eq. C₆₀ (blue dashed line). [2] = 1.0 × 10⁻⁶ M.

Binding studies of Trimer 2 with C₇₀

As for the previous fullerenes, in the case of C₇₀, no signs of complex formation were observed in the UV-Vis absorption titration experiment. However, quenching of fluorescence emission intensity upon addition of the guest did indicate interaction with C₇₀ (Figure 3.14). The association was quantified from the nonlinear fitting of the emission titration data to a 1:1 complexation model ($K_{\text{ass}} = 2.3 \times 10^3 \text{ M}^{-1}$) (Figure 3.14).

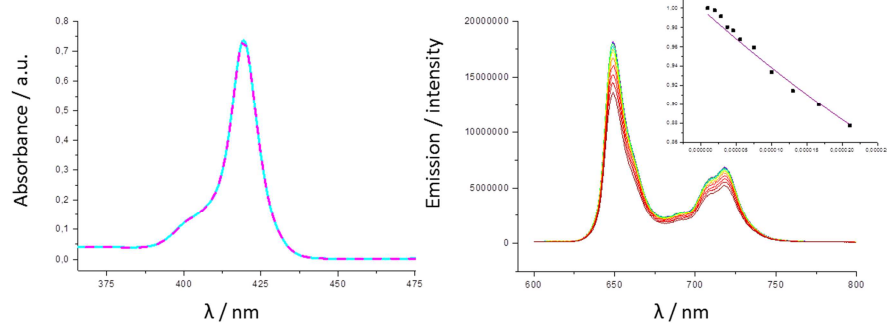


Figure 3.14 UV-Vis absorption complexation experiments with C₇₀; free receptor **2** (purple line); **2** + 10 eq. C₇₀ (blue dashed line); Right: fluorescence emission titration experiment of receptor **2** with C₇₀; right. [2] = 1.0 × 10⁻⁶ M; [C₇₀]_w = 5.0 × 10⁻⁵ M; Final host/guest ratio added = 1:10; inset: fluorescence emission titration data (change in intensity at 649 nm) for the binding of trimer **2** with C₇₀ in toluene fitted to the theoretical binding curves for a simple 1:1 complexation model.

3. Preorganized Receptor I: **Cyclic Porphyrin Trimer**

Binding studies of Trimer 2 with C₇₆ and C₇₈

C₇₆ and C₇₈ were selected as possible guests since their size is between C₇₀ and C₈₄. Titration experiments performed with C₇₆ indicated a weak interaction between **1** and C₇₆ (Figure 3.15). A slight quenching of the *Soret* band intensity and the fluorescence emission intensity upon addition of the fullerene was observed.

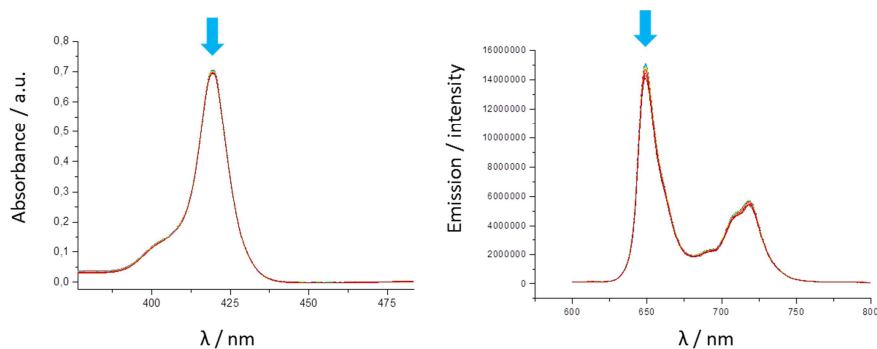


Figure 3.15 UV-Vis and fluorescence emission titration experiments with C₇₆. Arrows indicate the direction of the spectroscopic changes throughout the experiment. [2] = 1.0 × 10⁻⁶ M; [C₇₆]_w = 5.0 × 10⁻⁵ M; Final host/guest ratio added = 1:15.

In the case of C₇₈, no changes in either the absorption or the emission spectra evidenced the lack of interaction between the cyclic receptor **2** and C₇₈ (Figure 3.16).

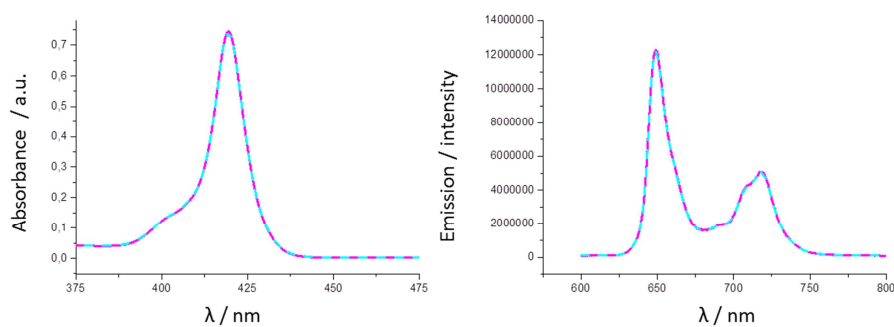


Figure 3.16 UV-Vis and fluorescence emission complexation experiments with C₇₈. Free receptor **2** (purple line); **2** + 20 eq. C₇₈ (blue dashed line). [2] = 3.4 × 10⁻⁶ M.

3. Preorganized Receptor I: **Cyclic Porphyrin Trimer**

3.3.2 Summary and Discussion

Receptor **2**, despite being designed to encapsulate C₈₄ did not show any evidences of interaction with this fullerene and also failed to encapsulate C₆₀ and C₇₈. Only in the fluorescence emission titration experiment performed with C₇₀, a clear decrease of the receptor emission intensity was observed which indicates inclusion complex formation with C₇₀.

The porphyrin cyclic trimer **XLVIII** reported by Anderson *et al.*⁷³ (Figure 3.20) was actually shown to encapsulate even larger fullerenes, despite having a smaller cavity, what indicates that trimer **2** cavity is actually big enough to accommodate the fullerenes what was confirmed by the modeling studies (Figure 3.21). The lack of interaction cannot be related with the inner cavity size, but must be related to other factors such as low flexibility of the receptor or the presence of bulky aryl substituent groups on the *meso* positions of the porphyrin subunits.

Preorganized cyclic receptors are known to show high interactions with fullerenes. At the same time, cyclic porphyrin receptors bearing flexible linkers are generally able to better adapt to the fullerene guests improving the association with the fullerene guests. In most cases the rigid analogue shows no interaction at all with the fullerenes whereas the flexible version was able to complex the guests with high association constants.

Some exceptions to this general lack of interaction associated to receptors bearing rigid linkers can be mentioned: The cyclic dimer **XLIII** reported by Ballester *et al.*^{67, 68} (Figure 3.22) bearing rigid linkers although not able to form inclusion complexes with C₆₀ did encapsulate C₇₀ with a reasonable associations constant ($K_{ass} = 2 \times 10^4 \text{ M}^{-1}$). The porphyrin cycle was able as well to form an inclusion complex with Sc₃N@C₈₀, although the association constant was not reported. It has to be pointed out that in this case the linkers were not totally rigid, since some flexibility was introduced by the

3. Preorganized Receptor I: **Cyclic Porphyrin Trimer**

presence of a methylene carbon, allowing the porphyrin units to twist and adapt to the fullerenes.

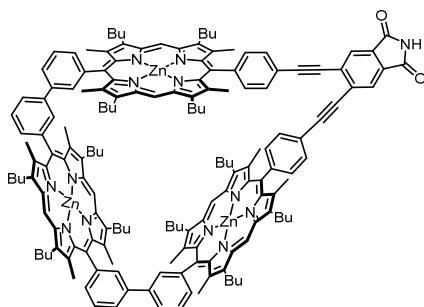


Figure 3.17 Cyclic porphyrin trimer **XLVIII**.

More interesting is the receptor **XLVIII** reported by Anderson *et al.*⁷³ (Figure 3.20). The small rigid cyclic porphyrin trimer, despite its low flexibility, is able to encapsulate a wide range of fullerenes from C_{60} to C_{96} and also did it with extremely high association constants. For instance the receptor was able to form an inclusion complex with C_{70} with an association of $1.6 \times 10^8 \text{ M}^{-1}$ in toluene, the highest association reported to date with this fullerene; Moreover the trimer was able to encapsulate C_{86} and $\text{La}@C_{82}$ with even higher associations ($> 10^9 \text{ M}^{-1}$). In this case the perfect combination of high preorganization of the receptor and appropriate cavity size lead to an extremely effective association.

It is important to notice that in our case as well as in Anderson's receptor, three porphyrin units are connected through relatively short rigid linkers, whereas in the rest of the examples reported, only two porphyrin units were connected through longer spacers what results in a bigger inner space where the porphyrin units are too far away from each other to allow a simultaneous interaction with the fullerenes.

All these results indicate that, even though flexibility plays an important role on the complexation ability of cyclic receptors, a receptor with three porphyrin units, relatively short rigid linkers and an appropriate cavity size as **2** (Figure 3.21) should be able to

3. Preorganized Receptor I: **Cyclic Porphyrin Trimer**

form inclusion complexes with fullerenes. Consequently, the lack of interaction cannot be related only to flexibility of the receptor but other factors should be involved. For instance, the presence of bulky mesityl groups at the *meso* positions of the porphyrin subunits might hinder the interaction between receptor **2** and the fullerene guests.

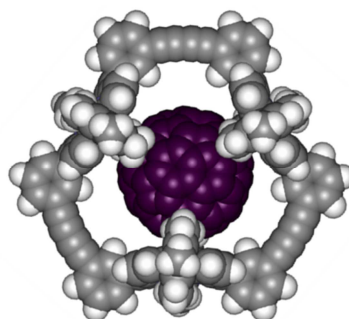


Figure 3.18 Energy-minimized structure (SCIGRESS) of the $C_{84}@2$ inclusion complex.

It is known from extended studies with tweezer-like porphyrin hosts that receptors bearing substituents at the *meso* positions of the porphyrin subunits interact with the fullerenes with higher associations than their unsubstituted analogues. Nevertheless, contrary to those tweezer-like porphyrin based hosts, most of the cyclic porphyrin receptors reported to date that successfully encapsulate fullerenes have *meso* unsubstituted porphyrin units.

Only cyclic receptors **XLII** and **XLIII** reported by Ballester *et al.*^{67, 68} (Figure 3.22) were able to encapsulate fullerenes despite of having bulky aryl substituents on the *meso* positions of the porphyrin units. In this case, solid state proofs of the complexes show that the porphyrin units are not oriented in a cofacial way but instead the porphyrin units are twisted forming a cone-shaped cavity that accommodates the guests.

3. Preorganized Receptor I: **Cyclic Porphyrin Trimer**

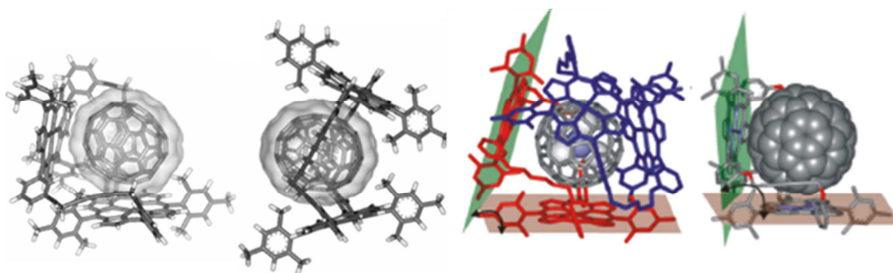


Figure 3.19 Solid state structures of $C_{70}@XLII$, $C_{70}@XLIII$, $Sc_3N@C_{80}@XLII$, $Sc_3N@C_{80}@XLIII$.

The cone-shape orientation is adopted even for the flexible version of the receptor, even though this receptor taking into account that the cavity size and the flexibility of its linkers should be able to encapsulate the fullerenes while keeping the porphyrin units in a cofacial manner. This could indicate that the aryl substituents on the *meso* positions prevent formation of inclusion complexes.

In an attempt to promote encapsulation of C_{84} , a 1:1 mixture of **2** and C_{84} was heated up to 398 K (Figure 3.23). Under these conditions the pendant groups are freely rotating, although the supramolecular complex would be destabilized at such high temperatures. However, this could be compensated by the stabilization coming from the complex formation. Unfortunately, such complex formation did not occur, as evidenced by the 1H -NMR spectra (Figure 3.23) recorded at room temperature, 398 K and after slow cooling down.

3. Preorganized Receptor I: **Cyclic Porphyrin Trimer**

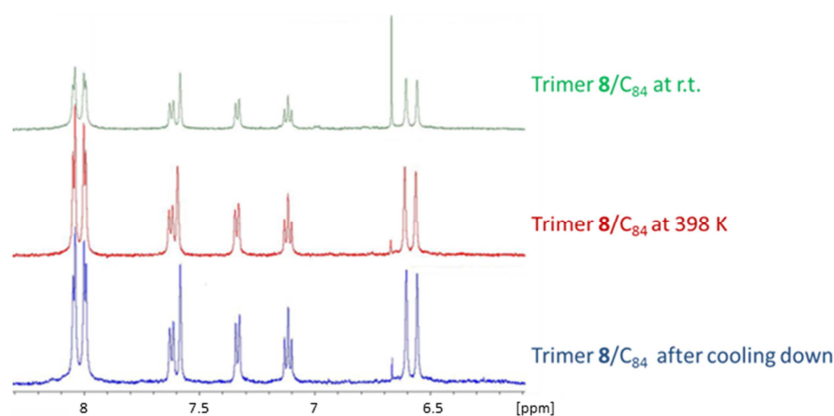


Figure 3.20 Selected region of the $^1\text{H-NMR}$ spectra of a **2** / C_{84} 1:0.5 mixture in toluene, at room temperature, 398 K and one month after cooling down. $[\mathbf{2}] = 1.0 \times 10^{-4}$ M.

3.4 Conclusions

The cyclic porphyrin trimer **2** has been successfully synthesized and characterized.

The formation of inclusion complexes with C_{60} , C_{70} , C_{76} , C_{78} and C_{84} was monitored by means of UV-Vis absorption and fluorescence emission spectroscopic techniques and $^1\text{H-NMR}$ spectroscopy.

Receptor **2** failed to form complexes with most of the guests. No interaction was observed with C_{60} , C_{78} and C_{84} .

Attempts to promote the encapsulation of fullerene C_{84} by heating up the reaction to promote free rotation of the bulky mesityl substituents and then slowly cooling down to room temperature were monitored by $^1\text{H-NMR}$. Such attempts were not successful.

Trimer **2** successfully formed inclusion complex with C_{70} . Although no changes were observed on the absorption spectrum of the receptor, a fluorescence emission titration

3. Preorganized Receptor I: **Cyclic Porphyrin Trimer**

experiment did evidence formation of the C₇₀@**2** host guest inclusion complex. The association was quantified ($K_{ass} = 2.3 \times 10^3 \text{ M}^{-1}$).

Titration experiments performed with C₇₆ indicate a weak complexation of the fullerene. Nevertheless the changes observed were too small to be considered. The association was not quantified.

**Chapter 4: Preorganized Receptor II: A Flexible
Cyclic Porphyrin Trimer**

4. Preorganized Receptor II: Flexible Cyclic Porphyrin Trimer

4.1 Design and Aim of the Project

The aim of this chapter is to prepare a cyclic porphyrin trimer able to form host-guest inclusion complexes with C_{84} and other fullerenes. As reported in chapter 3, the first attempt to prepare a preorganized receptor able to encapsulate C_{84} was not successful, since porphyrin cyclic trimer **2** was unable to encapsulate neither C_{84} nor C_{60} and only showed small indications of C_{70} encapsulation. The presence of bulky *meso*-substituents and the low flexibility of the receptor appear to hamper formation of the host-guest inclusion complex.

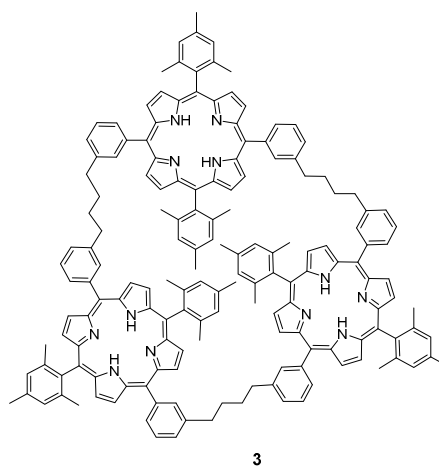


Figure 4.1 Flexible cyclic porphyrin trimer **3**

Two new variations of porphyrin cyclic trimers were thus designed and synthesized in order to overcome the challenge of C_{84} encapsulation. The first strategy is presented in this chapter and is based on the preparation of a flexible analogue of trimer **2** (namely trimer **3**, Figure 4.1). In a second approach, a rigid trimer bearing sterically unhindered *meso*-substituents will be described.⁹³

⁹³ See Chapter 5.

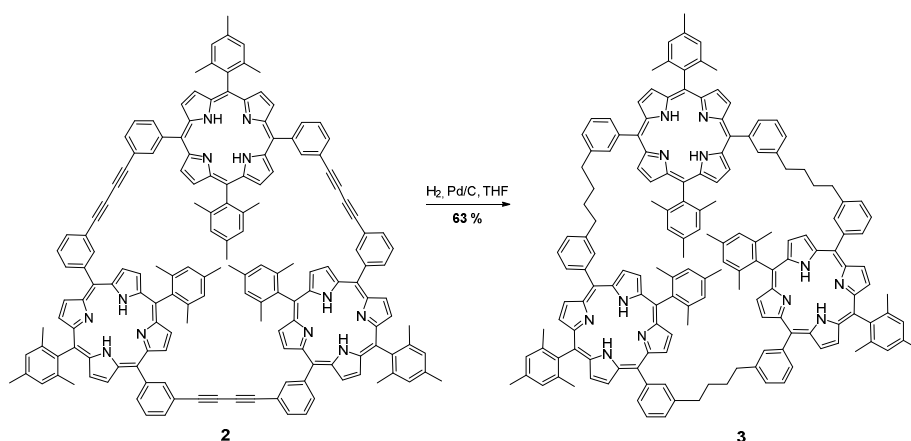
4. Preorganized Receptor II: Flexible Cyclic Porphyrin Trimer

The new target receptor **3** consists of a flexible version of trimer **2** whose synthesis can be simply achieved by palladium catalyzed hydrogenation of trimer **2**. The receptor flexibility is expected to allow the porphyrin units to better adapt to the fullerenes leading to a more successful encapsulation (Figure 4.1).

4.2 Synthesis and Characterization

4.2.1 Synthesis of Cyclic Porphyrin Trimer 3

Trimer **3** was obtained in a 63% yield by palladium catalyzed hydrogenation of the triple bonds of trimer **2** (Scheme 4.1). Alternative methods such as use of a high pressure reactor under 2.5 bar H₂, as reported in the literature⁶⁸, led to trimer **2** degradation. Trimer **3** was obtained with moderate yields when an H₂ balloon was used instead. The reaction progress could not be monitored by TLC due to similar retention factors of educt and product. Instead, filtrated diluted aliquots of the reaction mixture were directly analyzed by HPLC-ms using an ES-MM-APCI+ mass detector.



Scheme 4.1 Synthesis of trimer 3

4. Preorganized Receptor II: Flexible Cyclic Porphyrin Trimer

4.2.2 Characterization of Cyclic Porphyrin Trimer 3

The flexible receptor **3** was characterized by $^1\text{H-NMR}$ spectroscopy and mass spectrometry. The $^1\text{H-NMR}$ receptor shows a certain complexity due to the flexibility of the linkers and its low structural symmetry at 298 K (Figure 4.2).

In the high temperature $^1\text{H-NMR}$ experiments, the broad signals in the aromatic region collapse into major peaks, simplifying the spectrum. The integrals are consistent with the assignments. The N-H proton appears as a multiplet at room temperature. Upon increasing the temperature the N-H signal shifts downfield and gets sharper (Figure 4.2).

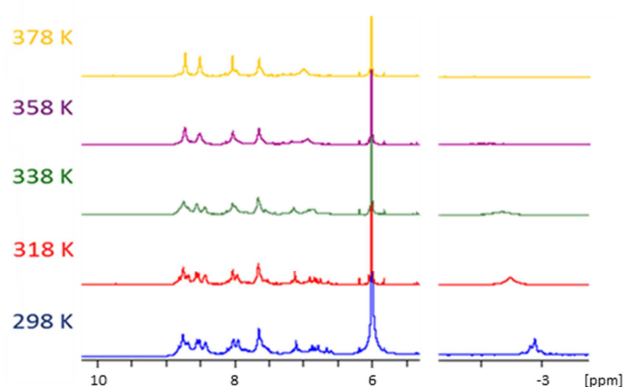


Figure 4.2 Cyclic trimer **3** high temperature $^1\text{H-NMR}$ studies in TCE.

Mass analysis of trimer **3** was performed by means of ESI+ MM-ES+APCI and MALDI-TOF spectroscopic techniques. MALDI-TOF spectrum is shown in Figure 4.3. In the spectrum the mass of the trimer is observed, the isotopic pattern matching the theoretical distribution (trimer **3** mass/z^+ : 2258, 1543, calculated mass/z^+ : 2258, 1670) (Figure 4.3).

4. Preorganized Receptor II: Flexible Cyclic Porphyrin Trimer

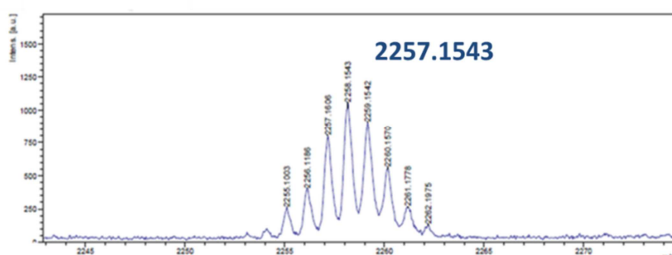


Figure 4.3 MALDI-TOF mass spectrum of the target receptor **3**.

4.3 Results and Discussion

4.3.1 Binding Studies of the Porphyrin Trimer **3** with Fullerenes.

The inclusion complex formation with C_{60} , C_{70} , C_{84} and $Sc_3N@C_{80}$ was studied by means of UV-Vis absorption and fluorescence emission spectroscopy, 1H -NMR spectroscopy and mass spectrometry.

Binding Studies of Trimer **3** with C_{60}

UV-Vis absorption and fluorescence emission titration experiments did not show any evidence of interaction with C_{60} (Figure 4.4).

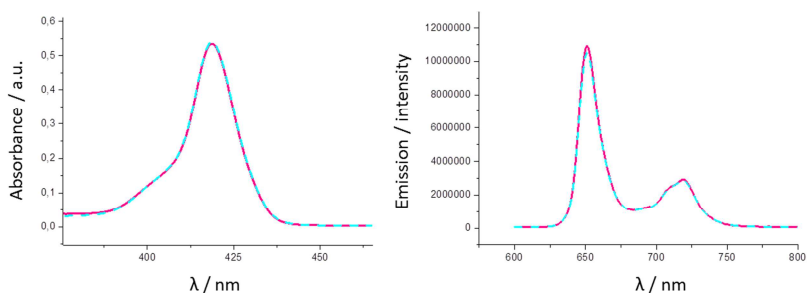


Figure 4.4 UV-Vis and fluorescence emission complexation experiments with C_{60} . Free receptor **3** (purple line); **3** + 23 eq. C_{60} (blue dashed line). $[3] = 1.0 \times 10^{-6}$ M.

4. Preorganized Receptor II: Flexible Cyclic Porphyrin Trimer

However, some quite small changes were observed in the trimer **3** $^1\text{H-NMR}$ spectrum after addition of 1 equivalent of C_{60} to a receptor solution at 10^{-4} M (Figure 4.5).

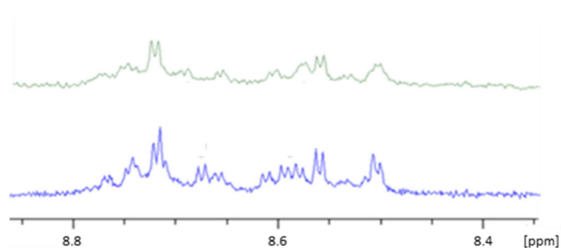


Figure 4.5 Selected regions of the $^1\text{H-NMR}$ spectra of the free receptor **3** and $3/\text{C}_{60}$ 1:1 mixture in toluene. $[\mathbf{3}] = 10^{-4}$ M

Also, mass analysis of 1:1 and 1:15 mixtures of the receptor and the fullerene evidenced formation of an inclusion complex. Both the masses of the free host and the 1:1 complex were identified. The masses appear double protonated (free receptor mass/ z^+ : 1129,4, calculated mass/ z^+ : 1130,2; complex mass / z^+ : 1489,9, calculated mass/ z^+ : 1490,1) (Figure 4.6).

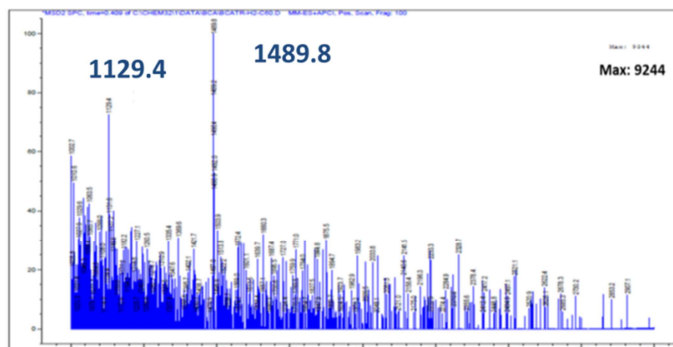


Figure 4.6 MM-ES+APCI spectrum of the 1:1 trimer $3/\text{C}_{60}$ mixture

4. Preorganized Receptor II: Flexible Cyclic Porphyrin Trimer

Binding Studies of Trimer 3 with C₇₀

Complexation of C₇₀ was also studied by means of UV-Vis absorption and fluorescence emission spectroscopy. Like for C₆₀, no changes in the absorption spectra of the receptor (Figure 4.7) were observed upon increasing the ratio of C₇₀.

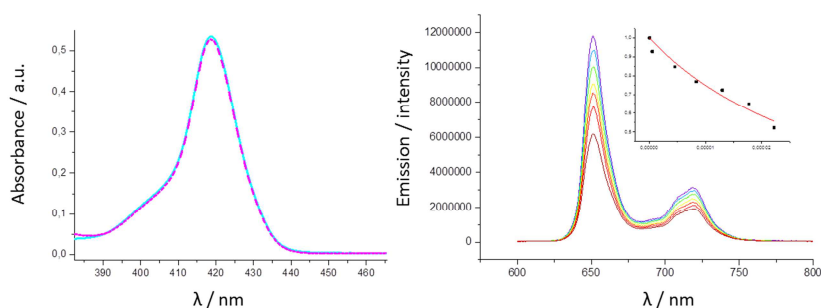


Figure 4.7 Left: UV-Vis absorption complexation experiments with C₇₀; free receptor **3** (pink line); **3** + 23 eq. C₇₀ (blue dashed line) [**3**] = 1.0 × 10⁻⁶ M. Right: fluorescence emission titration experiment; [**3**] = 1.0 × 10⁻⁶ M; [C₇₀]_w = 5.0 × 10⁻⁵ M; Final host/guest ratio added = 1:23; inset: fluorescence emission titration data (change in intensity at 651 nm) for the binding of trimer **3** with C₇₀ in toluene fitted to the theoretical binding curves for a simple 1:1 complexation model.

However, quenching of the fluorescence emission intensity did indicate interaction and inclusion complex formation. The association constant was quantified from the nonlinear fitting of the fluorescence emission titration data to a 1:1 complexation model ($K_{\text{ass}} = 2.8 \times 10^4 \text{ M}^{-1}$).

The ¹H-NMR spectrum of the 1:1 10⁻⁴ M solution with C₇₀ was recorded. Small changes on the aromatic region of the porphyrins were observed, indicating interaction (Figure 4.8). Mass analysis of the receptor C₇₀ mixture confirmed the formation of the 1:1 inclusion complex with C₇₀. Both the masses of the free host and the 1:1 complex were identified. The masses appear double protonated (free receptor mass/z⁺: 1129.8, calculated mass/z⁺: 1130.2; complex mass / z⁺: 1550.1, calculated mass/z⁺:1550.12;) (Figure 4.9).

4. Preorganized Receptor II: Flexible Cyclic Porphyrin Trimer

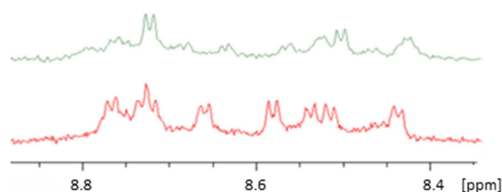


Figure 4.8 Selected regions of the $^1\text{H-NMR}$ spectra of the free receptor **3** and **3/C₇₀** 1:1 mixture in toluene. $[\mathbf{3}] = 10^{-4}$ M

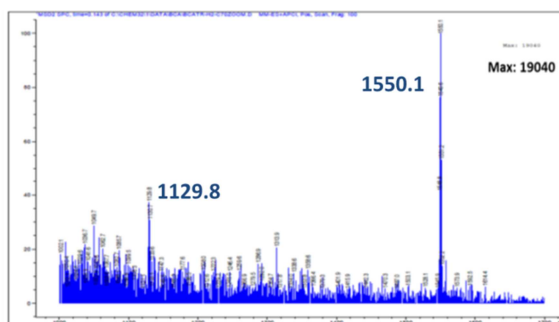


Figure 4.9 MM-ES+APCI spectrum of the 1:1 trimer **3/C₇₀** mixture

Binding studies of Trimer **3** with **C₈₄**

The inclusion complex formation with **C₈₄** was studied and characterized by UV-Vis absorption and fluorescence emission spectroscopy, $^1\text{H-NMR}$ spectroscopy and mass spectrometry.

Very small quenching of the *Soret* band was observed during the UV-Vis absorption titration experiment, indicating interaction with the fullerene (Figure 4.10).

In the fluorescence emission titration experiment significant quenching of the intensity confirmed the formation of an inclusion complex. The association was quantified from the nonlinear fitting of the titration data to a 1:1 complexation model ($K_{\text{ass}} = 6.1 \cdot 10^4 \text{ M}^{-1}$) (Figure 4.10).

4. Preorganized Receptor II: Flexible Cyclic Porphyrin Trimer

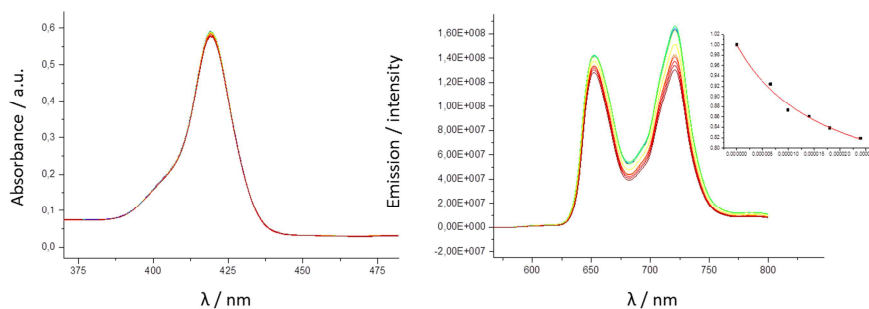


Figure 4.10 Absorption and fluorescence emission titration experiments of receptor **3** with C_{84} . $[3] = 1.0 \times 10^{-6}$ M; $[C_{84}]_w = 1.5 \times 10^{-5}$ M; Final host/guest ratio added = 1:24; insets: fluorescence emission titration data (change in intensity at 721 nm; right) for the binding of trimer **3** with C_{84} in toluene fitted to the theoretical binding curves for a simple 1:1 complexation model.

Mass analysis of receptor **3** and C_{84} mixture confirmed the formation of the 1:1 inclusion complex with C_{84} . Both the masses of the free host and the 1:1 complex were identified. The masses appear double protonated (free receptor mass/ z^+ : 1130,1, calculated mass/ z^+ : 1130,2; complex mass/ z^+ : 1633,2, calculated mass/ z^+ : 1634,1;) (Figure 4.11)

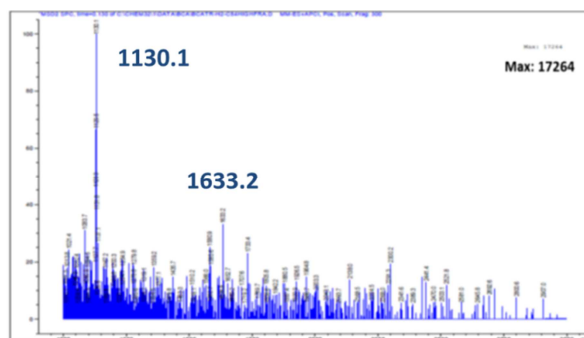


Figure 4.11 MM-ES+APCI spectrum of the 1:1 trimer **3**/ C_{84} mixture

4. Preorganized Receptor II: Flexible Cyclic Porphyrin Trimer

Binding Studies of Trimer **3** with Sc₃N@C₈₀

Regarding encapsulation of Sc₃N@C₈₀, results obtained from both UV-Vis absorption and fluorescence emission titrations indicated formation of an inclusion complex with the endohedral fullerene (Figure 4.12).

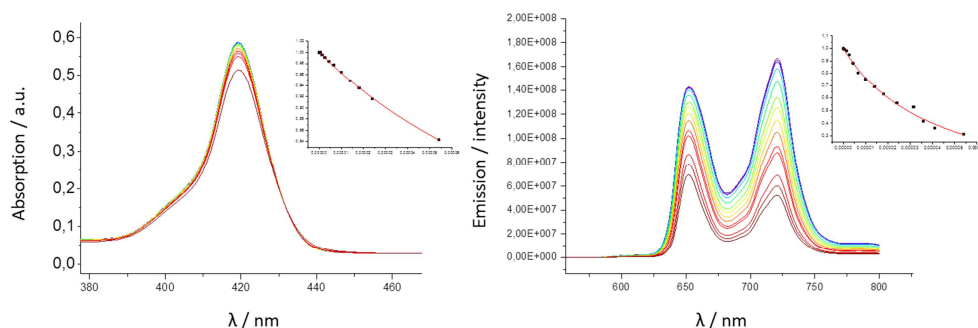


Figure 4.12 Absorption and fluorescence emission titration experiments of receptor **3** with C₈₄. [**3**] = 1.0 × 10⁻⁶ M; [C₈₄]_w = 1.5 × 10⁻⁵ M; Final host/guest ratio added = 1:50; inlets: UV-visible titration data (change in absorbance at 419; left) and fluorescence emission titration data (change in intensity at 721 nm; right) for the binding of **3** with C₈₄ in toluene fitted to the theoretical binding curves for a simple 1:1 complexation model.

On the UV-Vis absorption titration experiment, both the small quenching of the *Soret* band, as well as the emergence of a new band at 440 nm confirmed the inclusion. An isosbestic point was detected at 431 nm. The association constant was calculated from the nonlinear fitting of the changes on the absorption titration data to a 1:1 complexation model ($K_{\text{ass}} = 7 \times 10^3 \text{ M}^{-1}$).

In the fluorescence emission titration experiment considerable quenching of the emission intensity was observed upon addition of the endohedral fullerene, which confirmed the formation of the complex. The association constant was calculated from the nonlinear fitting of the changes on the fluorescence emission titration data to a 1:1 complexation model ($K_{\text{ass}} = 2.5 \times 10^4 \text{ M}^{-1}$).

4. Preorganized Receptor II: Flexible Cyclic Porphyrin Trimer

4.3.2 Summary and Discussion

The flexible receptor **3** bearing saturated linkers and mesityl pendant groups at the *meso* positions of the porphyrin units, unlike its rigid version **2**, was able to interact with C₇₀, C₈₄ and Sc₃N@C₈₀ and only failed to form inclusion complexes with C₆₀ at a receptor concentration of 10⁻⁶ M. The results are summarized in Table 4.1.

Table 4.1 Summary of the receptor **3** complexation studies with the different carbon guests.

Entry	Guest	Binding	$K_{\text{ass}}^{\text{q}}$ [x 10 ⁻⁴ M ⁻¹]	$K_{\text{ass}}^{\text{a}}$ [x 10 ⁻⁴ M ⁻¹]	$K_{\text{ass}}^{\text{f}}$ [x 10 ⁻⁴ M ⁻¹]
1	C ₆₀	✓	n.d.	n.d.	n.d.
2	C ₇₀	✓	n.d.	n.d.	2.8
3	C ₈₄	✓	n.d.	n.d.	6.1
4	ScN ₃ @C ₈₀	✓	0.7	n.d.	2.5

$K_{\text{ass}}^{\text{q}}$ = association constant calculated from the absorbance quenching; $K_{\text{ass}}^{\text{a}}$ = association constant calculated from the absorbance increase; $K_{\text{ass}}^{\text{f}}$ = association constant calculated from the fluorescence emission quenching data.

Porphyrin trimer **3**, despite having flexible linkers and a poor preorganization, still has a sizable inner space controlled by the three interlocked porphyrin subunits. The resulting minimum cavity might be too large for all three porphyrin units to simultaneously interact with the C₆₀. Probably for this reason, no interaction with C₆₀ was observed at 10⁻⁶ M.

Trimer **3** was indeed able to discriminate major fullerene C₆₀ from larger fullerenes merely by size. This is an advantage with respect to porphyrin dimers. In general

4. Preorganized Receptor II: **Flexible Cyclic Porphyrin Trimer**

flexible porphyrin dimers are able to adapt to small guests by adjusting the two porphyrin subunits to the fullerenes in a co-facial manner. The cavity size in porphyrin dimers can only be regulated by the length and flexibility of its linkers. Thus, the minimum cavity size cannot be regulated.

Trimer **3** despite having bulky mesityl-*meso* substituents that might hamper the fullerene guests to properly enter the receptor cavity is still able to interact with the fullerenes. Its less restrained geometry when compared with its rigid analog **2** allows the porphyrin units to adapt and interact with the fullerenes despite the bulky restricted cavity.

Regarding the calculated association constants for the encapsulation of the different fullerenes, trimer **3** showed the highest affinity towards the encapsulation of C₈₄ ($K_{\text{ass}} = 6.1 \times 10^{-4}$ M).

The association calculated for Sc₃N@C₈₀ ($K_{\text{ass}} = 2.5 \times 10^{-4}$ M) was found to be smaller than that for C₈₄ and comparable to the association calculated for the encapsulation of C₇₀ ($K_{\text{ass}} = 2.8 \times 10^{-4}$ M). These results contradict the preferred supramolecular interaction between porphyrins and endohedral fullerenes over smaller empty fullerenes reported in the literature.^{51, 58, 68} The low association could be related to the presence of the bulky substituents that would not allow proper interaction between the porphyrin units and the fullerene.

4.4 Conclusions

The cyclic porphyrin trimer **3** has been successfully synthesized and characterized.

The formation of inclusion complexes with C₆₀, C₇₀, C₈₄ and ScN₃@C₈₀ was monitored by means of UV-Vis absorption and fluorescence emission spectroscopic techniques, ¹H-NMR spectroscopy and mass spectrometry.

4. Preorganized Receptor II: **Flexible Cyclic Porphyrin Trimer**

Receptor **3** was able to successfully encapsulate C_{70} , C_{84} and $ScN_3@C_{80}$ at a receptor concentration of 10^{-6} M. No interaction was observed with the major fullerene (C_{60}) at that concentration; nevertheless both 1H -NMR spectroscopy and mass spectrometry evidenced such interaction at a receptor concentration of 10^{-4} M.

The association constants for the encapsulation of C_{70} , C_{84} and $Sc_3N@C_{80}$ were quantified in toluene from both the UV-Vis absorption and the fluorescence emission titration experiments.

Despite the general trend reported for porphyrins and porphyrin-based receptors, the association calculated for $Sc_3N@C_{80}$ was found to be on the same range than that found for C_{70} . The association constant calculated for C_{84} was found to double the values calculated for C_{70} and $Sc_3N@C_{80}$.

**Chapter 5: Preorganized Receptor III: A Sterically
Unhindered Cyclic Porphyrin Trimer**

UNIVERSITAT ROVIRA I VIRGILI

CYCLOTRIVERATRYLENE AND PORPHYRIN SCAFFOLDS FOR MOLECULAR RECOGNITION AND SELF-ASSEMBLY

Berta Camafort Blanco

Dipòsit Legal: T 677-2015

5. Preorganized Receptor III: A Sterically Unhindered Cyclic Porphyrin Trimer

5.1 Design and Aim of the Project

The aim of this chapter is to prepare a cyclic porphyrin trimer able to form host-guest inclusion complexes with C_{84} and other fullerenes. As reported in chapter 3, the first attempt to prepare such a preorganized receptor was not successful, since porphyrin cyclic trimer **2** was unable to encapsulate neither C_{84} nor C_{60} and only showed small indications for C_{70} encapsulation. Two main receptor characteristics, the presence of bulky *meso*-substituents and the low flexibility of the receptor linkers, were likely the reasons for this lack of interaction. In chapter 4, trimer **3** bearing flexible saturated linkers was synthesized and showed to be able to form host-guest inclusion complexes with C_{70} , C_{84} and $ScN_3@C_{80}$.

In this chapter, two different cyclic porphyrin-based receptors **4** and **5** bearing no *meso*-substituents or substituents with low steric demand, respectively, were designed to facilitate encapsulation of C_{84} .

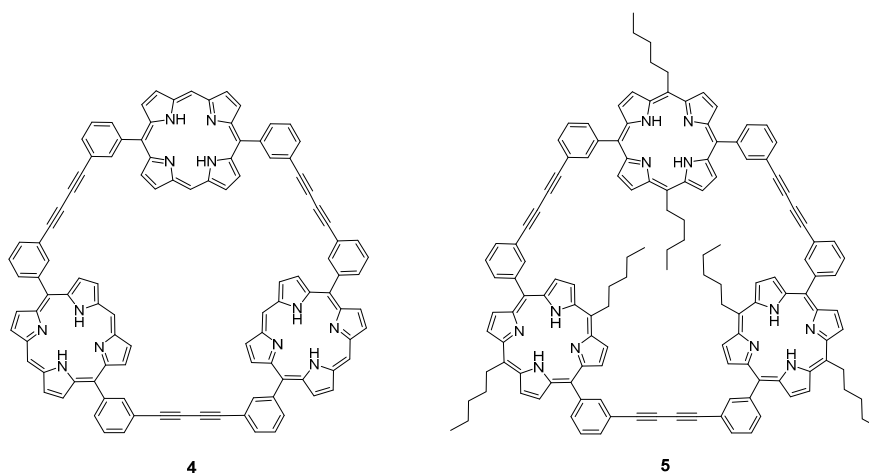


Figure 5.1 *Meso*-unsubstituted cyclic porphyrin trimer **4** and *meso*-pentyl-substituted cyclic porphyrin trimer **5**.

5. Preorganized Receptor III: A Sterically Unhindered Cyclic Porphyrin Trimer

Within trimer **4**, the *trans*-A₂B₂-type porphyrin building block is functionalized with two 3-ethynylphenyl *meso*-substituents, the remaining *meso*-positions being unsubstituted.

Trimer **5** *trans*-A₂B₂-type porphyrin building block is functionalized with four *meso*-substituents. Two of those substituents consist of 3-ethynylphenyl groups designed to connect the porphyrin units within trimer **5**. The porphyrin units are further equipped with sterically unhindered pentyl groups at their *meso* positions.

In this chapter, the synthesis, characterization and inclusion complex formation of **4** and **5** with fullerenes is discussed.

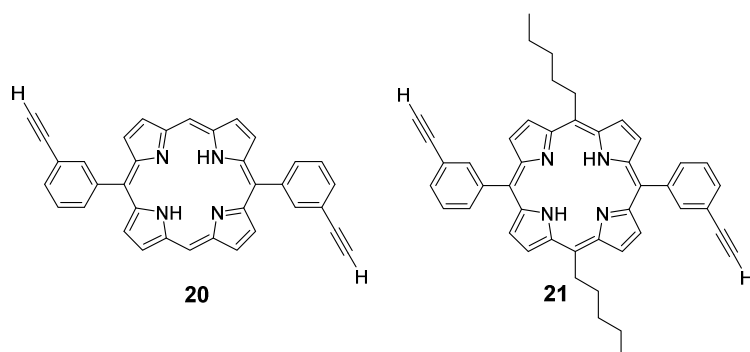


Figure 5.2 *trans*-A₂B₂-porphyrin building blocks **20** and **21**

5.2 Synthesis and Characterization

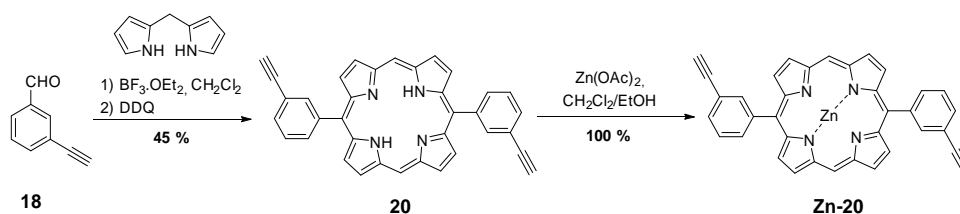
5.2.1 Synthesis of Cyclic Porphyrin Trimer **4**

The synthesis of the *meso*-unsubstituted porphyrin cyclic trimer **4** was initially attempted.

5. Preorganized Receptor III: A Sterically Unhindered Cyclic Porphyrin Trimer

Synthesis of Zinc-Metallated Porphyrin Building Block Zn-20

Porphyrin **20** was synthesized through acid catalyzed condensation of commercially available dipyrromethane and 3-ethynylbenzaldehyd followed by oxidation with DDQ. The desired porphyrin was obtained in a moderate yield. The porphyrin was then quantitatively metallated with zinc acetate.



Scheme 5.1 Synthesis of zinc metallated ligand Zn-20.

The porphyrin building block **20** was characterized by $^1\text{H-NMR}$ spectroscopy and mass spectrometry. The $^1\text{H-NMR}$ spectrum is shown in Figure 5.3.

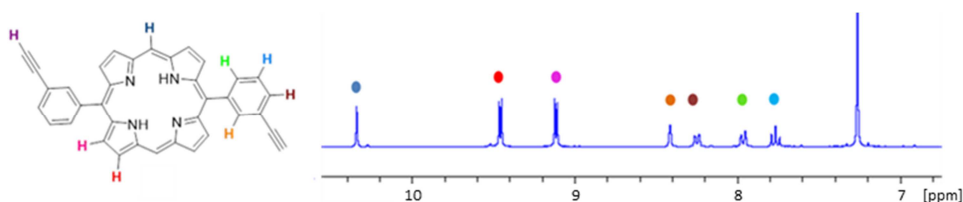


Figure 5.3 $^1\text{H-NMR}$ spectrum selected region of **20** in CDCl_3 .

Mass analysis of porphyrin **20** was performed by means MM-ES+APCI spectroscopy (**20** mass/ z^+ : 506.5, calculated mass/ z^+ : 510.1) (Figure 5.4).

5. Preorganized Receptor III: A Sterically Unhindered Cyclic Porphyrin Trimer

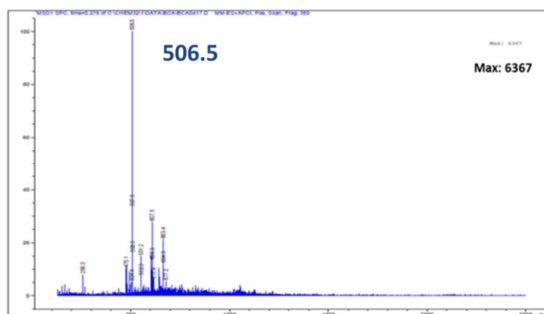


Figure 5.4 MMES+APCI mass spectrum of **20**.

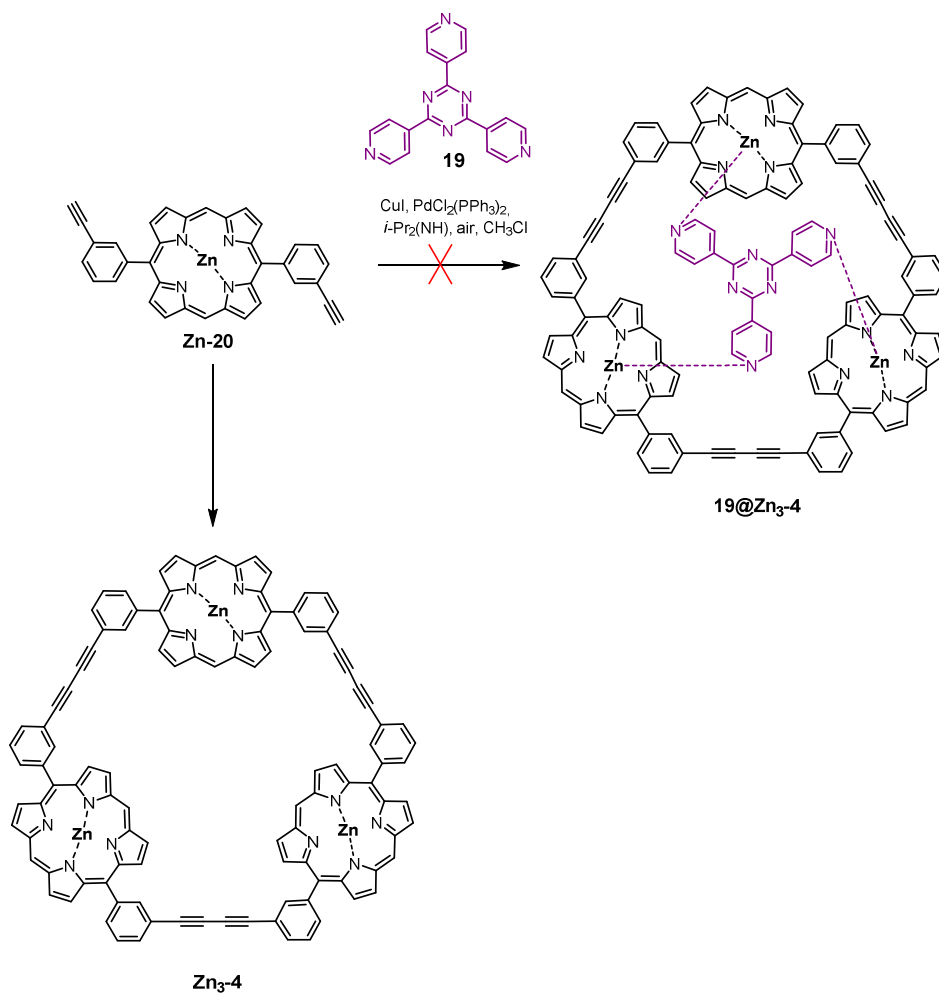
Synthesis of Cyclic Porphyrin Trimer **4**

Attempts to prepare the desired unsubstituted trimer **4** in a reasonable yield failed. Use of the procedure reported previously for the synthesis of cyclic porphyrin receptor **2** led only to traces of the template-free receptor. No indication of template directed trimer formation was observed.

In attempts to promote the template directed synthesis of the receptor **4**, a highly diluted solution of template **19** was added dropwise into a concentrated solution of porphyrin monomer. In this way the ratio of porphyrin ligand over the ratio of template **19** is maximized, forcing complexation of the template prior to coupling of the terminal alkynes.

This strategy led again to the formation of traces of the template-free receptor **4**. The synthesis of **4** in the absence of template **19** led to formation of the same amount of free receptor **4** as obtained through the template-directed strategy.

5. Preorganized Receptor III: A Sterically Unhindered Cyclic Porphyrin Trimer



Scheme 5.2 Synthetic attempts of cyclic porphyrin trimer **4**.

5.2.2 Synthesis of Cyclic Porphyrin Trimer **5**

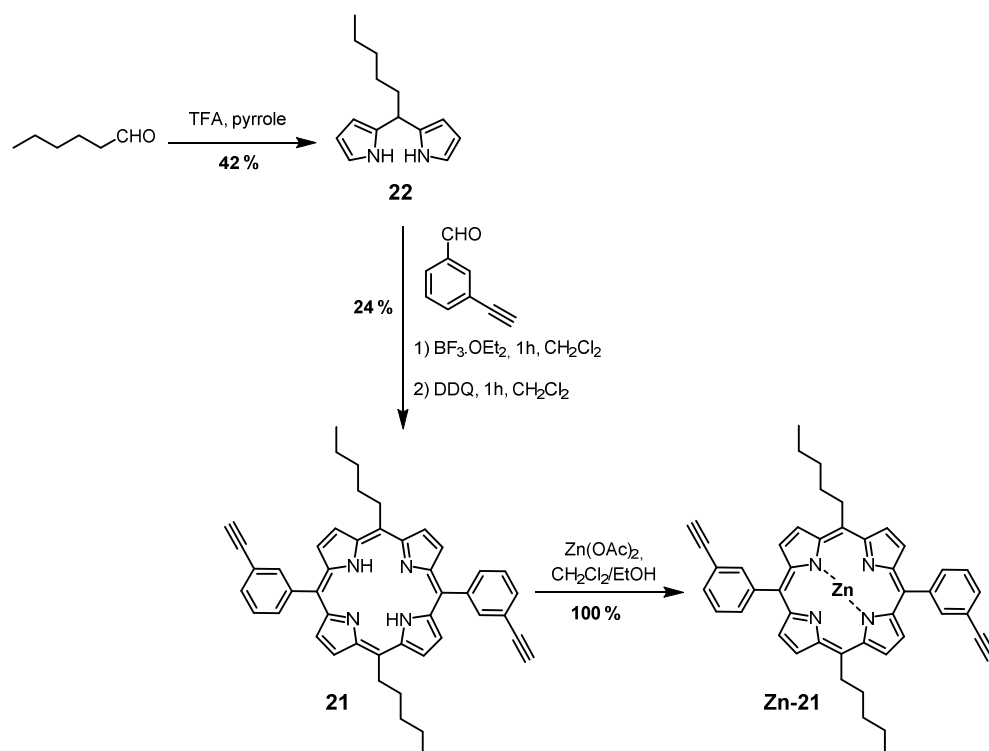
Trimer **5** bearing pentyl groups in *meso* position was then synthesized.

5. Preorganized Receptor III: A Sterically Unhindered Cyclic Porphyrin Trimer

Synthesis of Zinc-Metallated Porphyrin Building Block Zn-21

The synthesis of porphyrin trimer **5** started with the preparation of the dipyrrohexane **22**. Since both starting materials, pyrrole and hexanal, are liquid the isolation of the dipyrrohexane resulting from condensation in aqueous HCl solution was in this case not very efficient (conditions (b), Table 3.1). Moreover, the yield was considerably lower (24 %) than when a large excess of pyrrole and TFA (42 %) were employed (conditions (a), Table 3.1).

Acid catalyzed condensation of two equivalents of pyrrole and one equivalent of hexanal in the presence of TFA gave the desired dipyrrohexane **21** in reasonable yields.



Scheme 5.3 Synthesis of zinc-metallated porphyrin ligand **Zn-21**

5. Preorganized Receptor III: A Sterically Unhindered Cyclic Porphyrin Trimer

The hexane substituted porphyrin **21** was obtained in moderate yield through acid catalyzed condensation of commercially available 3-ethynylbenzaldehyde and dipyrrohexane followed by oxidation with DDQ. The porphyrin was then quantitatively metallated with zinc acetate

The porphyrin monomer was characterized by $^1\text{H-NMR}$ spectroscopy and mass spectrometry. The $^1\text{H-NMR}$ spectrum of porphyrin building block **21** is shown in Figure 5.3.

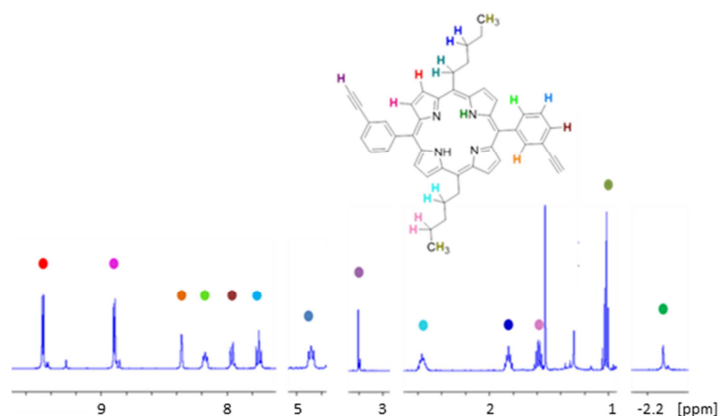


Figure 5.5 $^1\text{H-NMR}$ spectrum of the porphyrin building block **21** in CDCl_3

Mass analysis of metallated porphyrin **21** was performed by means of ESI+ mass spectrometry (**21** mass/ z^+ : 712.2512, calculated mass/ z^+ : 712.2544) (Figure 5.6).

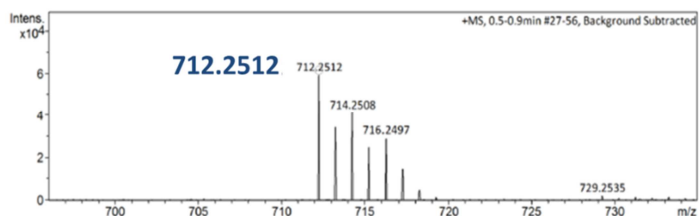


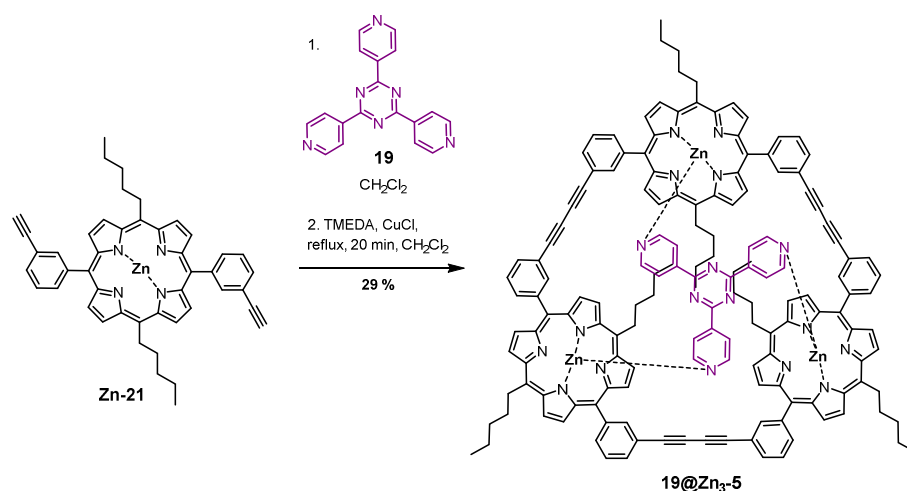
Figure 5.6 ESI+ mass spectra of the **21**.

5. Preorganized Receptor III: A Sterically Unhindered Cyclic Porphyrin Trimer

Synthesis of Cyclic Porphyrin Trimer 5

Porphyrin trimer **5** was prepared by template directed homocoupling of the metallated porphyrin **Zn-21**. Dropwise addition of template **19** in a highly diluted solution over a concentrated porphyrin ligand **21** solution followed by coupling of the terminal alkynes gave the desired complexed trimer **19@Zn₃-5** in moderate yields.

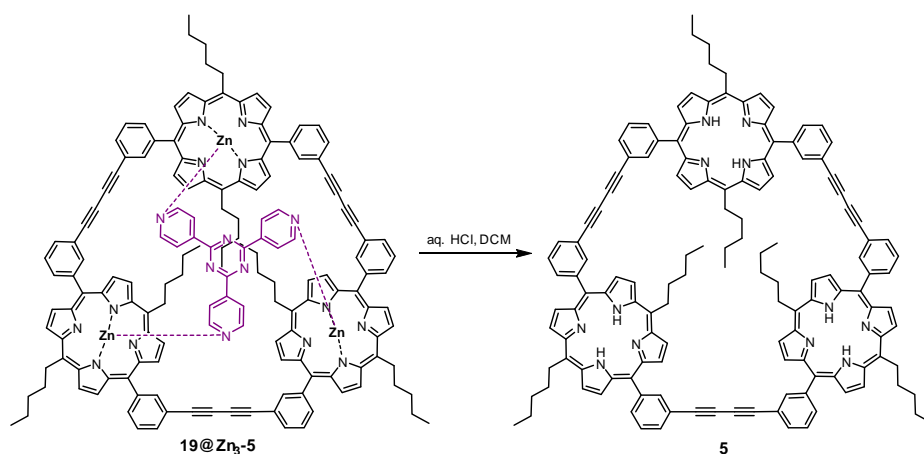
The *Sonogashira*-based conditions used previously were rejected in this case, because it was not possible to separate the oxidized catalyst employed for the coupling from the desired receptor. *Hay's* coupling conditions were used instead. Aqueous washings and filtration was the only purification required after refluxing the complex with TMEDA and CuCl for 20 min. Despite some concerns about TMEDA acting as a competing template to promote the formation of the porphyrin dimer, no such dimer was observed.



Scheme 5.4 Template directed synthesis of the **19@Zn₃-5**.

The template was released by protonation of the pyrrole with HCl to give the desired free-base porphyrin trimer **5** quantitatively.

5. Preorganized Receptor III: A Sterically Unhindered Cyclic Porphyrin Trimer



Scheme 5.5 Synthesis of cyclic porphyrin trimer **5**: Template removal.

5.2.3 Characterization of Cyclic Porphyrin Trimer **5**

The porphyrin trimer **5** was characterized by ¹H-NMR spectroscopy (Figure 5.7) and MALDI-TOF mass spectrometry.

The ¹H-NMR spectrum of receptor **5** shows a considerable complexity. This accounts for the flexibility of the receptor. Unlike for *meso*-mesityl-substituted porphyrins, where the bulky groups prevent movements of the porphyrin subunits within the trimer, the absence of bulky substituents allows the porphyrin units within trimer **5** to almost freely twist, leading to a more complicated spectrum. The integrals are consistent with the trimer. Aromatic region of the ¹H-NMR is shown in Figure 5.7

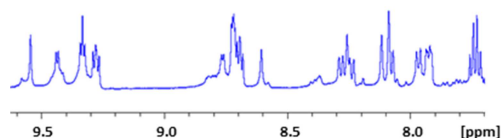


Figure 5.7 ¹H-NMR spectrum selected region of **5** in CDCl₃.

5. Preorganized Receptor III: A Sterically Unhindered Cyclic Porphyrin Trimer

Mass analysis of pentyl *meso*-substitute trimer **5** was performed by MALDI-TOF spectrometry (**5** mass/ z^+ : 1945.9748, calculated mass/ z^+ : 1945.9792) (Figure 5.8).

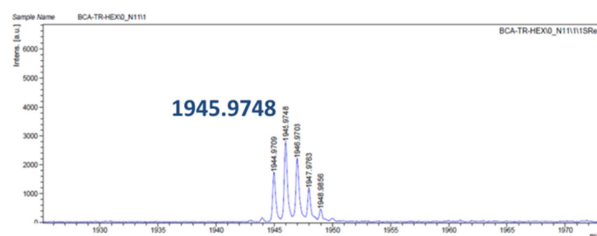


Figure 5.8 MALDI-TOF mass spectra of the porphyrin cyclic trimer **5**.

5.3 Results and Discussion

5.3.1 Binding Studies of the Porphyrin Trimer **5** with Fullerenes

Complexation studies were performed with C_{60} , C_{70} , C_{84} , $Sc_3N@C_{80}$ as well as a single walled carbon nanotube (SWCNT) and a bucky onion mixture, likely containing $C_{60}@C_{240}$. Inclusion complexes formation was monitored by UV-Vis absorption and fluorescence emission spectroscopy, 1H -NMR spectroscopy and mass spectrometry.

Binding Studies of Trimer **5** with C_{60}

No interaction between *meso*-pentyl-substituted trimer **5** and the major fullerene was observed. Continuous addition of C_{60} to a 10^{-6} M receptor solution did not cause any changes to neither the UV-Vis absorption nor the fluorescence emission spectra of the host.

5. Preorganized Receptor III: A Sterically Unhindered Cyclic Porphyrin Trimer

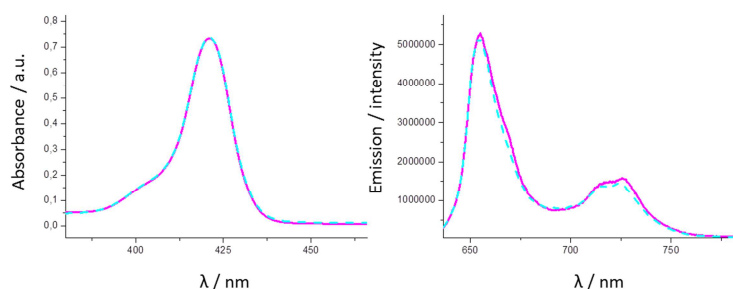


Figure 5.9 UV-Vis and fluorescence emission complexation experiments with C_{60} . Free receptor **5** (purple line); **5** + 17 eq. C_{60} (blue dashed line). $[5] = 1.0 \times 10^{-6}$ M.

However, ESI+ mass spectrometry of a trimer **5** / C_{60} mixture did indicate the formation of 1:1 complex. Both masses of the free host and the 1:1 complex were identified. The masses appear double protonated (Free receptor mass/ z^+ : 974.4; calculated mass/ z^+ : 974.0; complex C_{60} @**5** mass/ z^+ : 1334.0, calculated mass/ z^+ : 1334.0).

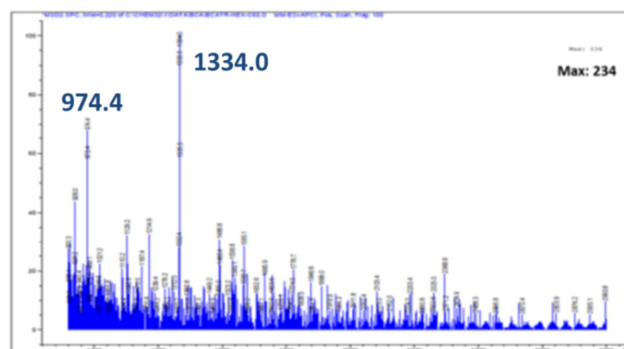


Figure 5.10 MMES+APCI mass spectra of the 1:1 **5** / C_{60} .

Binding Studies of Trimer **5** with C_{70}

Complexation of C_{70} was monitored by both UV-Vis absorption and fluorescence emission titration experiments.

5. Preorganized Receptor III: A Sterically Unhindered Cyclic Porphyrin Trimer

In the UV-Vis absorption titration experiment, quenching of the *Soret* band and the appearance of a new band corresponding to the absorption band of the complex formed at 436 nm evidenced interaction with the fullerene. The isosbestic point was observed at 428 nm. The association was quantified from the nonlinear fitting of both the quenching of the *Soret* band and the increasing absorption of the complex to a 1:1 complexation model ($K_{\text{ass}} = 9.7 \times 10^3 \text{ M}^{-1}$, $2.0 \times 10^4 \text{ M}^{-1}$).

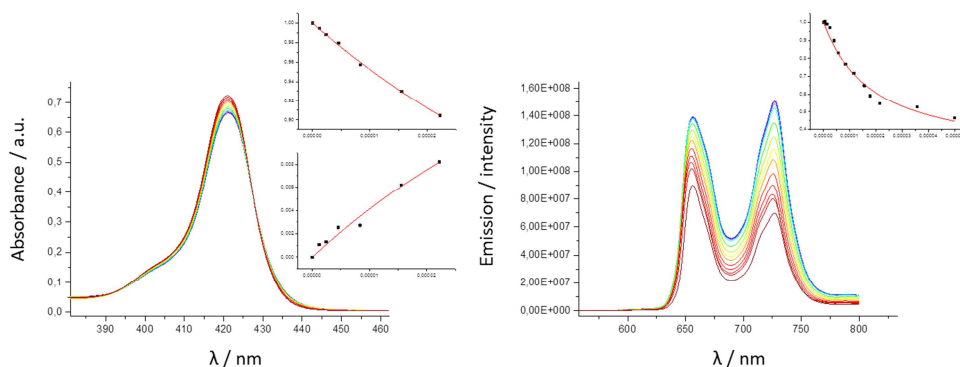


Figure 5.11 Absorption and fluorescence emission titration experiments of receptor **5** with C_{70} . $[\mathbf{5}] = 1.0 \times 10^{-6} \text{ M}$; $[\text{C}_{70}]_{\text{w}} = 5.0 \times 10^{-5} \text{ M}$; Final host/guest ratio added = 1:50; Inlets: UV-visible titration data (change in absorbance at 421 and 438 nm; left) and fluorescence emission titration data (change in intensity at 656 nm; right) for the binding of trimer **5** with C_{60} in toluene fitted to the theoretical binding curves for a simple 1:1 complexation model.

In the fluorescence emission titration experiment, quenching of the emission intensity was observed upon addition of the fullerene, indicating the formation of a complex with the fullerene. The association was quantified from the nonlinear fitting of the titration data to a 1:1 complexation model ($K_{\text{ass}} = 2.5 \times 10^4 \text{ M}^{-1}$). The associations calculated from both the absorption and the fluorescence titration experiments were in agreement with each other.

Mass analysis of the receptor **5** / C_{70} mixture confirmed the formation of the 1:1 complex with C_{70} . Both the masses of the free host and the 1:1 complex were identified. The masses appear double protonated (free receptor **5** mass/ z^+ : 974.0,

5. Preorganized Receptor III: A Sterically Unhindered Cyclic Porphyrin Trimer

calculated mass/ z^+ : 974.0; complex **C**₇₀@**5** mass / z^+ : 1394.3, calculated mass/ z^+ : 1394.0).

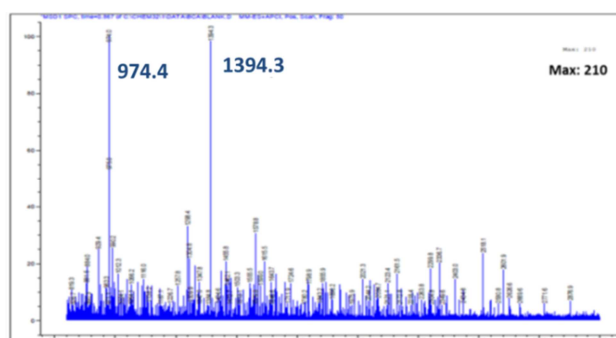


Figure 5.12 MM-ES+APCI spectrum of the 1:1 trimer **5** / **C**₇₀ mixture.

Binding Studies of Trimer **5** with **C**₈₄

Complex formation with **C**₈₄ was evidenced and characterized by UV-Vis absorption and fluorescence emission spectroscopy, ¹H-NMR spectroscopy and mass spectrometry.

In the case of **C**₈₄, a significant quenching and a small bathochromic shift of the *Soret* band were observed. A new band appeared at 437 nm, corresponding to the absorption band of the complex formed. An isosbestic point was observed at 429 nm. The association constant was quantified from the nonlinear fitting of the absorption titration data to a 1:1 complexation model ($K_{\text{ass}} = 3.8 \times 10^4 \text{ M}^{-1}$; $1.3 \times 10^4 \text{ M}^{-1}$).

5. Preorganized Receptor III: A Sterically Unhindered Cyclic Porphyrin Trimer

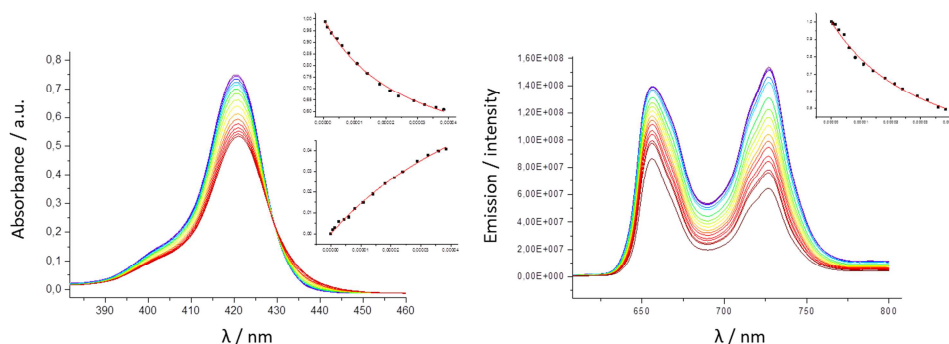


Figure 5.13 Absorption and fluorescence emission titration experiments of receptor **5** with C_{70} . $[5] = 1.0 \times 10^{-6} \text{ M}$; $[C_{84}]_w = 5.4 \times 10^{-5} \text{ M}$; Final host/guest ratio added = 1:38; inlets: UV-visible titration data (change in absorbance at 421 and 437 nm; left) and fluorescence emission titration data (change in intensity at 727 nm; right) for the binding of trimer **5** with C_{84} in toluene fitted to the theoretical binding curves for a simple 1:1 complexation model.

In the fluorescence emission titration experiment, strong quenching of the emission intensity was observed upon increasing the ratio of C_{84} , confirming formation of a strong complex with the fullerene. The association was quantified from the nonlinear fitting of the fluorescence emission titration data to a 1:1 complexation model ($K_{\text{ass}} = 2.9 \times 10^4 \text{ M}^{-1}$). The associations calculated from both the absorption and the fluorescence titration experiments were found to be in agreement with each other.

Mass analysis of the receptor **5** / C_{84} mixture confirmed the formation of the 1:1 inclusion complex with C_{70} . Both the masses of the free host and the 1:1 complex were identified. The masses appear double protonated (free receptor **5** mass/ z^+ : 973.2, calculated mass/ z^+ : 974.0; complex $C_{84}@5$ mass / z^+ : 1479.4, calculated mass/ z^+ : 1478.0).

5. Preorganized Receptor III: A Sterically Unhindered Cyclic Porphyrin Trimer

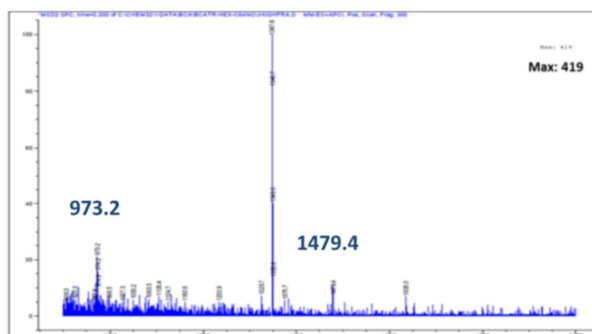


Figure 5.14 MM-ES+APCI spectrum of the 1:1 trimer **5** / C₈₄ mixture.

Binding Studies of the Trimer **5** with Sc₃N@C₈₀

Regarding Sc₃N@C₈₀, complex formation was evidenced by both UV-Vis absorption and fluorescence emission titration experiments with high association.

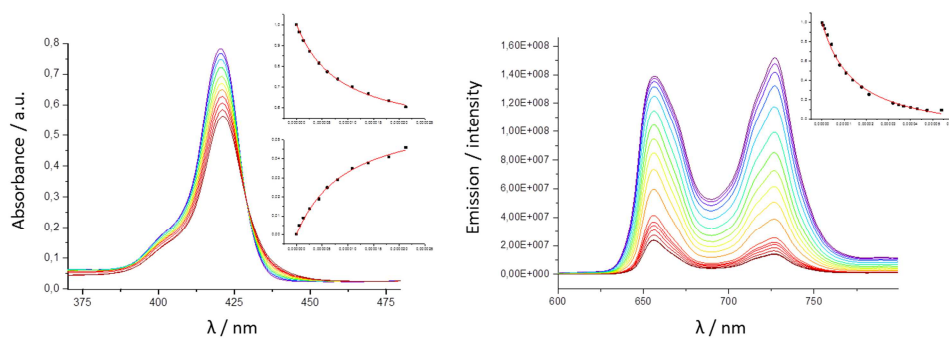


Figure 5.15 Absorption and fluorescence emission titration experiments of receptor **5** with C₇₀. [5] = 1.0 × 10⁻⁶ M; [Sc₃N@C₈₀]_w = 5.4 × 10⁻⁵ M; Final host/guest ratio added = 1:38; insets: UV-visible titration data (change in absorbance at 421 and 437 nm; left) and fluorescence emission titration data (change in intensity at 727 nm; right) for the binding of trimer **5** with Sc₃N@C₈₀ in toluene fitted to the theoretical binding curves for a simple 1:1 complexation model.

In the UV-Vis absorption titration experiment significant quenching and small red shift of the *Soret* band were observed. A new band appeared at 438 nm corresponding to

5. Preorganized Receptor III: A Sterically Unhindered Cyclic Porphyrin Trimer

the new complex formed. An isosbestic point was observed at 429 nm. The association was quantified from the nonlinear fitting of the absorption titration data to a 1:1 complexation model ($K_{\text{ass}} = 1.3 \times 10^5 \text{ M}^{-1}$ and $1.0 \times 10^5 \text{ M}^{-1}$).

In agreement with these results, strong fluorescence emission intensity quenching was observed upon addition of $\text{Sc}_3\text{N}@\text{C}_{80}$ to the receptor solution. The association constant was calculated from the nonlinear fitting of the emission data to a 1:1 complexation model ($K_{\text{ass}} = 7.2 \times 10^4 \text{ M}^{-1}$). The calculated association was found to be in agreement with that calculated from the UV-Vis absorption titration experiment.

5.3.2 Preliminary Binding Studies of Porphyrin Trimer 5 with Other Carbon Materials

Preliminary Binding Studies of the Trimer 5 with a Mixture of Bucky Onions Containing $\text{C}_{60}@\text{C}_{240}$

A preliminary binding study was performed with the *bucky onion* sample (the carbonaceous mixture containing undetermined amount of *bucky onions*). The complexation was studied in DMF. The interaction between trimer **5** and the nano-onions mixture was studied by means of UV-Vis absorption spectroscopy. The UV-VIS titration indicated interaction with the *bucky onions* solution. A strong quenching of the *Soret* band was observed. A new band appeared at 447 nm corresponding to the absorption of the complex formed. An isosbestic point was observed at 435 nm.

5. Preorganized Receptor III: A Sterically Unhindered Cyclic Porphyrin Trimer

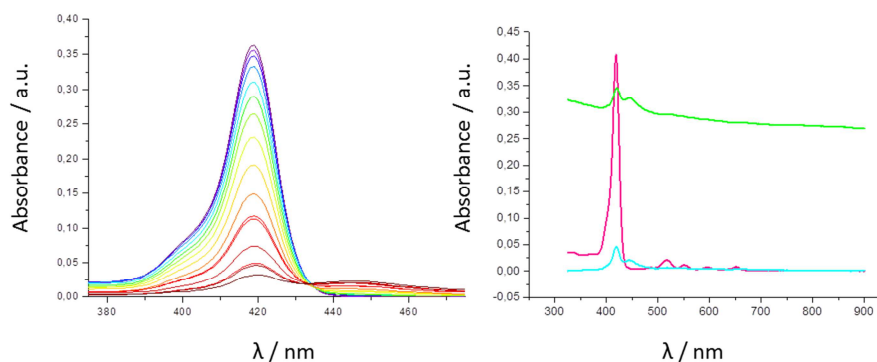


Figure 5.16 UV-Vis absorption titration experiments of receptor **5** with *bucky onions*. $[5] = 5.0 \times 10^{-7}$ M; $[CNO]_w = 0.036$ g/L; Final host/guest ratio added = n.d.. Left: Changes observed on the absorption spectrum upon addition of the guest; spectra normalized at 492 nm. Right: Absorption spectra of **5** (purple line), final **5** + mixture (green line), final **5** + mixture with the *bucky onion* solution in the reference cuvette (light blue line).

Preliminary Binding Studies of the Trimer **5** with a SWCNT

Regarding carbon nanotubes, a preliminary complexation study monitored by UV-Vis absorption spectroscopy was performed in THF. Changes observed on the UV-Vis spectrum of the trimer **5** upon addition of the guest clearly indicate interaction with the CNT. Addition of SWCNT to a solution of the receptor led to a strong quenching of the *Soret* band and the appearance of a new band at 440 nm. An isosbestic point was observed at 431 nm. After addition of a large excess of SWCNT, the *Soret* band of the receptor **5** was completely quenched, only the band corresponding to the new complex formed being observed.

Although the complexation could not be quantified in the case of SWCNTs, the titration experiment qualitatively indicates a high association with the CNOs, as can be observed in Figure 5.18.

Due to the scattering effect of the insolubilized SWCNT no fluorescence emission titration experiment could be performed. The decrease of the detected light in

5. Preorganized Receptor III: A Sterically Unhindered Cyclic Porphyrin Trimer

presence of insolubilized nanotubes cannot be therefore directly associated to the interaction.

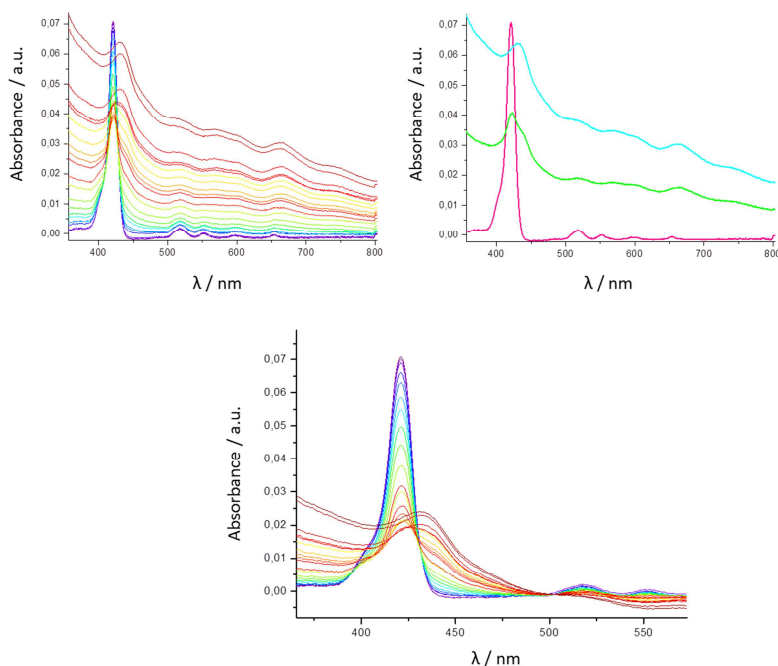


Figure 5.17 UV-Vis Absorption titration experiments of receptor **5** with SWCNT. $[5] = 5.0 \times 10^{-7}$ M; $[SWCNT]_w = 0.5$ g/L; Final host/guest ratio added = n.d.. Up Left: Changes observed on the absorption spectrum upon addition of the guest; spectra normalized at 1400 nm. Up Right: Absorption spectra of **5** (pink line), trimer **5** + SWCNT mixture (green line), two bands can still be observed corresponding to the free receptor **5** and the SWCNT complex; final trimer **5** + SWCNT (light blue line), only the complex absorption band is observed. *Soret* band appears completely quenched. Down: Changes observed on the absorption spectrum upon addition of the guest; spectra normalized at 502 nm.

The association constant cannot be quantified in the case of CNT. The size and wide variability of the carbon material does not allow the calculation of the concentration and consequently the association. Nevertheless, the titration experiment qualitatively indicates a high association with the nanotubes as can be seen in figure 5.18.

5. Preorganized Receptor III: A Sterically Unhindered Cyclic Porphyrin Trimer

5.3.3 Summary and Discussion

Receptor **5**, bearing sterically unhindered pentyl chains as *meso*-substituents, unlike its *meso*-mesityl-substituted analogue trimer **2**, was able to form complexes with C₇₀, C₈₄ and Sc₃N@C₈₀, the bucky onion sample (C₆₀@C₂₄₀) and SWCNT. The complexations were evidenced by means of UV-Vis absorption and fluorescence emission spectroscopy as well as mass spectrometry data.

Table 5.1 Summary of the receptor **5** complexation studies with the different carbon guests.

Entry	Guest	Binding	$K_{\text{ass}}^{\text{q}}$ [x 10 ⁻⁴ M ⁻¹]	$K_{\text{ass}}^{\text{a}}$ [x 10 ⁻⁴ M ⁻¹]	$K_{\text{ass}}^{\text{f}}$ [x 10 ⁻⁴ M ⁻¹]
1	C ₆₀	✓	n.d.	n.d.	n.d.
2	C ₇₀	✓	0.97	2.0	2.5
3	C ₈₄	✓	3.8	1.3	2.9
4	ScN ₃ @C ₈₀	✓	13	10	7.2
5	C ₆₀ @C ₂₄₀	✓	-	-	-
6	SWCNT	✓	-	-	-

$K_{\text{ass}}^{\text{q}}$ = association constant calculated from the absorbance quenching; $K_{\text{ass}}^{\text{a}}$ = association constant calculated from the absorbance increase; $K_{\text{ass}}^{\text{f}}$ = association constant calculated from the fluorescence emission quenching data.

As a general tendency, a bigger size of the carbon guest lead to a larger binding affinity. The largest binding constant was obtained for the endohedral fullerene

5. Preorganized Receptor III: A Sterically Unhindered Cyclic Porphyrin Trimer

ScN₃@C₈₀. Also, a strong quenching was observed for the complexation of the CNOs and the SWCNTs. The results are summarized in Table 5.1.

Trimer **5** failed to form inclusion complexes with C₆₀ at a receptor concentration of 10⁻⁶ M due to the weak binding. However, APCI-MM-ES+ mass spectrometry of a trimer **5** / C₆₀ mixture did indicate the formation of a 1:1 complex.

Receptor **5** was able to form complexes with C₇₀ at a 10⁻⁶ M despite of having a comparable diameter as C₆₀. The quantified association was in the range of 2 x 10⁴ M. Trimer **5** successfully encapsulates C₈₄ at 10⁻⁶ M. The calculated association constant was found to be larger than that for C₇₀. APCI-MM-ES+ mass spectrometry confirmed the formation of 1:1 complexes with both C₇₀ and C₈₄.

The highest association was calculated for the complexation of the endohedral fullerene ScN₃@C₈₀ and was found to be more than five times larger than those calculated for empty fullerenes. This preferred interaction between porphyrins and endohedral fullerenes over empty fullerenes has been already described.^{51, 56, 68}

Finally preliminary complexation studies were performed with both a *bucky onion* sample and SWCNT sample. UV-Vis absorption titration experiments were performed and evidenced a strong interaction with these carbon guests.

In the case of the CNOs, a strong quenching of the *Soret* band as well as the new band formed confirmed the interaction with the nested fullerene sample.

Regarding SWCNT, a very strong association was observed. After addition of a large excess of SWCNT, a complete quenching of the receptor **5** *Soret* band was observed. Only the band corresponding to the new complex formed was observed

Although complexation could not be quantified in the case of the *bucky onions* and SWCNTs, the titration experiments qualitatively indicate a strong association with both guests.

5. Preorganized Receptor III: **A Sterically Unhindered Cyclic Porphyrin Trimer**

The porphyrin cyclic trimer **5** bearing sterically hindered *meso*-substituents was able to encapsulate all the fullerene guests under study. As suggested in the hypothesis presented in chapter 3, the presence of bulky *meso*-substituents, is one of the main reasons for the lack of complexation observed for trimer **1**. In this case, the presence of small *meso*-substituents allowed the trimer to successfully form complexes with the fullerenes.

When comparing these results with those of the small cavity trimer **XLVIII** reported by Anderson *et al.*, the smaller trimer was able to encapsulate a wide range of fullerenes with extremely high associations. Trimer **5** did not show such high association constants, but it was found to be more selective since it discriminates the most abundant fullerene C₆₀ from larger fullerenes merely by its size, as has been as well reported for trimer **3**.

5.4 Conclusions

The synthesis of cyclic porphyrin trimer **4** was attempted. Trimer **4** could not be prepared in reasonable yields and therefore was discarded as a target receptor.

On the contrary, cyclic porphyrin trimer **5** has been successfully synthesized and characterized.

The formation of complexes with C₆₀, C₇₀, C₈₄ and ScN₃@C₈₀ was monitored by means of by UV-Vis absorption and fluorescence emission spectroscopic techniques and mass spectrometry.

Receptor **5** was able to successfully encapsulate C₇₀, C₈₄ and ScN₃@C₈₀ at a receptor concentration of 10⁻⁶ M. No interaction was observed with the major fullerene (C₆₀) at that concentration; nevertheless mass spectrometry evidenced such interaction and the formation of the 1:1 inclusion complex. The association constants for the encapsulation of C₇₀, C₈₄ and Sc₃N@C₈₀ were quantified in toluene from both the

5. Preorganized Receptor III: **A Sterically Unhindered Cyclic Porphyrin Trimer**

UV-Vis absorption and the fluorescence emission titration experiments. Formation of 1:1 complexes with C₇₀ and C₈₄ was confirmed by APC-MM-ES+ mass spectrometry experiments. As reported previously for porphyrins and porphyrin-based receptors, trimer **5** showed the strongest interaction towards the endohedral fullerene Sc₃N@C₈₀.^{51, 68}

Finally preliminary complexation studies were performed with both the *bucky onion* sample and the SWCNT. The association with these guests was monitored by UV-Vis absorption spectroscopy. The UV-Vis titration experiments with both the CNOs and the SWCNTs showed the strongest *Soret* band quenching yet observed.

**Chapter 6: Preorganized Receptor IV: Enlarged
Cyclic Porphyrin Trimer for Giant
Carbon *Nano Onions*. Preliminary
Studies.**

UNIVERSITAT ROVIRA I VIRGILI

CYCLOTRIVERATRYLENE AND PORPHYRIN SCAFFOLDS FOR MOLECULAR RECOGNITION AND SELF-ASSEMBLY

Berta Camafort Blanco

Dipòsit Legal: T 677-2015

6. Preorganized Receptor IV: Enlarged Cyclic Porphyrin Trimer for Giant Carbon Nano Onions. Preliminary Studies.

6.1 Design and Aim of the Project

The aim of this project is the preparation of a giant porphyrin cyclic receptor that could potentially encapsulate $C_{60}@C_{240}$ and eventually achieve separation of $C_{60}@C_{240}$ from a *bucky onion* mixture. The encapsulation, solubilization and isolation of *bucky onions* has not been so far reported in the literature. Only Echegoyen *et al.* reported in 2008 the encapsulation of pyridyl-functionalized carbon *nano onions* by zinc tetra-phenyl porphyrins (ZnTPP).^{83e}

The encapsulation, inclusion complex characterization and isolation of giant *bucky onions* such as $C_{60}@C_{240}$ are specially challenging processes due to the big size and extremely low solubility of the nested fullerene.

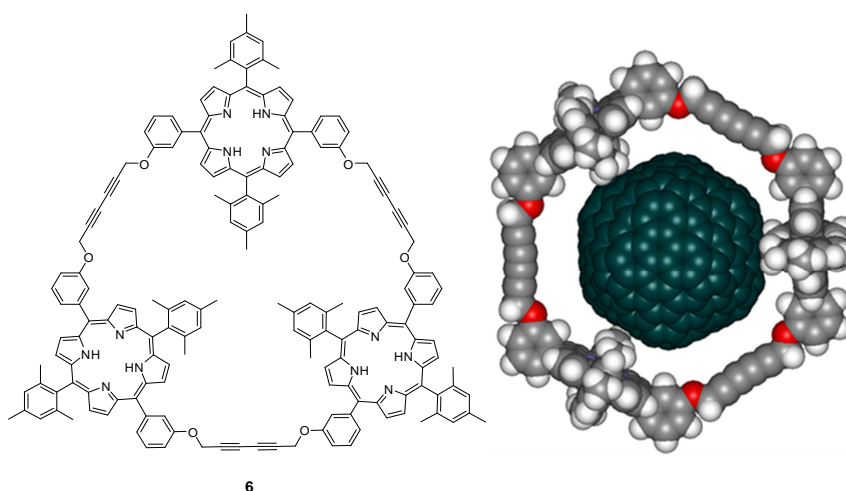


Figure 6.1 Trimer receptor 6. Optimized structure of trimer 6 complex with a $C_{60}@C_{240}$ *bucky onion*.

6. Preorganized Receptor IV: **Enlarged Cyclic Porphyrin Trimer for Giant Carbon Nano Onions. Preliminary Studies.**

The cavity size is an important aspect of the receptor design. First the trimer cavity should be big enough to allow the encapsulation of the giant guest. Furthermore, the porphyrin units should be able to interact with the guest and discriminate it by size criteria from other *bucky onions*. To approach the encapsulation of the *bucky onion* $C_{60}@C_{240}$, two different trimers **6** and **7** were designed.

In cyclic porphyrin trimer **6**, the porphyrin units are connected through long hexadiynyldioxo linkers. The longer hexadiynyldioxo connectors, when compared with those used in trimer **2** (chapter 3), provide the cyclic trimer with a wider cavity, better suited for the encapsulation of $C_{60}@C_{240}$. The presence of the extra oxo-methylene spacers to connect the porphyrin units with the acetylene linkers introduces some flexibility, allowing the porphyrin units to better adapt to the guest despite the overall rigidity of the receptor (Figure 6.1).

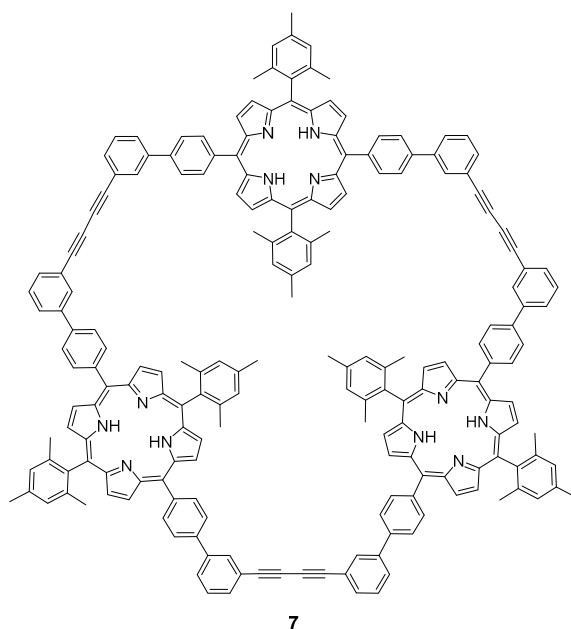


Figure 6.2 Trimer receptor **7**.

6. Preorganized Receptor IV: **Enlarged Cyclic Porphyrin Trimer for Giant Carbon Nano Onions. Preliminary Studies.**

Within cyclic porphyrin trimer **7**, the porphyrin units are connected through rigid 1,4-diphenylbuta-1,3-diyne linkers. The long linkers connected through *meso*-aryl substituents provide the trimer with cavity also suitable for the encapsulation of the $C_{60}@C_{240}$ *bucky onion* (Figure 6.2).

Within trimer **6**, the *trans*- A_2B_2 -type porphyrin building block **23** is functionalized with four *meso*-substituents. Two of these substituents consist of propargyl groups designed to connect the porphyrin units within the trimer. The porphyrin units were further equipped with mesityl groups (Figure 6.3).

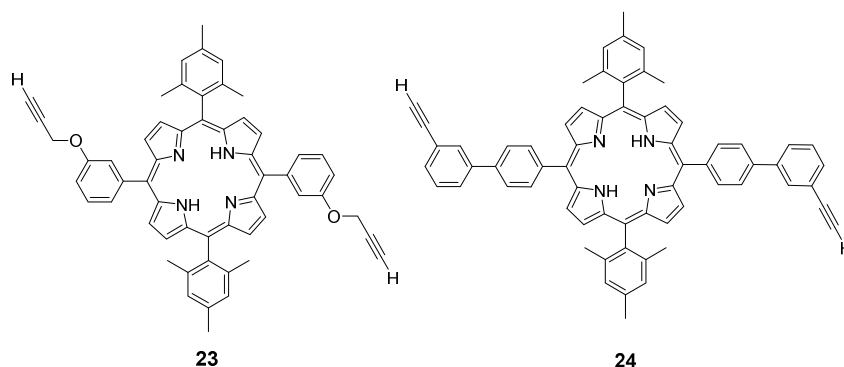


Figure 6.3 *Trans*- A_2B_2 -type porphyrin building blocks **23** and **24**.

Similarly, for trimer **7** *trans*- A_2B_2 -type porphyrin building block **24** is functionalized with four *meso*-substituents, two of them being 3-ethynyl-1,1'-biphenyl groups designed to connect the porphyrin units within the trimer. The porphyrin units were further equipped with mesityl groups on their *meso* positions (Figure 6.3).

In this chapter, the synthesis and characterization of trimers **6** and **7** as well as the preliminary complexation studies with the sample containing a mixture of *bucky onions* are discussed.

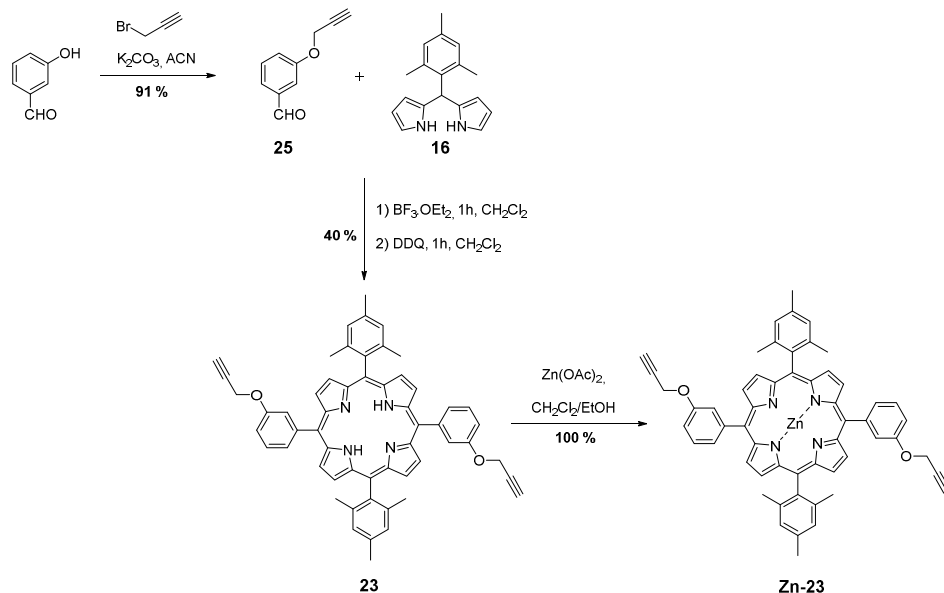
6. Preorganized Receptor IV: Enlarged Cyclic Porphyrin Trimer for Giant Carbon Nano Onions. Preliminary Studies.

6.2 Synthesis and Characterization

6.2.1 Synthesis of Cyclic Porphyrin Trimer 6

Synthesis of Zinc Metallated Porphyrin Building Block Zn-20

The synthesis of the cyclic porphyrin trimer started with the preparation of the porphyrin **23** building block. The commercially available 3-hydroxybenzaldehyde was alkylated quantitatively with propargyl bromide in acetonitrile in the presence of potassium carbonate. Acid catalyzed condensation of 5-mesityldipyrromethane **16** and 3-propargyloxibenzaldehyde **25** in the presence of BF_3 etherate followed by oxidation with DDQ gave the desired porphyrin **23** in moderate yield. The porphyrin was then quantitatively metallated with zinc acetate in DCM / EtOH (Scheme 6.1).



Scheme 6.1 Synthesis of zinc metallated ligand Zn-23.

6. Preorganized Receptor IV: Enlarged Cyclic Porphyrin Trimer for Giant Carbon Nano Onions. Preliminary Studies.

The free base porphyrin **23** and the metallated porphyrin ligand **Zn-23** were characterized by $^1\text{H-NMR}$ spectroscopy and mass spectrometry. The $^1\text{H-NMR}$ spectrum is shown in Figure 6.4.

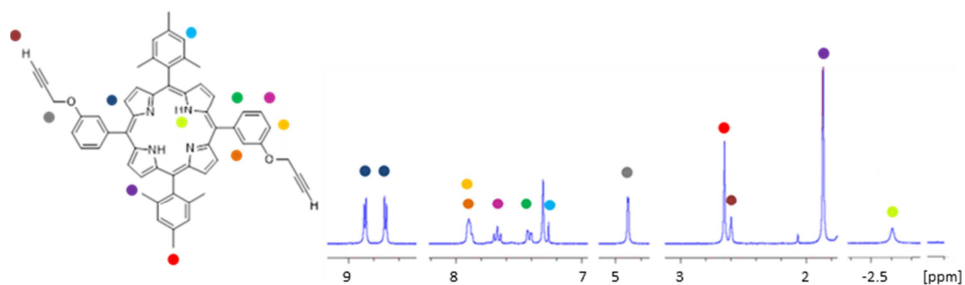


Figure 6.4 $^1\text{H-NMR}$ spectrum of **23** in CDCl_3

The MM-ES+APCI mass spectrum of the zinc metallated porphyrin **Zn-23** is shown in Figure 6.5. Both the masses of the free base porphyrin **23** and the zinc-metallated ligand **Zn-23** are observed (**23** mass/ z^+ : 807,3, calculated mass/ z^+ : 807,4; **Zn-23** mass/ z^+ : 869,1, calculated mass/ z^+ : 869,3).

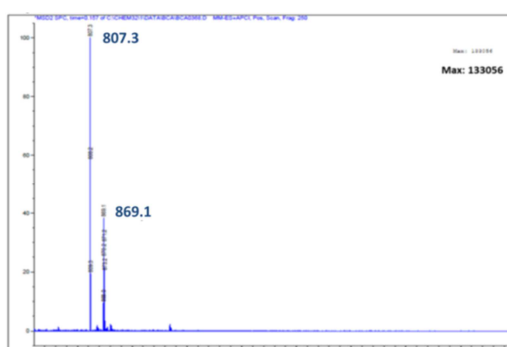


Figure 6.5 MM-ES+APCI mass spectrum of **Zn-23**.

6. Preorganized Receptor IV: Enlarged Cyclic Porphyrin Trimer for Giant Carbon Nano Onions. Preliminary Studies.

Template Directed Synthesis of Cyclic Porphyrin Trimer 6

Template directed homocoupling of the terminal alkynes was selected as the synthetic strategy for ring closure of the zinc-metallated 3-propargyloxy-porphyrin ligand **Zn-23** to give the desired porphyrin trimer **6**.

As shown in Figure 6.6, commercially available 2,4,6-tri-4-pyridyl-1,3,5-triazine **19**, previously used as template for the synthesis of smaller trimers **2** and **5**, is too small in this case to properly preorganize three **Zn-23** ligands around its binding sites. Therefore, a larger template such as **26** was selected.

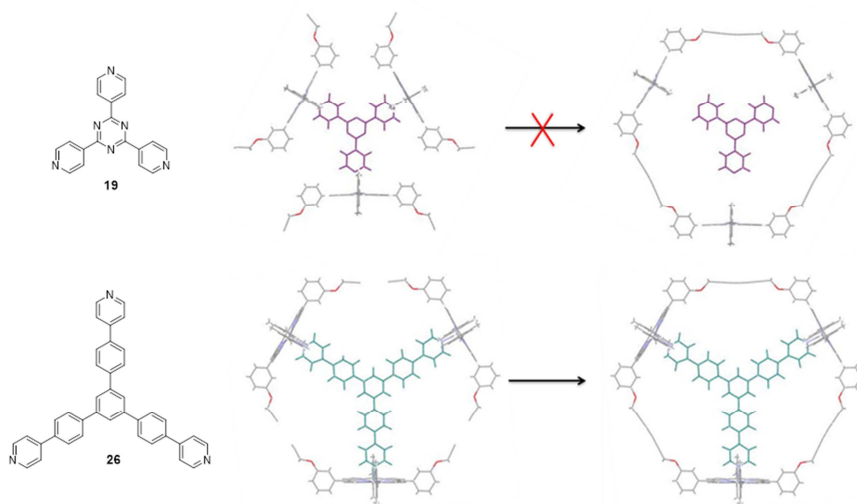
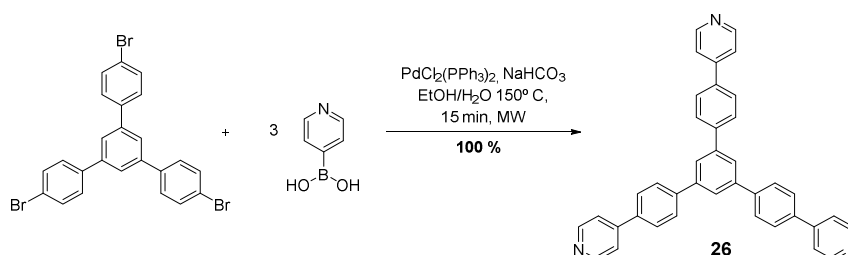


Figure 6.6 Templates **19** and **26**. Template ability on porphyrin **Zn-23** preorganization.

Trimeric template **26** was prepared in excellent yields through a *Suzuki* coupling of commercially available 1,3,5-tris-(4-bromophenyl)benzene and 4-pyridyl boronic acid under microwave irradiation (Scheme 6.2).

6. Preorganized Receptor IV: Enlarged Cyclic Porphyrin Trimer for Giant Carbon Nano Onions. Preliminary Studies.



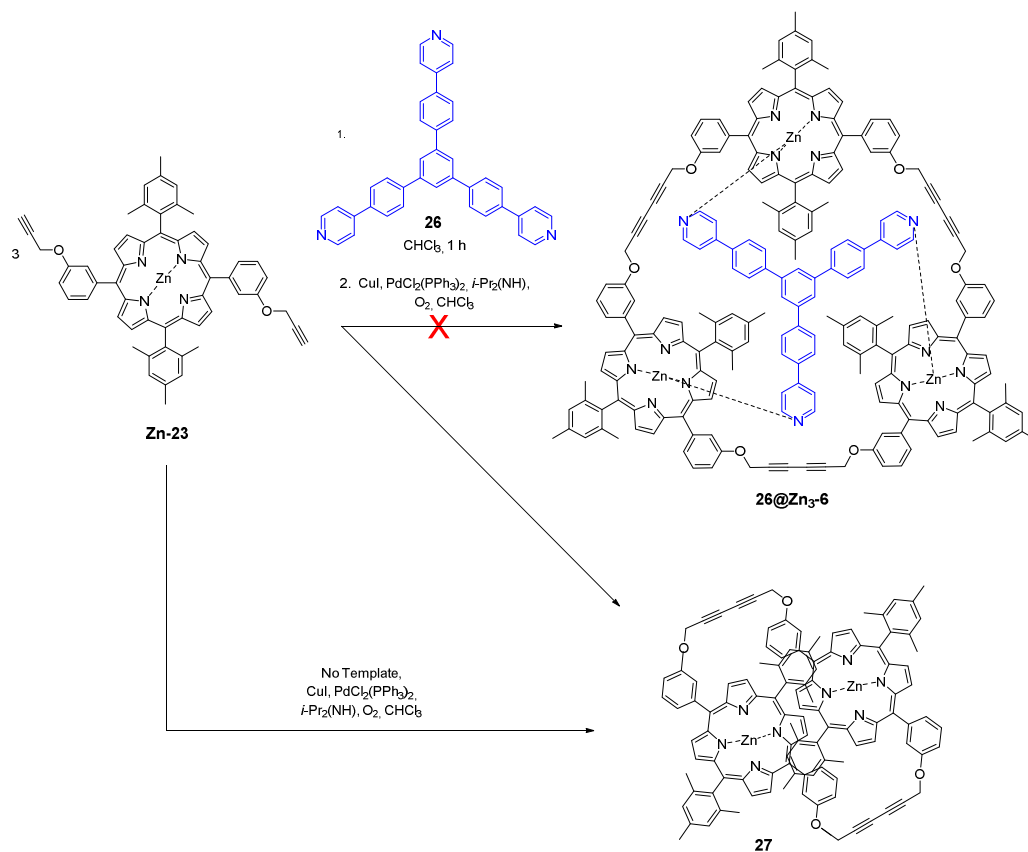
Scheme 6.2 Synthesis of template **26**.

A 1:3 template / metallated porphyrin **Zn-23** solution was sonicated for 3-5 h before the addition of the *Sonogashira*-derived catalyst solution (CuI , $\text{PdCl}_2(\text{PPh}_3)_2$ and isopropylamine). Unfortunately, the template directed homocoupling of the porphyrin ligands failed to give the target porphyrin trimer **26@Zn₃-6**. Apart from insoluble linear oligomers, the exclusive formation of dimer **27** was observed.^{67, 68} Similar results were obtained when the reaction was performed in the absence of template (Scheme 6.3).

Further attempts to achieve the above-mentioned transformation, such as increasing the ratio of template added to the reaction mixture also failed to promote formation of the desired trimer. On the contrary, a clear negative template effect was observed. Upon increasing the ratio of template, the amount of dimer **27** decreased until no dimer formation was observed at all, whereas linear oligomers were produced. These observations indicate that template **26** does actually interact with the porphyrin ligands but is unable to promote the required preorganization of the ligands prior to porphyrins' coupling to form trimer **6**.

The additional degrees of freedom introduced by the *O*-methylene fragment in the case of porphyrin ligand **23** might be responsible for the template inability to promote a proper orientation of the terminal alkynes during coupling. This additional flexibility would allow the template-complexed porphyrin **26@Zn-23** to react with porphyrin **Zn-23** units, resulting in formation of linear arrays.

6. Preorganized Receptor IV: Enlarged Cyclic Porphyrin Trimer for Giant Carbon Nano Onions. Preliminary Studies.



Scheme 6.3 Synthetic attempts of **26@Zn₃-6**.

6.2.2 Synthesis of Cyclic Porphyrin Trimer 7

Trimer **7** was then synthesized. Instead of porphyrin ligand **23**, the much better preorganized porphyrin ligand **24** would fulfill the requirements to achieve a proper orientation of the terminal alkynes when complexed to the template **26** before the coupling of the terminal alkynes. The low degree of freedom of the new porphyrin ligand **24** would only allow the terminal alkynes to move within one plane promoting

6. Preorganized Receptor IV: **Enlarged Cyclic Porphyrin Trimer for Giant Carbon Nano Onions. Preliminary Studies.**

the homocoupling of the porphyrin ligands complexed to template **26** and formation of trimer **7** (Figure 6.7).

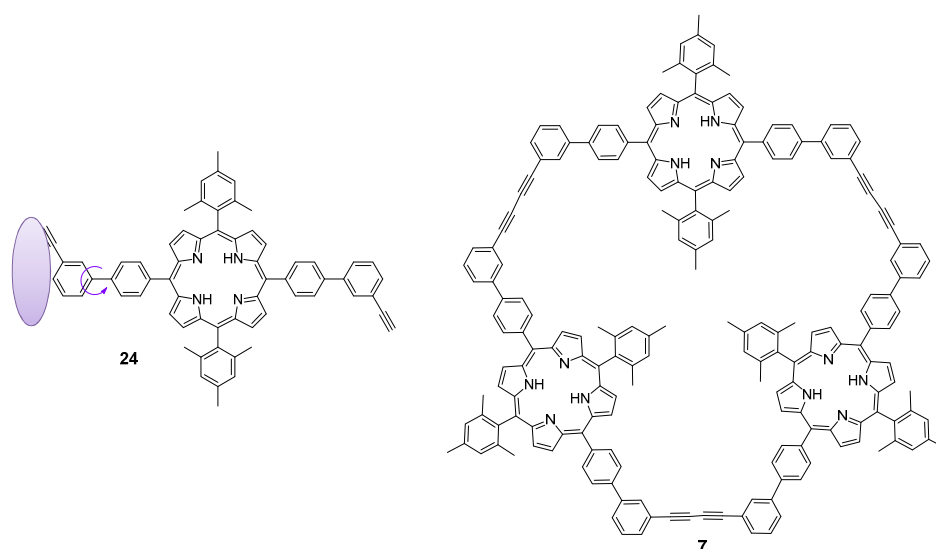
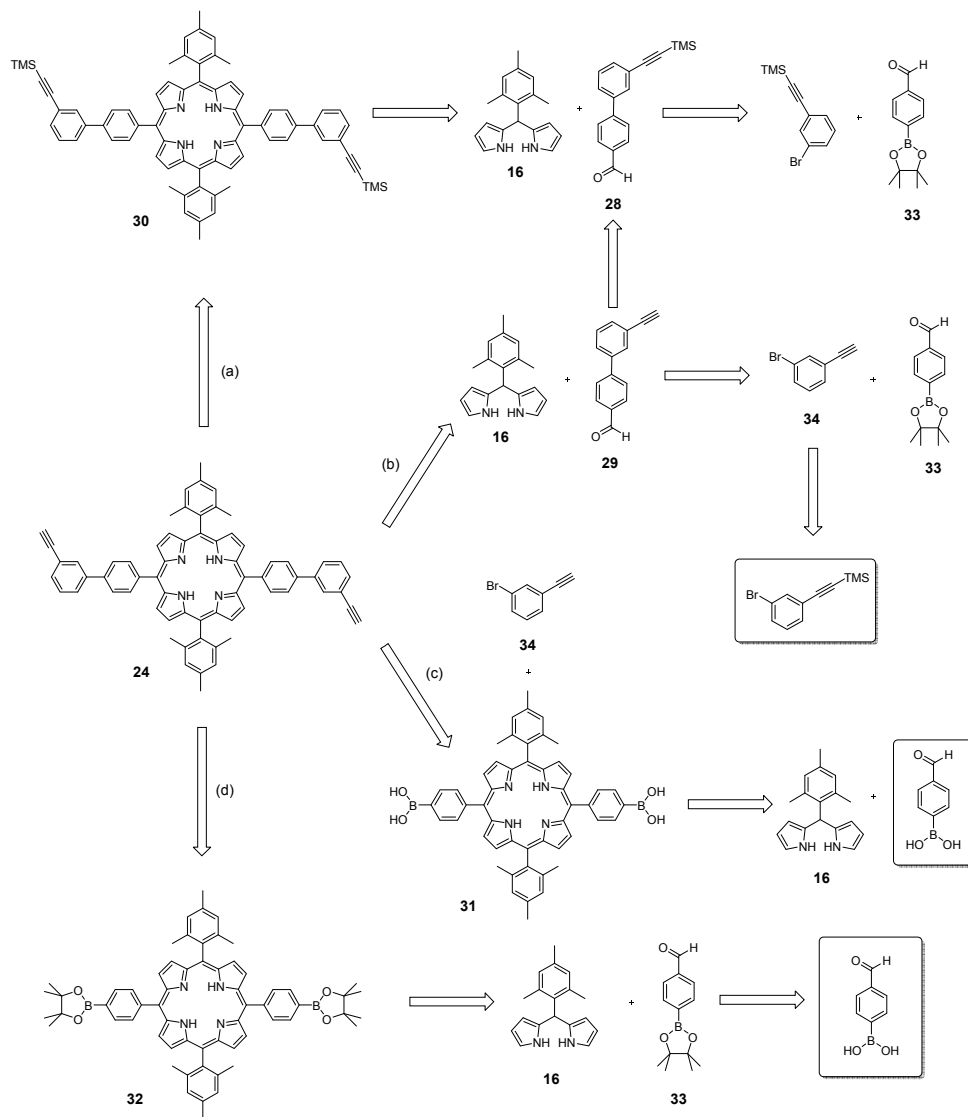


Figure 6.7 Porphyrin building block **24**. porphyrin cyclic trimer **7**

Synthesis of Zinc Metallated Porphyrin Building Block Zn-24

Four different routes were proposed for the synthesis of the rigid porphyrin ligand **24**. Routes (a) and (b) start with ethynyl-biphenylaldehyde building block derivatives **28** and **29** prior to formation of the porphyrin building blocks **24** and **30**, whereas routes (c) and (d) start with boronic acid porphyrin derivatives **31** and **32** that are further functionalized to give the desired porphyrin building block (Scheme 6.4).

6. Preorganized Receptor IV: Enlarged Cyclic Porphyrin Trimer for Giant Carbon Nano Onions. Preliminary Studies.

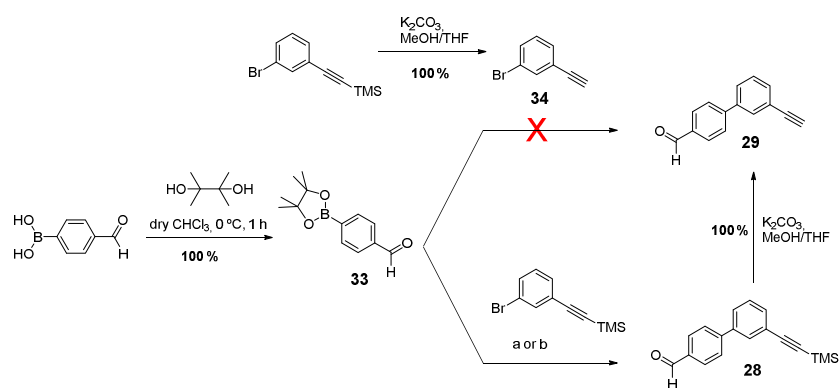


Scheme 6.4 Retrosynthetic routes (a-d) towards the synthesis of porphyrin building block 24.

6. Preorganized Receptor IV: Enlarged Cyclic Porphyrin Trimer for Giant Carbon Nano Onions. Preliminary Studies.

Synthesis of Zinc Metallated Porphyrin Building Block Zn-24: Routes (a) and (b).

Synthetic routes (a) and (b) were initially selected. The commercially available (4-formylphenyl)boronic acid was protected with commercially available pinacol to give **33** in excellent yields. The TMS-protected ethynyl-naphthalene aldehyde building block **28** was then prepared *via* a *Suzuki* coupling under microwave irradiation, starting from aldehyde **33** and the commercially available TMS-protected 1-bromo-3-ethynylbenzene. *Suzuki* coupling of previously deprotected bromide **34** did not succeed (Scheme 6.5).



Scheme 6.5 Synthesis of ethynyl-naphthalene aldehyde building blocks **28** and **29**

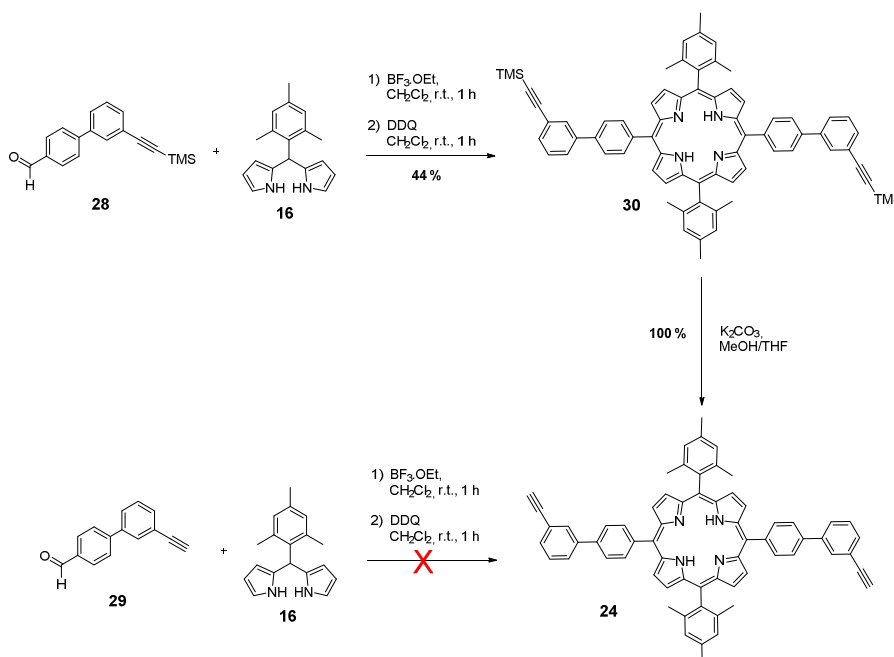
Table 6.1 Screening of Suzuki coupling parameters for the synthesis of **28**.

	<i>Reagents</i>	<i>Solvent</i>	<i>Temperature</i>	<i>Time</i>	<i>Yield</i>
a	PdCl ₂ (PPh ₃) ₂ , NaHCO ₃	EtOH/H ₂ O	150 °C (MW)	15 min - 1h	46 %
b	Pd(OAc) ₂ , Na ₂ CO ₃ aq.	DME	80 °C (MW)	2 - 8 h	97 %

Two different Suzuki coupling conditions were screened and are summarized in Table 6.1. Initially, we selected the previously employed conditions for the synthesis of

6. Preorganized Receptor IV: Enlarged Cyclic Porphyrin Trimer for Giant Carbon Nano Onions. Preliminary Studies.

template **26** (conditions a: PdCl₂(PPh₃)₂, NaHCO₃ in EtOH/H₂O). In this particular case the yields obtained were not as high as expected, the desired aldehyde was obtained in a 46 yield after microwave irradiation at 150 °C and different time ranges (from 15 min to 1 h). Conditions b (Pd(OAc)₂ and aq. Na₂CO₃ in DME) gave the desired building block in excellent yields after 2 h MW irradiation at 80 °C.



Scheme 6.6 Synthetic attempts of free base porphyrin **24**

Acid catalyzed condensation of the TMS-protected ethynyl-biphenylaldehyde **28** and mesityl dipyrromethane **16** in the presence of BF₃ etherate followed by oxidation with DDQ gave the desired TMS-protected porphyrin **30** in moderate yields. As usually, *cis*-A₂B₂-porphyrin and A₃B-porphyrin were also obtained due to the scrambling of the aldehydes under acid catalysis (Scheme 6.6).

6. Preorganized Receptor IV: **Enlarged Cyclic Porphyrin Trimer for Giant Carbon Nano Onions. Preliminary Studies.**

Unfortunately, due to impurities of the commercially available TMS-protected (3-bromophenyl)ethynyl starting material, six additional products were observed after removal of the trimethylsilyl protective group with potassium carbonate in MeOH / THF.

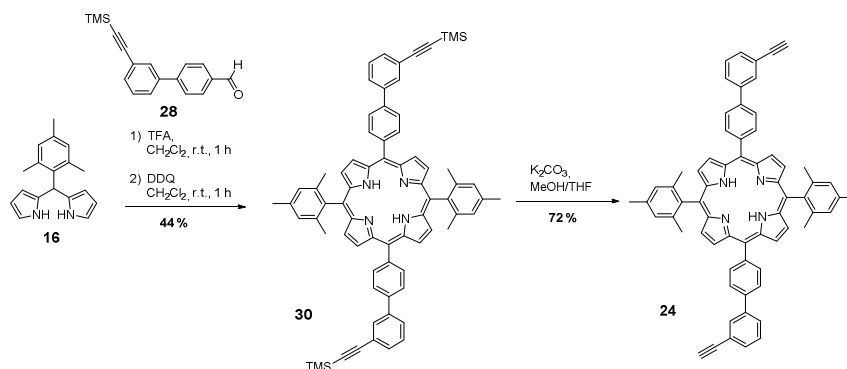
In summary, a total of nine different products were obtained after the first synthetic attempt resulting from both the scrambling of the aldehydes during acid catalyzed condensation reaction and the impurities of the commercially available starting material.

The condensation conditions were further studied in order to reduce the scrambling and to avoid formation of the *cis*-A₂B₂- and the A₃B-porphyrin. It was observed that if TFA was used instead of BF₃·OEt as acid catalyst, only one porphyrin was obtained, without detectable formation of scrambling side products (Scheme 6.7), as previously reported by Lindsey *et al.*⁹⁰ The number of different products was reduced from nine to three, corresponding to the *trans* A₂B₂-porphyrins.

To reduce the number of side *trans*-A₂B₂-porphyrins resulting from the starting material impurities, purification of commercially available starting material was achieved prior to reaction. Nevertheless, the final number of porphyrins obtained was reduced to only two. These porphyrins were almost not detectable by TLC due to retention times overlap. In the mass spectra both porphyrins could be differentiated by only 15 mass units and in the ¹H-NMR spectrum of the porphyrin mixture, only the signals corresponding to the desired porphyrin could be identified.

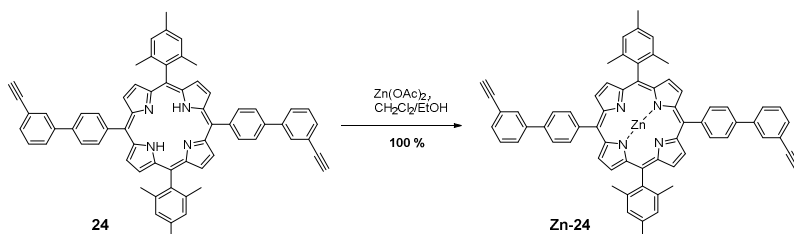
HPLC semi-preparative separation was required for the isolation of the desired porphyrin since other techniques such as column chromatography, preparative TLC or gel permeation chromatography (GPC) failed. The purification was performed with the free base porphyrin since the difference in retentions factors observed between the free base porphyrins was found to be slightly bigger than that for the zinc metallated ones.

6. Preorganized Receptor IV: Enlarged Cyclic Porphyrin Trimer for Giant Carbon Nano Onions. Preliminary Studies.



Scheme 6.7 Synthesis of porphyrin ligand **24**.

Finally, the HPLC-purified free base porphyrin building block **24** was metallated with zinc acetate in EtOH / DCM to give the **Zn-24** porphyrin ligand quantitatively (Scheme 6.8).

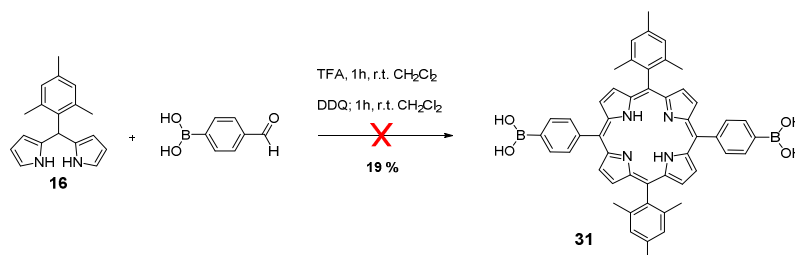


Scheme 6.8 Synthesis of zinc metallated porphyrin ligand **Zn-24**.

Synthesis of Zinc Metallated Porphyrin Building Block Zn-24: Routes (c) and (d)

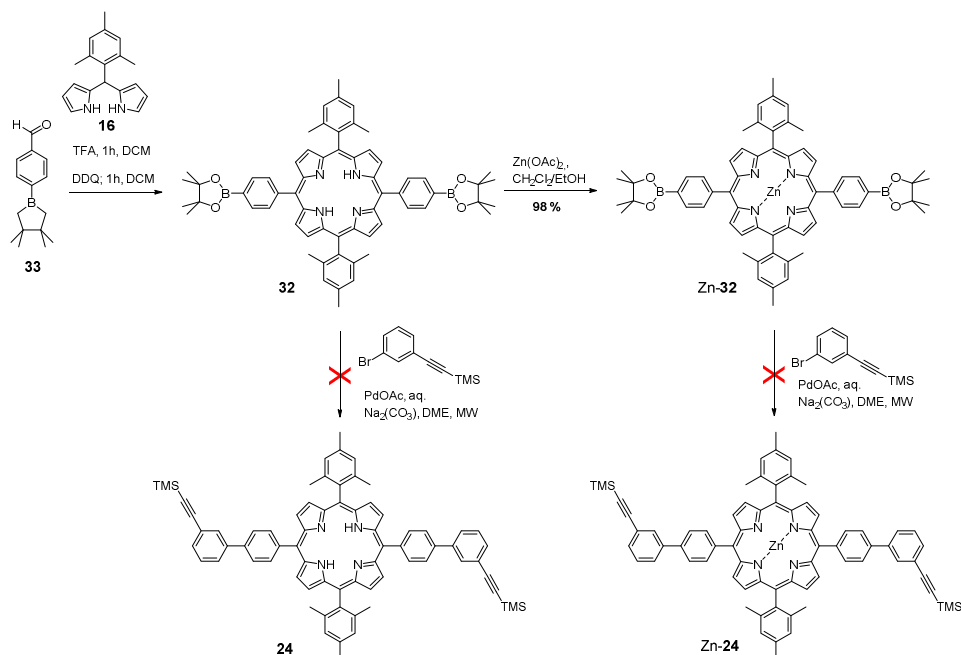
In parallel to routes (a) and (b), synthetic routes (c) and (d) were explored to overcome the synthesis of the porphyrin ligand, avoiding time-consuming HPLC semi-preparative purification. Unfortunately, preparation of the required boronic acid porphyrin derivative **31** from the commercially available boronic acid failed (Scheme 6.9).

6. Preorganized Receptor IV: Enlarged Cyclic Porphyrin Trimer for Giant Carbon Nano Onions. Preliminary Studies.



Scheme 6.9 Synthetic attempts of boronic acid porphyrin derivative **31**.

Protection of the commercially available boronic acid prior to TFA-catalyzed condensation with mesityl dipyrromethane building block **16** was thus attempted. Further oxidation with DDQ gave the boronic acid derivative porphyrin **32** in moderate yield. Porphyrin **32** was further quantitatively metallated with zinc acetate in EtOH/DCM. Unfortunately, neither coupling of the free base **32** nor the metallated porphyrin **Zn-32** with commercially available TMS-protected bromide gave the desired porphyrin building block **24** (Scheme 6.10).



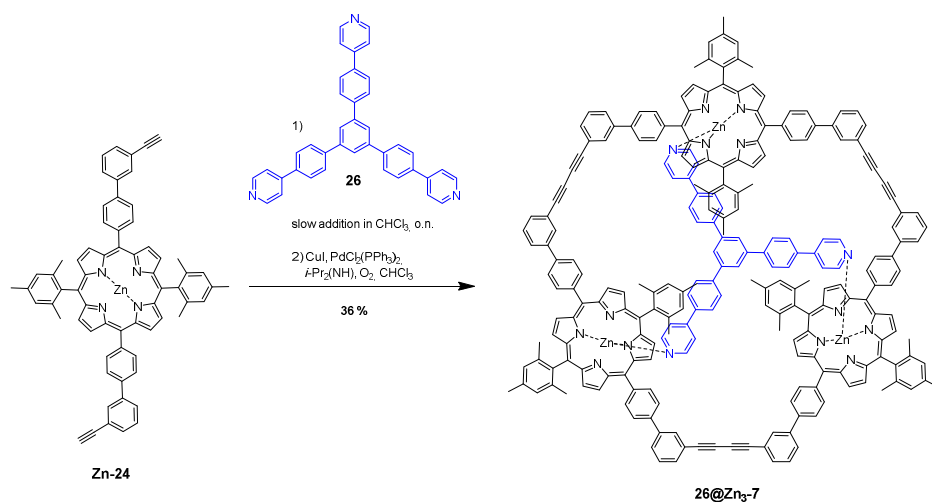
6. Preorganized Receptor IV: Enlarged Cyclic Porphyrin Trimer for Giant Carbon Nano Onions. Preliminary Studies.

Scheme 6.10 Synthesis attempts of zinc-metallated porphyrin ligand **Zn-24**

Template Directed Synthesis of Cyclic Porphyrin Trimer **7**

As in previous chapters, template assisted ring closure through homocoupling of the terminal alkynes was selected as a synthetic approach for the preparation of the cyclic porphyrin trimer **7**. Previously synthesized trimeric template **26** was selected to preorganize the metallated porphyrin monomers and promote formation of the desired cyclic porphyrin trimer **7**.

A 1:3 template **26** / **Zn-24** ligand solution was sonicated for 3 to 5 h prior to the addition of the *Sonogashira*-derived catalyst solution (CuI, PdCl₂(PPh₃)₂ and isopropylamine). No evidences of trimer formation were observed. Instead, exclusive formation of insoluble linear oligomers was found (Scheme 6.11).



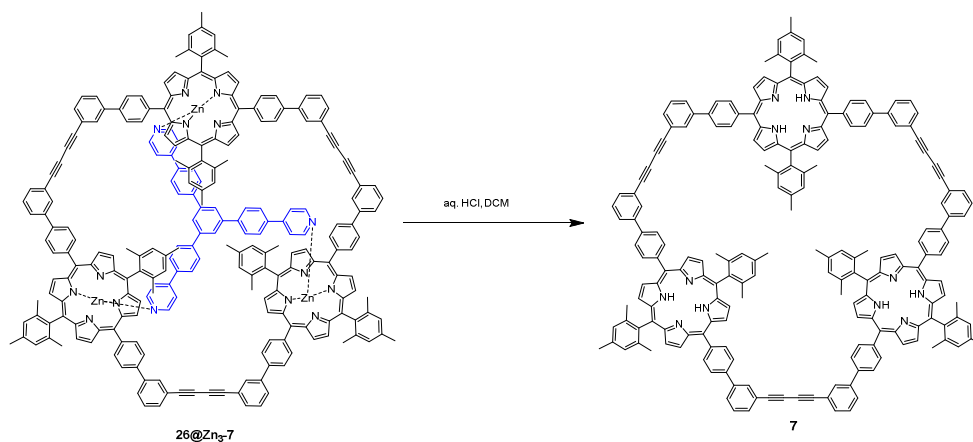
Scheme 6.11 Template-directed synthesis of complex **26@Zn₃-7**.

In attempts to promote the preorganization of the porphyrin ligands around the template binding sites, the effective concentration of porphyrin monomer was

6. Preorganized Receptor IV: **Enlarged Cyclic Porphyrin Trimer for Giant Carbon Nano Onions. Preliminary Studies.**

increased by dropwise addition of a highly diluted solution of template **26** over a concentrated solution of porphyrin ligand **Zn-24** over 5 h. In this way the template complex formation is favored and furthermore, the low concentration of the solution minimizes the chances of rapid formation of the major kinetic linear oligomer products.

The reaction mixture was stirred for further 7 h prior to the addition of *Sonogashira*-derived catalyst solution. Homocoupling of the terminal alkynes gave the desired complex **26@Zn₃-7** in moderate yields. The reaction was monitored by TLC. The catalyst solution was added several times until no further formation of trimer was observed. The complex was purified by preparative TLC (cyclohexane / CHCl₃ 7:3).



Scheme 6.12 Synthesis of the **7**: Template removal.

6.2.3 Characterization of Cyclic Porphyrin Trimer **7**

The porphyrin trimer **7** was characterized by both ¹H-NMR spectroscopy and MALDI-TOF mass spectrometry. The ¹H-NMR spectrum is shown in Figure 6.8.

6. Preorganized Receptor IV: **Enlarged Cyclic Porphyrin Trimer for Giant Carbon Nano Onions. Preliminary Studies.**

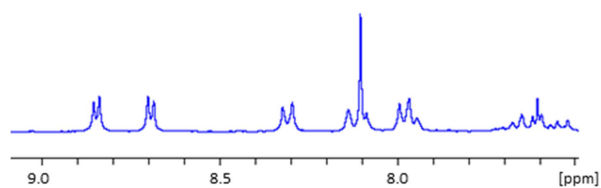


Figure 6.8 Selected region of $^1\text{H-NMR}$ spectrum of the cyclic porphyrin trimer **7** in CDCl_3 .

Mass analysis of trimer **7** was performed by means of MALDI-TOF spectrometry (**7** mass/z^+ : 2691.2930, calculated mass/z^+ : 2691.1704) (Figure 6.9).

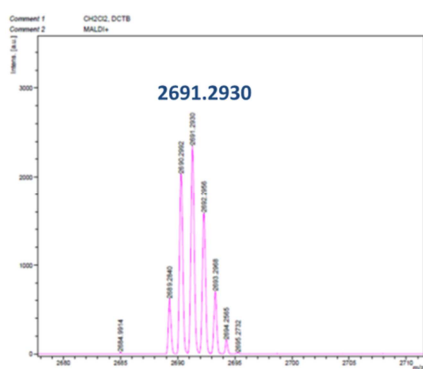


Figure 6.9 MALDI-TOF spectrum of the target cyclic porphyrin trimer **7**.

6. Preorganized Receptor IV: Enlarged Cyclic Porphyrin Trimer for Giant Carbon *Nano Onions*. Preliminary Studies.

6.3 Results and Discussion

6.3.1 Preliminary Complexation Studies of Porphyrin Trimer **7** with a *Bucky Onion* Mixture Solution

A preliminary complexation study was performed in DMF. The changes on the receptor absorbance were monitored by UV-Vis spectroscopy upon addition of the *bucky onion* solution. The concentration of *bucky onion* solution was increased whereas the concentration of receptor **7** was kept constant. The absorbance quenching observed indicates interaction with the guest. No shifting of the *Soret* band was observed. No formation of a new absorption band was detected (Figure 6.10).

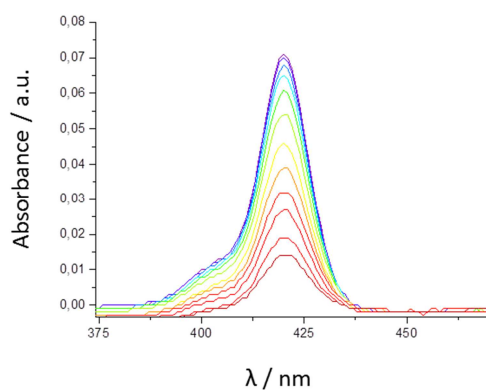


Figure 6.10 UV-Vis absorption complexation experiments with CNOs; free receptor. $[7] = 5.0 \times 10^{-7}$ M; $[CNOs]_w = 0.036$ g/L; Final host/guest ratio added = n.d.

6. Preorganized Receptor IV: **Enlarged Cyclic Porphyrin Trimer for Giant Carbon Nano Onions. Preliminary Studies.**

6.3.2 Summary and Discussion

Receptor **7** bearing rigid 1,4-diphenylbuta-1,3-diyne linkers and mesityl pendant groups on the *meso*-positions of the porphyrin units was designed to form inclusion complex with a C₆₀@C₂₄₀ *bucky onion* guest. Preliminary UV-Vis absorption titration studies were performed with a CNOs sample (a heterogeneous mixture of *bucky onions*). Quenching of the trimer **7** *Soret* band evidenced interaction between the receptor and the guest.

6.4 Conclusions

The cyclic porphyrin trimer **6** synthesis was attempted. No trimer **6** formation was observed. Instead, **27** was exclusively isolated. A negative template effect was observed, since formation of linear arrays was promoted upon addition of more than one equivalent of template. Cyclic porphyrin trimer **7** has been successfully synthesized and characterized.

Preliminary complexation studies performed with a carbon *onion* sample were monitored by UV-Vis absorption spectroscopy. Changes observed on the receptor **7** *Soret* band evidenced interaction with the *bucky onion* sample in DMF.

Chapter 7: Experimental Part

UNIVERSITAT ROVIRA I VIRGILI

CYCLOTRIVERATRYLENE AND PORPHYRIN SCAFFOLDS FOR MOLECULAR RECOGNITION AND SELF-ASSEMBLY

Berta Camafort Blanco

Dipòsit Legal: T 677-2015

7.1 General Information and Instrumentation

All commercial reagents and solvents, unless otherwise noted, were purchased at reagent grade from Acros, ABCR, Aldrich and Fluka and used as received. Anhydrous solvents were obtained from solvent purification system SPS-400-6 from Innovative Technologies. Solvents for flash chromatography (FC), preparative TLC, plug filtrations and extractions were of technical quality. CHCl_3 was distilled under *vacuum* before use. For all aqueous solutions deionized water was used.

All reactions, except porphyrin metallations as well as *Hay* and *Sonogashira*-based couplings, were performed under an inert atmosphere by applying a positive pressure of Argon using dry solvents. *Hay* and *Sonogashira*-based catalyst solutions were freshly distilled prior its use. Pyrrole was freshly distilled under *reduced pressure* before use.

Evaporation and concentration under *reduced pressure* was performed at water aspirator pressure; drying in vacuo at 10^{-2} Torr. Thin-layer chromatography (TLC) was conducted on silica gel pre-coated TLC-plates SIL G-25 UV254 (Macherey-Nagel) glass supported and visualized by UV light (254 or 366 nm) and/or KMnO_4 stain. Column chromatography and plug filtrations were carried out with silica gel SDS (Silica Gel 60 A; particle size 0.040–0.063 mm). Flash chromatography (FC) was carried out at an overpressure of 0.1 - 0.6 bar. For automated flash column chromatography a CombiFlash Companion apparatus running RediSep® columns was used. HPLC chromatograms were recorded on an Agilent Technologies 1100 (UV-detector).

Melting points (M.p.) were measured either on a Büchi B-540 melting-point apparatus in open capillaries or in a Mettler Toledo DSC822 differential scanning calorimeter. "Decomp" refers to decomposition.

7. Experimental Part

^1H -NMR and ^{13}C -NMR spectra were measured at 293 K, unless otherwise specified, on Bruker Avance 300 (300 MHz for ^1H -NMR and 75 MHz for ^{13}C -NMR), Bruker Avance 400 (400 MHz for ^1H -NMR and 100 MHz for ^{13}C -NMR) and Bruker Avance 500 (500 MHz for ^1H -NMR and 125.75 MHz for ^{13}C -NMR) NMR spectrometers. Deuterated solvents used are indicated in each case. Chemical shifts (δ) are reported in ppm relative to the signal of tetramethylsilane. Residual solvent signals in the ^1H and ^{13}C NMR spectra were used as an internal reference. Coupling constants (J) are given in Hz. The apparent resonance multiplicity is described as s (singlet), bs (broad singlet), d (doublet), dd (doublet of doublet), dt (doublet of triplet), t (triplet), q (quartet) and m (multiplet). The number of signal inducing protons and their positioning are given. Complete signal assignments from 1D and 2D NMR spectroscopy were based on COSY, HSQC, HMBC correlations and phase sensitive DEPTQ45 and DEPTQ135 spectra.

High-resolution mass analysis was performed in Bruker MALDI-TOF or Waters LCT Waters LCT (HPLC/MS-TOF; ESI or APCI mode) spectrometers.

Infrared spectra (IR) were recorded on FTIR Bruker spectrometer model Alpha with an ATR accessory.

UV-Vis spectra were recorded on a double beam UV-Vis Shimadzu spectrophotometer (UV-1800 model) as well as UV-Vis Lambda 2 and Lambda 35 (Perkin Elmer) spectrophotometers. The spectra were measured in toluene and DMF in a quartz cuvette (1 cm). For titration experiments involving SWCNT, UV-Vis-NIR spectra were recorded on a Cary 5000 (Varian) spectrophotometer.

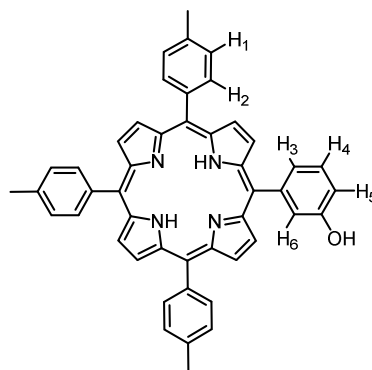
Fluorescence spectra were recorded on a Horiba Jobin Yvon System as well as Fluoromax 3 and Fluoromax 3P (Jobin Yvon) spectrofluorimeter. The spectra were measured in toluene and DMF in a quartz cuvette (1 cm).

UV-Vis and fluorescence titration were analyzed by fitting the whole series spectra using software Origin Pro 9.0 (Origin Lab).

7.2 Synthetic procedures

7.2.1 Flexible Receptor: A CTV-Based Acyclic Porphyrin Tripod

Synthesis of 5-(3-propargyloxyphenyl)-10,15,20-tolyl-porphyrin **8**⁹⁵



A solution of 3-hydroxybenzaldehyde (4.021 g, 32.9 mmol) in propionic acid (200 mL) was warmed to 120 °C under vigorous stirring. 4-tolualdehyde (11.65 mL, 99 mmol) was added and the reaction was protected from light to reduce the formation of polymerization products prior addition of pyrrole (9.14 mL, 132 mmol). The reaction mixture was refluxed under vigorous stirring for 1 h. After cooling down to r.t., the propionic acid was evaporated under reduced pressure and the crude was taken up in a small amount of CHCl₃. The porphyrins were precipitated by addition of hexane and filtrated off. The porphyrin mixture was purified by column chromatography (SiO₂; CHCl₃). Porphyrin **8** was isolated (1.107 g, 5%) as a purple solid.

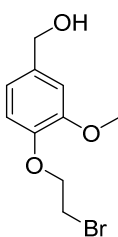
⁹⁵ Johnstone, K. M.; Yamaguchi, K.; Gunter, M. J. *Org. Biomol. Chem.* **2005**, *3*, 3008.

7. Experimental Part

¹H-NMR (400 MHz, CDCl₃): δ = -2.77 (s, 2 H; NH), 2.7 (s, 9 H; CH₃), 7.19 (dd, 1 H; ³J(H,H) = 8.25 Hz, J(H,H) = 2.63 Hz, H₃), 7.52-7.57 (m, 1 H; H₆), 7.55 (d, 6 H; ³J(H,H) = 7.76 Hz, H₂), 7.62 (t, 1 H; J(H,H) = 1.96 Hz, H₄), 7.77 (dt, 1 H; ³J(H,H) = 7.78 Hz, J(H,H) = 1.28 Hz, H₅), 8.10 (d, 6 H; ³J(H,H) = 7.76 Hz, H₁), 8.85-8.88 (s, 8 H; β -pyrrolic H).

LR-MM-ES+APCI-MS *m/z*: calculated for C₄₇H₃₇N₄O₁⁺: 673.0; found: 673.3 ([MH]²⁺).

Synthesis of (4-(2-bromoethoxy)-3-methoxyphenyl)methanol **5**⁹⁶



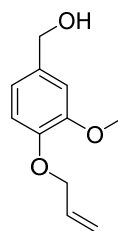
Commercially available vanillyl alcohol (2 g, 12.97 mmol) and K₂CO₃ (8.96 g, 64.9 mmol) were stirred in DMF (25 mL) for 30 min at r.t.. Dibromoethane (11.22 mL, 130 mmol) was added and the reaction mixture was heated for 18 h at 55 °C. The solvent was evaporated under reduced pressure, the crude was redissolved in EtOAc and the organic fraction was washed with water, 1 M NaOH and brine and dried over MgSO₄. The solvent was removed under *vacuum* and the yellow oil was purified by column chromatography (SiO₂; EtOAc / Hexane 20:80) to give the (4-(2-bromoethoxy)-3-methoxyphenyl)methanol **5** (3.142 g, 74 %) as a white solid.

⁹⁶ (a) Wei, Q.; Seward, G. K.; Hill, P. A.; Patton, B.; Dimitrov, I. E.; Kuzma, N. N.; Dmochowski I. J.; *J. Am. Chem. Soc.* **2006**, *128*, 13274. (b) Taratula, O.; Hill, P. A.; Bai, Y.; Khan, N. S.; Dmochowski, I. *J. Org. Lett.* **2011**, *13*, 1414.

7. Experimental Part

¹H-NMR (300 MHz, CDCl₃): δ = 1.65 (t, ³J(H,H) = 5.80, 1 H, CH₂OH), 3.66 (t, ³J(H,H) = 6.63 Hz, 2 H, OCH₂CH₂Br), 3.93 (s, 3H, OCH₃), 4.41 (t, ³J(H,H) = 6.63 Hz, OCH₂CH₂Br), 4.63 (d, ³J(H,H) = 5.84 Hz, 2 H, CH₂OH), 6.88 (dd, J(H,H) = 1.60 Hz, ³J(H,H) = 8.04 Hz, 1 H; ArH), 6.90 (d, ³J(H,H) = 8.04 Hz, 1 H; ArH), 6.96 (d, J(H,H) = 1.60 Hz, 1 H; ArH).

Synthesis of (4-(allyloxy)-3-methoxyphenyl)methanol **12**^{96a}

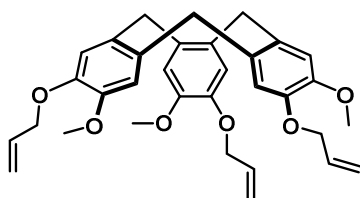


Commercially available vanillyl alcohol (2 g, 12.97 mmol) and K₂CO₃ (1.8 g, 12.97 mmol) were stirred in acetone (25 mL) for 30 min. Allyl bromide (1.5 mL, 17.3 mmol) was added and the reaction mixture was refluxed for 4 hours. The reaction mixture was allowed to cool down and the acetone was removed under *vacuo*. The crude product was redissolved in CH₂Cl₂ and washed with water, 1M NaOH and brine and dried over MgSO₄. The solvent was removed under reduced pressure and the reaction crude was purified by flash chromatography (SiO₂, EtOAc / Hexane 20:80) to afford the (4-(allyloxy)-3-methoxyphenyl)methanol **12** (2.443 g, 97 % yield) as a white product.

¹H-NMR (300 MHz, CDCl₃): δ = 1.58 (t, ³J(H,H) = 6.00 Hz, 1 H; CH₂OH), 3.90 (s, 3 H; OCH₃), 4.62 (d, ³J(H,H) = 5.14 Hz, 2 H; OCH₂CH), 4.63 (d, ³J(H,H) = 3.62 Hz, 2 H; CH₂OH), 5.30 (dd, ³J(H,H) = 20.18 Hz, J(H,H)₂ = 1.54 Hz, 1 H; CH₂CHCH₂), 5.42 (dd, ³J(H,H) = 20.26 Hz, J(H,H) = 1.54 Hz, 1 H; CH₂CHCH₂), 6.09 (m, 1 H; CH₂CHCH₂), 6.86 (s, 2 H; ArH), 6.94 (s, 1 H; ArH).

7. Experimental Part

Synthesis of 2,7,12-Trimethoxy-3,8,13-tris(2-propenyloxy)-10,15-dihydro-5H-tribenzo[a,d,g] cyclononene **13**^{96a}

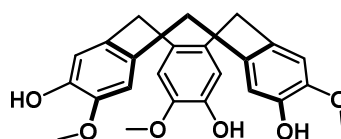


A solution of the allyl protected vanillyl alcohol **12** (0.5 g, 2.574 mmol) in MeOH (5 mL) was cooled in an ice bath. Perchloric acid (1.1 mL, 12.87 mmol) was dropwise added and the reaction mixture was stirred at r.t. for 18 h. The allyl protected CTV was extracted into CH₂Cl₂ and further washed with water until neutral pH was achieved. The organic fraction was further washed with brine and dried over Na₂SO₄. The crude product was digested in ether overnight and the white product was collected by filtration and washed with ether to afford the desired protected CTV **13** (213 mg, 47 %) as a white product.

¹H-NMR (400 MHz, CDCl₃): δ = 3.52 (d, ³*J*(H,H) = 10.15 Hz, 3 H; OCH₂CH), 3.83 (s, 9 H; OCH₃), 4.58 (m, 6 H; OCH₂CH), 4.75 (d, ²*J*(H,H) = 15.14 Hz, 3 H; ArCH₂Ar), 5.25 (dd, ³*J*(H,H) = 10.25 Hz, *J*(H,H) = 1.4 Hz, 3 H; CH₂CHCH₂), 5.38 (dd, ³*J*(H,H) = 10.20 Hz, *J*(H,H) = 1.40 Hz, 3 H; CH₂CHCH₂), 6.05 (m, 3 H; ArCH₂Ar), 6.78 (s, 3 H; ArH), 6.83 (s, 3 H; ArH).

7. Experimental Part

Synthesis of cyclotriguaiacylene **10**^{96a}

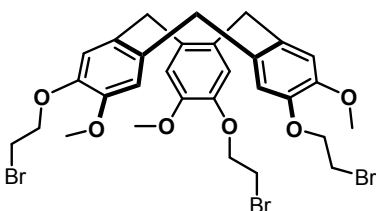


Allyl protected CTV-triphenol **13** (400 mg, 0.757 mmol), Pd(OAc)₂ (15.29 mg, 0.068 mmol) and PPh₃ (29.8 mg, 0.113 mmol) were dissolved in THF (12.5 mL). Diethylamine (4.7 mL, 45.4 mmol) and water (2.5 mL) were added and the reaction mixture was submitted to MW irradiation for 20 minutes at 120 °C. The solvent was evaporated under reduced pressure and the aqueous phase was extracted with ethyl acetate. The organic layers were washed with 1 M HCl, water and brine and were over Na₂SO₄. The solvent was removed under reduced pressure and the crude product was triturated in EtOH to give the desired CTV-triphenol **10** (247 mg, 80 %) as a white powder.

¹H-NMR (400 MHz, CDCl₃): δ = 3.50 (d, 3 H; ²J(H,H) = 13.68 Hz, ArCH₂Ar), 3.85 (s, 9 H; OCH₃), 4.71 (d, 3 H; ²J(H,H) = 13.68 Hz, ArCH₂Ar), 5.39 (s, 3 H; OH), 6.79 (s, 3 H; ArH), 6.88 (s, 3 H; ArH).

7. Experimental Part

Synthesis of 2,7,12-tris(2-bromoethoxy)-3,8,13-trimethoxy-10,15-dihydro-5H-tribenzo[a,d,g] [9]annulene **9**⁹⁶

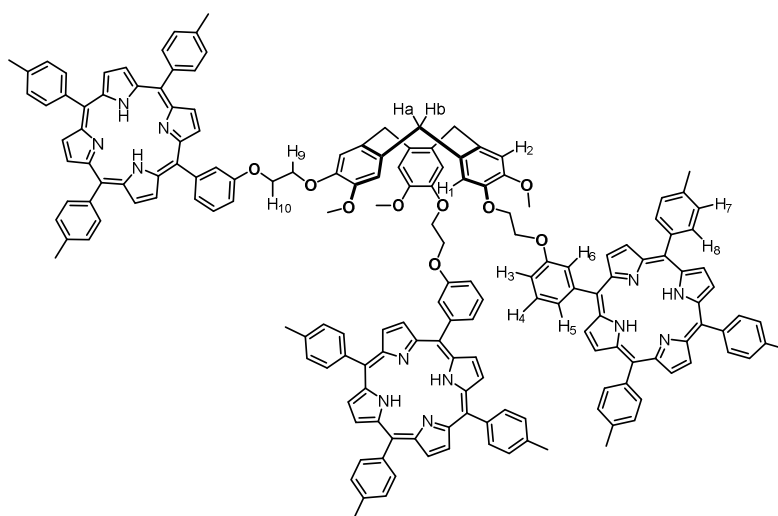


A suspension of CTV-triphenol **10** (0.054 g, 0.132 mmol), 1,2-dibromoethane (3.43 mL, 3.970 mmol) and cesium carbonate (0.646 g, 1.983 mmol) was stirred in ACN (20 mL) for 42 h at 55 °C. The solvent was removed under reduced pressure and the crude product was taken up in CHCl_3 . The suspension was filtered through celite and washed with CHCl_3 . The solvent was removed under *vacuo* and the crude was purified with column chromatography to afford the CTV-bromide **9** (46 mg, 48 %) as a yellowish oil.

¹H-NMR (500 MHz, CDCl_3): δ = 3.54 (d, 3 H; $^2J(\text{H,H}) = 13.93$ Hz, ArCH_2Ar), 3.56 (t, 6 H; $^3J(\text{H,H}) = 6.71$ Hz, $\text{OCH}_2\text{CH}_2\text{Br}$), 3.83 (s, 9 H; OCH_3), 4.27 (td, 6 H, $^3J(\text{H,H}) = 6.79$ Hz, $^2J(\text{H,H}) = 1.58$ Hz, $\text{OCH}_2\text{CH}_2\text{Br}$), 6.83 (s, 3 H; ArH), 6.91 (s, 3 H; ArH).

7. Experimental Part

Synthesis of CTV-porphyrin receptor **1**



CTV-bromide **8** (0.025 g, 0.034 mmol) and porphyrin **9** (0.092 g, 0.137 mmol) were dissolved in DMF (30 mL). Cesium carbonate (0.168 g, 0.514 mmol) was added and the suspension was vigorously stirred at 55 °C for 48 h. The solvent was removed under reduced pressure and the crude was taken up in CHCl₃, filtered through celite and washed with CHCl₃. The crude was filtrated through silica and eluted with CHCl₃ and the fractions containing the desired receptor were collected and purified by column chromatography (SiO₂, EtOAc / Hexane 8:2; CHCl₃ / Hexane 7:3) to afford the CTV-porphyrin **1** (67 mg, 70 %) as a purple solid.

¹H-NMR (500 MHz, CDCl₃): δ = -2.76 (s, 6 H; NH), 2.64 (s, 18 H; *cis*-CH₃), 2.70 (s, 9 H; *trans*-CH₃), 3.43 (d, 3 H; ²J(H,H) = 14.01 Hz, H_a), 3.67 (s, 9 H; OCH₃), 4.28-4.39 (m, 12 H, OCH₂CH₂O), 4.60 (d, 3 H; ³J(H,H) = 14.01 Hz, H_b), 6.77 (s, 3 H; H₂), 6.94 (s, 3 H; H₁), 7.27 (dd 3 H; ³J(H,H) = 8.34, J(H,H) = 2.60, H₃), 7.48-7.58 (m, 21 H; H₅ + H₈), 7.79-7.80 (m, 6 H, H₄ + H₆), 8.06-8.10 (m, 18 H, H₇), 8.84 (s, 12H; β-pyrrolic-H), 8.85 (s, 12H; β-pyrrolic-H).

7. Experimental Part

¹³C-NMR (125.75 MHz, CDCl₃): δ = 21.47 (*cis*-CH₃ + *trans*-CH₃), 36.39 (C-H_a + C-H_b), 56.21 (OCH₃), 66.80 (OCH₂CH₂O), 68.55 (OCH₂CH₂O), 114.08 (C-H₂), 114.16 (C-H₃), 117.21 (C-H₁), 119.36 (C), 120.18 (C), 120.31 (C), 121.27 (C-H₆), 127.40 (C-H₈), 127.47 (C-H₄), 127.98 (H₅), 131.01 (β-pyrrolic C), 131.84 (C), 133.26 (C), 134.50 (C-H₇), 137.31 (C), 137.32 (C), 139.24 (C), 139.32 (C), 143.63 (C), 146.92 (C), 148.79 (C), 157.02 (C).

IR (ATR): $\tilde{\nu}$ = 3314, 3021, 2919, 2850, 1598, 1574, 1506, 1469, 1399, 1347, 1259, 1218, 1179, 1090, 1022, 996, 965, 797, 730 cm⁻¹.

LR-MM-ES+APCI-MS *m/z*: calculated for C₁₇₂H₁₃₈N₁₂O₉⁺: 1253.0; found: 1253.0 ([MH]²⁺).

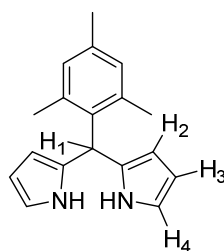
HR-FT-MALDI-MS *m/z*: calculated for C₁₇₂H₁₃₈N₁₂O₉⁺: 2505.0743; found: 2505.0127 ([MH]⁺).

UV/Vis (toluene): λ_{max} (ε) = 420 nm (766482 mol⁻¹ dm³ cm⁻¹);

M.p. 256-268 °C

7.2.2 Preorganized Receptor I: A Cyclic Porphyrin Trimer

Synthesis of mesityldipyrromethane **16**⁹⁷



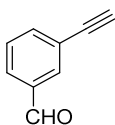
To 200 mL of 0.18 M aq. HCl, pyrrole (8.47 mL, 122 mmol) was added, followed by the addition of mesitylaldehyde (6 mL, 40.70 mmol). The reaction mixture was stirred at r.t. for 3 h. The sticky solid, was filtered off and washed with water. The reaction crude was then sonicated in cyclohexane. The mesityldipyrromethane **16** was afforded (2.875 g, 27 %) as a white product.

¹H-NMR (300 MHz, CDCl₃): δ = 2.06 (s, 6H; *ortho*-CH₃), 2.28 (s, 3H; *para*-CH₃), 5.93 (bs, 1 H; H₁), 6.00-6.02 (m, 2H; H₂), 6.16-6.19 (m, 2H; H₃), 6.65-6.67 (m, 2H; H₄), 6.87 (s, 2H; *ArH*), 7.94 (bs, 2H; NH).

⁹⁷ Rohand, T.; Dolusic, E.; Ngo, T. H.; Maes, W.; Dehaen, W. *ARKIVOC*, **2007**, 307

7. Experimental Part

Synthesis of 3-ethynylbenzaldehyde **18**⁹⁸



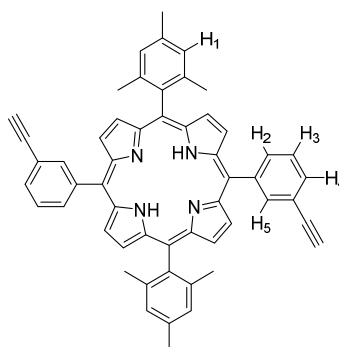
To a solution of commercially available 3-((trimethylsilyl)ethynyl)benzaldehyde (0.5 g, 2.471 mmol) in MeOH / THF 1:1 (40 mL) K_2CO_3 (2.39 g, 17.3 mmol) was added and the suspension was stirred at r.t. for 4 h. The suspension was filtered and the solvent removed under reduced pressure. CH_2Cl_2 was added and the organic phase was washed with water, brine and dried over $MgSO_4$. The solvent was removed under vacuum to yield the 3-ethynylbenzaldehyde **18** (275 mg, 86 %) as a white product that was used in the next steps without further purification.

¹H-NMR (300 MHz, $CDCl_3$): δ = 3.21 (s, 1 H, $C\equiv C-H$), 7.52 (t, 1 H, *ArH*), 7.71 (d, 1 H, *ArH*), 7.89 (d, 1 H, *ArH*), 8.00 (s, 1 H, *ArH*), 10.01 (s, 1 H, *CHO*).

⁹⁸ de Miguel, G.; Wielopolski, M.; Schuster, D. I.; Fazio, M. A.; Lee, O. P.; Haley, C. K.; Ortiz, A. L.; Echegoyen, L.; Clark, T.; Guldi, D. M. *J. Am. Chem. Soc.* **2011**, *133*, 13036.

7. Experimental Part

Synthesis of 5,15-bis(3-ethynylphenyl)-10,20-dimesitylporphyrin **14**⁹⁹



A solution of 5-mesityldipyrromethane **16** (100 mg, 0.378 mmol) and 3-ethynylbenzaldehyde **18** (49 mg, 0.378 mmol) in CH₂Cl₂ (10 mL) was degassed for 15 min under an Argon flow. The flask was protected from light to reduce the formation of polymerization products. BF₃·OEt₂ (10 μL, 0.079 mmol) was added and the reaction mixture was stirred for 1 h at room temperature. DDQ (86 mg, 0.378 mmol) was added and the reaction mixture was allowed to stir for an extra hour. Triethylamine was added and the reaction mixture was stirred for 5 min. The solvent removed under *vacuum* and the crude was filtered through silica to remove the polymerization products. The resulting purple crude was purified by preparative TLC chromatography (Cyclohexane:CHCl₃ 7/3) to obtain the desired porphyrin **14** (112 mg, 40%) as a purple product.

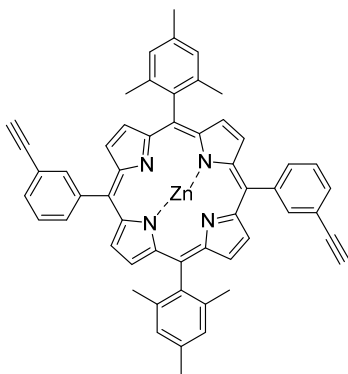
¹H-NMR (400 MHz, CDCl₃): δ = -2.63 (s, 2 H; NH), 1.86 (s, 12 H; *ortho*-CH₃), 2.65 (s, 6 H; *para*-CH₃), 3.17 (s, 2 H; CH), 7.31 (s, 4 H; H₁), 7.72 (t, 2H; ³J(H,H) = 7.70 Hz, H₃), 7.93 (d, 2 H; ³J(H,H) = 8.03 Hz, H₄), 8.23 (d, 2 H; ³J(H,H) = 8.03 Hz, H₂), 8.38 (s, 2 H; H₅), 8.73 (d, 4 H; ³J(H,H) = 4.83 Hz, β-pyrrolic H), 8.79 (d, 4 H; ³J(H,H) = 4.83 Hz, β-pyrrolic H).

⁹⁹ Yu L.; Lindsey, J. S. *J. Org. Chem.*, **2001**, 66, 7402.

7. Experimental Part

LR-MM-ES+APCI-MS m/z : calculated for $C_{54}H_{43}N_4^+$: 747.3; found: 747.3 ($[M]^+$).

Synthesis of zinc metallated 5,15-bis(3-ethynylphenyl)-10,20-dimesitylporphyrin Zn-14⁹⁹

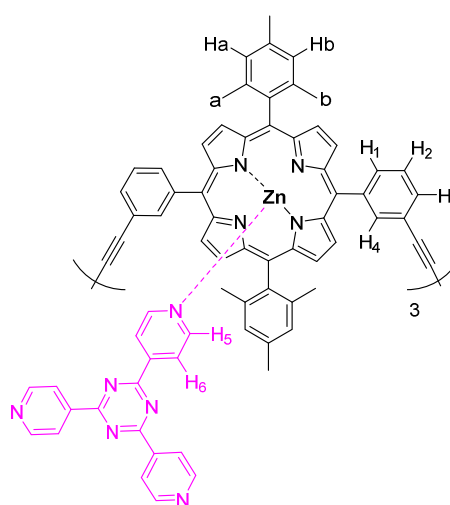


To a solution of free base porphyrin **14** (215 mg, 0.288 mmol) in CH_2Cl_2 / EtOH (3:1; 60 mL) zinc acetate (528 mg, 2.88 mmol) was added and the suspension was stirred at r.t. under open air for two hours. The solvent was evaporated and the crude was taken up in CH_2Cl_2 . The organic fraction was washed with water, brine and dried over $MgSO_4$. The organic fraction was filtered through silica to remove the remaining acetate. The solvent was removed under reduced pressure to afford the metallated porphyrin Zn-**14** (228 mg, 98 %) as a purple product that was used on the next step without further purification.

LR-MM-ES+APCI-MS m/z : calculated for $C_{54}H_{43}N_4Zn^+$: 809.2; found: 809.1 ($[M]^+$).

7. Experimental Part

Synthesis of template complexated trimer **19@Zn₃-2**¹⁰⁰



A solution of zinc metallated porphyrin **Zn-14** (63 mg, 0.078 mmol) and commercially available 2,4,6-tri(pyridin-4-yl)-1,3,5-triazine trimeric template (7.3 mg, 0.023 mol) in CHCl_3 (100 mL) was sonicated for 2 h. Dichlorobis(triphenylphosphine)-palladium (II) (36 mg, 0.052 mmol), CuI (20 mg, 0.104 mmol) and *i*-Pr₂NH (3 mL) were added and the reaction mixture was stirred under air for 30 min. The product was purified with preparative TLC (Cyclohexane / CHCl_3 7:3) to obtain the complex **19@Zn₃-2** (21 mg, 30 %) as a purple-blueish solid that was directly submitted to template release process under acidic conditions.

¹H-NMR (300 MHz, CDCl_3): δ = 1.54 (s, 18 H; *ortho*-CH₃(a)), 1.84 (s, 18 H; *ortho*-CH₃(b)), 2.55 (s, 18 H; *para*-CH₃), 2.68 (d, 6 H; ³*J*(H,H) = 6.47 Hz, H₆), 6.05 (d, 6 H; ²*J*(H,H) = 6.47 Hz, H₅), 6.99 (s, 6 H; H_aH_b), 7.22 (s, 6 H; H_aH_b), 7.64 (t, 6 H;

¹⁰⁰ Procedure adapted from O'Sullivan, M. C.; Sprafke, J. K.; Kondratuk, D. V.; Rinfray, C.; Claridge, T. D. W.; Saywell, A.; Blunt, M. O.; O'Shea, J. N.; Beton, P. H.; Malfois M.; Anderson, H. L. *Nature*, **2011**, *469*, 72.

7. Experimental Part

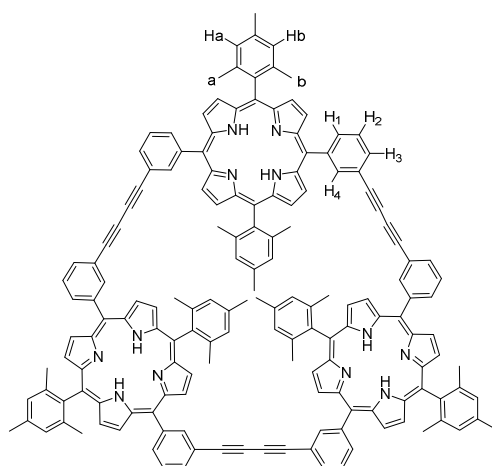
$^3J(\text{H,H}) = 7.78 \text{ Hz}$, H_2), 7.85 (dd, 6 H; $^3J(\text{H,H}) = 7.90 \text{ Hz}$, $J(\text{H,H}) = 1.26 \text{ Hz}$, H_3), 8.00 (dd, 6 H; $^2J(\text{H,H}) = 7.90 \text{ Hz}$, $^2J(\text{H,H}) = 1.26 \text{ Hz}$, H_1), 8.55 (d, 12 H; $^2J(\text{H,H}) = 4.83 \text{ Hz}$, β -pyrrolic H), 8.68 (d, 12 H; $^3J(\text{H,H}) = 4.83 \text{ Hz}$, β -pyrrolic H), 8.68 (s, 6 H; H_4).

LR-MM-ES+APCI-MS m/z : calculated for $\text{C}_{180}\text{H}_{127}\text{N}_{18}\text{Zn}_3^+$: 1367.9; found: 1368.0 ($[\text{MH}]^{2+}$).

LR-MM-ES+APCI-MS m/z : calculated for $\text{C}_{162}\text{H}_{115}\text{N}_{12}\text{Zn}_3^+$: 1212.0; found: 1212.9 ($[\text{MH}]^{2+}$).

LR-FT-MALDI-MS m/z : calculated for $\text{C}_{162}\text{H}_{115}\text{N}_{12}\text{Zn}_3^+$: $\text{C}_{162}\text{H}_{115}\text{N}_{12}\text{Zn}_3^+$: 2422.7; found: 2424.9.

Synthesis of cyclic porphyrin trimer **2**



Conc. HCl was added dropwise to a solution of **19@Zn₃-2** (120 mg, 0.044 mmol) in CH_2Cl_2 until acid pH was achieved or the solution turn deep green colored. Then the solution was washed with water until the solution turn reddish. It was further washed with brine and dried over the minimum amount of Na_2SO_4 . The solvent was evaporated under reduced pressure to give the desired receptor **5** (96 mg, 98 %) as a purple solid.

7. Experimental Part

¹H-NMR (500 MHz, CDCl₃): δ = -2.82 (s, 6 H; N-H), 1.64 (s, 18 H; *ortho*-CH₃ (a)), 1.76 (s, 18 H; *ortho*-CH₃ (b)), 2.58 (s, 18 H; *para*-CH₃ (c)), 7.18 (s, 6 H; H_a), 7.22 (s, 6 H; H_b), 7.07 (t, 6 H; ³J(H,H) = 7.86 Hz, H₂), 7.93 (dt, 6 H; ³J(H,H) = 7.86 Hz, J(H,H) = 1.29 Hz, H₃), 8.21-8.23 (m, 24 H; H₁ and H₄), 8.60 (d, 24 H; ³J(H,H) = 4.79 Hz, β-pyrrolic H), 8.66 (d, 24 H; ³J(H,H) = 4.79 Hz, β-pyrrolic H).

¹³C NMR (125.75 MHz, CDCl₃): δ = 21.42 (*para*-CH₃ (c)), 21.44 (*ortho*-CH₃ (a)), 21.57 (*ortho*-CH₃ (b)), 117.71 (C), 118.57 (C), 120.32 (C), 126.86 (C-H₂), 127.69 (C-H_b), 127.73 (C-H_a), 130.36 (β-pyrrolic C), 130.92 (β-pyrrolic C), 131.55 (C-H₃), 133.73 (C), 134.87 (C-H₁), 137.72 (C), 138.14 (C), 138.15 (C-H₄), 139.21 (C), 139.40 (C), 142.39 (C), 165.40 (C), 165.44 (C).

IR (ATR): $\tilde{\nu}$ = 3323, 9219, 2850, 1725, 1591, 1510, 1466, 1438, 1376, 1338, 1260, 1217, 1190, 1090, 1012, 969, 914, 852, 799, 723, 694, 607, 566, 508, 466, 442, 406 cm⁻¹.

UV/Vis (toluene): $\lambda_{\text{max}} (\epsilon) = 419 \text{ nm} (785944 \text{ mol}^{-1} \text{ dm}^3 \text{ cm}^{-1})$;

LR-MM-ES+APCI-MS *m/z*: calculated for C₁₆₂H₁₂₁N₁₂⁺: 1118.0; found: 1117.9; ([MH]²⁺).

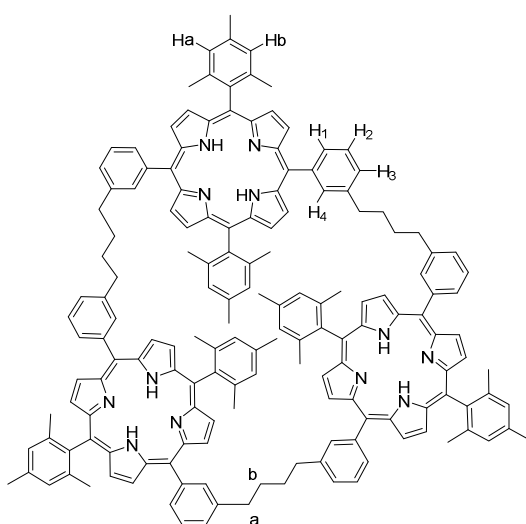
HR-FT-MALDI-MS *m/z*: calculated for C₁₆₂H₁₂₁N₁₂⁺: 2233.9792; found: 2233,9790 ([MH]⁺).

M.p. 358-360 °C (decomp)

7. Experimental Part

7.2.3 Preorganized Receptor II: A Flexible Cyclic Porphyrin Trimer

Synthesis of cyclic porphyrin trimer **3**¹⁰¹



To a 10 ml THF solution of porphyrin trimer **2** (38 mg, 0.017 mmol) Pd/C (47 mg, 0.044 mmol) was added and the suspension was stirred under H₂ atmosphere for 4 h until total conversion was attained. The reaction was monitored by HPLC-ms (MM-ES+APCI mode). Once no starting material was detected the suspension was filtered through celita, eluting with THF. The solvent was evaporated and taken up in CH₂Cl₂ and filtrated through silica. No further purification was required. Cyclic porphyrin trimer **3** was afforded as a purple solid (24 mg, 63%)

¹H-NMR (500 MHz, CDCl₃): δ = -2.86 to -2.75 (ts, 6 H; N-H), 1.48 (bs, 18 H; CH₃), 1.71 (bs, 18 H; CH₃), 2.00 (bs, 12; CH₂(b)), 2.34 (bs, 18 H; CH₃), 2.93 (bs, 12; CH₂(a));

¹⁰¹ Procedure adapted from Tashiro, K.; Aida, T.; Zheng, J.-Y.; Kinbara, K.; Saigo, K.; Sakamoto, S.; Yamaguchi, K.; *J. Am. Chem. Soc.* **1999**, *121*, 9477

7. Experimental Part

6.63-6.85 (m, 6 H; H_aH_b), 7.08 (bs, 6 H, H_aH_b), 7.43-7.65 (m, 12 H; Aromatic-H $H_2 + H_3$), 7.90-8.61 (m, 12 H; $H_1 + H_4$), 8.34-8.43 (m, 6 H; (β -pyrrolic H)), 8.47-8.53 (m, 6 H; (β -pyrrolic H)), 8.62-8.77 (m, 12 H; (β -pyrrolic H))

^{13}C NMR (125.75 MHz, CDCl_3): δ = 21.16 (CH_3), 21.30 (CH_3), 21.35 (CH_3), 21.37 (CH_3), 21.47 (CH_3), 21.49 (CH_3), 31.93 (CH_2 (b)), 36.20 (CH_2 (a)), 36.30 (CH_2 (a)), 118.00 (C), 118.02 (C), 119.42 (C), 119.44 (C), 123.97 (C), 124.46 (C), 126.61 (CH_2), 126.80 (CH_2), 127.27 (H_3), 127.30 (H_3), 127.39 (H_aH_b), 127.43 (H_aH_b), 127.49 (H_aH_b), 127.56 (H_aH_b), 127.68 (H_aH_b), 129.89 (β -pyrrolic C), 131.30 (β -pyrrolic C), 132.28 (C- H_1), 132.37 (C- H_4), 135.19 (C), 135.64 (C), 137.18 (C), 137.34 (C), 137.39 (C), 138.27 (C), 138.35 (C), 139.00 (C), 139.11 (C), 139.17 (C), 139.18 (C), 139.21 (C), 140.84 (C), 140.86 (C), 140.90 (C), 141.77 (C), 141.88 (C).

IR (ATR): $\tilde{\nu}$ = 3316, 3202, 3047, 2953, 2919, 2851, 2528, 2321, 2214, 2186, 2107, 2040, 1970, 1917, 1773, 1717, 1650, 1600, 1562, 1463, 1440, 1400, 1376, 1349, 1305, 1283, 1261, 1229, 1215, 1179, 1127, 1089, 1071, 1052, 1012, 985, 972, 914, 852, 800, 731, 711, 679, 647, 610, 568, 550, 535, 462, 441 cm^{-1} .

LR-MM-ES+APCI-MS m/z : calculated for $\text{C}_{162}\text{H}_{145}\text{N}_{12}^+$: 1129.6; found: 1129.8 ($[\text{MH}]^{2+}$).

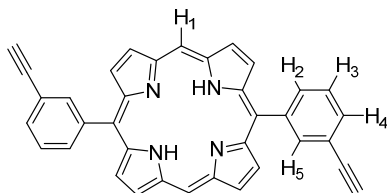
HR-FT-MALDI-MS m/z : calculated for $\text{C}_{162}\text{H}_{145}\text{N}_{12}^+$: 2258,1670; found: 2258,1543 ($[\text{MH}]^+$).

UV/Vis (toluene): λ_{max} (ϵ) = 419 nm (534541 $\text{mol}^{-1} \text{dm}^3 \text{cm}^{-1}$);

7. Experimental Part

7.2.4 Preorganized Receptor III: A Sterically Unhindered Cyclic Porphyrin Trimer

Synthesis of 5,15-bis(3-ethynylphenyl)porphyrin **20**¹⁰²



A solution of the commercially available dipyrromethane (309 mg, 2.05 mmol) and the previously deprotected 3-ethynylbenzaldehyde **18** (275 mg, 0.205 mmol) in CH_2Cl_2 was degassed under a stream of Argon for 15 min. The flask was protected from light to reduce the formation of polymerization products. $\text{BF}_3 \cdot \text{OEt}$ (47 μL , 0.369 mmol) was added and the reaction mixture that was stirred at r.t. for 1 h. DDQ was added and the reaction was further stirred for another hour. Triethylamine was added the reaction was stirred for 5 min. The reaction mixture was filtered through silica to remove the polymerization products and the solvent was removed under *vacuum* to give the purple crude that was purified by flash chromatography (Cyclohexane / CHCl_3 7:3) to obtain the desired free base porphyrin **20** (472 mg, 45 %) as a purple product.

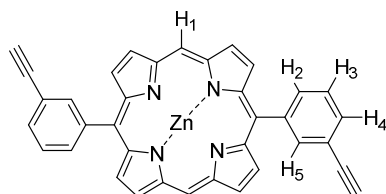
¹H-NMR (300 MHz, CDCl_3): δ = -3.16 (s, 2 H; N-H), 3.20 (s, 2 H; C \equiv C-H), 7.78 (t, 2 H; ³J(H,H) = 7.69 Hz, H₃), 7.96 (bd, 2 H; ³J(H,H) = 7.64 Hz, H₂), 8.26 (bd, 2 H; ³J(H,H) = 7.67 Hz, H₄), 8.42 (s, 2 H; H₅), 9.06 (d, 4 H; ³J(H,H) = 4.55 Hz, β -pyrrolic H), 9.42 (d, 4 H; ³J(H,H) = 4.56 Hz, β -pyrrolic H), 10.35 (s, 2 H; H₁).

LR-MM-ES+APCI-MS *m/z*. calculated for $\text{C}_{36}\text{H}_{23}\text{N}_4^+$: 511.3; found: 511.2 ($[\text{M}]^{2+}$).

¹⁰² Procedure adapted from ref. 4

7. Experimental Part

Synthesis of zinc metallated 5,15-bis(3-ethynylphenyl)porphyrin **Zn-20**¹⁰²



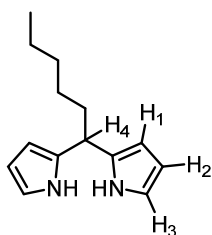
To a solution of free base porphyrin **20** (250 mg, 0.490 mmol) in CH_2Cl_2 / EtOH (3:1; 30 mL), zinc acetate (898 mg, 4.90 mmol) was added and the suspension was stirred at r.t. under open air for 18 h. Solvent was evaporated under reduce pressure, the crude was taken up in CH_2Cl_2 . The organic fraction was washed with water, brine and dried over MgSO_4 . The solvent was removed under *vacuum* and the reaction crude was filtrated through silica to remove the excess of zinc acetate to afford the zinc metallated porphyrin **Zn-21** (278 mg, 94%) as a purple solid.

¹H-NMR (300 MHz, CDCl_3): δ = 3.19 (s, 2 H; $\text{C}\equiv\text{C-H}$), 7.76 (t, 2 H; $^3J(\text{H,H}) = 7.67$ Hz, H_2), 7.96 (dt, 2 H; $^3J(\text{H,H}) = 7.67$ Hz, $J(\text{H,H}) = 1.40$ Hz, H_2), 8.25 (d, 2 H; $^3J(\text{H,H}) = 7.67$ Hz, H_4), 8.41 (bs, 2 H; H_5) 9.11 (d, 4 H; $^3J(\text{H,H}) = 4.53$ Hz, β -pyrrolic H), 9.45 (d, 4 H; $^3J(\text{H,H}) = 4.57$ Hz, β -pyrrolic H), 10.34 (s, 2 H; H_1).

LR-MM-ES+APCI-MS m/z : calculated for $\text{C}_{36}\text{H}_{23}\text{N}_4\text{Zn}^+$: 573.3; found: 573.1 ($[\text{MH}]^{2+}$).

7. Experimental Part

Synthesis of dipyrrohexane **22**¹⁰³



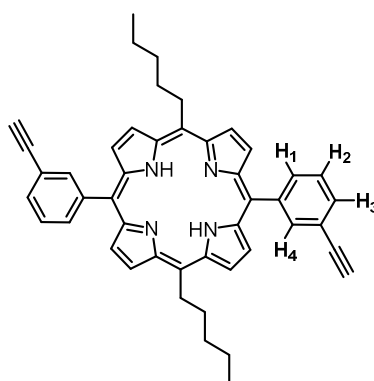
A solution of hexanal (2.45 mL, 19.97 mmol) and pyrrole (34.6 mL, 499 mmol) was degassed under an Argon flow for 5 min. The reaction flask was protected from light to reduce the formation of polymerization products prior to addition of TFA (0.3 mL, 3.99 mmol). The reaction mixture was then stirred at r.t. for 1 h and quenched with 0.1 M NaOH. Ethyl acetate was added and the organic phase was washed with water, brine and dried over MgSO₄. The solvent was removed at reduced pressure. The brown oil was sonicated in cyclohexane and was further purified by flash chromatography (Cyclohexane / EtOAc 8:2) to give the desired dipyrrohexane (1.8 g, 42 %) as a white solid.

¹H-NMR (400 MHz, CDCl₃): δ = 3.91 (t, 3 H, ³J(H,H) = 6.35 Hz, CH₃), 1.32 (bs, 6 H; CH₂(CH₂)₃CH₃), 1.91-1.98 (m, 2 H; CH₂(CH₂)₃CH₃), 3.94 (t, 1 H; ³J(H,H) = 7.59 Hz, H₁), 6.08-6.21 (m, 2 H; H₂) 6.16-6.20 (m, 2 H; H₃), 6.56-6.60 (m, 2 H; H₄), 7.57 (bs, 2 H; N-H).

¹⁰³ (a) Seo, K. D.; Lee, M. J.; Song, H. M.; Kang H. S.; Kim, H. K. *Dyes Pigments*, **2012**, *94*, 143
(b) Halime, Z.; Lachkar, M.; Matsouki, N.; Charalambidis, G.; di Vaira, M.; Coutsolelos A. G.; Boitrel, B. *Tetrahedron*, **2006**, *62*, 3056.

7. Experimental Part

Synthesis of 5,15-bis(3-ethynylphenyl)-10,20-dipentylporphyrin **21**¹⁰²



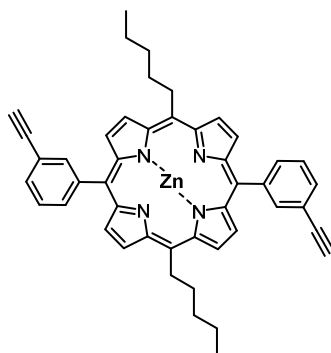
A solution of dipyrrohexane **22** (900 mg, 4.16 mmol) and 3-ethynylbenzaldehyde (558 mg, 4.16 mmol) in CH_2Cl_2 was degassed under a stream of Argon for 15 min. The reaction flask was protected from light to reduce the formation of polymerization products and then $\text{BF}_3 \cdot \text{OEt}$ (95 μL , 0.749 mmol) was added to the reaction mixture that was allowed to stir at r.t. for 1 h. DDQ (944 mg, 4.16 mmol) was added and the reaction was stirred for another hour and further quenched with trimethylamine. The solvent was removed under reduced pressure. CH_2Cl_2 was added and the reaction crude was filtrated through silica to eliminate the polymerization products. The resulting purple crude was purified by flash chromatography (Cyclohexane / CHCl_3 7:3) to afford the free base porphyrin **21** (648 mg, 34 %) as a purple product.

$^1\text{H-NMR}$ (400 MHz, CDCl_3): δ = -2.69 (s, 2 H; N-H), 0.99 (t, 6 H; $^3J(\text{H,H}) = 7.42$ Hz, CH_3), 1.53-1.58 (m, 4 H; CH_2CH_3), 1.78-1.84 (m, 4 H; $\text{CH}_2\text{CH}_2\text{CH}_3$), 2.48-2.57 (m, 4 H; $\text{CH}_2(\text{CH}_2)_2\text{CH}_3$), 3.18 (s, 2 H; $\text{C}\equiv\text{CH}$), 4.93 (t, 4 H; $^3J(\text{H,H}) = 8.09$ Hz, $\text{CH}_2(\text{CH}_2)_3\text{CH}_3$), 7.72 (t, 2 H; $^3J(\text{H,H}) = 7.73$ Hz, H_2), 7.93 (dt, 2 H; $^3J(\text{H,H}) = 7.94$ Hz, $J(\text{H,H}) = 1.38$ Hz, H_3), 8.15-8.18 (m, 2 H; H_1), 8.34-8.35 (m, 2 H; H_4), 8.90 (d, 4 H; $^3J(\text{H,H}) = 4.73$ Hz, β -pyrrolic H), 9.50 (d, 4H; $^2J(\text{H,H}) = 4.73$ Hz, β -pyrrolic H)

7. Experimental Part

LR-MM-ES+APCI-MS m/z : calculated for $C_{46}H_{43}N_4^+$: 651.4; found: 651.3 ($[MH]^+$).

Synthesis of zinc metallated 5,15-bis(3-ethynylphenyl)-10,20-dipentylporphyrin **Zn-21**¹⁰²



To a solution of free base porphyrin **21** (270 mg, 0.415 mmol) in CH_2Cl_2 / EtOH (3:1; 30 mL), zinc acetate (761 mg, 4.15 mmol) was added and the suspension was stirred at r.t. under open air for 18 h. The reaction mixture was directly filtrated through silica to remove the excess of zinc acetate and the solvent was removed under reduced pressure to afford the zinc metallated porphyrin **Zn-21** (278 mg, 94%) as a purple solid.

¹H-NMR (400 MHz, $CDCl_3$): δ = 0.99 (t, 6 H; $^3J(H,H)$ = 7.27 Hz, CH_3), 1.52-1.58 (m, 4 H; CH_2CH_3), 1.78-1.82 (m, 4 H; $CH_2CH_2CH_3$), 2.49-2.51 (m, 4 H; $CH_2(CH_2)_2CH_3$), 3.18 (s, 2 H; $C\equiv CH$), 4.86 (t, 4 H; $^3J(H,H)$ = 8.00 Hz, $CH_2(CH_2)_3CH_3$), 7.72 (t, 2 H; $^3J(H,H)$ = 7.69 Hz, H_2), 7.93 (bd, 2 H; $^3J(H,H)$ = 7.65 Hz, H_2), 8.15 (bt, 2 H; $^3J(H,H)$ = 6.22 Hz, H_2), 8.33 (bs, 2 H; H_2), 8.87 (d, 4 H; $^3J(H,H)$ = 4.67 Hz, β -pyrrolic H), 9.44 (d, 4 H; $^3J(H,H)$ = 4.75 Hz, β -pyrrolic H).

¹³C-NMR (125.75 MHz, $CDCl_3$): δ = 14.16 (CH_3), 22.80 (CH_2CH_3), 32.85 ($CH_2CH_2CH_3$), 35.65 ($CH_2(CH_2)_3CH_3$), 38.70 ($CH_2CH_2(CH_2)_2CH_3$), 83.96 ($C\equiv CH$), 118.55 (C), 120.46 (C), 126.55 ($C-H_2$), 128.95 (β -pyrrolic C), 129.63 (C), 131.22 ($C-H_3$), 132.01

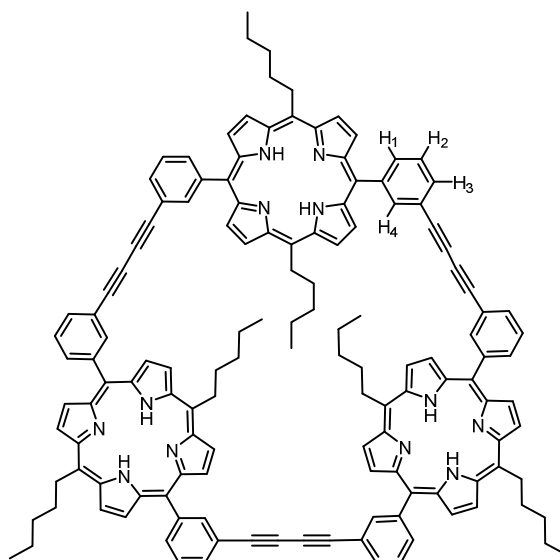
7. Experimental Part

(β -pyrrolic C), 132.68 (C), 134.67 (C-H₁), 137.59 (C-H₄), 143.27 (C), 149.71 (C), 150.35 (C).

LR-MM-ES+APCI-MS *m/z*: calculated for C₄₆H₄₃N₄⁺: 712.3; found: 712.3 ([MH]⁺).

HR-FT-MALDI-MS *m/z*: calculated for C₄₆H₄₃N₄⁺: 712.2544; found: 712.2512 ([MH]⁺).

Synthesis of cyclic porphyrin trimer **5**



Porphyrin **Zn-21** (54 mg, 0.076 mmol) was dissolved in the minimum amount of CHCl₃ (5 mL) and a solution of commercially available 2,4,6-tri-4-pyridyl-1,3,5-triazine (7.8 mg, 0.025 mmol) in CHCl₃ (300 mL) was dropwise added. The reaction solution was then stirred for 5 h and then CuCl (254 mg, 5.29 mmol) and TMEDA (79 μ L, 5.29 mmol) were added. The reaction was then refluxed for 1 h under open air until total consumption of starting material was observed. The solvent was removed under reduced pressure and the reaction crude was dissolved in CH₂Cl₂. The organic fraction was washed with water, brine and dried over MgSO₄. Purification with preparative TLC (Cyclohexane / CHCl₃ 7:3) afforded **19@Zn₃-5** as a purple-blueish solid

7. Experimental Part

(**LR-MM-ES+APCI-MS** m/z calculated for $C_{156}H_{127}N_{18}Zn_3^+$: 1067.9 (template free); found: 1068.2 ($[MH]^{2+}$)). The complexed receptor was dissolved in the minimum amount of $CHCl_3$ and conc. HCl was added dropwise until acidic pH was achieved and the solution turn deep green colored. Then the solution was washed with water until the solution turn reddish. It was further washed with brine and dried over the minimum amount of Na_2SO_4 . The crude was filtrated through silica and the solvent was evaporated under reduced pressure to give the desired receptor **5** (10 mg, 28 %) as a purple solid.

1H -NMR (500 MHz, $CDCl_3$): δ = -2.90- -2.74 (m, 6 H; NH), 0.76 (t, 6 H; CH_3), 0.86 (t, 6 H; CH_3), 0.98 (t, 6 H; CH_3), 1.23-1.48 (m, 12 H; CH_2CH_3), 1.52-1.83 (m, 12 H; $CH_2CH_2CH_3$), 2.33-2.54 (m, 12 H; $CH_2CH_2CH_2CH_3$), 4.80 (t, 4 H; $^3J(H,H) = 7.76$ Hz, $CH_2CH_2CH_2CH_2CH_3$), 4.86 (t, 4 H; $^3J(H,H) = 7.76$ Hz, $CH_2CH_2CH_2CH_2CH_3$), 4.94-5.03 (m, 4 H; $CH_2CH_2CH_2CH_2CH_3$), 7.74 (q, 6 H; $^3J(H,H) = 7.48$ Hz, H_2), 7.95 (dd, 6 H; $^3J(H,H) = 20.86$ Hz, $^3J(H,H) = 7.88$ Hz, H_3), 8.06-8.13 (m, 6 H; H_1), 8.22-8.30 (m, 6 H; H_4), 8.57-8.85 (m, 12 H; β -pyrrolic H), 9.25-9.62 (m, 12 H; β -pyrrolic H).

^{13}C -NMR (125.75 MHz, $CDCl_3$): δ = 13.79 (CH_3), 14.03 (CH_3), 14.12 (CH_3), 14.13 (CH_3), 22.57 ($CH_2CH_2CH_3$), 22.66 ($CH_2CH_2CH_3$), 22.69 ($CH_2CH_2CH_3$), 22.76 ($CH_2CH_2CH_3$), 35.08 ($CH_2(CH_2)_3CH_3$), 35.14 ($CH_2(CH_2)_3CH_3$), 38.21 ($CH_2(CH_2)_2CH_3$), 38.27 ($CH_2(CH_2)_2CH_3$), 116.98 (C), 117.21 (C), 119.10 (C), 119.11 (C), 120.06 (C), 120.12 (C), 120.15 (C), 120.33 (C), 126.64 (C-H₂), 126.74 (C-H₂), 126.79 (C-H₂), 127.83 (β -pyrrolic C), 131.46 (β -pyrrolic C), 131.81 (C-H₃), 131.95 (C-H₃), 134.41 (C-H₁), 134.78 (C), 135.36 (C), 137.42 (C-H₁), 137.91 (C), 138.46 (C), 138.54 (C), 139.04 (C-H₄), 142.63 (C), 143.05 (C), 143.08 (C), 147.08 (C), 147.62 (C), 147.68 (C).

IR (ATR): $\tilde{\nu}$ = 3315, 3202, 3047, 2919, 2851, 2321, 2214, 2186, 2166, 2149, 2112, 2085, 2052, 2014, 1982, 1773, 1716, 1650, 1600, 1562, 1463, 1448, 1439, 1400, 1375, 1349, 1305, 1283, 1263, 1228, 1215, 1179, 1128, 1089, 1071, 1053, 1011, 986, 972, 915, 851, 800, 730, 713, 678, 647, 609, 576, 549, 535, 463, 442, 418 cm^{-1} .

7. Experimental Part

LR-MM-ES+APCI-MS *m/z*: calculated for C₁₃₈H₁₂₁N₁₂⁺: 1946.9; found: 1946.7 ([M]⁺).

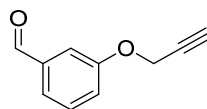
LR-MM-ES+APCI-MS *m/z*: calculated for C₁₃₈H₁₂₁N₁₂⁺: 973.9; found: 974.0 ([M]²⁺).

HR-FT-MALDI-MS *m/z*: calculated for C₁₃₈H₁₂₁N₁₂⁺: 1946.9792; found: 1945.9748 ([M]⁺).

UV/Vis (toluene): λ_{max} (ε) = 421 nm (738094 mol⁻¹ dm³ cm⁻¹);

7.2.5 Preorganized Receptor IV: Enlarged Cyclic Porphyrin Trimer.

Synthesis of 3-allyloxybenzaldehyde **25**⁶⁷

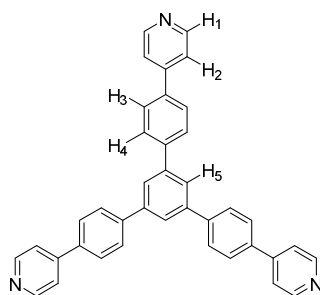


To a solution of 3-hydroxybenzaldehyde (1 g, 8.19 mmol) and propargylbromide (1.34 ml, 12.28 mmol) in dry CH₃CN, K₂CO₃ (1.7 g, 12.28 mmol) was added and the suspension was stirred for 18 h at 60 °C. The precipitate was filtered off, washed with water, brine and dried over MgSO₄. The crude was purified through column chromatography (SiO₂; Hexane / EtOAc 8:2) to afford the 3-(prop-2-yn-1-yloxy)benzaldehyde **25** (1.2 g, 91%) as a yellow oil.

¹H-NMR (300 MHz, CDCl₃): δ = 2.49 (t, 1 H; ⁴J(H,H) = 2.47 Hz, CH), 4.58 (d, 2 H; ⁴J(H,H) = 2.48 Hz, CH₂), 7.06-7.09 (m, 1 H; ArH), 7.28-7.32 (m, 3 H; ArH), 9.79 (s, 1 H, COH).

7. Experimental Part

Synthesis of 4,4'-(5'-(4-(pyridin-4-yl)phenyl)-[1,1':3',1''-terphenyl]-4,4''-diyl)dipyridine **26**¹⁰⁴



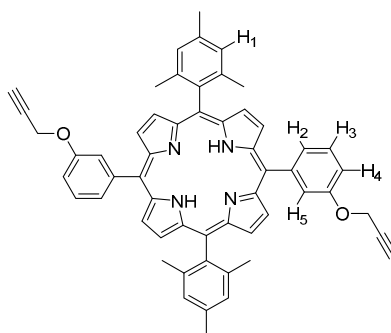
A mixture of 4,4''-dibromo-5'-(4-bromophenyl)-1,1':3',1''-terphenyl (0.5 g, 0.921 mmol), pyridine boronic acid (0.407, 3.31 mmol), sodium carbonate (1.171 g, 11.05 mmol) and tetrakis(triphenylphosphine)-palladium (0.064 g, 0.055 mmol) in EtOH / H₂O (16.5:3.5; 2.5 mL) were degassed under an Argon flow. The reaction mixture was submitted to MW irradiation at 150 °C for 15 min. The reaction mixture was cooled down to r.t., the crude product was extracted into CH₂Cl₂ and was washed with water, brine and dried over MgSO₄. The solvent was removed under vacuum to afford the trimeric template **26** (497 mg, 100 %) as a white solid.

¹H-NMR (300 MHz, CDCl₃): δ = 7.58 (dd, 6 H; ²J(H,H) = 6.18 Hz, ³J(H,H) = 2.78 Hz, H₂), 7.82 (dd, 12 H; H₃ + H₄), 7.90 (s, 3 H; H₅), 8.70 (dd, 6 H; ³J(H,H) = 6.18 Hz, ³J(H,H) = 2.78 Hz, H₁),

¹⁰⁴ Howard; H. R.; Bishop, W. U.S. Histamine-3 receptor antagonists. U.S. Patent 20,050,245,543, April 15, 2005.

7. Experimental Part

Synthesis of 5,15-dimesityl-10,20-bis(3-(prop-2-yn-1-yloxy)phenyl)porphyrin **23**⁶⁷



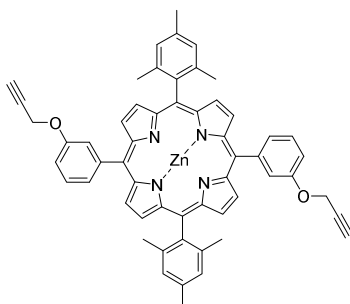
A solution of mesityl substituted dipyrromethane **16** (100 mg, 0.378 mmol) and 3-(prop-2-yn-1-yloxy)benzaldehyde **25** (86 mg, 0.378 mmol) in CH_2Cl_2 (10 mL) was degassed for 15 min under an Argon flow. The reaction was protected from light to reduce the formation of polymerization products. $\text{BF}_3 \cdot \text{OEt}_2$ (10 μL , 0.079 mmol) was added and the reaction mixture was stirred for 1 h at r.t.. DDQ (86 mg, 0.378 mmol) was added and the reaction mixture was allowed to stir for an extra hour. Triethylamine was added and the reaction mixture was stirred for 5 min. The solvent was removed under *vacuo* and the crude was taken up in CHCl_3 and was filtered through silica to remove the polymerization products. The resulting purple solid was purified by preparative TLC chromatography (cyclohexane / CHCl_3 7:3) to obtain the desired porphyrin **23** (182 mg, 60 %) as a purple product.

¹H-NMR (300 MHz, CDCl_3): δ = -2.61 (s, 2 H; *NH*), 1.86 (s, 12 H; *ortho-CH*₃), 2.60 (s, 2 H; *CH*), 2.65 (s, 6H; *para-CH*₃), 4.90 (d, 4 H; ³*J*(H,H) = 2.01 Hz, *CH*₂), 7.30 (s, 4 H; H₁), 7.41 (dd, 2 H; ³*J*(H,H) = 8.48 Hz, *J*(H,H) = 1.77 Hz, H₂), 7.67 (t, 2 H; ³*J*(H,H) = 7.92 Hz, H₃), 7.89 (s, 4 H; H₄ + H₅), 8.71 (d, 4 H; ³*J*(H,H) = 4.79 Hz, β -pyrrolic *H*), 8.87 (d, 4 H; ³*J*(H,H) = 4.79 Hz, β -pyrrolic *H*).

LR-MM-ES+APCI-MS *m/z*: calculated for $\text{C}_{56}\text{H}_{47}\text{N}_4\text{O}_2^+$: 807.4; found: 807.3 ($[\text{MH}]^+$).

7. Experimental Part

Synthesis of zinc metallated 5,15-dimesityl-10,20-bis(3-(prop-2-yn-1-yloxy)phenyl)porphyrin Zn-23⁶⁷



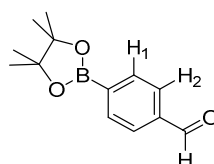
To a solution of free base porphyrin **23** (120 mg, 0.149 mmol) in CH_2Cl_2 / EtOH (3:1; 30 mL) zinc acetate (273 mg, 1.49 mmol) was added and the suspension was stirred at r.t. under air for 6 hours. The solvent was evaporated under reduced pressure. The crude was taken up in CH_2Cl_2 and filtered through silica to remove the remaining acetate. The solvent was removed under *vacuo* to afford the metallated porphyrin Zn-**14** (127 mg, 98 %) as a purple product.

¹H-NMR (300 MHz, CDCl_3): δ = 1.91 (s, 12 H; *ortho-CH*₃), 2.58 (s, 2 H; *CH*), 2.69 (s, 6H; *para-CH*₃), 4.83 (d, 4 H; ³*J*(H,H) = 2.01 Hz, *CH*₂), 7.34 (s, 4 H; *H*₁), 7.38 (dd, 2 H; ³*J*(H,H) = 8.48 Hz, *J*(H,H) = 1.77 Hz, *H*₂), 7.67 (t, 2 H; ³*J*(H,H) = 7.92 Hz, *H*₃), 7.93 (s, 4 H; *H*₄ + *H*₅), 8.85 (d, 4 H; ³*J*(H,H) = 4.79 Hz, β -pyrrolic *H*), 9.00 (d, 4 H; ³*J*(H,H) = 4.79 Hz, β -pyrrolic *H*).

LR-MM-ES+APCI-MS *m/z*. calculated for $\text{C}_{56}\text{H}_{44}\text{N}_4\text{O}_2\text{Zn}^+$: 869.3; found: 869.1 ($[\text{M}]^+$).

7. Experimental Part

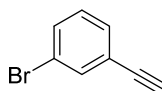
Synthesis of 4-(4,4,5,5-tetramethyl-1,3,2-dioxaborolan-2-yl)benzaldehyde **33**¹⁰⁵



Pinacol (252 mg, 2.13 mmol) was added to a solution of 4-formylphenylboronic acid (320 mg, 2.13 mmol) in chloroform. The mixture was stirred at 0 °C for 1 h. The solvent was removed under reduced pressure to afford 4-(4,4,5,5-tetramethyl-1,3,2-dioxaborolan-2-yl)benzaldehyde **33** (499 mg, 100%) as a white solid.

¹H-NMR (400 MHz, CDCl₃): δ = 1.37 (s, 12 H; CH₃); 7.87 (d, ³J(H,H) = 7.64 Hz, 2 H; H₂), 7.96 (d, ³J(H,H) = 7.64 Hz, 2 H; H₁), 10.06 (s, 1 H; COH).

Synthesis of 1-bromo-3-ethynylbenzene **34**¹⁰⁶



To a solution of [(3-bromophenyl)ethynyl](trimethyl)silane (0.5 g, 1.974 mmol) in MeOH / THF 1:1 (40 mL), K₂CO₃ (2.50 g, 13.82 mmol) was added and the suspension was stirred at r.t. for 4 h. The suspension was filtered and the solvent removed under reduced pressure. CH₂Cl₂ was added and the organic phase was washed with water, brine and dried over MgSO₄. The solvent was removed under vacuum to yield the

¹⁰⁵ Nicolas, M.; Fabre, B.; Gilles Marchand, G.; Simonet, J. *Eur. J. Org. Chem.* **2000**, 1703.

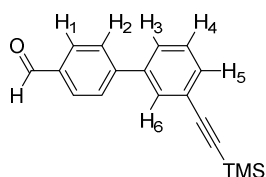
¹⁰⁶ Malamas, M. S.; Barnes, K.; Johnson, M.; Hui, Y.; Zhou, P.; Turner, J.; Huc, Y.; Wagner, E.; Fan, K.; Chopra, R.; Olland, A.; Bard, J.; Pangalos, M.; Reinhart, P.; Robichaud, A. J. *Bioorg. Med. Chem.* **2010**, *18*, 630.

7. Experimental Part

1-bromo-3-ethynylbenzene **34** (0.349 g, 98 %) as a clear oil that was used in the next steps without further purification.

¹H-NMR (400 MHz, CDCl₃): δ = 4.29 (s, 1 H, C≡C-H), 7.28–7.30 (m, 1 H, ArH), 7.43–7.46 (m, 1 H, ArH), 7.57–7.59 (m, 1 H, ArH), 7.63–7.64 (m, 1 H, ArH).

Synthesis of 3'-((trimethylsilyl)ethynyl)-[1,1'-biphenyl]-4-carbaldehyde **28**¹⁰⁷



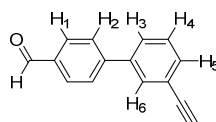
A suspension of Pd(OAc)₂ (0.147 mg, 0.099 mmol) and PPh₃ (105 mg, 0.395 mmol) in DME (18 mL) was stirred for 10 min at r.t.. Commercially available ((3-bromophenyl)ethynyl)trimethylsilane (250 mg, 0.987 mmol) and 2 M Na₂CO₃ solution (1.7 mL, 3.55 mmol) were added and the reaction mixture was further stirred for 5 min. The protected boronic acid **33** was added and the reaction mixture was submitted to MW irradiation for 4 h at 80 °C. The solvent was then removed under reduced pressure and the reaction crude was redissolved in CH₂Cl₂. The organic phase was washed with water, brine and dried over MgSO₄. The solvent was removed under *vacuo*. The viscous oil was sonicated in MeOH to afford the 3'-((trimethylsilyl)ethynyl)-[1,1'-biphenyl]-4-carbaldehyde **28** (268 mg, 97%) as a white solid.

¹⁰⁷ Procedure adapted from Opsenica, I.; Filipovic, V.; Nuss, J. E.; Gomba, L. M.; Opsenica, D.; Burnett, J. C.; Rick Gussio, R.; Bogdan A. Solaja, B. A.; Bavari, S. *Eur. J. Med. Chem.* **2012**, 53, 374

7. Experimental Part

¹H-NMR (500 MHz, CDCl₃): δ = 0.27 (s, 9 H; TMS), 7.42 (t, 1 H; ³J(H,H) = 7.76 Hz, H₄), 7.50-7.52 (m, 1 H; H₃), 7.58 (dd, 1 H; ³J(H,H)₁ = 7.55 Hz, J(H,H)₂ = 1.58 Hz, H₅), 7.74-7.76 (m, 3 H; H₆ + H₂), 7.96 (d, 2 H; ³J(H,H) = 8.35 Hz, H₁), 10.06 (s, 1 H; CHO)

Synthesis of 3'-ethynyl-[1,1'-biphenyl]-4-carbaldehyde **29**¹⁰⁷

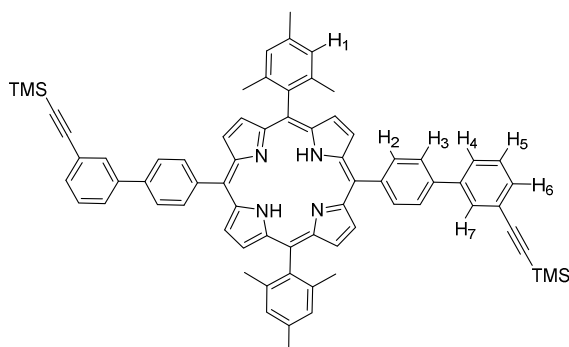


To a solution of **28** (0.2 g, 0.718 mmol) in MeOH / THF (1:1; 5 mL), K₂CO₃ (0.9 g, 5.03 mmol) was added and the suspension was stirred at r.t. for 4 h. The suspension was filtered off and the solvent removed under reduced pressure. The crude was taken up in CH₂Cl₂ and the organic phase was washed with water, brine and dried over MgSO₄ to afford the desired 3'-ethynyl-[1,1'-biphenyl]-4-carbaldehyde **29** (139 mg, 94 %) as a white solid.

¹H-NMR (300 MHz, CDCl₃): δ = 7.42-7.52 (m, 3 H; H₃ + H₄), 7.64 (m, 2 H; H₆ + H₅), 7.76 (d, 2H; ³J(H,H) = 8.22 Hz, H₂), 7.87 (d, 2H; ³J(H,H) = 8.30 Hz, H₁), 10.06 (s, 1 H; CHO).

7. Experimental Part

Synthesis of 5,15-dimesityl-10,20-bis(3'-((trimethylsilyl)ethynyl)-[1,1'-biphenyl]-4-yl)porphyrin **30**¹⁰²



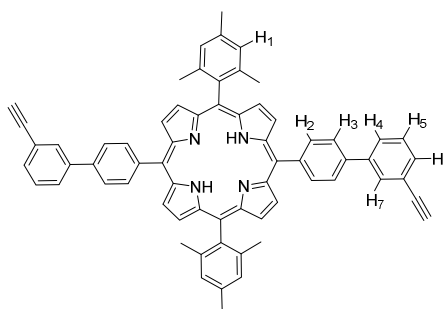
A solution of 5-mesityldipyrromethane **16** (190 mg, 0.178 mmol) and aldehyde **28** (200 mg, 0.718 mmol) in CH₂Cl₂ (60 mL) was degassed for 15 min under an Argon flow. The reaction was protected from light to reduce the formation of polymerization products. TFA (105 μ L, 1.365 mmol) was added and the reaction mixture was stirred at r.t. for 1 h. DDQ (163 mg, 0.718 mmol) was added and the reaction mixture was allowed to stir for another hour. Triethylamine was added and the reaction and the reaction mixture was stirred for 5 min. The solvent was removed under vacuum and the crude was filtered through silica to remove the polymerization products. The resulting purple crude was purified by preparative TLC chromatography (Cyclohexane / CHCl₃ 7:3) to obtain the desired porphyrin **30** (330 mg, 44 %) as a purple product.

¹H-NMR (400 MHz, CDCl₃): δ = -2.55 (s, 2 H; N-H), 0.34 (s, 18 H; TMS), 1.88 (s, 12 H, *ortho*-CH₃), 2.65 (s, 6 H; *para*-CH₃), 7.31 (s, 4 H; H₁), 7.54-7.59 (m, 4 H; H₄ + H₅), 7.88 (dt, 2 H; ³J(H,H) = 7.63 Hz, J(H,H) = 1.61 Hz, H₆), 7.99 (d, 4 H; ³J(H,H) = 8.38 Hz, H₂), 8.07 (bs, 2 H; H₇), 8.32 (d, 4 H; ³J(H,H) = 8.38 Hz, H₃), 8.74 (d, 4 H; ³J(H,H) = 4.79 Hz, β -pyrrolic H), 8.88 (d, 4 H; ³J(H,H) = 4.79 Hz, β -pyrrolic H).

LR-MM-ES+APCI-MS *m/z*. calculated for C₇₂H₆₆N₄Si₂⁺: 1043.5; found: 1043.3 ([M]⁺).

7. Experimental Part

Synthesis of 5,15-bis(3'-ethynyl-[1,1'-biphenyl]-4-yl)-10,20-dimesitylporphyrin **24**



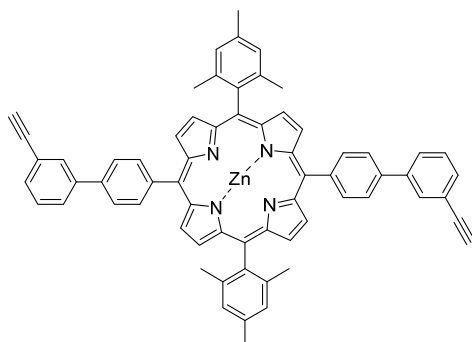
To a solution of porphyrin **30** (37 mg, 0.035 mmol) in MeOH / THF (1:1; 20 mL), K_2CO_3 (34 mg, 0.248 mmol) was added and the suspension was stirred at r.t. for 4 h. The suspension was filtered off and the solvent removed under reduced pressure. The crude was taken up in CH_2Cl_2 and the organic phase was washed with water, brine and dried over $MgSO_4$. The solvent was removed under vacuum and the crude was purified through preparative HPLC (Chiralpak IA, Hexane / IPA 99:1) to afford the deprotected porphyrin **24** (23 mg, 72 %) as a purple solid.

1H -NMR (400 MHz, $CDCl_3$): δ = -2.57 (s, 2 H; N-H), 1.86 (s, 12 H, *ortho-CH*₃), 2.64 (s, 6 H; *para-CH*₃), 7.29 (s, 4 H; *H*₁), 7.53-7.62 (m, 4 H; *H*₄ + *H*₅), 7.91 (bd, 2 H; $^3J(H,H) = 7.14$ Hz, *H*₆), 7.97 (d, 4 H; $^3J(H,H) = 7.98$ Hz, *H*₂), 8.07 (bs, 2 H; *H*₇), 8.31 (d, 4 H; $^3J(H,H) = 8.01$ Hz, *H*₃), 8.72 (d, 4 H; $^3J(H,H) = 4.62$ Hz, β -pyrrolic *H*), 8.87 (d, 4 H; $^3J(H,H) = 4.62$ Hz, β -pyrrolic *H*).

LR-MM-ES+APCI-MS *m/z*: calculated for $C_{66}H_{51}N_4^+$: 899.4; found: 900.0 ($[MH]^+$).

7. Experimental Part

Synthesis of zinc metallated 5,15-bis(3'-ethynyl-[1,1'-biphenyl]-4-yl)-10,20-dimesitylporphyrin **Zn-24**¹⁰²



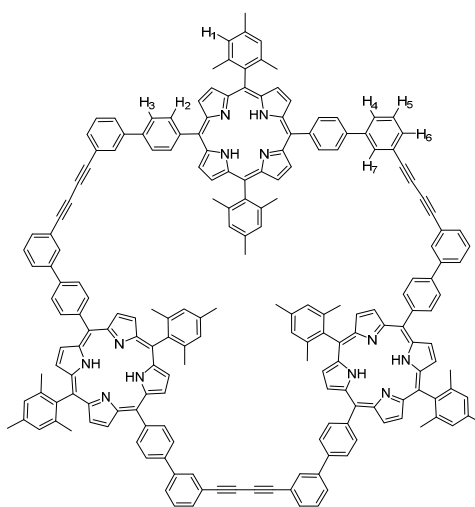
To a solution of free base porphyrin **24** (58 mg, 0.065 mmol) in CH_2Cl_2 / EtOH (3:1; 15 mL), zinc acetate (118 mg, 0.65 mmol) was added and the suspension was stirred at r.t. under air for 18 h. The solvent was evaporated under reduced pressure. The crude was taken up in CH_2Cl_2 and further filtered through silica to remove the remaining acetate. The solvent was removed under reduced pressure to afford the metallated porphyrin **Zn-14** (60 mg, 97 %) as a purple product that was used on the next step without further purification.

¹H-NMR (300 MHz, CDCl_3): δ = 1.85 (s, 12 H, *ortho-CH*₃), 2.64 (s, 6 H; *para-CH*₃), 7.29 (s, 4 H; *H*₁), 7.56-7.61 (m, 4 H; *H*₄ + *H*₅), 7.92 (bd, 2 H; ³*J*(H,H) = 7.67 Hz, *H*₆), 7.97 (d, 4 H; ³*J*(H,H) = 8.14 Hz, *H*₂), 8.08 (bs, 2 H; *H*₇), 8.32 (d, 4 H; ³*J*(H,H) = 8.14 Hz, *H*₃), 8.80 (d, 4 H; ³*J*(H,H) = 4.68 Hz, β -pyrrolic *H*), 8.95 (d, 4 H; ³*J*(H,H) = 4.65 Hz, β -pyrrolic *H*).

LR-MM-ES+APCI-MS *m/z*. calculated for $\text{C}_{66}\text{H}_{49}\text{N}_4\text{Zn}^+$: 961.3; found: 961.0 ($[\text{MH}]^+$).

7. Experimental Part

Synthesis of porphyrin cyclic trimer **7**



Zinc metallated porphyrin **Zn-24** (19 mg, 0.02 mmol) was dissolved in the minimum amount of CHCl_3 (5 mL). A diluted solution of template **26** (3.54 mg, 0.013 mmol) (10^{-2} M) in 400 mL CHCl_3 was dropwise added and the solution was further stirred for 18 h. Dichlorobis(triphenylphosphine)-palladium (II) (9.24 mg, 0.013 mmol), CuI (5 mg, 0.026 mmol) and isopropylamine (5 mL) were added and the reaction mixture was stirred under **open air**. Catalyst mixture was further added until no further trimer formation is observed. The amount of solvent was reduced under reduced pressure and the solution was filtrated through silica to remove the polymerization products. The solvent was removed under reduced pressure and the crude was purified by flash chromatography (SiO_2 , Cyclohexane / CH_2Cl_2 60:40) to remove the oxidized catalyst and then was further purified by preparative TLC (SiO_2 , Cyclohexane / CH_2Cl_2 60:40) to afford the **26@Zn₃-7** complex as a purple-blueish product (**LR-MM-ES+APCI-MS** *m/z*: calculated for $\text{C}_{237}\text{H}_{166}\text{N}_{15}\text{Zn}_3^+$: 1440.5 (template free); found: 1441.0 ($[\text{MH}]^{2+}$)). The complexated receptor was redissolved in the minimum amount of CHCl_3 and conc. HCl was added dropwise until acid pH was attained and the solution turn deep green colored. Then the solution was washed with water until the solution turn reddish. The organic fraction was further washed with brine and dried over the minimum amount of

7. Experimental Part

Na₂SO₄. The solvent was evaporated under reduced pressure to give the desired receptor 5 (6 mg, 34 %) as a purple solid.

¹H-NMR (500 MHz, CDCl₃): δ = -2.61 (s, 6 H; N-H), 1.83 (s, 36 H; *ortho*-CH₃), 2.60 (s, 18 H; *ortho*-CH₃), 7.52-7.67 (m, 4 H; ; H₄ + H₅), 7.94-7.98 (m, 2 H; H₆), 7.98 (d, 4H; ³J(H,H) = 8.12 Hz, H₂), 8.10 (bs, 4 H; H₁), 8.14 (bs, 2 H; H₇), 8.31 (d, 4 H; ³J(H,H) = 8.11 Hz, H₃), 8.69 (d, 4 H; ³J(H,H) = 4.64 Hz, β-pyrrolic H), 8.84 (d, 4 H; ³J(H,H) = 4.64 Hz, β-pyrrolic H).

¹³C-NMR (125.75 MHz, CDCl₃): δ = 21.42 (*para*-CH₃), 21.60 (*ortho*-CH₃), 118.44 (C), 118.77 (C), 119.11 (C), 122.55 (C-H₂), 123.97 (C-H₃), 124.19 (C), 124.47 (C), 125.31 (C-H₅), 127.74 (C-H₁), 128.19 (C), 128.80 (C), 129.22 (C), 130.88 (β-pyrrolic C), 131.79 (β-pyrrolic C), 133.78 (C-H₆), 135.10 (C-H₄), 137.74 (C), 138.42 (C-H₂), 139.11 (C), 139.37 (C), 141.23 (C), 141.62 (C), 165.33 (C).

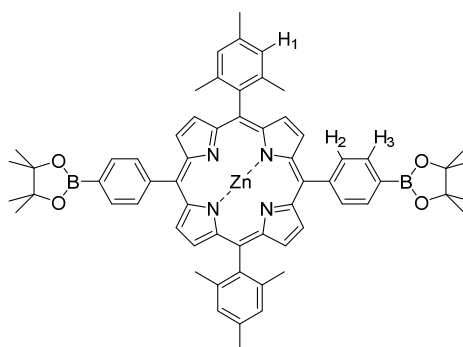
LR-MM-ES+APCI-MS *m/z*: calculated for C₁₉₈H₁₄₅N₁₂⁺: 1346.8; found: 1349.7 ([MH]²⁺).

HR-FT-MALDI-MS *m/z*: calculated for C₁₉₈H₁₄₅N₁₂⁺: 2692.1704; found: 2691.2930 ([MH]⁺).

UV/Vis (toluene): λ_{max} (ε) = 420 nm (141589 mol⁻¹ dm³ cm⁻¹);

7. Experimental Part

Synthesis of zinc metallated 5,15-dimesityl-10,20-bis(4-(4,4,5,5-tetramethyl-1,3,2-dioxaborolan-2-yl)phenyl)porphyrin Zn-**32**¹⁰²



A solution of 5-mesityldipyrromethane **16** (92 mg, 0.348 mmol) and 4-(4,4,5,5-tetramethyl-1,3,2-dioxaborolan-2-yl)benzaldehyde **33** (81 mg, 0.348 mmol) in CH₂Cl₂ (40 mL) was degassed for 15 min under an Argon flow. The reaction was protected from light to reduce the formation of polymerization products, TFA (51 μL, 0.661 mmol) was added and the reaction mixture was stirred at r.t. for 1 h. DDQ (79 mg, 0.348 mmol) was added and the reaction mixture was allowed to stir for another hour. Triethylamine was added and the reaction mixture was stirred for 5 min. The solvent was removed under vacuum and the crude was filtered through silica to remove the polymerization products. Purification by preparative column chromatography (SiO₂, Cyclohexane / CHCl₃ 7:3) afforded porphyrin **32** as a purple product (**LR-MM-ES+APCI-MS** *m/z*: calculated for C₆₂H₆₆B₂N₄O₄⁺: 951.5; found: 951.7 ([MH]⁺). The free base porphyrin **32** (63 mg, 0.0661 mmol) was redissolved in CH₂Cl₂ / EtOH (3:1; 20 mL) and zinc acetate (139 mg, 0.757 mmol) was added and the suspension was stirred at r.t. under air for 18 h. The solvent was evaporated. The crude was taken up in CH₂Cl₂ and was filtered through silica to remove the remaining acetate. The solvent was removed under reduced pressure to afford the metallated porphyrin Zn-**32** (66 mg, 19 %) as a purple product.

7. Experimental Part

¹H-NMR (300 MHz, CDCl₃): δ = 1.50 (s, 24 H; B(OC(CH₃)₂)₂), 1.83 (s, 12 H, *ortho*-CH₃), 2.63 (s, 6 H; *para*-CH₃), 7.28 (s, 4 H; H₁), 8.18 (d, 4 H; ³J(H,H) = 8.03 Hz, H₂), 8.56 (d, 4 H; ³J(H,H) = 8.03 Hz, H₃), 8.76 (d, 4 H; ³J(H,H) = 4.66 Hz, β-pyrrolic H), 8.87 (d, 4 H; ³J(H,H) = 4.66 Hz, β-pyrrolic H).

LR-MM-ES+APCI-MS *m/z*: calculated for C₆₂H₆₃B₂N₄O₄Zn⁺: 1013.4; found: 1013.7 ([M]⁺).

Part II: CTV-Based Self-Assembled Columnar Structures

UNIVERSITAT ROVIRA I VIRGILI

CYCLOTRIVERATRYLENE AND PORPHYRIN SCAFFOLDS FOR MOLECULAR RECOGNITION AND SELF-ASSEMBLY

Berta Camafort Blanco

Dipòsit Legal: T 677-2015

Chapter 8: Introduction

8.1 CTV-Based Self-Assembled Columnar Structures

CTV-based bowl-shaped molecules are able to self-assemble into macroscopic well-organized architectures such as columnar aggregates, supramolecular polymers or liquid crystals. Within the columns, the molecules are stacked on top of each other in a regular arrangement stabilized by non-covalent interactions such as π - π stacking or hydrogen bonding (Figure 8.1).^{108,109,110}

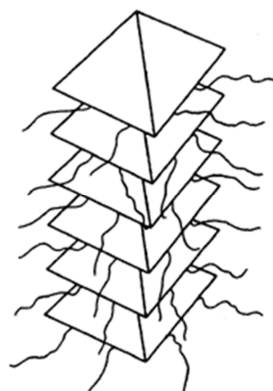


Figure 8.1 Schematic representation of CTV-based pyramidic columnar aggregates.

Such self-assembled architectures are known as pyramidic or bowl-like columnar aggregates. These concepts were first introduced by Zimmermann in 1985¹⁰⁹ and Lin

¹⁰⁸ (a) Hardie, M. J. "Cyclotrimeratrylene and Cryptophanes" in: *Supramolecular Chemistry: from Molecules to Nanomaterials*, Vol. 3, P. A. Gale, J. W. Steed (eds.), J. Wiley & Sons, Chichester, 2012, 895. (b) Hardie, M. J. *Chem. Soc. Rev.*, **2010**, 39, 516.

¹⁰⁹ (a) Collet, A. *Tetrahedron* **1987**, *47*, 5725. (b) Zimmermann, H.; Poupko, R.; Luz, Z.; Billard, J. *Z. Naturforsch.*, **1985**, *40a*, 149. (c) Zimmermann, H.; Poupko, R.; Luz, Z.; Billard, J. *Z. Naturforsch.*, **1986**, *41a*, 1137.

¹¹⁰ (a) Peterca, M.; Percec, V.; Imam, M. R.; Leowanawat, P.; Nirunutsy, K.; Heiney, P. A. *J. Am. Chem. Soc.* **2008**, *130*, 14840. (b) Percec, V.; Imam, M. R.; Peterca, M.; Wilson, D. A.; Heiney, P. A. *J. Am. Chem. Soc.* **2009**, *131*, 12941. (c) Roche, C.; Sun, H.-J.; Prendergast, M. E.; Leowanawat, P.; Partridge, B. E.; Heiney, P. A.; Araoka, F.; Graf R.; Spiess, H. W.; Zeng, X.; Ungar, G.; Percec, V. *J. Am. Chem. Soc.* **2014**, *136*, 7169.

8. Introduction

in 1987¹¹¹ to describe a new type of columnar liquid crystals. This new variations of discotic mesogens were composed by bowl-shaped rigid central cores with pyramidal symmetry to which side chains were symmetrically attached. Initially the “pyramidic” concept was referred to CTV-based mesophases but other bowl-like molecules such as calixarenes¹¹² metacyclophanes¹¹³ and cyclotetraveratrylene (CTTV)¹¹⁴ have been reported as central cores able to form columnar aggregates and mesophases.

8.2 Pyramidic Liquid Crystals

Pyramidic columnar aggregates are known to express liquid crystalline behavior. Such mesomorphic behavior depends on several factors such as the central core substitution pattern, the length and nature of the peripheral groups or the position and nature of the linkers.

The formation of CTV-based pyramidic liquid crystals was first described by Zimmermann *et al.* in 1985.^{109b} Zimmermann reported two different series of hexa-substituted CTVs connected through either ester- or ether groups to peripheral alkyl chains (**L** and **LI**, Figure 8.2).

When the CTVs (**L** and **LI**) were substituted with sufficient long alkyl chains, mesomorphic behavior was observed. Alkyloxy hexa-substituted CTV central cores bearing $6 \geq n \leq 12$ alkyl chains as well as all the studied ester derivatives ($n = 8 - 15$) expressed liquid crystalline behavior.

¹¹¹ Lin, L. *Mol. Cryst. Liq. Cryst.* **1987**, *41*, 146.

¹¹² Yang, F.; Guo, H.; Vicens, J. *J. Incl. Phenom. Macrocycl. Chem.* **2014**, *80*, 177. (b) Yonetake, K.; Nakayama, T.; Ueda, M. *J. Mater. Chem.* **2001**, *11*, 761.

¹¹³ Bonsignore, S.; Cometti, G.; Dalcanale, E.; Du Vosel, A. *Liquid Crystals*, **1990**, *8*, 639. (b) Cometti, G.; Dalcanale, E.; Du Vosel, A.; Levelut, A.-M. *J. Chem. Soc.; Chem. Commun.* **1990**, 163.

¹¹⁴ Lunkwitz, R.; Tschierske, S.; Diel, S. *J. Mater. Chem.* **1997**, *7*, 2001.

8. Introduction

Later in 1986, Zimmermann *et al.* reported the hexa-substituted CTV-based mesogens **LII** bearing long alky chains connected through benzoyloxy groups (Figure 8.2).^{109c}

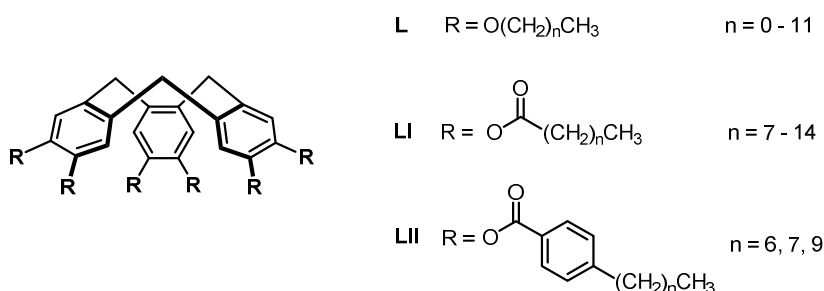


Figure 8.2 CTV-based monomers **L**, **LI** and **LII**.¹⁰⁹

In 1997, Hexa-functionalized CTVs bearing mono and bis-substituted benzoate derivatives (Figure 8.3).¹¹⁵

All CTVs functionalized with monosubstituted benzoate derivatives **LIII**, **LIV** and **LV** were found to be birefringent at room temperature. The hexa-functionalized CTV **LIV** bearing 3,4-disubstituted benzoate derivatives only showed mesomorphic behavior upon cooling down from the isotropic liquid. In the case of the CTV-based 3,5-disubstituted benzoate derivative **LV** no mesophase was detected.

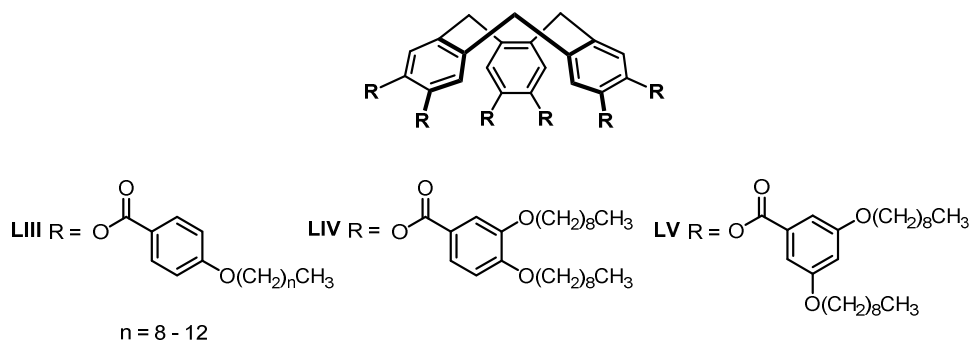


Figure 8.3 CTV-based monomers **LIII**, **LIV** and **LV**.¹¹⁵

¹¹⁵ Vo, L. P. M. S. Thesis, San Jose State University, USA, 1997.

8. Introduction

These results suggest that high substitution of the directly attached benzoate derivatives might interfere with the efficient CTV stacking inducing poorer mesophases upon increasing the number of alkyl chains. In the case of CTV **8**, the alkyl chains created sufficient steric hindrance to completely disrupt the formation of a mesophase.

In 1990, du Vosel *et al.* reported the synthesis of six different series of metacyclophane-based monomers (**LVI** – **LXI**) and studied the effect of the number and nature of the side chains, as well as the nature of the connectors on the thermal behavior of the metacyclophane-based pyramidal aggregates. None of the octa-substituted metacyclophane-based monomers (series **LVI-LVIII**, Figure 8.4) showed liquid crystalline behavior, independently on the length and the nature of the substituents (Figure 8.4).¹¹³

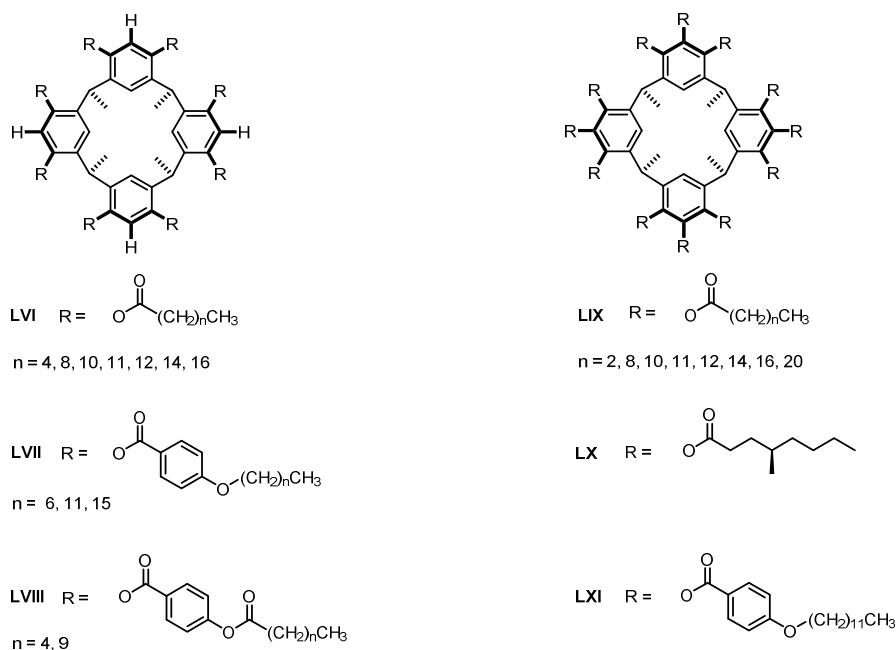


Figure 8.4 Metacyclophane-based monomers **LVI**, **LVII**, **LVIII**, **LIX**, **LX** and **LXI**.¹¹³

Metacyclophane-based central core functionalization with twelve peripheral chains was required to promote formation of thermotropic mesophases (**LIX** – **LXI**). Within the dodeca-substituted metacyclophane series, only those bearing non-branched alkyl

8. Introduction

chains (series **LIX**; $11 \leq n \leq 17$) directly attached to the central core through ester-linkers expressed liquid crystalline behavior. Mesophases were not observed when the central core was attached to short alkyl chains ($n \leq 9$) or when the peripheral chains were too long ($n \geq 21$). The dodeca-substituted metacyclophane **LXI** bearing benzyloxy linkers did not express liquid crystalline behavior.

These results suggested that short alkyl chains formed too stable columnar aggregates that did not express mesomorphic behavior whereas the steric hindrance of the long alkyl chains disrupted the formation of the columnar aggregates.

Also in this particular case of high substituted pattern of the central core, the presence of bulky benzyloxy connectors directly attached to the central core inhibit the formation of mesophases. The steric hindrance of the benzyloxy peripheral groups did not allow planar distribution of the phenyl rings destabilizing the core stacking and the mesomorphic behavior.

8.2.1 Introducing Chirality into the CTV-Based Pyramidic Aggregates

Chirality can be introduced through two different approaches. The first approach consists of functionalizing the central cores with peripheral groups containing asymmetric carbons, typically, branched alkyl chains.¹¹⁰

The second strategy consists of the unsymmetrical functionalization of the CTV central core. The tri-substituted ($R_1 \neq R_2$) and nona-substituted CTV-based monomers lack symmetry planes and they are structurally chiral, despite not possessing asymmetric tetrahedral carbons (Figure 8.5).

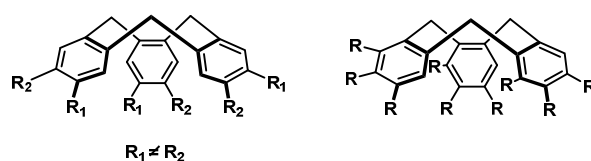


Figure 8.5 Substitution dependent chirality of CTV derivatives

8. Introduction

Tri-Substituted CTV-Based Aggregates

In 1987, Malthête and Collet reported the first tri-substituted CTV-based columnar aggregate **LXII** able to express liquid crystalline behavior.¹¹⁶

They suggested that tri-substituted CTVs substituted with elongated alkyl chains would not be able to promote the formation of mesophases due to the insufficient space filling around the central core. To ensure such space filling, they selected triangular-shaped 3,4,5-tris(*p*-*n*-dodecyloxybenzyloxy)benzoyloxy groups (DOBOB) as peripheral substituents (Figure 8.6).

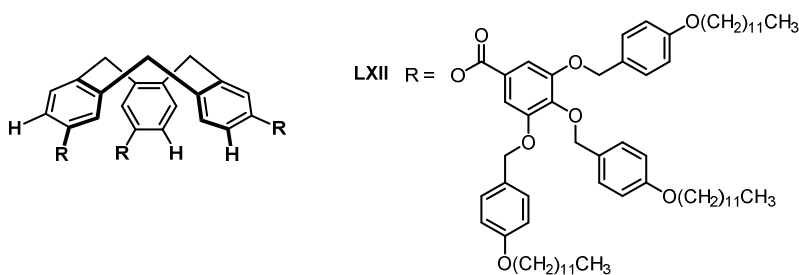


Figure 8.6 CTV-based monomer **LXII**.¹¹⁶

In contrast to the data reported previously, suggesting that sufficient space filling and long alkyl chains are required for the CTV-based monomers to express liquid crystalline behavior, tri-substituted CTV-based mesogens bearing short alkyl chains reported by Yan-Ming *et al.* and Xiao-Lan *et al.* indicate otherwise.^{117,118}

YanMing *et al.*¹¹⁷ reported in 2009 the mesomorphic behavior of the CTV-based monomers **LXIII** and **LXIV** tri-functionalized with small peripheral groups. Both **LXIII** and **LXIV** did express liquid crystalline behavior at high temperature (Figure 8.7).

¹¹⁶ Malthête, J.; Collet, A. *J. Am. Chem. Soc.* **1987**, *107*, 7544.

¹¹⁷ Yan-Ming, D.; Dan-Mei, C.; Er-Man, Z.; Xiao-Lan, H.; Zhi-Qun, Z. *Sci. China Ser. B*, **2009**, *52*, 986.

¹¹⁸ Dan-Mei, C.; Yan-Ming, D.; Bing-Xing, S.; Xue-Hui, Y.; Yan-Jie, L.; Xiao-Lan, H. *Chem. Res. Chinese. U.* **2009**, *25*, 579.

8. Introduction

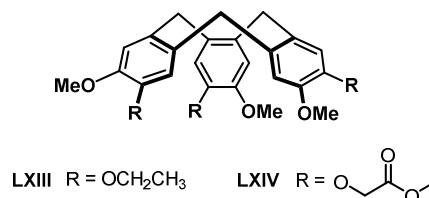


Figure 8.7 CTV-based monomers **LXIII** and **LXIV**.¹¹⁷

For CTV-monomer **LXIV** bearing small peripheral methyl groups a poorer mesomorphic behavior as well as lower liquid crystalline temperature range was observed.

Despite of the presence of ester groups that could potentially engage intermolecular hydrogen bonding, the ester moieties were directly attached to the CTV central core that seemed to inhibit the formation of H-bonding interaction. For this reason, the crystalline textures observed for **LXIII** and **LXIV** were very similar.

Also in 2009 Xiao-Lan *et al.* reported the synthesis and mesomorphic behavior of tri-substituted CTVs **LXV** and **LXVI** bearing relatively short alkyl chains. They investigated the effect of the number of carbons as well as the odd/even effect had on the mesophase characteristics. They reported that all of the CTV-based derivatives displayed thermotropic liquid crystalline behavior despite the short alkyl chains, the low substitution pattern and the low space filling achieved by the peripheral groups (Figure 8.8).

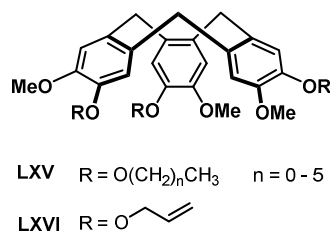


Figure 8.8 CTV-based monomers **LXV** and **LXVI**.¹¹⁸

The CTV-based mesogens melting points were found to be exclusively dependent on the length of the peripheral alkyl chains. Upon increasing the number of carbons the

8. Introduction

structure organization was reduced. The longer alkyl chains prevent the regular CTV stacking reducing the order of the structure and promoting the formation of mesophases.

Nona-Substituted CTV-Based Aggregates

In 2002 Zimmermann *et al.* reported a series of nona-alkanoyloxy substituted CTVs **LXVII** and compared these columnar aggregates with the previously reported hexa-substituted CTV-analogues (Figure 8.9).¹¹⁹

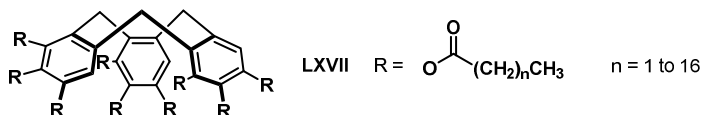


Figure 8.9 CTV-based monomer **LXVII**.¹¹⁹

When introducing three more peripheral groups in *ortho* position to the methylene CTV carbon, the CTV-derivative becomes structurally chiral. Moreover, the extra peripheral substituents might promote destabilization of the crown form towards the saddle conformation.

The crown form is the only stable conformation for tri- and hexa-substituted CTVs. In nona-substituted derivatives, an equilibrium between the crown and saddle form is established at high temperature, although the crown conformation is favored at room temperature (Figure 8.10). Since the isomerization at room temperature is extremely slow, both isomers could be separated by column chromatography and their properties were studied separately.

Zimmermann reported the formation of racemic CTV-crown mesophases as well as CTV-saddle mesophases when the central core was substituted with sufficient long

¹¹⁹ Zimmermann, H.; Bader, V.; Poupko, R.; Wachtel, E. J.; Luz, Z. *J. Am. Chem. Soc.* **2002**, *124*, 15286.

8. Introduction

side chains ($n \geq 4$ for the saddle and $n \geq 5$ for the crown form). The mesophases were characterized by DSC, POM microscopy and X-ray diffraction.

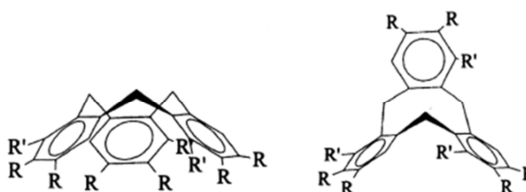


Figure 8.10 Schematic representation of crown and saddle conformations.

Later in 2009 Zimmermann *et al.* reported the separation of the previously synthesized racemic CTV-mesogen **LXVIII** into its neat enantiomers and studied its mesomorphic behaviour (Figure 8.11).¹²⁰ The aggregate was characterized by DSC, X-ray diffraction and chiral dichroism. In comparison with the racemate, the chiral mesophases were found to be more disordered and better tightly packed, so that their tendency towards crystallization was decreased.

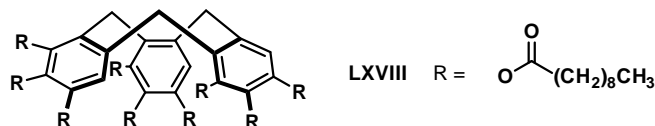


Figure 8.11 CTV-based monomer **LXVIII**.¹²⁰

The chirality of the CTV-mesogens might be transferred and amplified to the columnar aggregate, promoting the formation of a macroscopic helix. However, Zimmermann's attempts to identify such helical macroscopic arrangement were not successful. No X-ray evidences of the helical character of the columns were obtained. Besides the possibility that the detection techniques employed were not sufficient, there are indications that no helical arrangements were formed.

¹²⁰ Luz, Z.; Poupko, R.; Wachtel, E. J.; Zimmermann, H. *Phys. Chem. Chem. Phys.* **2009**, *11*, 9562.

8. Introduction

8.2.2 Hydrogen Bonding Promoted Columnar Twisting

Hydrogen bonds constitute an interesting and unique type of intermolecular interactions, due to both their intermediate energies between strong covalent bonds and weak van der Waals interactions and their directionality.

The introduction of moieties able to engage hydrogen bonding interactions within columnar assemblies and mesophases, as well as to stabilize and address the formation of helical macroscopic structures has been widely reported.¹²¹

As an example, Nuckolls *et al.* reported in 2004 the synthesis, mesomorphic behavior and chiral amplification phenomena of four hexa-substituted aromatic rings, bearing three amide groups able to engage H-bonding interactions and three dodecyloxy chains that would promote the formation of mesophases (Figure 8.12).^{121c}

From the four prepared monomer, **LXIX**, **LXXI**, **LXXII**, were able for form stable mesophases. In the case of **LXX**, The bulky substituents did not allowed the stacking of the monomers inhibiting the formation of a mesophase.

In the case of **LXXII**, the presence of the three amide groups promoted the formation of a macroscopic helix. Since the amide rotation is lower than 90° out of the plane of the benzene ring, the molecules were only complementary with all amides in the same rotation phase. This promoted the formation of three helices of hydrogen bonds emerging around the outer column.

¹²¹ (a) Vera, F.; Serrano, J. L.; Sierra T. *Chem. Soc. Rev.* **2009**, *38*, 781. (b) Ishihara, S.; Furuki, Y.; Takeoka, S. *Polym. Advan. Technol.* **2008**, *19*, 1097. (c) Bushey, M- L.; Nguyen, T.-Q.; Zhang, W.; Horoszewski, D.; Nuckolls, C. *Angew. Chem. Int. Ed.* **2004**, *43*, 5446. (d) Bushey, M- L.; Hwang, A.; Stephens, P. W.; Nuckolls, C. *Angew. Chem.* **2002**, *14*, 2828. (e) Lightfoot, M. P.; Mair, F. S.; Pritchard R. G.; Warren, J. E. *Chem. Commun.* **1999**, 1945. (f) Ranganathan, D.; Kurur, S.; Gilardi, R.; Karle, I. L. *Biopolymers*, **2000**, *54*, 289. (g) Wan den Hout, K. P.; Martín-Rapún, R.; Vekemans, J. A. J. M.; Meijer, E. W. *Chem. Eur. J.* **2007**, *13*, 8111.

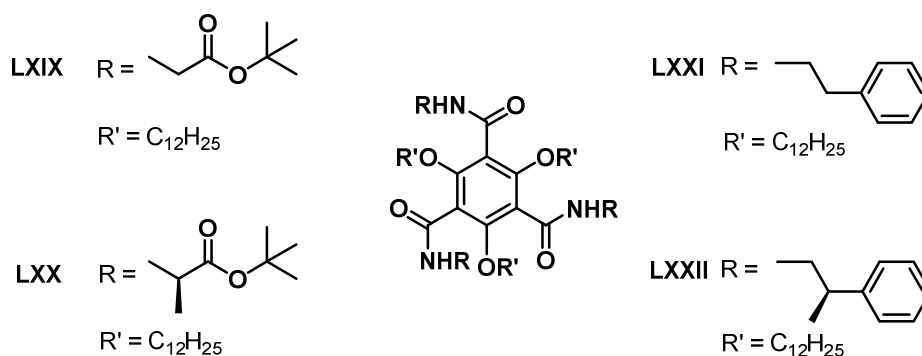


Figure 8.12 Hexa-substituted monomers LXIX, LXX, LXXI, LXXII.^{121c}

The hydrogen bonds extend along the column through intermolecular interactions between the different mesogenic units. The propagation of the hydrogen bonds along the column forces the columnar aggregate to acquire a twisted macroscopic architecture. As a consequence, the chirality is amplified from the monomers to the supramolecular columnar organization.

The Urea Moiety

Urea molecules self-associate through strong, highly specific and directional hydrogen bonding interactions, thus making them very interesting moieties to be introduced in columnar aggregates or mesophases.¹²²

8.3 Amplification of Chirality on Supramolecular Aggregates

In the amplification of chirality processes a small proportion of chiral molecules results in a significantly enhanced chiral effect. In the case of chiral amplification in helical

¹²² (a) Steed, J. W.; Atwood, J. L. *Supramolecular Chemistry*, Wiley, Chichester, **2009**. (b) Shukla, A.; Isaacs, E. D.; Hamann, D. R.; Platzman, P. M.; *Physical Review B*, **2001**, *64*, 052101. (c) de Loos, M.; Ligtenbarg, A. G. J.; van Esch, J.; Kooijman, H.; Spek, A. L.; Hage, R.; Kellogg, R. M.; Feringa, B. L. *Eur. J. Org. Chem.*, **2000**, 3675.

8. Introduction

supramolecular aggregates, this means that either a small number of chiral molecules or monomers dictate the helical handedness of the aggregate predominantly composed of achiral compounds or in case of chiral monomers, that the major enantiomer dictates the helicity of the whole aggregate. These phenomena can be easily monitored by CD Spectroscopy, since an induced CD signal appears when low quantity of the chiral molecules is added. This CD Spectra have a nonlinear amplified intensity and in some cases, the addition of less than a 5 % of chiral molecules gives to a saturated CD signal, with same intensities as in the enantiomerically pure compound spectrum. Two different behaviours can be identified within the chiral amplification: The “Sergeants and soldiers” and the “Majority Rules”.¹²³

The “Sergeants and soldiers” principle implies control of the helicity of large numbers of cooperative achiral units, the “soldiers”, by a few chiral units, the “sergeants”. The chirality of the sergeants, which are in a very low concentration, is transferred to the supramolecular aggregate composed of achiral molecules, inducing a preferred homochiral helix.

The “Majority Rules” principle implies control of the helicity of a mixture of enantiomers by the major one. In this case, a slight excess of one enantiomer leads to a strong bias toward the helicity corresponding to the major one.

In 2010, Meijer *et al.* reported a systematic study of the “Majority Rules” chiral amplification phenomena.^{123a} Upon addition of trialkylbenzene-1,3,5-tricarboxamide monomer (*S*)-**LXXIII** to the enantiopure aggregate of (*R*)-**LXXIII** at a concentration of 2×10^{-5} M, the CD spectra remained constant until 40 % ee was reached, up to which a saturated CD signal was observed. This evidenced a strong nonlinear dependence on the chirality transfer from a small portion of chiral molecule to a fully homochiral

¹²³ (a) Smulders, M. M. J.; Filot, I. A. W.; Leenders, J. M. A.; van der Schoot, P.; Palmans, A. R. A.; Schenning A. P. H. J.; Meijer, E. W. *J. Am. Chem. Soc.* **2010**, *132*, 611.
(b) Brunsfeld, L.; Lohmeijer, B. G. G.; Vekenmans, J. A. J. M.; Meijer, E. W. *J. Incl. Phenom. Macro.* **2001**, *41*, 61

8. Introduction

supramolecular system. Addition of further (S)-LXXIII led to the reduction of the CD intensity becoming zero at the racemic mixture. A negative CD signal appeared after further addition of (S)-LXXIII. The CD Spectra of the consecutive additions of (S)-LXXIII to the enantiopure aggregate as well as the neat helicity plot are shown in Figure 8.12.

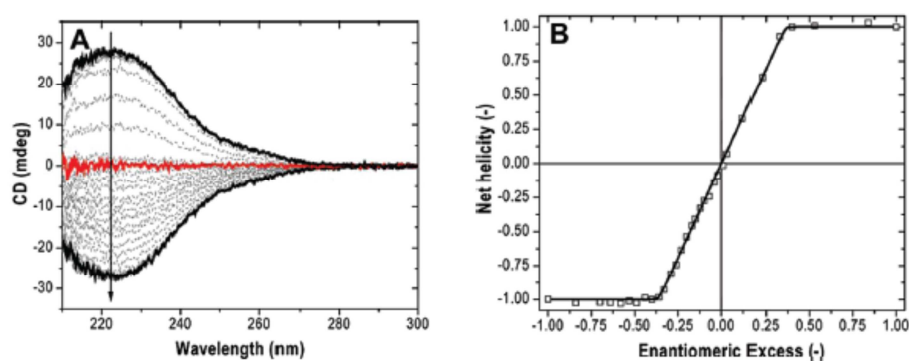


Figure 8.12 CD spectra for mixtures of (S)-LXXIII and (R)-LXXIII recorded at 20 °C. Arrow indicates the change upon going from pure (R)-LXXIII to pure (S)-LXXIII.

8. Introduction

Part II: General Objectives

The goal of the second part of the thesis is the preparation and characterization of chiral CTV-based pyramidic monomers. Their potential for self-assembly into macroscopic columnar aggregates which are stabilized by non-covalent π - π and hydrogen bonding interactions is examined. Two different CTV-monomer **35** and **36** were designed.

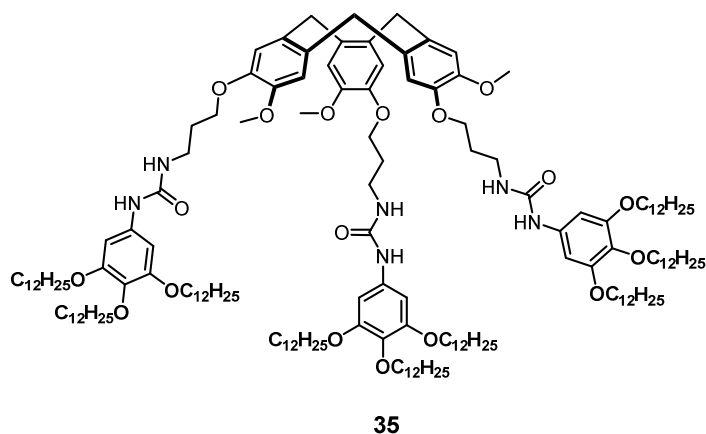


Figure 8.13 CTV-monomer **35**.

CTV-monomer **35** consists of a CTV tri-substituted bearing nine 3,4,5-*tris*(dodecyloxy)benzene pendant legs. In the case of CTV-monomer **36**, an extra methylene group is introduced within the peripheral legs.

CTV-monomers are known to form pyramidic mesophases when connected to sufficiently long side chains. The long dodecyloxy chains are introduced to promote the formation of a liquid crystalline phase. The incorporation of the nine alkyl chains is expected to compensate the low-substitution pattern of the central core. Urea moieties were introduced linked through a propyl backbone to the CTV central core in attempts to promote a formation of a macroscopic helix. The presence of the urea moieties is

Part II: General Objectives

expected to stabilize the helical arrangement within the columnar aggregate, maximizing the intermolecular interactions.

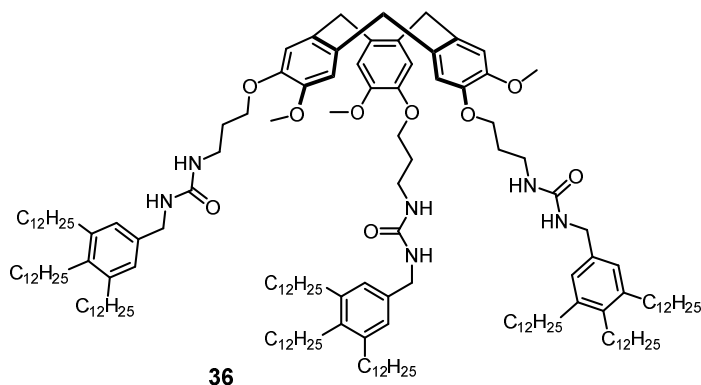


Figure 8.14 CTV-monomer **36**.

The synthetic attempts, characterization, self-assembly as well as mesogenic behavior of the resulting columnar aggregates will be studied by means of $^1\text{H-NMR}$, DSC, and POM microscopy and the results discussed. “Majority Rules” chiral amplification studies will be performed to investigate the ability of the CTV-monomers to induce chirality to the macroscopic level.

**Chapter 9: CTV-Based Pyramidic Monomers for
Chiral Columnar Aggregates.**

UNIVERSITAT ROVIRA I VIRGILI

CYCLOTRIVERATRYLENE AND PORPHYRIN SCAFFOLDS FOR MOLECULAR RECOGNITION AND SELF-ASSEMBLY

Berta Camafort Blanco

Dipòsit Legal: T 677-2015

9. CTV-Based Pyramidic Monomers for Chiral Columnar Aggregates.

9.1 Design and Aim of the Project

The goal of the project is the synthesis of a chiral CTV-based pyramidic monomer able to self-assemble into macroscopic columnar aggregates stabilized by non-covalent π - π stacking and hydrogen bonding interactions.

The designed target CTV-monomer **35** consists of a CTV tri-substituted with 3,4,5-*tris*(dodecyloxy)benzene pendant legs. The incorporation of the nine alkyl chains is expected to compensate the low-substitution pattern of the central core. The long dodecyloxy chains are expected to promote the formation of a liquid crystalline phase.

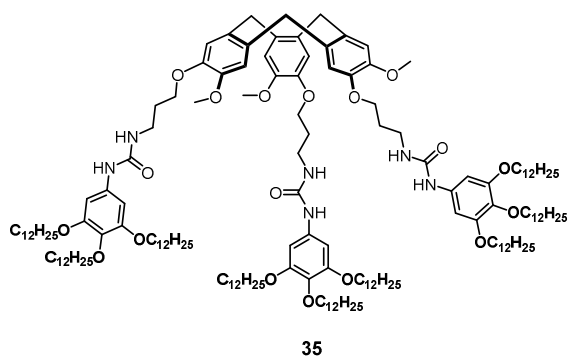


Figure 9.1 CTV-based pyramidic monomer **35**

Due to the tri-substitution pattern, the pyramidic CTV-monomer **35** becomes structurally chiral. In an attempt to promote the chirality transfer from the monomer into the macroscopic columnar aggregate, generating a macroscopic helix, urea moieties were linked through a propyl backbone to the CTV central core. In this way, the bulky tri-substituted aromatic groups are not directly attached to the central core which could likely destabilize the stacking of the monomers.

As already pointed out, the urea moiety has a strong, highly specific and directional hydrogen bonding ability, and can thus act as a powerful self-assembling moiety for

9. CTV-Based Pyramidic Monomers for Chiral Columnar Aggregates.

the pyramidic monomers. In addition, the directionality of the urea hydrogen bonding would should promote a twist of the CTV-monomers along the aggregation axis, promoting the formation of a macroscopic helix.

The helical arrangement of the pyramidic columnar aggregate would allow all the urea moieties of one CTV-monomer to interact with all of the N-H protons of the neighboring CTV-monomer. This would stabilize the helical arrangement within the pyramidic columnar aggregate, maximizing the intermolecular interactions, as suggested by molecular mechanics molecular modeling (Figure 9.2).

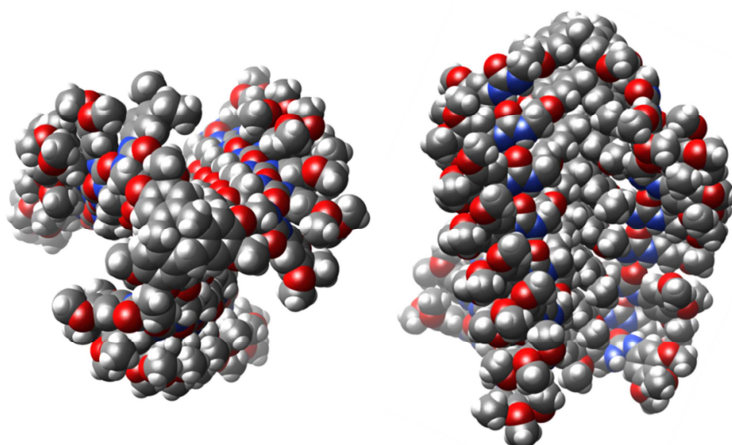


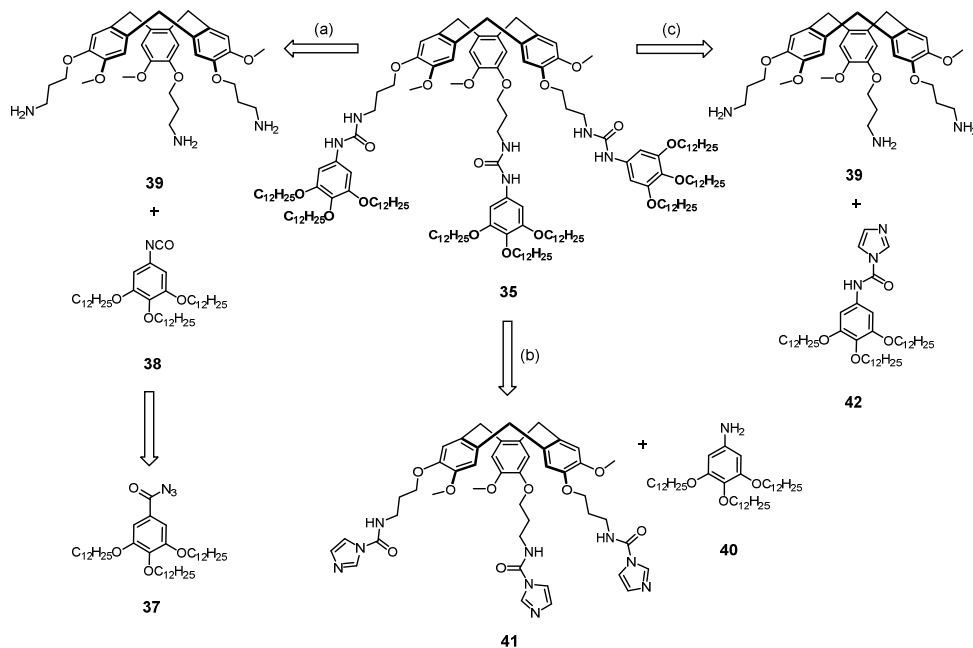
Figure 9.2 Top and side views of the optimized molecular structure of the pyramidal columnar aggregate. The urea moieties promote the formation of a macroscopic helix.

Finally, since CTV-monomers are known to form pyramidic mesophases when connected to sufficiently long side chains *via* ether or ester linkages, the mesogenic behavior of the resulting columnar aggregates will be as well discussed.

9.2 Synthesis and Characterization

The target CTV-based monomer could be prepared, among other strategies, through two main synthetic approaches (Scheme 9.1).

9. CTV-Based Pyramidic Monomers for Chiral Columnar Aggregates.



Scheme 9.1 Retrosynthetic routes proposed for CTV monomer **35**.

In the first synthetic strategy (route (a); Scheme 9.1), the urea is formed through a *Curtius* rearrangement of the acyl azide **37** to give the corresponding isocyanate intermediate **38** that further should react with the CTV-amino derivative building block **39** to give the desired CTV-monomer **35**.

In the second approach (routes (b) and (c); Scheme 9.1), either the 3,4,5-*tris*(dodecyloxy)aniline **40** or the CTV-amino **39** building blocks undergo a nucleophilic attack through the corresponding acyl activated carbamoyl imidazole building block **41** and **42** to give the desired monomer.

9.2.1 Synthesis of CTV Monomer **35**. Route (a)

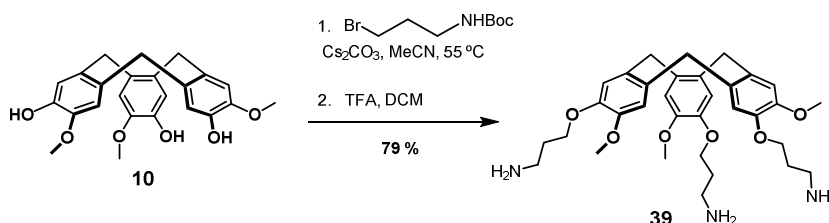
The route (a) was initially selected to prepare the target monomer **35**. This route involves preparation of 1,2,3-*tris*(dodecyloxy)-5-isocyanatobenzene **38** and the amino derivative **39** as building blocks.

9. CTV-Based Pyramidic Monomers for Chiral Columnar Aggregates.

Synthesis of the Amino Derivative Building Block **39**

The CTV-amino derivative building block **39** was synthesized from the previously prepared CTV triphenol **10**.

Triphenol **10** was successfully alkylated with commercially available *N*-Boc-protected propyl bromide in the presence of cesium carbonate in acetonitrile. The protected CTV-amino derivative was further deprotected with TFA to give the corresponding TFA salt. The CTV-amino derivative building block **39** was isolated in very good overall yield after neutralization with base (Scheme 9.2).

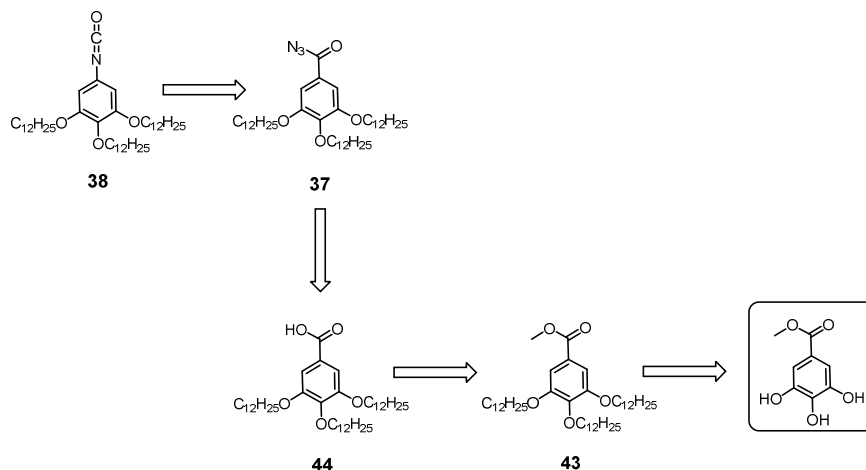


Scheme 9.2 Synthesis of CTV-amino derivative building block **39**.

Synthesis of the Isocyanate Building Block **38**

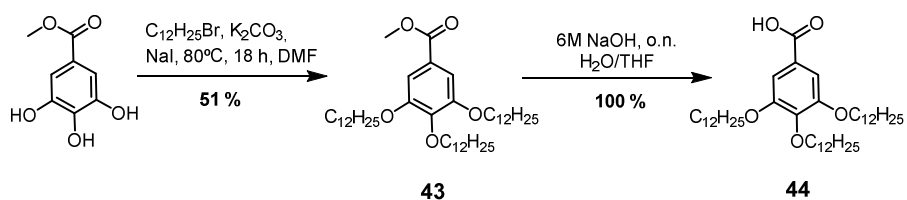
The isocyanate building block **38** can be prepared in a four steps synthesis starting from the commercially available methyl gallate (Scheme 9.3).

9. CTV-Based Pyramidic Monomers for Chiral Columnar Aggregates.



Scheme 9.3 Retrosynthetic route to the isocyanate building block **38**.

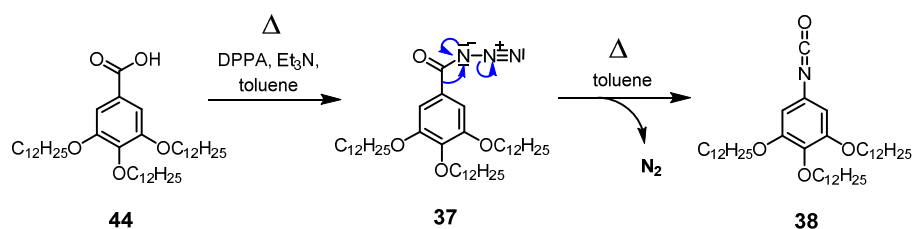
Alkylation of commercially available methyl gallate with dodecyl bromide in the presence of K_2CO_3 and NaI in DMF gave the desired methyl *tris*(dodecyloxy)benzoate **43** in a moderate yield. Further deprotection of the methyl ester with NaOH in H_2O / THF gave the desired benzoic acid **44** quantitatively (Scheme 9.4).



Scheme 9.4 Synthesis of *tris*(dodecyloxy)benzoic acid **44**.

For the synthesis of the isocyanate building block, the carboxylic acid was typically heated in the presence of DPPA and Et_3N to give the acyl azide that then further undergoes a *Curtius* rearrangement to give the isocyanate in a one-pot reaction (Scheme 9.5).

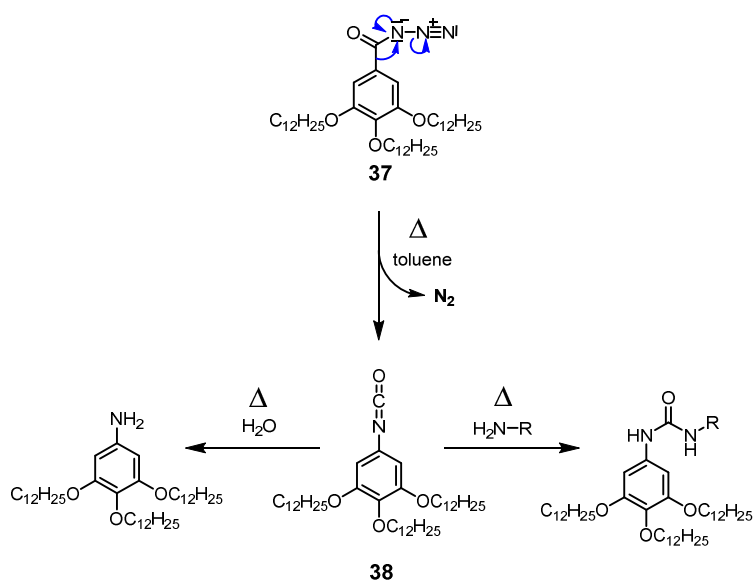
9. CTV-Based Pyramidic Monomers for Chiral Columnar Aggregates.



Scheme 9.5 Synthetic attempt for the 3,4,5-tris(dodecyloxy)benzoyl azide **37** and its *Curtius* rearrangement to the isocyanate building block **38**.

The *Curtius* Rearrangement

The *Curtius* rearrangement is a thermal decomposition of the carboxylic azide that produces an isocyanate after nitrogen elimination. This intermediate may be isolated, or directly made to react with amines to produce ureas or hydrolyzed with water to give amines (Scheme 9.5). In the strategy followed for the synthesis of the desired CTV-monomer **35**, the isocyanate building block was directly reacted, without further purification, to the desired urea.

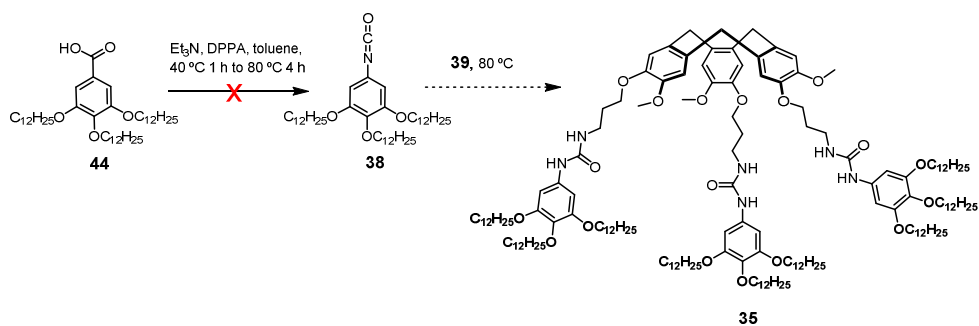


Scheme 9.6 *Curtius* rearrangement: Isocyanate formation and its reaction and hydrolysis products.

9. CTV-Based Pyramidic Monomers for Chiral Columnar Aggregates.

Synthesis of the CTV-Urea **35**

Initial attempts to synthesize the CTV urea derivative **35** from the carboxylic acid building block did not succeed, starting materials **44** and **39** being exclusively recovered. IR spectroscopy analysis of the crude product indicated that neither the desired urea **35** nor the isocyanate intermediate **38** were formed.



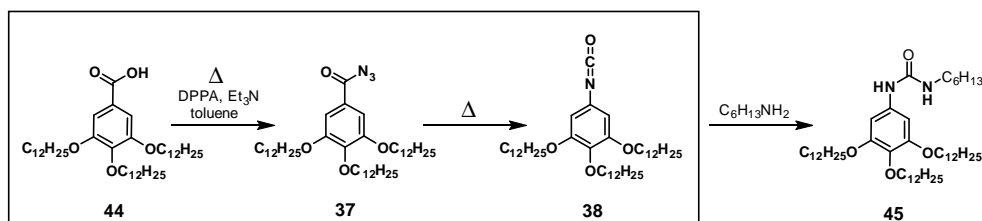
Scheme 9.7 Synthetic attempts of CTV target molecule **35**.

Isocyanate Formation: Key Step Optimization

To optimize isocyanate **38** formation step and promote the subsequent formation of the target urea **35**, the synthesis of the acyl azide **37**, the isocyanate **38** and the urea **35** were performed in a reactor provided with an IR probe. Such IR-reactor allows observation of the IR spectra profile of the reaction mixture in real time. The formation and consumption of the carboxylic azide **37**, isocyanate **38** as well as the consumption of DPPA was thus monitored by infrared spectroscopy. Analysis of the spectroscopic data allows the optimization of the reaction conditions.

Initially, commercially available hexylamine was selected as a model reaction for optimization, avoiding the unnecessary consumption of the CTV-amino building block **39** (Scheme 9.8). The reaction was performed in toluene. The IR spectra profile of the reaction mixture was recorded after addition of each reactive species, which allowed identification of the reagents and solvent profile and its subsequent decrease. For instance, the toluene profile was subtracted from the experiment prior to data analysis. The model reaction conditions are summarized in Table 9.1.

9. CTV-Based Pyramidic Monomers for Chiral Columnar Aggregates.



Scheme 9.8 Model reaction for key step optimization: acyl azide formation (a) and *Curtius* rearrangement (b). Synthetic final step: urea formation (c).

Typically the reaction is first initially heated at 40 °C in the presence of the DPPA and Et₃N to promote formation of the acyl azide. The reaction mixture is then further heated at 80 °C to promote the rearrangement and formation of the isocyanate (Scheme 9.8). Nevertheless, in this particular case, the reaction was performed at constant temperature of 80 °C to avoid baseline variations.

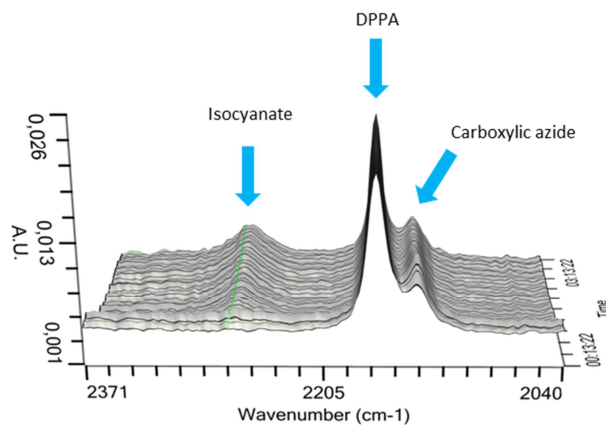


Figure 9.3 Key step optimization: Monitoring of the isocyanate formation IR spectra profile over time; Wavenumber interval: 2020-2370 cm⁻¹; time interval: 13 min - 3h 13 min.

In the typical 3D reaction profile shown in Figure 9.3, the IR intensity is plotted against the wavenumber over time. After addition of the DDPA a very intense peak appears at 2170 cm⁻¹. After 10 minutes heating, formation of a new peak was observed at 2140 cm⁻¹ that corresponds to the acyl azide building block **39**. After approximately 1 h a new peak at 2270 cm⁻¹ accounting for the formation of isocyanate **38** was observed. The intensities of both DPPA and carboxylic azide **37** peaks decreased as isocyanate **38** intensity increases.

9. CTV-Based Pyramidic Monomers for Chiral Columnar Aggregates.

In this first study, the reaction was stirred at 80 °C for 5 h while being monitored. Then, hexylamine was added and the reaction mixture was allowed to run for 18 additional hours. The isocyanate consumption profile after addition of the hexylamine indicating formation of the urea is shown in Figure 9.4.

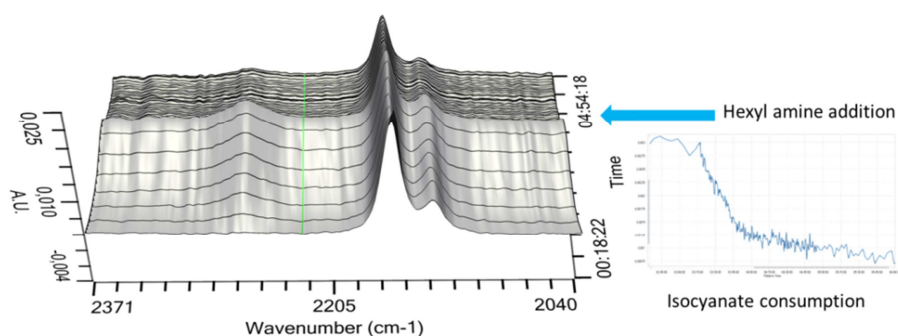
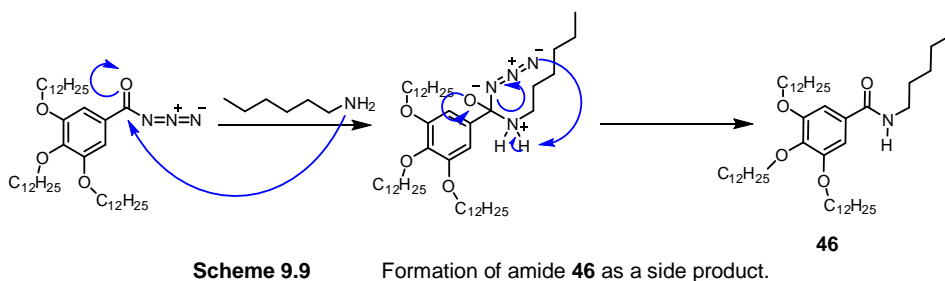


Figure 9.4 Monitoring of isocyanate formation and consumption. Left: IR spectra profile over time. Right: Isocyanate consumption profile after addition of the hexyl amine (2270 cm^{-1}).

When the IR profile was analyzed, it was observed that within the 5 h reaction still a big amount of DPPA as well as the acyl azide **37** remained unreacted. Moreover, further analysis of the crude revealed that, besides the desired urea, the non-desired amide **46** was as well formed as a consequence of the reaction between the non-rearranged acyl azide **37** and the hexylamine (Scheme 9.9).¹²⁴ Consequently, the desired urea was obtained in only moderate yield (Table 9.1).



¹²⁴ (a) Montalbetti, C. A. G. N.; Falque, V. *Tetrahedron*, **2005**, *61*, 10829. (b) Inouye, K.; Watanabe, K.; Shin, M. *J. Chem. Soc., Perkin Trans. 1*, **1977**, 1905.

9. CTV-Based Pyramidic Monomers for Chiral Columnar Aggregates.

In attempts to maximize the formation of the isocyanate, the reaction was first allowed to run overnight. Analysis of the IR spectra indicated that isocyanate **38** concentration was maximal after 3.5 h reaction. Then, its intensity started to decrease. After 18 h there was almost no isocyanate left (Figure 9.5).

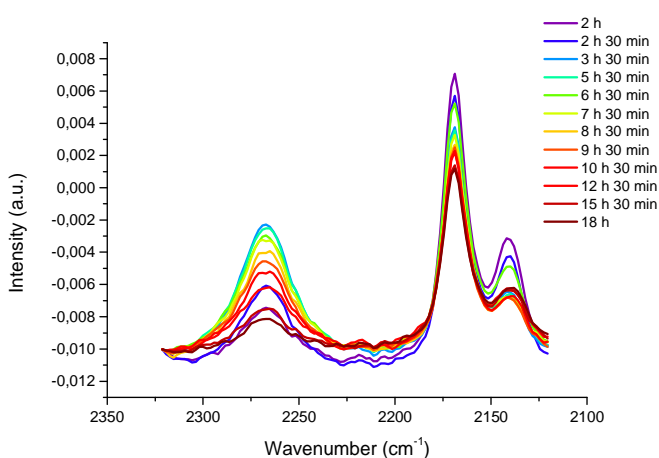


Figure 9.5 Isocyanate formation reaction IR profile recorded at selected times.

In the plotted IR profile monitored over the time it can be observed that formation of isocyanate **38** starts before the total conversion of carboxylic acid **44** occurs, while the acyl azide **37** is not totally formed and a big amount of DPPA remains unreacted (Figure 9.3) Moreover, when the isocyanate **38** reaches its maximum intensity after 3.5 h, a considerable amount of acyl azide **37** remains unreacted. This limits the amount of isocyanate **38** that can be formed and also allows the formation of side products.

In attempts to promote the full conversion of the carboxylic acid **44** towards the acyl azide **37** prior to the *Curtius* rearrangement, the reaction was initially heated at 40 °C. Typically, at this temperature the acyl azide is formed but does not rearrange into the isocyanate. In this way the isocyanate formation could be promoted in a controlled way only after total conversion of the carboxylic acid would take place. Unfortunately, when the reaction was performed at such low temperature, no isocyanate **38** formation was observed by IR.

9. CTV-Based Pyramidic Monomers for Chiral Columnar Aggregates.

Table 9.1 Conditions screened for the reaction optimization

	<i>Time</i>	<i>DPPA, Et₃N</i> <i>Equivalents</i>	<i>Hint</i>	<i>Urea</i> <i>formation</i>	<i>Amide</i> <i>formation</i>	<i>Yield</i>
a	5 h	1.1	-	✓	amide	54 %
b	18 h	1.1	-	✗	-	-
c	3.5 h	1.1	-	✓	amide	66 %
d	3.5-6 h	1.1	T = 40 °C	✗	-	-
e	3.5 h	2.2	-	✓	amide	71 %

Finally, only by increasing the equivalents of carboxylic acid building block, DPPA and Et₃N, the isocyanate **38** formation could be improved. The 3,4,5-*tris*-(dodecyloxy)-*N*-hexylbenzamide **46** was finally obtained in 78 % yield (Table 9.1).

Isocyanate Formation: Key Step Optimization under MW Conditions

The isocyanate formation step was then further studied under microwave conditions. The reaction was initially heated for 1 h at both 80 °C and 100 °C in a pressured vessel. The IR profile analysis determined that when heating at 100 °C more isocyanate was formed within the 1 hour. The reaction was then allowed to run at 100 °C until a decrease in isocyanate intensity was observed. The maximum intensity of isocyanate was reached after 1 h 15 min (Figure 9.6)

9. CTV-Based Pyramidic Monomers for Chiral Columnar Aggregates.

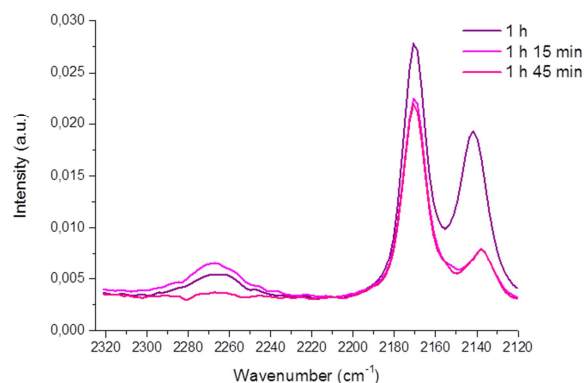


Figure 9.6 Isocyanate formation reaction IR profile in toluene at selected times.

Once the conditions were optimized for the model reaction in toluene, the urea formation was attempted with the CTV-amino derivative building block **39**. Unfortunately, this building block was highly insoluble in toluene, so the reaction was then run in THF.

The isocyanate formation in toluene was compared with that in THF at the same conditions (MW, 100 °C, 1 h 15 min). As it is observed in Figure 9.7, formation of the isocyanate was favored in THF.

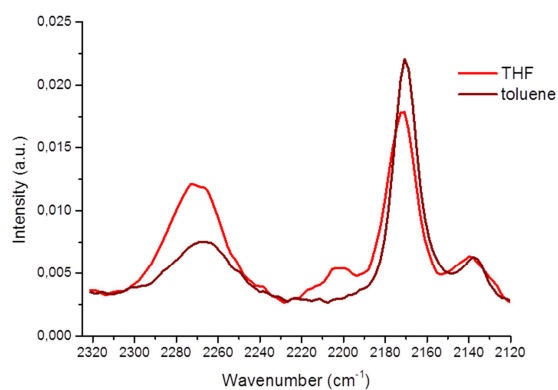


Figure 9.7 Isocyanate formation reaction IR profile in THF and toluene.

9. CTV-Based Pyramidic Monomers for Chiral Columnar Aggregates.

As in toluene, the reaction was allowed to run at 100 °C. The IR spectra profile was monitored at different times. The maximum intensity of the isocyanate peak was observed after 1 h and 15 min under MW irradiation. After 1 h 45 min the peak intensity dropped due to decomposition of the isocyanate intermediate (Figure 9.8).

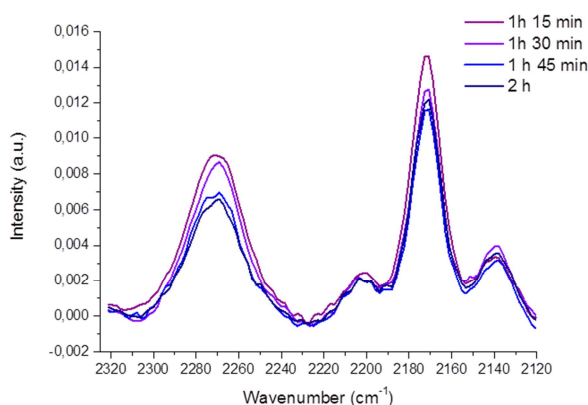
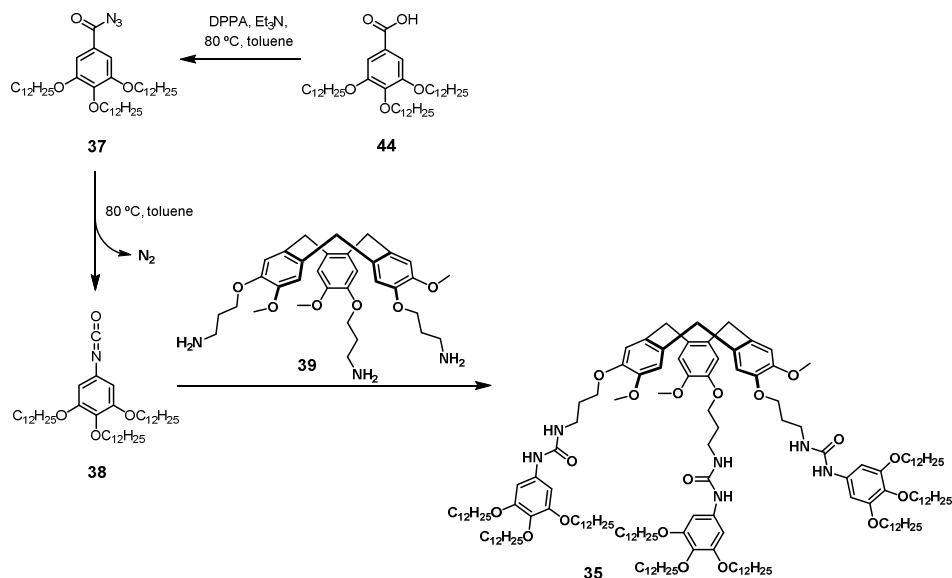


Figure 9.8 Isocyanate formation reaction IR profiles in THF at selected times.

Synthesis of the Target CTV Monomer **35**

Finally, the desired urea **35** was synthesized. The *tris*(dodecyloxy)benzoic acid **44** was heated in THF for 1.25 h at 100 °C. Then amine **39** was added and the reaction was allowed to run for one extra hour (Scheme 9.10). The solvent was evaporated and the mixture was directly submitted for an external mass analysis. However, attempts to purify the desired urea by column chromatographic were unsuccessful, so the sample was submitted to HPLC. The HPLC-MS analysis confirmed the presence of the desired CTV-monomer **35** but, unfortunately, the desired product could not be isolated from the crude mixture, so the yield is therefore unknown.

9. CTV-Based Pyramidic Monomers for Chiral Columnar Aggregates.



Scheme 9.10 Synthesis of desired CTV-monomer 35.

9.2.2 Synthesis of CTV Monomer 35. Route (b)

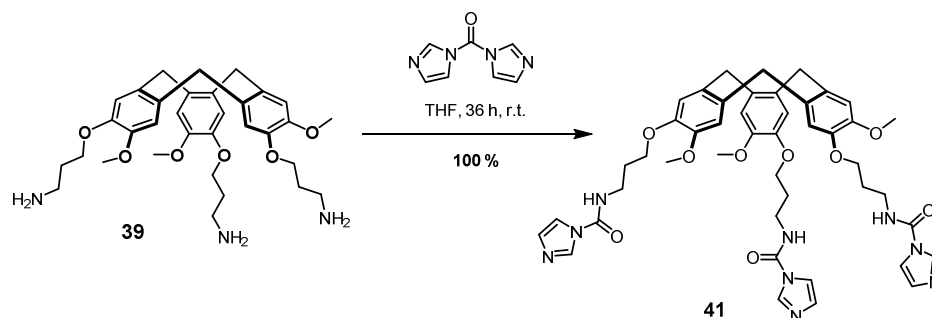
After attempts to isolate the CTV-monomer 35 prepared through the synthetic route (a) failed, the synthesis of the CTV-based target monomer 35 was approached through the synthetic route (b) (Scheme 9.1).

The synthesis started with the preparation of the CTV-carbamoyl imidazole building block 47 and the *tris*-(dodecyloxy)aniline building block 48.

Synthesis of CTV-Carbamoyl Imidazole Building Block 47

The CTV-carbamoyl-imidazole building block 47 was synthesized starting from the CTV-amino derivative building block 39. Stirring compound 39, in the presence of carbonyl imidazole (CDI) gave the activated CTV amino derivative in excellent yields (Scheme 9.11). Decomposition of the carbamoyl imidazole is observed at room temperature. For this reason, the carbamoyl imidazole was readily prepared before its use and kept under argon atmosphere at 5 °C.

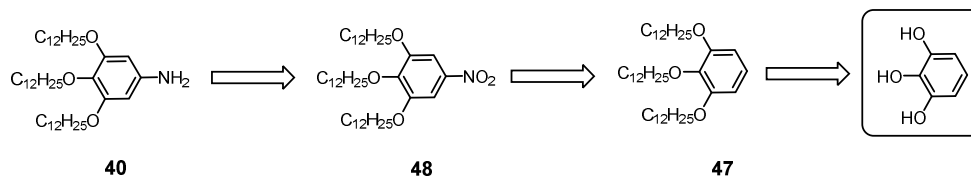
9. CTV-Based Pyramidic Monomers for Chiral Columnar Aggregates.



Scheme 9.11 Synthesis of CTV-carbamoyl imidazole building block **41**.

Synthesis of *Tris*-(dodecyloxy)aniline Building Block **48**

The *tris*-(dodecyloxy)aniline building block **48** was synthesized through a three step synthetic pathway starting from commercially available 1,2,3-triphenol (Scheme 9.12).

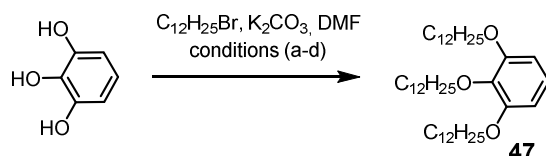


Scheme 9.12 Retrosynthetic approach of the 3,4,5-*tris*-(dodecyloxy)aniline building block **40**.

The synthesis started with the alkylation of commercially available 1,2,3-triphenol with dodecylbromide. The different conditions explored and are shown in Table 9.2. Alkylation of the commercially available triphenol with dodecylbromide in the presence of potassium carbonate in DMF was achieved in excellent yields.

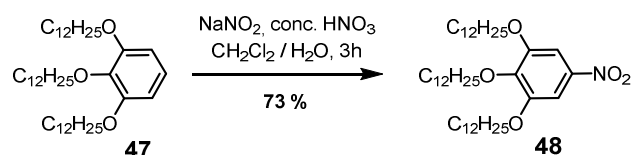
9. CTV-Based Pyramidic Monomers for Chiral Columnar Aggregates.

Table 9.2 Conditions screened for the synthesis of 1,2,3-*tris*-(dodecyloxy)benzene **47**.



	<i>Heating</i>	<i>Temperature</i>	<i>Time</i>	<i>Yield</i>
a	MW	100 °C	2 h	31 %
b	MW	100 °C	6 h	81 %
d	Δ	80 °C	18 h	97 %

The introduction of the nitro group was achieved in good yields (Scheme 9.13). Initially, the reaction could not be reproduced when preparing large amounts of nitrobenzene **48**. The yield dropped to 30 % or even no conversion occurred when the reaction was scaled-up.



Scheme 9.13 Introduction of the nitro group, synthesis of nitrobenzene **48**.

The relative amount of solvent was found to be relevant for the reaction performance. Currently, when scaling-up a reaction procedure, a lower relative amount of solvent is employed, which in this particular case lead to a considerable yield drop. When the solvent ratio was corrected, reproducibility was achieved at high scale.

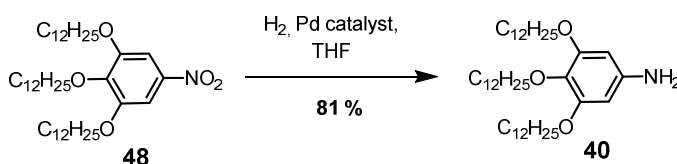
For the last synthetic step, both palladium black and palladium over carbon were screened as catalysts to reduction the nitro group. The aniline building block was obtained in very good yields. The conditions screened are shown in Table 9.3.

9. CTV-Based Pyramidic Monomers for Chiral Columnar Aggregates.

Only starting material was recovered after attempted reduction with H₂ using palladium black as catalyst over a 12 h reaction (entry a, Table 9.3).

The 3,4,5-*tris*-(dodecyloxy)aniline **40** was successfully synthesized starting from 1,2,3-*tris*-(dodecyloxy)-5-nitrobenzene **48** after reduction of the nitro group with H₂ in the presence of palladium over carbon. Due to similar retention times of both educt and product, the reaction could not be monitored by TLC. In the first attempt, the reaction was stopped after 12 h when 25 % of the starting material was still unreacted and only 49 % yield was achieved. When the reduction was allowed to proceed for 18 h the yields were improved up to 81 %.

Table 9.3 Conditions screened for the synthesis of the aniline building block **40**.



	<i>Pd catalyst</i>	<i>Time</i>	<i>Yield</i>
a	Pd black, H ₂	12 h	0 %
b	Pd / C, H ₂	12 h	49 %
c	Pd / C, H₂	18 h	81 %

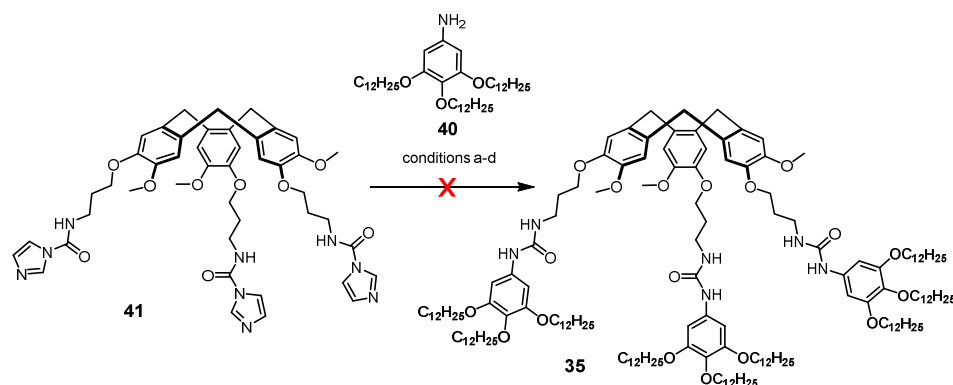
Synthesis of CTV-Based Monomer **35**

In the last synthetic step the 3,4,5-*tris*-(dodecyloxy)aniline building block **40** performs a nucleophilic attack towards the activated CTV-carbamoyl imidazole to form the desired urea.

Attempts to prepare the desired urea by following conditions reported for the synthesis of ureidopyrimidinone derivatives, previously described in our group^{41a} (Table 9.4) exclusively lead to degradation of the CTV-carbamoyl imidazole building block **41**.

9. CTV-Based Pyramidic Monomers for Chiral Columnar Aggregates.

Table 9.4 Conditions screened for the synthetic attempts of CTV-monomer **35**.



	Solvent	Time	Temperature	Heating	Product
a	THF	48 h	Reflux	Δ	degradation
b	DCM	48 h	Reflux	Δ	degradation
c	DCM	6 h	60 °C	MW	degradation
d	THF	4 h	80 °C	MW	degradation

In aromatic amines the non-bonding electron pair of aromatic amines is delocalized over the aromatic ring which leads to a decrease of their nucleophilic character. Due to this low availability of the non-bonding electron pair, aniline derivatives are unable to perform the nucleophilic attack of the carbamoyl imidazole activated carbonyl group (Figure 9.9).

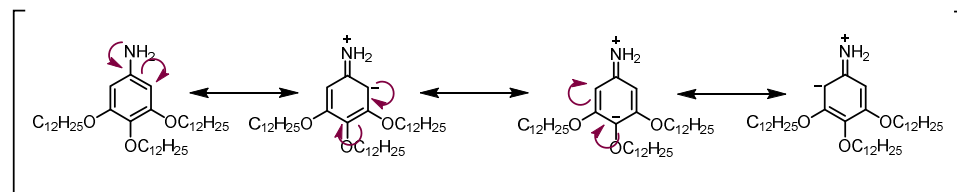


Figure 9.9 Resonance structures of aromatic amine building block **40**.

9. CTV-Based Pyramidic Monomers for Chiral Columnar Aggregates.

However, anilide anions are more reactive nucleophiles due to the high availability of the non-bonding electron pair (Figure 9.10).

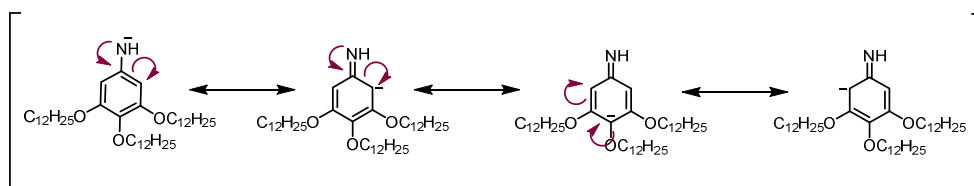


Figure 9.10 Resonance structures of anilide.

In attempts to activate the nucleophilic attack of 3,4,5-*tris*-(dodecyloxy)aniline **40** to the carbamoyl imidazole, the aniline building block **40** was pre-treated with a base to promote formation of the anilide nucleophile. Screened conditions are summarized in Table 9.5.

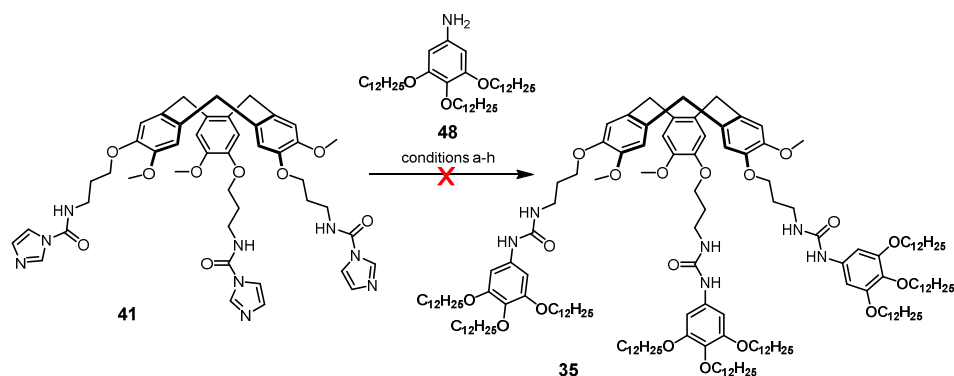
Pre-treatment with triethylamine did not promote the urea formation (entries a-b, Table 9.5). These conditions¹²⁵ successful for aliphatic amines were not suitable for the activation of the aromatic amine building block **48**. The material was recovered. The imidazole derivative partially decomposed.

The pre-treatment of the aniline derivative building block with a strong base such as *n*-BuLi has been reported to provide a convenient synthetic protocol for the formation of aromatic ureas.¹²⁵ Unfortunately, attempts to promote the urea formation in THF after pre-activation of the 3,4,5-*tris*-(dodecyloxy)aniline building block with *n*-BuLi prior to the addition of the CTV-carbamoyl imidazole building block did not succeed either (entries c-d, Table 9.5).

¹²⁵ Bertrand, M. B.; Wolfe, J. P. *Tetrahedron*, **2005**, *61*, 6449.

9. CTV-Based Pyramidic Monomers for Chiral Columnar Aggregates.

Table 9.5 Screened conditions for the preparation of the desired CTV-monomer **35**



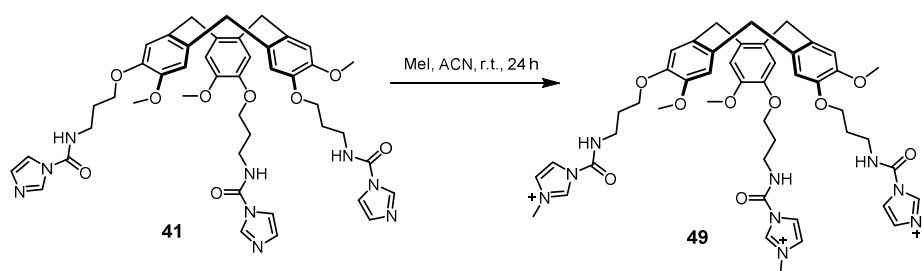
	<i>Equivalents</i>	<i>Solvent</i>	<i>Base</i>	<i>Time</i>	<i>Temperature</i>	<i>Yield</i>
a	5	DCM	Et ₃ N	4 h	60 °C (MW)	0 %
b	5	DCM	Et ₃ N	48 h	Reflux	0 %
c	3.3	THF	<i>n</i> -BuLi	18 h	r.t.	0 %
d	5	THF	<i>n</i> -BuLi	48 h	Reflux	0 %
f	3.3	THF / DMF	<i>n</i> -BuLi	48 h	r.t. to reflux	0 %
g	3.3	THF / DMF	<i>n</i> -BuLi	48 h	< 0 to reflux	0 %
h	3.3	THF / DMF	<i>n</i> -BuLi	48 h	< 0 to reflux	0 %

To improve the solubility of the building blocks, DMF was added to the reaction solution (entry f, Table 9.5). In the presence of DMF, after the pre-treatment of the aniline building block with *n*-BuLi, a product was isolated that did not correspond to the desired urea **35**. The product obtained seems to be the result of a cross-reaction with the degraded THF. *n*-BuLi is known to attack the acidic protons in α position to the ether group of the solvent. Solubility of the building block achieved in DMF and THF degradation allow the formation of the non-desired side product.

9. CTV-Based Pyramidic Monomers for Chiral Columnar Aggregates.

To avoid such cross-reactions, the reaction was repeated under temperature control. The temperature was kept under 0 °C during the addition of the *n*-BuLi and then the reaction mixture was allowed to reach room temperature and further refluxed for 48 h (entry e, Table 9.5). Only starting material was isolated. The carbamoyl imidazole derivative partially decomposed.

In the last attempt to promote the formation of the desired urea, the acyl imidazole leaving group was activated to increase its reactivity towards a nucleophilic attack (Scheme 9.14)



Scheme 9.14 Synthesis of acyl activated CTV-carbamoyl imidazolium 51

As shown in Figure 9.11 the imidazole was *N*-methylated to give the corresponding resonance-stabilized imidazolium salt leaving group.

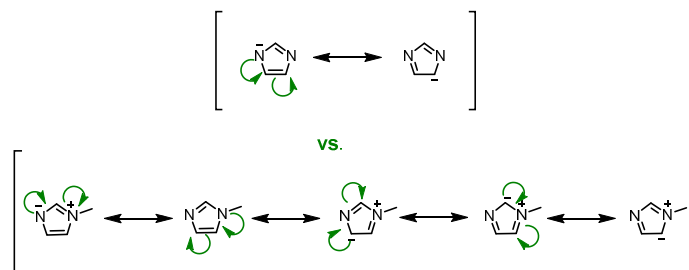
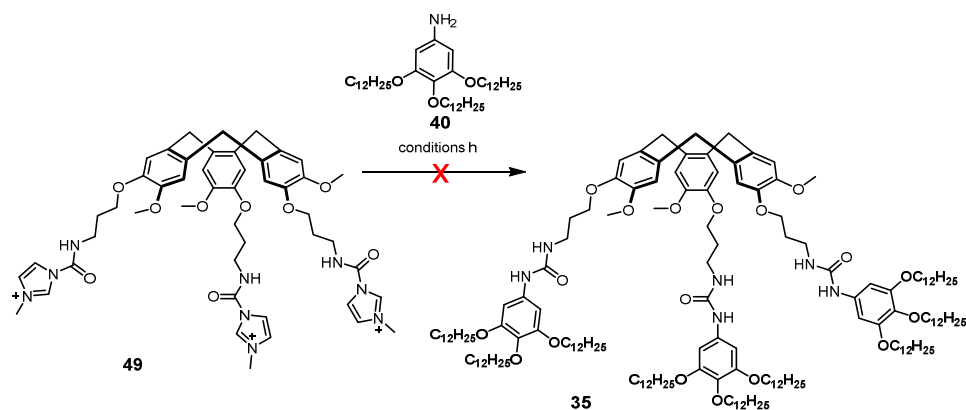


Figure 9.11 Resonance structures for the imidazole and imidazolium salt leaving groups.

Unfortunately, activation of the leaving group did not promote the formation of the desired urea (Scheme 9.15).

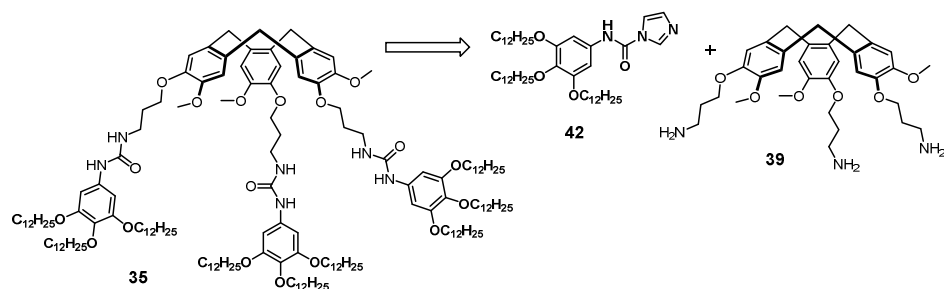
9. CTV-Based Pyramidic Monomers for Chiral Columnar Aggregates.



Scheme 9.15 Synthetic attempt of target CTV-monomer **35**.

9.2.3 Synthesis of CTV Monomer **35**: Route (c)

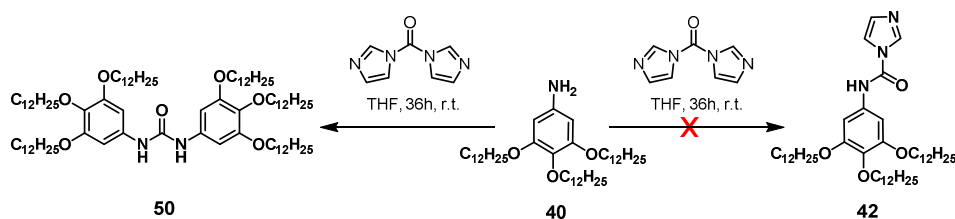
In the last synthetic approach, the preparation of the CTV-monomer **35** was attempted starting from the CTV-amino derivative building block **39** and the 3,4,5-*tris*-(dodecyloxy)phenyl carbamoyl imidazole derivative **42** following route (c) (Scheme 9.16). This synthetic pathway was initially rejected to avoid formation of the symmetric urea during the preparation of the carbamoyl imidazole building block.



Scheme 9.16 Retrosynthetic approach (c) for the preparation of the CTV-monomer **35**.

As expected, the symmetric urea **50** was formed when attempting the synthesis of the carbamoyl imidazole building block **42** even when working at low carbonyl diimidazole equivalents. No carbamoyl imidazole **42** was isolated (Scheme 9.17).

9. CTV-Based Pyramidic Monomers for Chiral Columnar Aggregates.



Scheme 9.17 Synthetic attempts of carbamoyl imidazole building block **42**.

9.3 Summary and Discussion

In the first synthetic approach towards the preparation of the CTV-monomer **35**, the target molecule was prepared starting from 3,4,5-*tris*-(dodecyloxy)benzoic acid building block **44** and the CTV-amino derivative building block **39**. The carboxylic acid **44** was heated in the presence of DPPA and Et₃N to give the acyl azide that further underwent a *Curtius* rearrangement and gave the isocyanate building block **38**. The isocyanate was then further reacted with the CTV-amino derivative building block **39** and gave the desired urea **35** in a one-pot reaction.

The isocyanate formation was depicted as the key step reaction and was optimized. For that aim the reaction was monitored by an IR probe incorporated into an IR reactor that allowed real time *in situ* monitoring of the reaction IR profile.

The IR monitoring evidenced that the isocyanate **38** formation reached its maximum after 3.5 h reaction and its IR intensity dropped afterwards. Attempts to promote the full conversion of the carboxylic acid **44** and the acyl azide **37** as well as improving the isocyanate **38** yield by initially heating the reaction at 40 °C and by performing the reaction under an argon flow did not succeed.

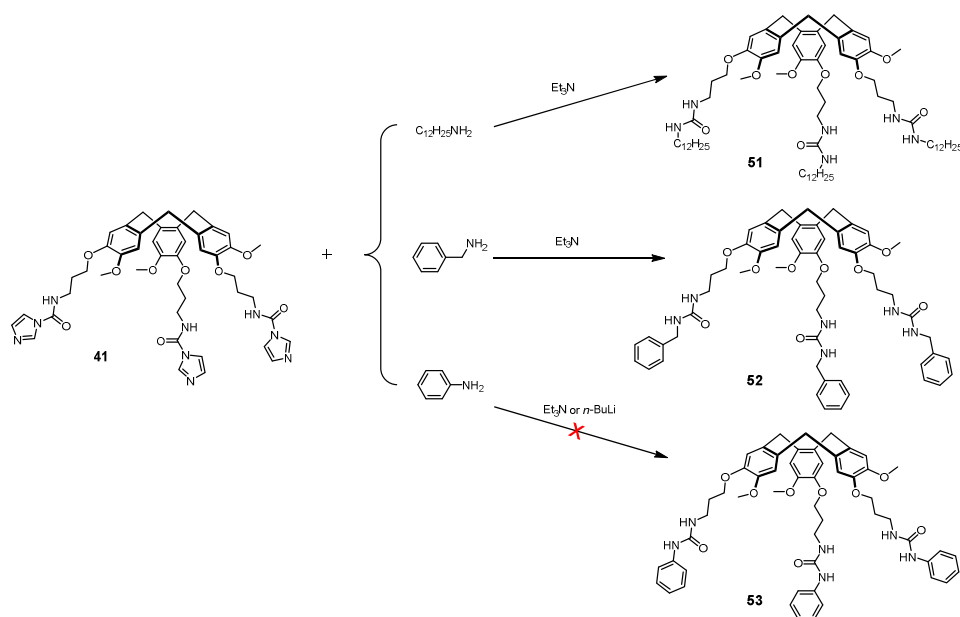
The key step reaction was further optimized in THF and under MW irradiation. The best conditions identified MW irradiation for 1 h and 15 min, when the corresponding amine was added to the reaction mixture.

Although the target molecule mass was detected in the reaction crude, the desired CTV-monomer **35** could not be isolated.

9. CTV-Based Pyramidic Monomers for Chiral Columnar Aggregates.

In the second approach, the synthesis of CTV-monomer **35** was attempted starting from the CTV-carbamoyl imidazole building block **41** and the corresponding aromatic amine **40**. The low availability of the non-bonding electron pair of the aromatic amine hampered the urea formation reaction. Despite the attempts to promote the nucleophilic attack by pre-treatment of the aniline building block **40** with Et_3N or $n\text{-BuLi}$ and by activation of the imidazole leaving group as imidazolium salt the desired CTV-monomer **35** could not be synthesized.

To confirm this hypothesis, the urea formation reaction between the activated CTV-carbamoyl imidazole and three different commercially available amines was studied: dodecylamine, benzyl amine and aniline (Scheme 9.18).



Scheme 9.18 Urea formation model reactions with commercially available dodecylamine, benzylamine and aniline

In the presence of Et_3N in DCM both alkylated and benzylated ureas were successfully synthesized. Pre-treatment of the aniline with either Et_3N or $n\text{-BuLi}$ failed to give the desired aromatic urea. Although the pre-treatment of anilines with $n\text{-BuLi}$ was reported for the synthesis of aromatic ureas, in this particular case it can be unambiguously

9. CTV-Based Pyramidic Monomers for Chiral Columnar Aggregates.

affirmed that such method did not promote the formation of the desired CTV-monomer **35**.

9.4 Conclusions

The synthesis of the target molecule **35** was attempted following three different synthetic pathways.

In the first approach, the CTV-monomer **35** was prepared starting from the isocyanate building block **38** and the CTV-amino derivative building block **39**. The reaction was optimized with the use of an IR-reactor that allowed *in situ* monitoring of chemical reactions by FTIR. Best conditions for the formation of the isocyanate and the final urea were obtained in THF under MW irradiation. Although the desired CTV-monomer was detected by mass spectrometry, the target molecule **35** could not be isolated.

The second approach deals with the synthesis of the CTV-monomer **35** starting from the CTV-carbamoyl imidazole building block **41** and the corresponding aromatic amine **40**. Unfortunately, the low availability of the non-bonding electron pair of the aniline hampers the nucleophilic attack and the urea formation. Attempts to promote such attack by activation of both the aromatic amine and the imidazole leaving group did not promote the formation of the desired urea.

In the third approach, the synthesis of the CTV-monomer **35** was attempted starting from the CTV-amino derivative **39** and the carbamoyl imidazole building block **42**. Unfortunately, the carbamoyl imidazole building block **42** could not be prepared and the symmetric urea **52** was obtained instead.

9. CTV-Based Pyramidic Monomers for Chiral Columnar Aggregates.

**Chapter 10: CTV-Based Pyramidic Monomers for
Chiral Columnar Aggregates II**

UNIVERSITAT ROVIRA I VIRGILI

CYCLOTRIVERATRYLENE AND PORPHYRIN SCAFFOLDS FOR MOLECULAR RECOGNITION AND SELF-ASSEMBLY

Berta Camafort Blanco

Dipòsit Legal: T 677-2015

10. CTV-Based Pyramidic Monomers for Chiral Columnar Aggregates II

10.1 Design and Aim of the Project

The goal of this chapter is the synthesis of a chiral CTV-based pyramidic monomer able to self-assemble into macroscopic columnar aggregates stabilized by non-covalent π - π stacking and hydrogen bonding interactions. Such columnar aggregates might express liquid crystalline behavior. The structural chirality of the trisubstituted CTVs might be transferred to the macroscopic columnar aggregate promoting the formation of a macroscopic helix.

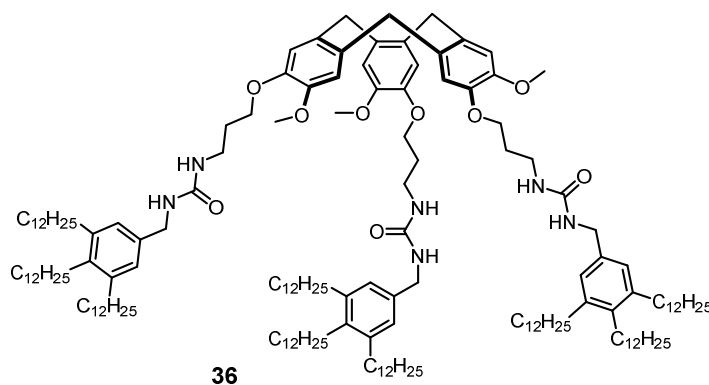


Figure 10.1 CTV-Based pyramidic monomer **36**.

In chapter 9, the synthetic attempts to prepare CTV-monomer **35** were not successful, due to problems during the preparation of the urea moiety. Thus, a new target molecule **36** was designed (Figure 10.1). In the new structure, an extra methylene group is introduced within the pendant legs, and thus 3,4,5-tridodecylbenzyl amine **54** (Figure 10.2) was selected as a nucleophilic building block to form the desired CTV-monomer **36**.

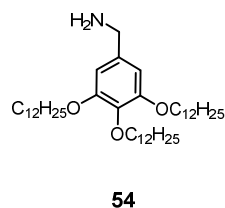


Figure 10.2 3,4,5-Tridodecylbenzyl amine building block **54**.

10. CTV-Based Pyramidic Monomers for Chiral Columnar Aggregates II

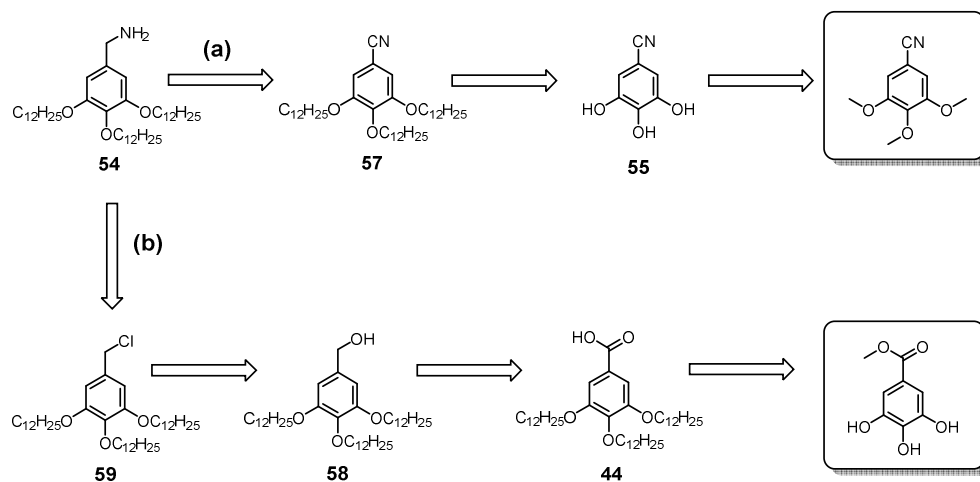
10.2 Synthesis and Characterization

10.2.1 Synthesis of CTV Monomer 36

The synthesis of the target monomer **36** started with the preparation of the benzylamine building block **54**.

Synthesis of 3,4,5-Tris(dodecyloxy)benzylamine Building Block **54**

Two different synthetic strategies were initially proposed for the preparation of **54**. In route (a) benzylamine **54** was approached through a three step synthesis starting from commercially available trimethoxybenzonitrile. In route (b) the synthesis could be achieved through a four step reaction starting from commercially available methyl gallate (Scheme 10.1).



Scheme 10.1 Retrosynthetic pathways of for benzylamine building block **54**.

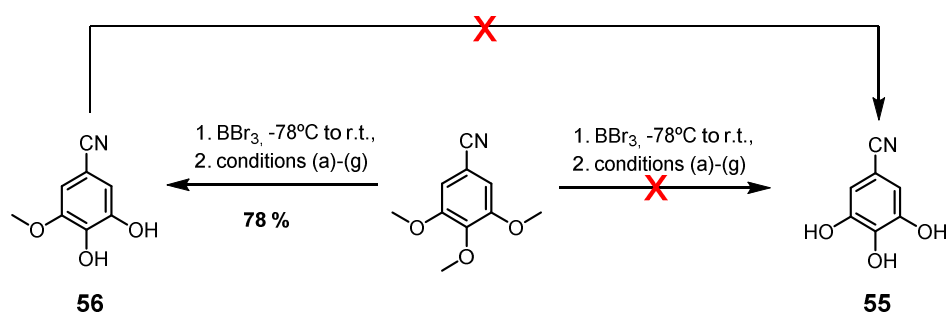
Synthesis of the 3,4,5-Tris(dodecyloxy)benzylamine **54**: Route (a)

Synthetic route (a) was initially selected. Demethylation of commercially available trimethoxybenzonitrile was attempted following a procedure described by Marder *et*

10. CTV-Based Pyramidic Monomers for Chiral Columnar Aggregates II

a.¹²⁶ (Scheme 10.1). Unfortunately, the desired trihydroxybenzonitrile **55** was not obtained. Addition of BBr_3 at -78°C and further stirring at room temperature in DCM produced exclusively monomethylated benzonitrile **56**, which precipitated out of the solution as a pure product in a 78 % yield (entry a, Table 10.1).

Table 10.1 Conditions screened for 3,4,5-trihydroxybenzonitrile **55** synthetic attempts.



	<i>BBr₃</i> equiv.	Time	Temperature	Solvent	Product
a	3,9	18 h	r.t	CH_2Cl_2	monomethylated
b	3,9	72 h	r.t	CH_2Cl_2	monomethylated
c	3,9	18 h	reflux	CH_2Cl_2	monomethylated
d	8	72 h	reflux	CH_2Cl_2	monomethylated
f	8	18	reflux	$\text{CH}_2\text{Cl}_2/\text{DMF}$	starting material
g	8	18	reflux	$\text{CH}_2\text{Cl}_2/\text{THF}$	starting material

In attempts to promote the total conversion of the starting material, the reaction conditions were screened. Increasing the number of reagent equivalents, reaction

¹²⁶ An, Z.; Yu, J.; Domercq, B.; Jones, S. C.; Barlow, S.; Kippelen, B.; Marder, S. R. *J. Mater. Chem.*, **2009**, *19*, 6688.

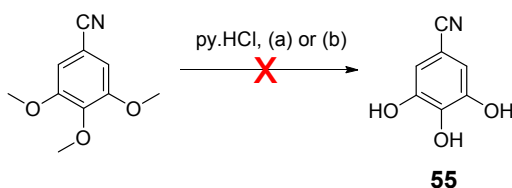
10. CTV-Based Pyramidic Monomers for Chiral Columnar Aggregates II

temperature or reaction time did not promote the synthesis of the desired building block **55** (entry b - d, Table 10.1).

Finally, DMF and THF were added to the reaction mixture to increase the solubility of the intermediate and to promote the total conversion of the benzonitrile (entries f - g, Table 10.1). However, starting material was exclusively recovered.

Alternatively, the demethylation conditions described by Wadgaonkar *et al.*¹²⁷ and Rao *et al.*¹²⁸ were also tested. Starting material was exclusively recovered after heating the reaction mixture in the presence of pyridine hydrochloride (py·HCl) (Table 10.2).

Table 10.2 Conditions screened for 3,4,5-trihydroxybenzonitrile **55** synthetic attempts.



	<i>Equivalents</i>	<i>Time</i>	<i>Temperature</i>	<i>Heating</i>	<i>Product</i>
a	15	1 h	220 °C	MW	starting material
b	15	18 h	150 °C	Sealed tub	starting material.

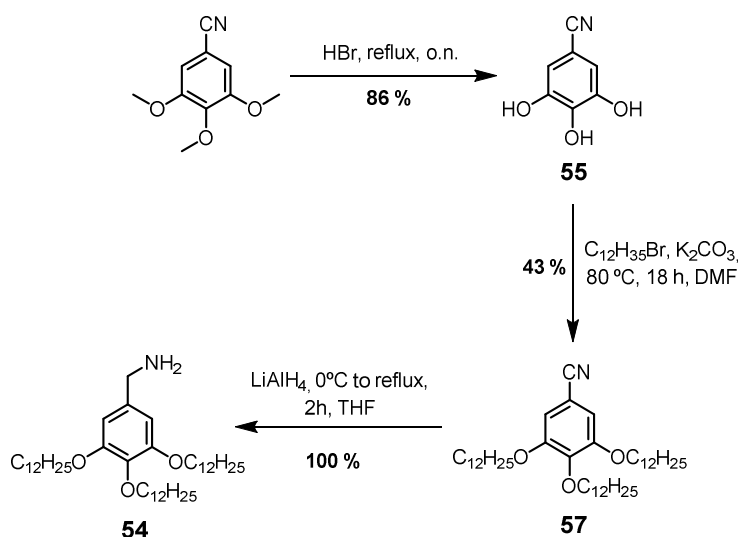
¹²⁷ Kulkarni, P. P.; Kadam, A. J.; Mane, R. B.; Desai, U. V.; Wadgaonkar, P. P. *J. Chem. Res.-S.* **1999**, 394.

¹²⁸ Yao, H.; So M.-K.; Rao, J. *Angew. Chem. Int. Ed.* **2007**, *46*, 7031.

10. CTV-Based Pyramidic Monomers for Chiral Columnar Aggregates II

Finally, total demethylation of commercially available trimethoxybenzonitrile was achieved in good yields after refluxing the starting material in HBr solution as reported by Learmonth *et al.*¹²⁹ (Scheme 10.2).

The triphenol **55** was then O-alkylated with dodecylbromide in the presence of potassium carbonate in DMF, in moderate yield. Finally reduction of the nitrile group with LiAlH₄ in THF gave the desired benzylamine **54** in excellent yields (Scheme 10.2).



Scheme 10.2 Synthesis of 3,4,5-tris(dodecyloxy)benzylamine building block **54** [route (a)].

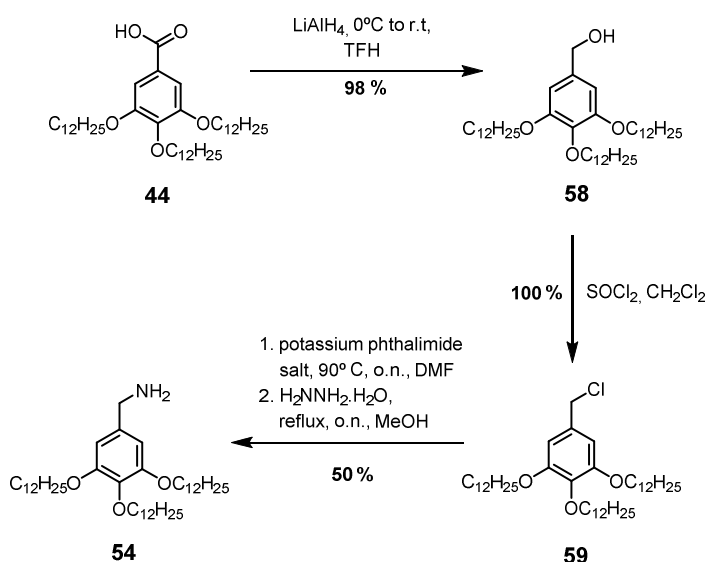
Synthesis of the 3,4,5-tris(dodecyloxy)benzylamine **54**. Route (b)

Simultaneously to route (a), the desired benzylamine **54** was prepared starting from the previously synthesized 3,4,5-tris(dodecyloxy)benzoic acid **44** by saponification of methyl trihydroxybenzoate.

¹²⁹ Kiss, L. E.; Ferreira, H. S.; Torrão, L.; Bonifacio, M. J.; Palma, P. N.; Soares-da-Silva, P.; Learmonth D. A. *J. Med. Chem.*, **2010**, 53, 3396.

10. CTV-Based Pyramidic Monomers for Chiral Columnar Aggregates II

Reduction of carboxylic acid **44** with LiAlH_4 in THF gave the 3,4,5-tris(dodecyloxy)benzyl alcohol **58** in excellent yield. The alcohol was then chlorinated with thionyl chloride in excellent yield. *Gabriel's* reaction with phthalimide potassium salt in DMF and further treatment with monohydrated hydrazine in methanol gave the desired tris(dodecyloxy)benzylamine building block **54** in moderate yield (Scheme 10.3).



Scheme 10.3 Synthesis of 3,4,5-tris(dodecyloxy)benzyl amine building block **54** [route (b)].

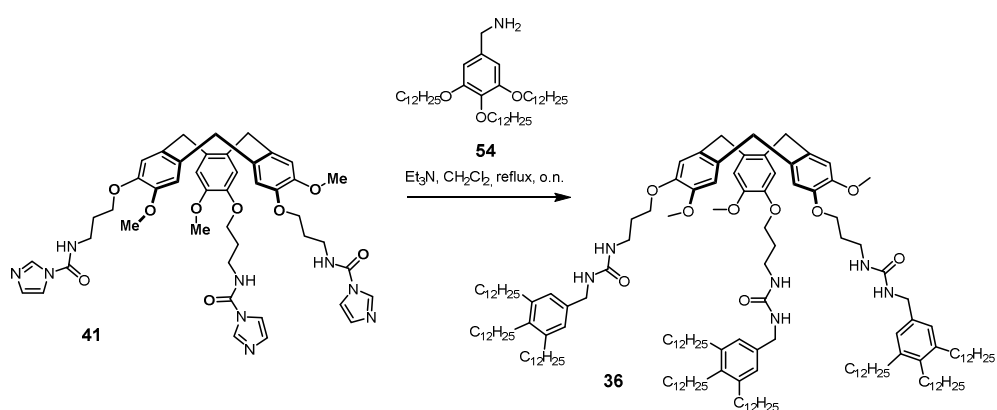
Synthesis of the Target Molecule CTV-Monomer **36**

The synthesis of the desired urea **36** was attempted through base catalyzed nucleophilic acyl substitution. After stirring the mixture of CTV-based carbamoyl imidazole **41** and tris(dodecyloxy)benzylamine **54** in the presence of triethylamine at room temperature, only starting material was recovered (entry a, Table 10.3).

The desired CTV-monomer **36** was obtained after refluxing the starting materials in DCM in the presence of Et_3N for 18 h. The final product was obtained after modification of 3 positions in an overall yield of 43%. The compound was purified by column chromatography (CH_2Cl_2 / MeOH 98:2).

10. CTV-Based Pyramidic Monomers for Chiral Columnar Aggregates II

Table 10.3 Conditions screened for the synthesis of target CTV-monomer **36**.



	<i>Et₃N</i> Equivalents	<i>Time</i>	<i>Temperature</i>	<i>Solvent</i>	<i>Yield</i>
a	3,3	18 h	r.t	CH ₂ Cl ₂	0 %
b	3.3	24 h	Reflux	CH₂Cl₂	43 %
c	3.3	24 h	Reflux	THF	32 %
d	3.3	48 h	Reflux	CH ₂ Cl ₂	40 %

10.2.2 Target Molecule **36** Characterization

CTV-Monomer **36** was characterized by ¹H-NMR and mass spectrometry. In the ¹H-NMR spectrum all significant protons were identified (Figure 10.3).

10. CTV-Based Pyramidic Monomers for Chiral Columnar Aggregates II

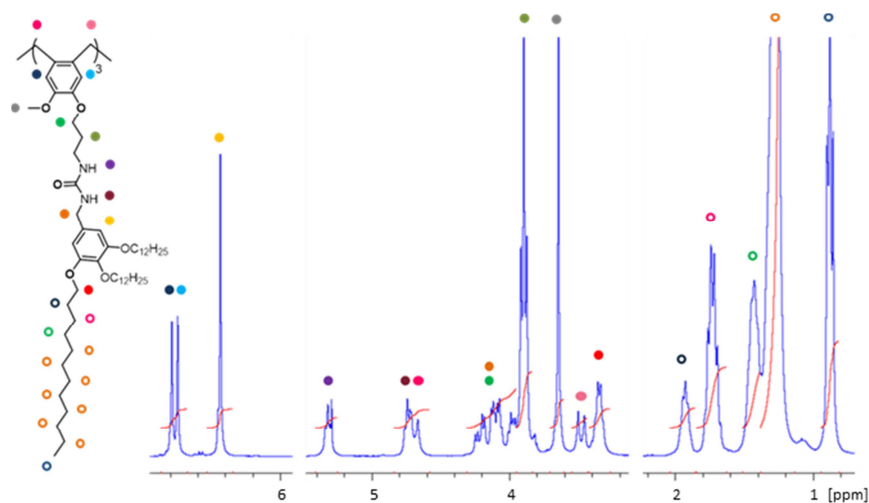


Figure 10.3 $^1\text{H-NMR}$ spectrum of CTV-porphyrin **36** in CDCl_3 .

Mass analysis of CTV-monomer **36** was performed by means of MALDI-TOF spectrometry. In Figure 10.4 the detected mass of the CTV-monomer **36** is shown (found mass/z^+ : 2659.1859, calculated mass/z^+ : 2660.1267).

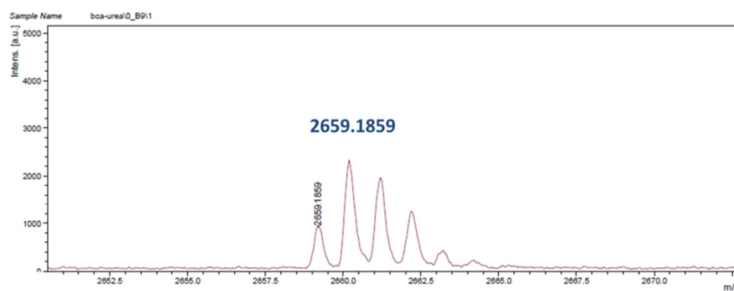


Figure 10.4 MALDI-TOF mass spectrum of CTV-monomer **36**.

The UV-Vis spectrum and CD spectra of both enantiomers were recorded in CH_2Cl_2 and are shown in Figure 10.5.

10. CTV-Based Pyramidic Monomers for Chiral Columnar Aggregates II

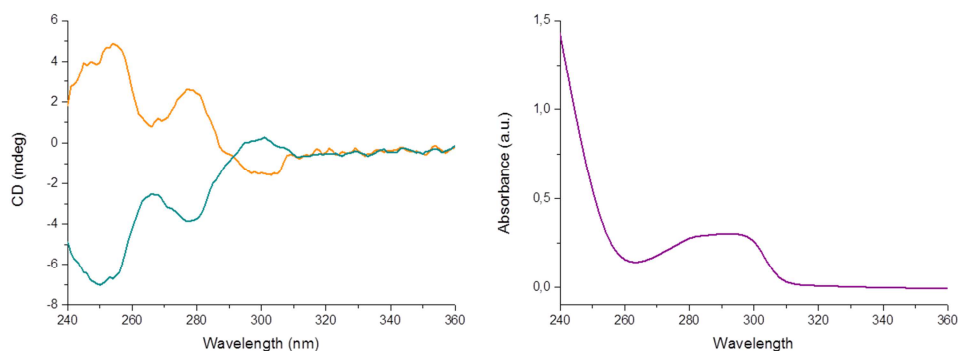


Figure 10.5 CD and UV-Vis spectrum of CTV-monomer **36** in DCM.

Attempts to record the CD spectra in polar competitive solvents were not successful, since monomer **36** was not soluble in either methanol or ethanol. Also, strong absorption of DMSO prevented the spectra to be recorded in that solvent.

10.3 Results and Discussion

10.3.1 Self-Assembly, Chiral Amplification and Mesomorphic Behavior. Preliminary Studies

Self-Assembly Studies: $^1\text{H-NMR}$

The aggregation of the CTV-monomer units was first studied by $^1\text{H-NMR}$ spectroscopy. Formation of columnar aggregates depends on various factors such as concentration, temperature and solvent polarity. The changes on the $^1\text{H-NMR}$ spectrum were recorded upon changing the CTV-monomer **36** concentration, the temperature and the solvent.

10. CTV-Based Pyramidic Monomers for Chiral Columnar Aggregates II

¹H-NMR Self-Assembly Studies at Different Concentrations

The formation of columnar aggregates would be promoted at higher concentrations, whereas highly diluted solutions would promote disaggregation of the columnar stacking. Thus, ¹H-NMR spectra of **36** were recorded at different concentrations in CDCl₃ (Figure 10.6). An upfield shift of the urea N-H_a proton was observed upon decreasing the CTV-monomer **36** concentration, indicating changes on the chemical environment of urea moieties at different concentrations. No changes of the CTV-central core proton signals were observed.

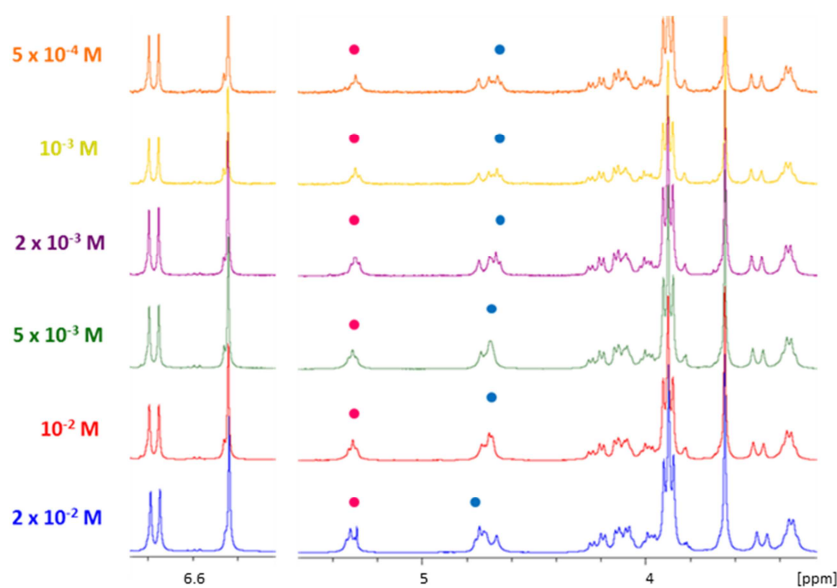


Figure 10.6 ¹H-NMR spectra of CTV **36** in CDCl₃ at different concentrations.

The small changes observed upon decreasing the concentration could indicate no stacking or a weak interaction between the CTV-monomers. However, it could also be assumed that the columnar aggregate was already present at the lowest concentration of 5×10^{-4} M, as it is otherwise expected. In this scenario, increasing the concentration would not have a strong effect on the spectra.

10. CTV-Based Pyramidic Monomers for Chiral Columnar Aggregates II

¹H-NMR Self-Assembly Studies at High Temperatures

To gain more insight into the columnar aggregation process, high temperature ¹H-NMR experiments at different concentrations were performed.

The non-covalent interactions present in the supramolecular aggregate are strongly dependent on temperature. The strength of such interactions and, therefore, the formation and length of the columnar aggregates should decrease as the temperature increases.

The ¹H-NMR spectra of CTV-monomer **36** were thus recorded at different temperatures. At both concentrations, a similar behavior was observed (2×10^{-2} M and 2×10^{-3} M; Figure 10.7). The urea N-H protons considerable shift upfield upon raising the temperature. The aromatic CTV-protons shift downfield as the singlets collapse.

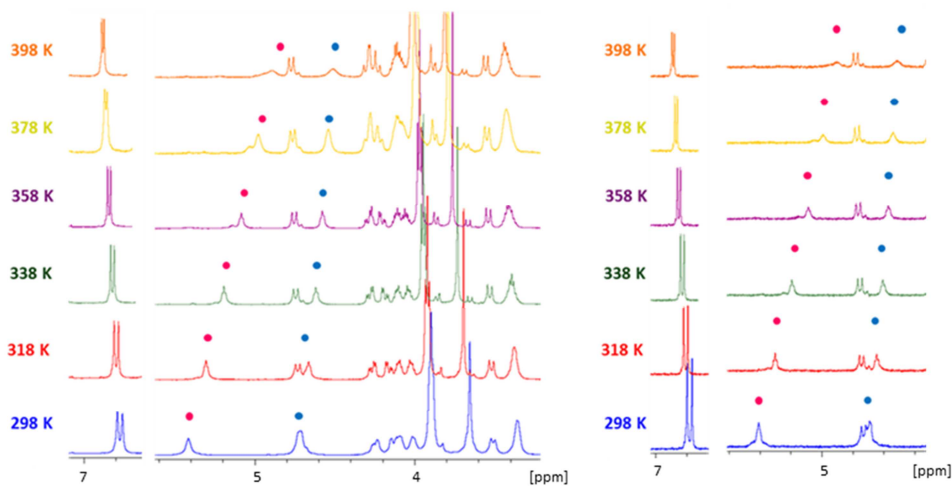


Figure 10.7 ¹H-NMR spectra of CTV **36** in TCE at different temperatures. Left: $[36] = 2 \times 10^{-2}$ M; Right $[36] = 2 \times 10^{-3}$ M.

¹H-NMR Self-Assembly Studies. Addition of Competitive Solvent

Increasing amounts of a polar competitive solvent (DMSO) were added to a 10^{-2} M solution of CTV-monomer **36** and the ¹H-NMR spectra were recorded (Figure 10.8).

10. CTV-Based Pyramidic Monomers for Chiral Columnar Aggregates II

The addition of DMSO is expected to disrupt the hydrogen bond interactions between the urea moieties, although this would not necessarily inhibit the aggregation since the columnar architecture is also stabilized by π - π interactions.

Addition of DMSO (1-8 equivalents) promoted the downfield shifting of both urea protons, The shift of N-H_b being nevertheless more pronounced. After addition of 8 equivalents of DMSO the urea protons eventually collapsed. No further experiments could be recorded since after addition of 10 equivalents the signal locking was inhibited.

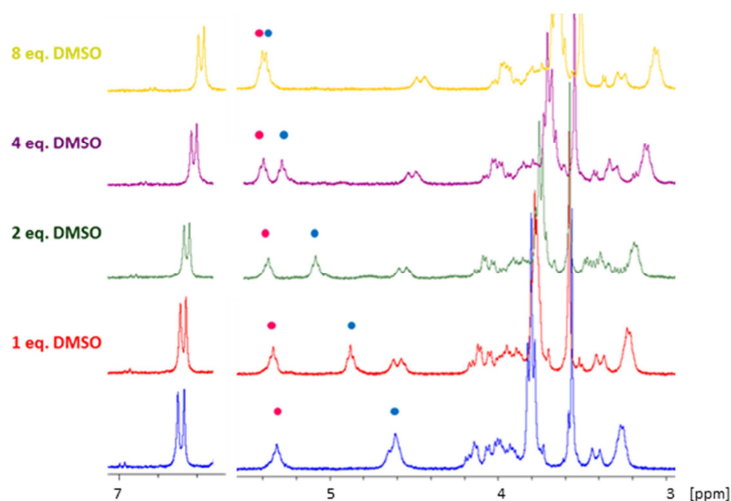


Figure 10.8 $^1\text{H-NMR}$ spectra of CTV **36** in TCE. $[\mathbf{36}] = 10^{-2}$ M. DMSO addition.

The $^1\text{H-NMR}$ experiments recorded at different conditions evidenced changes on the aggregation of the monomers, specifically on the H-bonding interactions. However, almost no changes were observed on the aromatic region of the CTV. Only at high temperatures did the experiment indicate changes on the chemical environment of the aromatic CTV protons.

The data collected through the $^1\text{H-NMR}$ experiments is not conclusive and therefore the formation of columnar aggregates cannot be confirmed by this method.

10. CTV-Based Pyramidic Monomers for Chiral Columnar Aggregates II

Chiral Amplification Studies: Circular Dichroism

A majority rules experiment was performed in order to investigate the chiral amplification behavior of the CTV-monomer **36**. The changes on the CD spectra of the enantiopure CTV-monomer **36** 2×10^{-5} M solution were recorded upon decreasing the enantiomeric excess of the solution (Figure 10.9).

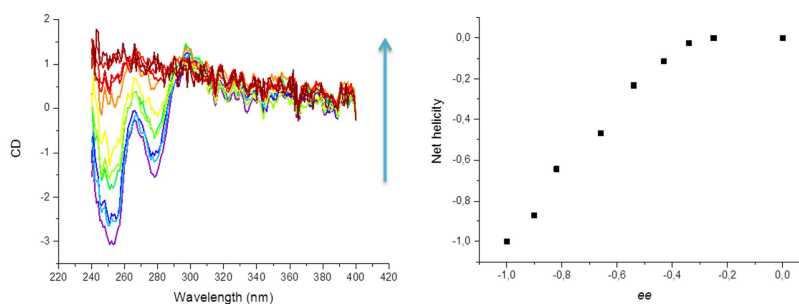


Figure 10.9 Majority rules experiment: Left: CD spectra recorded upon decreasing the ee of the CTV-monomer **36** solution; arrow indicates the changes upon going from enantiomerically pure sample to racemic mixture. Right: Net helicity plotted vs. the ee of the solution.

The majority rules principle implies control of the helicity of an enantiomeric mixture by the most abundant enantiomer. Typically, a small excess of one enantiomer leads to a strong bias toward the helicity corresponding to it. On the contrary, in the absence of any chiral amplification phenomena, a linear increase of the helicity is expected upon increasing the concentration of one enantiomer.

In this particular case, a minimum ee of 0.3 is required for the solution to express chirality and after this minimum ee is reached, a linear increase of helicity is observed.

No chiral amplification phenomena could be assumed, since the chirality increases in a linear manner. Instead, an unusual effect was observed below 0.3 ee. The complete loss of chirality could indicate columnar aggregate disruption.

Although the urea moieties were introduced to promote the chirality transfer from the CTV-monomers to the macroscopic column, the high H-bonding directionality of the

10. CTV-Based Pyramidic Monomers for Chiral Columnar Aggregates II

urea moieties and the non-planarity of the CTV central core could be responsible for this lack of chiral expression and column disaggregation at low enantiomeric excess concentrations.

Mesomorphic Behavior Studies: Thermal and Microscopic Studies

Thermogravimetry Analysis (TGA) and Differential Scanning Calorimetry (DSC)

A thermogravimetry analysis was performed in order to identify the temperature range for the differential scanning calorimetry to be performed. A small mass decrease was observed beyond 100 °C that is attributed to entrapped and solvent loss. Heating over 293 °C caused CTV-monomer **36** decomposition (Figure 10.10).

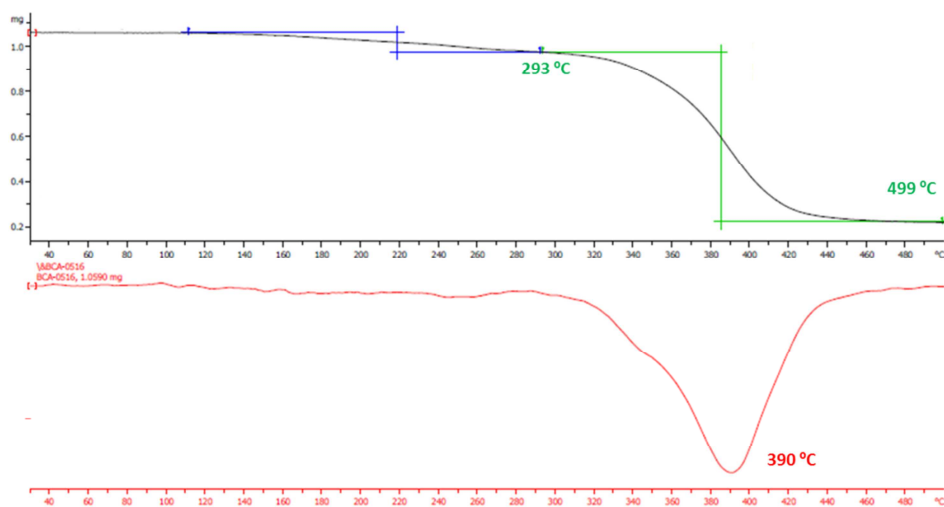


Figure 10.10 TGA thermogram of CTV-monomer **36**

Differential scanning calorimetry of CTV-monomer **36** was performed. Five heating slopes and four cooling slopes were performed. Within the first heating, the sample temperature was increased gradually (5 °C / min) just above the melting point. The sample was then cooled down to -80 °C. On the subsequent slopes, the sample was heated up to 250 °C and further cooled to -80 °C (Figure 10.11).

10. CTV-Based Pyramidic Monomers for Chiral Columnar Aggregates II

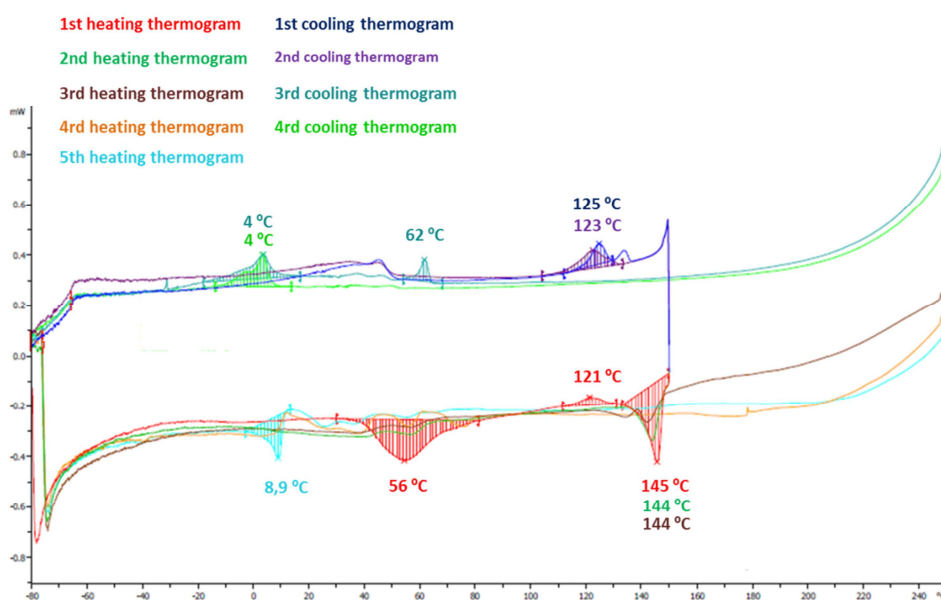


Figure 10.11 DSC thermograms of CTV-monomer **36**

During the first heating, an endothermic peak appears in the region 50-60 °C. After further heating an exothermic peak appears at 121 °C that undergoes clearing at 159 °C. The melting temperature is reproducible in all three first heating slopes. On the cooling slope three exothermic peaks are observed at 122 °C, 62 °C and 4 °C. The endothermic peak at 56 °C is not clearly observed on the 2nd and 3rd heating thermograms, but could not be discarded.

The endothermic peak observed at 56 °C in the first heating run, could be attributed to either formation of a mesophase or to evaporation of entrapped solvent. The fact that an equivalent exothermic peak is observed on the first cooling slope (62 °C) rules out the evaporation of solvent and could indicate formation of a mesophase.

Polarized Optical Microscopy (POM) Images

The mesophase formation was further investigated by means of hot-stage polarized optical microscopy. The CTV-monomer sample was observed under crossed polarized light and the changes at different temperatures monitored.

10. CTV-Based Pyramidic Monomers for Chiral Columnar Aggregates II

In Figure 10.12 the POM images at selected temperatures are shown. The sample was initially slowly heated above the melting transition, then cooled down and again heated up to the melting transition. Birefringent textures were observed during the second heating slope, compatible with the formation of mesophases. However, no typical patterns could be identified.

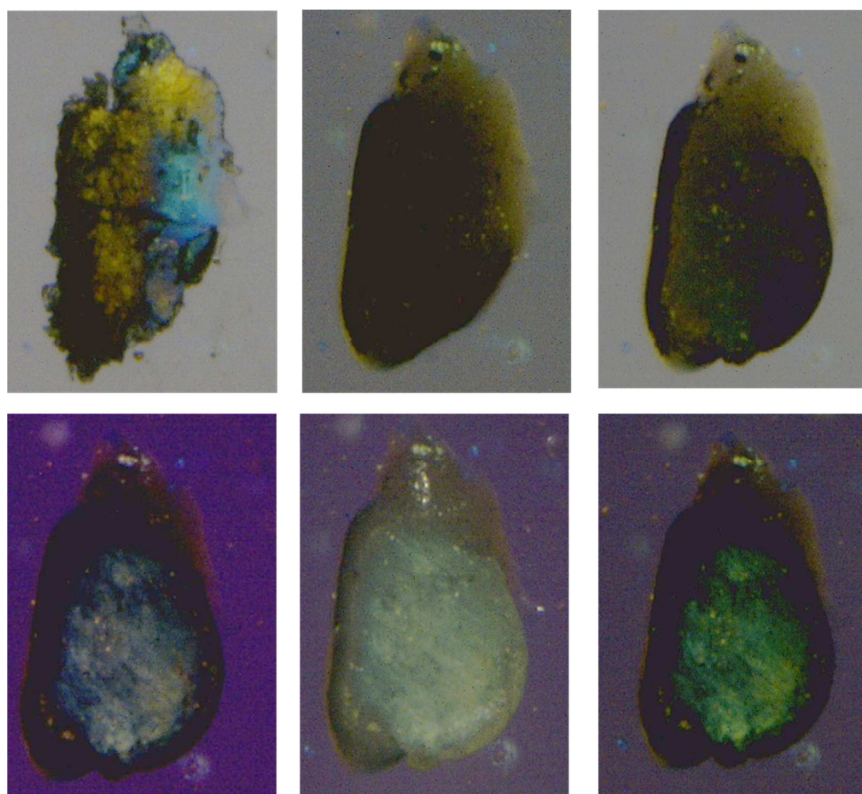


Figure 10.12 POM images at different temperatures. Top: Textures observed before and after melting transition (138 °C, 160 °C, 170 °C). Down: Textures observed after slow cooling down from melted sample (T = 67-62 °C).

10.3.2 Summary and Discussion

The CTV-monomer **36** was synthesized and characterized. The self-assembly of **36**, its mesomorphic behavior and its ability to promote chirality transfer to the macroscopic

10. CTV-Based Pyramidic Monomers for Chiral Columnar Aggregates II

level were studied by $^1\text{H-NMR}$ and CD spectroscopy as well as calorimetry and microscopic studies.

The aggregation of the CTV-monomers was monitored. The urea N-H protons suffered considerable shifting upon changing the concentration, the temperature or upon addition of a competitive solvent. However, almost no changes were observed on the aromatic region of the CTV. For these reason, the formation of a columnar aggregate cannot be confirmed.

No chiral amplification was identified at the selected concentration. Nevertheless, the majority rules experiment indicated that a minimum ee of 0.3 was required for the sample to express chirality. This could indicate disruption of the columnar aggregates below that ratio.

TGA indicated decomposition of the CTV-monomer above 390 °C. Within DSC thermograms, various transition temperatures were identified. Besides melting transition another transition was identified within first heating and cooling slopes that could be attributed to the formation of mesophases.

Images recorded under cross polarized light during hot-stage POM experiment confirmed the apparition of birefringent textures around the observed transition temperatures. Although this could indicate formation of mesophases, no typical patterns were identified. These might be the consequence of the low stability of the mesophases. The low substitution pattern and the presence of the urea moieties able to engage into strong H-bonding interactions could stabilize the columnar aggregate inhibiting the mesomorphic behavior, as reported by Marcelis *et al.* for triphenylene derivatives.¹³⁰

¹³⁰ Paraschiv, I.; Tomkinson, A.; Giesbers, M.; Sudhölter, E. J. R.; Zuilhof, H.; Marcelis, A. *T. M. Liq. Cryst.* **2007**, *34*, 1029.

10. CTV-Based Pyramidic Monomers for Chiral Columnar Aggregates II

10.4 Conclusions

The CTV-monomer **36** was synthesized and characterized.

The aggregation of the CTV-monomers was monitored by means of $^1\text{H-NMR}$ experiments. The formation of a columnar aggregate could not be confirmed.

Majority rules chiral amplification studies were performed in DCM, but no such behavior was observed. Moreover, it was observed that a minimum ee of 0.3 was required for the sample to express chirality. This could indicate formation of columnar aggregates above that ratio.

The mesomorphic behavior was also investigated by DSC and POM. A phase transition around 60 °C was identified within the first heating and cooling thermograms. The POM images recorded at that temperature could indicate liquid crystalline behavior.

Chapter 11: Experimental Part II

UNIVERSITAT ROVIRA I VIRGILI

CYCLOTRIVERATRYLENE AND PORPHYRIN SCAFFOLDS FOR MOLECULAR RECOGNITION AND SELF-ASSEMBLY

Berta Camafort Blanco

Dipòsit Legal: T 677-2015

11.1 General Information and Instrumentation

All commercial reagents and solvents, unless otherwise noted, were purchased at reagent grade from Acros, ABCR, Aldrich, and Fluka and used as received. All reactions were performed under an inert atmosphere by applying a positive pressure of Argon using dry solvents. Anhydrous solvents were obtained from solvent purification system SPS-400-6 from Inovative Technologies. For all aqueous solutions deionised water was used.

Solvents for flash chromatography (FC), preparative TLC, plug filtrations and extractions were of technical quality except for CHCl_3 , which was distilled under *vacuum* before use. Evaporation and concentration in *vacuo* was performed at water aspirator pressure; drying in *vacuo* at 10^{-2} Torr.

Thin-layer chromatography (TLC) was conducted on silica gel pre-coated TLC-plates SIL G-25 UV254 (Macherey-Nagel) glass supported and visualized by UV light (254 or 366 nm) and/or KMnO_4 stain. Column chromatography and plug filtrations were carried out with silica gel SDS (Silica Gel 60 A; particle size 0.040–0.063 mm). Flash chromatography (FC) was carried out at an overpressure of 0.1 - 0.6 bar. For automated flash column chromatography a CombiFlash Companion apparatus running RediSep® columns was used. HPLC chromatograms were recorded on an Agilent Technologies 1100 (UV-detector).

Melting points (M.p.) were measured either on a Büchi B-540 melting-point apparatus in open capillaries or in a Mettler Toledo DSC822 differential scanning calorimeter. "Decomp" refers to decomposition.

$^1\text{H-NMR}$ and $^{13}\text{C-NMR}$ spectra were measured at 293 K, unless specified so, on Bruker Avance 300 (300 MHz for $^1\text{H-NMR}$ and 75 MHz for $^{13}\text{C-NMR}$), Bruker Avance 400 (400 MHz for $^1\text{H-NMR}$ and 100MHz for $^{13}\text{C-NMR}$) and Bruker Avance 500

11. Experimental Part II

(500 MHz for ^1H -NMR and 125.75 MHz for ^{13}C -NMR) NMR spectrometers. Deuterated solvents used are indicated in each case. Chemical shifts (δ) are reported in ppm relative to the signal of tetramethylsilane. Residual solvent signals in the ^1H and ^{13}C NMR spectra were used as an internal reference. Coupling constants (J) are given in Hz. The apparent resonance multiplicity is described as s (singlet), bs (broad singlet), d (doublet), dd (doublet of doublet), dt (doublet of triplet), t (triplet), q (quartet) and m (multiplet). The number of signal inducing protons and their positioning are given. Complete signal assignments from 1D and 2D NMR spectroscopy were based on COSY, HSQC, HMBC correlations and phase sensitive DEPTQ45 and DEPTq135 spectra.

High-resolution mass analysis was performed in Bruker MALDI-TOF or Waters LCT Waters LCT (HPLC/MS-TOF; ESI or APCI mode) spectrometers

Infrared spectra (IR) were recorded on FTIR Bruker spectrometer model Alpha with an ATR accessory. Spectral range from 4000 to 400 cm^{-1} . Bands locations are given in cm^{-1} .

UV-Vis spectra were recorded on a double beam UV-Vis Shimadzu spectrophotometer (UV-1800 model) CH_2Cl_2 in a quartz cuvette with an edge length of 1 cm_b .

Circular dichroism spectra were measured with a Chirascan circular dichroism spectrometer from Applied Photophysics, with simultaneous measurement of UV-Vis and CD spectra. The spectra were measured in CH_2Cl_2 in a quartz cuvette.

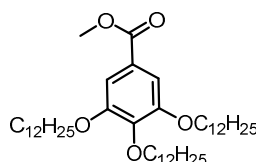
DSC thermograms were recorded on a Mettler Toledo DSC822 differential scanning calorimeter.

TGA analysis was performed on a Mettler Toledo TGA/SDTA851 thermogravimeter provided with an MT1 type balance.

11.2 Synthetic procedures

11.2.1 CTV-based Pyramidic Monomers for Chiral Columnar Aggregates

Methyl 3,4,5-tris(dodecyloxy)benzoate **43**¹³¹



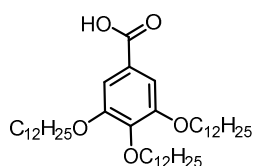
To a solution of commercially available methyl gallate (0.5 g, 2.72 mmol) in DMF (50 ml), K_2CO_3 (1.5 g, 10.86 mmol), NaI (1.63 g, 10.86 mmol) and dodecylbromide (2.63 mL, 10.86 mmol) were added. The reaction mixture was heated at 80 °C for 18 h. The reaction mixture was poured into water, extracted with ethyl acetate and the combined organic phases were washed with brine and dried over $MgSO_4$. The solvent was removed under reduced pressure. MeOH was added and the suspension was sonicated and filtered to give the tris(dodecyloxy) methyl ester **43** (1.321 mg, 71 %) as a white solid.

¹H-NMR (400 MHz, $CDCl_3$): δ = 0.85-90 (m, 9H; CH_2CH_3), 1.19-1.40 (m, 48 H; $CH_2(CH_2)_8CH_3$), 1.42-1.51 (m, 6 H; $CH_2(CH_2)_8CH_3$), 1.70-1.84 (m, 6 H; OCH_2CH_2), 3.88 (s, 3 H, OCH_3), 3.98-4.03 (m, 6 H; OCH_2), 7.24 (bs, 2 H, ArH).

¹³¹ Barbera, J.; Puig, L.; Romero, P.; Serrano, J. L.; Sierra, T. *J. Am. Chem. Soc.* **2006**, *128*, 4487.

11. Experimental Part II

3,4,5-tris(dodecyloxy)benzoic acid **44**¹³¹

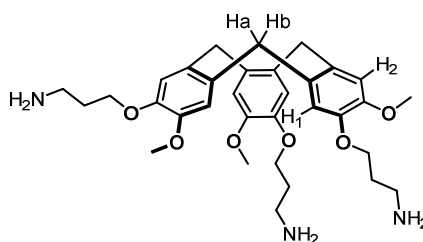


Methyl 3,4,5-tris(dodecyloxy)benzoate **43** (1.017 g, 1.476 mmol) was refluxed in 6 M NaOH H₂O / THF (1:1; 80 ml) solution for 18 h. The reaction mixture was then cooled down and conc. HCl was added until acid pH was attained. The mixture was extracted into CH₂Cl₂ and the combined extracts were washed with water, brine and dried over MgSO₄. The solvent was removed under reduced pressure and the reaction crude was sonicated in MeOH to afford the benzoic acid **44** (0.877, 88 %) as a white product.

¹H-NMR (400 MHz, CDCl₃): δ = 0.86-0.90 (m, 9H; CH₃), 1.22-1.40 (m, 48 H; (CH₂)₈CH₃), 1.44-1.51 (m, 6 H; CH₂(CH₂)₈CH₃), 1.72-1.85 (m, 6 H; OCH₂CH₂), 4.01-4.06 (m, 6 H; OCH₂), 7.32 (s, 2 H, ArH).

11. Experimental Part II

Synthesis of 3,3',3''-((3,8,13-trimethoxy-10,15-dihydro-5H-tribenzo[a,d,g][9]annulene-2,7,12-triyl)tris(oxy))tris(propan-1-amine) **39**^{132, 132}



A suspension of CTV-triphenol **10** (1.715 g, 4.2 mmol), commercially available tert-butyl(3-bromopropyl)carbamate (3.7 g, 15.54 mmol) and cesium carbonate (8.2 g, 25.2 mmol) in CH₃CN (100 mL) was stirred at 55 °C for 18 h. The solvent was removed under reduced pressure, the crude product was taken up in CHCl₃ and the suspension was filtered through celite and the solvent removed under *vacuo*. The product was directly used on the next step without further purification. The crude (3.7 g, 4.2 mmol) was redissolved in TFA / CH₂Cl₂ (1:1, 150 mL) and the reaction mixture was stirred at r.t. for 3 h. The reaction mixture was quenched by the addition of Et₂O. The white precipitate was filtrated and redissolved with NaOH 10 % solution and CH₂Cl₂. The organic extracts were washed with brine and dried over the minimum amount of Na₂SO₄. The solvent was removed under reduced pressure to afford the CTV triamino **39** (1.932, 79 %) as a white solid.

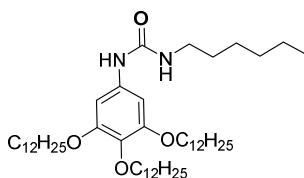
¹H-NMR (400MHz, CDCl₃): δ = 1.42 (s, 6 H, NH₂), 1.88-1.94 (m, 6 H; OCH₂CH₂CH₂N), 2.86 (t, 6 H; ³J(H,H) = 6.64 Hz, CH₂NH₂), 3.52 (d, 3 H; ³J(H,H) = 13.86 Hz, H_aH_b), 3.80

¹³² Dam, H. H.; Reinhoudt, D. N.; Verboom, W. *New J. Chem.* **2007**, *31*, 1620.

11. Experimental Part II

(s, 9 H; OCH_3), 3.99-4.13 (m, 6 H; OCH_2CH_2), 4.74 (d, 3 H; $^2J(\text{H},\text{H}) = 13.86$ Hz, H_aH_b), 6.82 (s, 3 H; H_2), 6.86 (s, 3 H; H_1).

Synthesis of 1-hexyl-3-(3,4,5-tridodecylphenyl)urea **46**¹²⁴

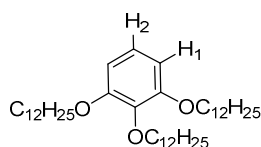


A mixture of 3,4,5-tris(dodecyloxy)benzoic acid **44** (40 mg, 0.121 mmol), Et_3N (20 μL , 0.146 mmol) and DPPA (31 μL , 0.146 mmol) in toluene (5 mL) was stirred at 40 °C for 1 h to promote the formation of the benzyl azide. The reaction was then stirred at 80 °C for 4 h to promote the Curtius rearrangement and the formation of the isocyanate. The reaction mixture was then cooled down and hexylamine (18 μL , 0.134 mmol) was added. The reaction was then heated for 18 h at 80 °C. The solvent was removed under reduced pressure and the reaction crude was sonicated in MeOH to afford the urea **46** (67 mg, 71 %) as a white product.

¹H-NMR (400MHz, CDCl_3): $\delta = 0.86$ - 0.91 (m, 12 H; CH_3), 1.24-1.35 (m, 54 H; $(\text{CH}_2)_8\text{CH}_3$ and $\text{NCH}_2\text{CH}_2(\text{CH}_2)_3\text{CH}_3$), 1.43-1.50 (m, 6 H; $\text{OCH}_2\text{CH}_2\text{CH}_2(\text{CH}_2)_8\text{CH}_3$), 1.56-1.63 (m, 2 H; $\text{NCH}_2\text{CH}_2(\text{CH}_2)_3\text{CH}_3$), 1.70-1.83 (m, 6 H; OCH_2CH_2), 3.39-3.44 (m, 2 H; NCH_2), 3.96-4.02 (m, 6 H; OCH_2), 6.93 (s, 2 H; ArH).

11. Experimental Part II

Synthesis of 1,2,3-tris(dodecyloxy)benzene **47**¹²⁹

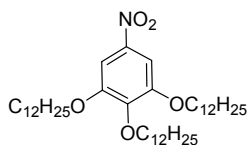


A suspension of pyragallol (2 g, 15.86 mmol), 1-bromododecane (13 mL, 52.3 mmol) and K₂CO₃ (14.47 g, 105 mmol) in DMF (80 mL) was heated at 80 °C for 18 h. The reaction mixture was poured on to ice-water. The solution was filtered off and the precipitate was sonicated in MeOH to afford the 1,2,3-tris(dodecyloxy)benzene **47** (9.729, 97 %) as a white product.

¹H-NMR (400 MHz, CDCl₃): δ = 0.88 (t, 9 H; ³J(H,H) = 6.88 Hz, CH₃), 1.26 (m, 48 H; (CH₂)₈CH₃), 1.41-1.50 (m, 6H; CH₂(CH₂)₈CH₃), 1.70-1.82 (m, 6 H; OCH₂CH₂), 3.96 (t, 6 H; ³J(H,H) = 6.57 Hz, OCH₂CH₂), 6.54 (d, 2 H; ³J(H,H) = 8.32 Hz, H₁), 6.90 (t, 1 H; ³J(H,H) = 8.31 Hz, H₂).

11. Experimental Part II

Synthesis of 1,2,3-tris(dodecyloxy)-5-nitrobenzene **48**¹³³



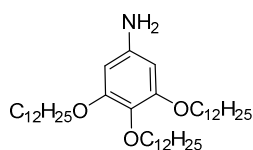
To a solution of 1,2,3-tris(dodecyloxy)benzene **47** (300 mg, 0.475 mmol) and NaNO₂ (17 mg, 0.238 mmol) in CH₂Cl₂ / water (5 mL, 10:0.5) conc. HNO₃ (91 μL, 1.426 mmol) was dropwise added and the reaction mixture was stirred for 3 h. The organic layer was washed with water, brine and dried over MgSO₄. The solvent was removed under reduced pressure and the crude was sonicated in MeOH to afford the substituted nitrobenzene **48** (235 mg, 73 %) as a white solid.

¹H-NMR (400 MHz, CDCl₃): δ = 0.88 (t, 9 H; ³J(H,H) = 6.81 Hz, CH₂CH₃), 1.27 (m, 48 H; CH₂(CH₂)₈CH₃), 1.44-1.53 (m, 6 H; CH₂(CH₂)₈CH₃), 1.70-1.87 (m, 6 H; OCH₂CH₂), 4.01-4.07 (m, 6 H; OCH₂CH₂), 7.47 (s, 2 H; ArH).

¹³³ Lincker, F.; Bourgun, P.; Masson, P.; Didier, P.; Guidoni, L.; Bigot, J.-Y. Nicoud, J.-F. Donnio, B.; Guillon, D. *Org. Lett.* **2005**, *7*, 1505.

11. Experimental Part II

Synthesis of 3,4,5-tris(dodecyloxy)aniline **40**¹³⁴



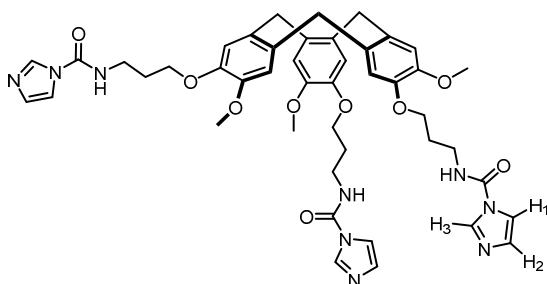
A solution of tridodecyloxy-nitrobenzene **48** (4.408 g, 6.52 mmol) THF (100 mL) was stirred for 18 h in the presence of Pd/C (441 mg, 10 %, 4.14 mmol) under H₂ atmosphere. The reaction mixture was then filtered over celite, and the solvent was removed under vacuum to afford brownish oil which was then sonicated in MeOH to afford the aniline **40** (3.413 g, 81 %) as a white solid.

¹H-NMR (400 MHz, CDCl₃): δ = 0.87 (t, 9 H; ³J(H,H) = 6.81 Hz, CH₂CH₃), 1.25 (m, 48 H; CH₂(CH₂)₈CH₃), 1.44-1.46 (m, 6H; CH₂(CH₂)₈CH₃), 1.67-1.80 (m, 6 H; OCH₂CH₂), 3.45 (s, 2 H; NH₂), 3.83 (t, 2 H; ³J(H,H) = 6.58 Hz, *para*-OCH₂CH₂), 3.90 (t, 4 H; ³J(H,H) = 6.58 Hz, *meta*-OCH₂CH₂), 5.90 (s, 2 H; ArH).

¹³⁴ Yelamaggad, C. V.; Achalkumar, A. S.; Rao, D. S. S.; Prasad, S. K. *J. Org. Chem.* **2007**, *72*, 8308.

11. Experimental Part II

Synthesis of N,N',N''-(((3,8,13-trimethoxy-10,15-dihydro-5H-tribenzo[a,d,g][9]annulene-2,7,12-triyl)tris(oxy))tris(propane-3,1-diyl))tris(1H-imidazole-1-carboxamide) **41**¹²⁶

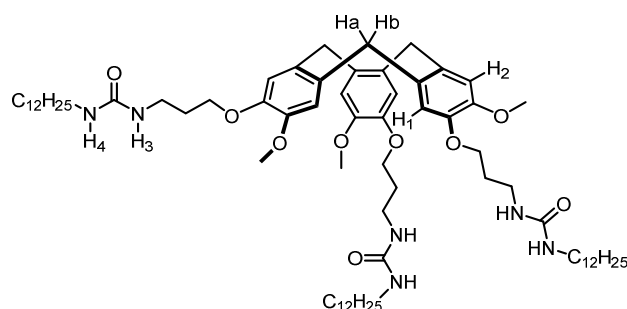


CTV-triamine (330 mg, 0.569 mmol) and CDI (554 mg, 3.42 mmol) were suspended in THF and the reaction mixture was stirred at r.t. for 36 h. The solvent was removed under reduced pressure, the crude was taken up in CH_2Cl_2 and the organic phase was washed with water, brine and dried with MgSO_4 . The solvent was removed under *vacuo* to afford the CTV-CI **41** (491 mg, 100 %) as a yellow solid that was kept under Argon at 5 °C until its use.

¹H-NMR (400 MHz, CDCl_3): δ = 2.12-2.15 (m, 6 H; $\text{CH}_2\text{CH}_2\text{CH}_2$), 3.57 (d, 3 H; ³ $J(\text{H,H})$ = 13.86 Hz, H_aH_b), 3.62-3.68 (m, 6 H; $\text{CH}_2\text{CH}_2\text{NH}$), 3.74 (s, 9 H; OCH_3), 4.05-4.25 (m, 6 H; OCH_2CH_2), 4.77 (d, 3 H; ³ $J(\text{H,H})$ = 13.80 Hz, H_aH_b), 6.82 (s, 3 H; H_2), 6.85 (s, 3 H; H_1), 6.95, bs, 3 H; imidazole- H_2), 7.35 (bs, 3 H; imidazole- H_1), 7.38 (bt, 3 H; ³ $J(\text{H,H})$ = 4.82 Hz, NH), 8.10 (bs, 3 H; imidazole- H_3).

11. Experimental Part II

Synthesis of 1,1',1''-(((3,8,13-trimethoxy-10,15-dihydro-5H-tribenzo[a,d,g][9]annulene-2,7,12-triyl)tris(oxy))tris(propane-3,1-diyl))tris(3-dodecylurea) 51¹²⁶



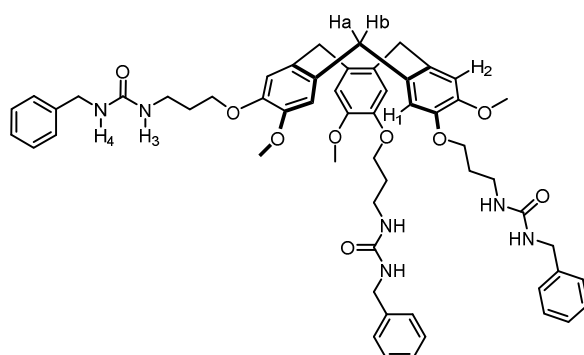
A solution of the CTV-Cl **41** (0.01 g, 0.012 mmol) and the dodecylamine (7.1 mg, 0.038 mmol) and Et₃N (5.3 μ L, 0.038 mmol) in CH₂Cl₂ (5 mL) were stirred at r.t. for 24 h. The solution was treated with 10 % aq. HCl and extracted with CHCl₃. The organic phase was washed with brine, and dried over MgSO₄. The solvent was removed under reduced pressure and the reaction crude was purified with column chromatography (SiO₂; Hex / EtOAc 80:20) to afford the desired urea **51** (0.032 g, 67 %) as a yellow solid.

¹H-NMR (400 MHz, CDCl₃): δ = 0.89 (t, 9 H; CH₂CH₃), 1.24 (bs, 48 H; (CH₂)₈CH₃), 1.36-1.46 (m, 6 H; CH₂(CH₂)₈CH₃), 1.57-1.81 (m, 6 H; NCH₂CH₂), 1.90-1.98 (m, 6 H; OCH₂CH₂CH₂N), 3.05-3.12 (m, 6 H; NCH₂), 3.33-3.35 (m, 6 H; OCH₂CH₂CH₂N), 3.50 (d, 3 H; ³J(H,H) = 13.94 Hz, H_aH_b), 3.81 (s, 9 H; OCH₃), 3.98-3.14 (m, 6 H; OCH₂CH₂CH₂N), 4.48 (t, 3 H; ³J(H,H) = 5.52 Hz, N-H₄), 4.73 (d, 3 H; ³J(H,H) = 13.68 Hz, H_aH_b), 5.16 (t, 3 H; ³J(H,H) = 5.49 Hz, N-H₃), 6.81 (s, 3 H; H₂), 6.83 (s, 3 H; H₁),

11. Experimental Part II

Synthesis of 1,1',1''-(((3,8,13-trimethoxy-10,15-dihydro-5H-tribenzo[a,d,g][9]annulene-2,7,12-triyl)tris(oxy))tris(propane-3,1-diyl))tris(3-benzylurea) **52**^{Error!}

Marcador no definido.

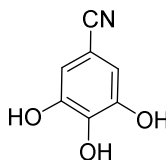


A mixture of the CTV-Cl **41** (0.012 g, 0.014 mmol) and benzylamine (5.02 μ L, 0.046 mmol) and Et₃N (6.4 μ L, 0.046 mmol) in dry CH₂Cl₂ was stirred at rt for 24h. The solution was treated with 10% aq. HCl and extracted with CHCl₃ (x 3). The organic phase was washed with brine, dried (MgSO₄) and concentrated to afford the desired urea **52** (0.014 g, 100 %) as a white solid.

¹H-NMR (400 MHz, CDCl₃): δ = 185-196 (m, 6 H; OCH₂CH₂CH₂N), 3.28-3.33 (m, 6 H; OCH₂CH₂CH₂N), 3.47 (d, 3 H; ²*J*(H,H) = 13.79 Hz, H_aH_b), 3.67 (s, 9 H; OCH₃), 3.91-3.96 (m, 6 H; OCH₂CH₂CH₂N), 4.14-4.29 (m, 6 H; NCH₂Ph), 4.68 (d, 3 H; ²*J*(H,H) = 13.79 Hz, H_aH_b), 4.90 (t, 3 H; ³*J*(H,H) = 5.72 Hz, N-H₄), 5.29 (t, 3 H; ³*J*(H,H) = 5.12 Hz, N-H₃), 6.75 (s, 3 H; H₂), 6.78 (s, 3 H; H₁), 7.13-7.23 (m, 15 H; BnH).

11.2.2 CTV-Based Pyramidic Monomers for Chiral Columnar Aggregates II

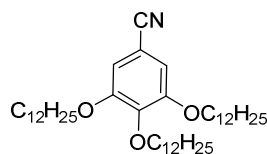
Synthesis of 3,4,5-trihydroxybenzonitrile **55**¹²⁹



A suspension of the commercially available 3,4,5-Trimethoxybenzonitrile (0.2 g, 1.035 mmol) in 48% aqueous HBr (10 mL) was refluxed overnight. Then the reaction was cooled down to r.t. and poured onto ice-water. The precipitate was filtered off, washed with water dissolved in EtOAc and dried over MgSO₄ to give the triphenol **55** (0.134 g, 86 %).

¹H-NMR (400 MHz, CDCl₃): δ = 7.26 (s, 2 H; ArH).

Synthesis of tert-butyl 3-((2-(benzyloxy)acetamido)methyl)benzylcarbamate **57**¹³⁵



K₂CO₃ (386 mg, 2.79 mmol) and 1-bromododecane (0.62 mL, 2.57) were added to a solution of 3,4,5-trihydroxybenzonitrile **55** (111 mg 0.735 mmol) in DMF (5 mL) and the reaction mixture was then stirred at 80 °C for 18 h. After cooling down to r.t., the crude

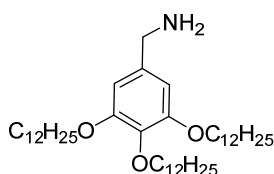
¹³⁵ An, Z.; Yu, J.; Domercq, B.; Jones, S. C.; Barlow, S.; Kippelen B.; Marder, S. R. *J. Mater. Chem.* **2009**, *19*, 6688.

11. Experimental Part II

was taken up in CH_2Cl_2 and the organic extracts were washed with water, brine and dried over MgSO_4 . The solvent was removed under reduced pressure to give 3,4,5-tris(dodecyloxy)benzonitrile **57** (205 mg, 43%) as a white solid.

$^1\text{H-NMR}$ (400MHz, CDCl_3): δ = 0.88 (t, 9H; $^3J(\text{H,H})$ = 6.98 Hz, CH_3), 1.23-1.39 (m, 48 H; $(\text{CH}_2)_8\text{CH}_3$), 1.43-1.51 (m, 6 H; $\text{OCH}_2\text{CH}_2\text{CH}_2$, $\text{CH}_2(\text{CH}_2)_8\text{CH}_3$), 1.70-1.84 (m, 6 H; OCH_2CH_2), 4.01 (t, 6 H; $^3J(\text{H,H})$ = 6.55 Hz, OCH_2), 7.25 (s, 2 H, *ArH*).

Synthesis of (3,4,5-tris(dodecyloxy)phenyl)methanamine **54**¹³⁵

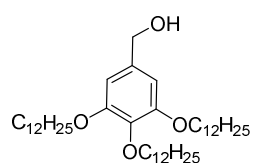


A suspension of LiAlH_4 (13 mg, 0.351 mmol) in dry THF (4 mL) was added to a solution of 3,4,5-tri(n-dodecyloxy)benzonitrile **57** (100 mg, 0.152 mmol) in THF (6 mL) at 0 °C. The reaction mixture was allowed to warm up to r.t. and was further refluxed for 2 h. The reaction mixture was then cooled down to 0 °C. The reaction mixture was quenched by dropwise addition of ice-cold water and 20 % aq. NaOH solution. The mixture was extracted into EtOAc and the organic extracts were washed with water, brine and dried over MgSO_4 . The solvent was removed under reduced pressure and the yellowish product was sonicated in MeOH and filtered off to afford the tris(dodecyloxy) substituted benzylamine **54** (98 mg, 97 %) as a white product.

$^1\text{H-NMR}$ (400MHz, CDCl_3): δ = 0.88 (t, 9H; $^3J(\text{H,H})$ = 6.95 Hz, CH_3), 1.22-1.38 (m, 48 H; $(\text{CH}_2)_8\text{CH}_3$), 1.42-1.50 (m, 6 H; $\text{OCH}_2\text{CH}_2\text{CH}_2$), 1.70-1.83 (m, 6 H; $\text{OCH}_2\text{CH}_2\text{CH}_2$), 3.63 (t, 2 H; $^3J(\text{H,H})$ = 6.70 Hz, $\text{H}_2\text{NCH}_2\text{Ar}$), 3.93 (t, 2 H; $^3J(\text{H,H})$ = 6.60 Hz, OCH_2CH_2), 3.97 (t, 4 H; $^3J(\text{H,H})$ = 6.51 Hz, OCH_2CH_2), 4.59 (s, 2 H; NH_2), 6.44 (s, 2 H, *ArH*).

11. Experimental Part II

Synthesis of (3,4,5-tris(dodecyloxy)phenyl)methanol **58**¹³⁶



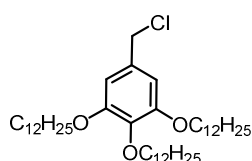
A suspension of LiAlH_4 in THF (1 M, 4.91 mL, 1.91 mmol) was added to a solution of 3,4,5-tris(dodecyloxy)benzoic acid **44** (1.44 g, 2.133 mmol) in THF (30 ml) at 0 °C. The resulting mixture was allowed to warm up to r.t. and was further stirred for 18 h. The mixture was cooled down and the excess of LiAlH_4 was quenched by water addition. The mixture was extracted with CH_2Cl_2 . The combined organic layers were washed with water, brine and dried over MgSO_4 . The solvent was removed under reduced pressures and the reaction crude was sonicated in MeOH to afford the tris(dodecyloxy) substituted benzyl alcohol **58** (1.387 g, 98 %) as a white solid.

¹H-NMR (400MHz, CDCl_3): δ = 0.86-0.90 (m, 9H; CH_3), 1.22-1.39 (m, 48 H; $(\text{CH}_2)_8\text{CH}_3$), 1.41-1.51 (m, 6 H; $\text{OCH}_2\text{CH}_2\text{CH}_2$), 1.70-1.83 (m, 6 H; OCH_2CH_2), 3.92-3.99 (m, 6 H; OCH_2), 4.59 (d, 2 H; $^3J(\text{H,H}) = 5.99$ Hz, $\text{H}_2\text{NCH}_2\text{Ar}$), 6.56 (s, 2 H, ArH).

¹³⁶ Fischer, G. M.; Daltrozzo, E.; Zumbusch, A. *Angew. Chem. Int. Ed.* **2011**, *50*, 1406.

11. Experimental Part II

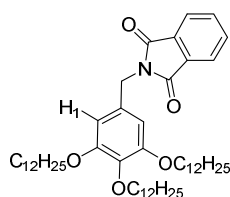
Synthesis of 5-(chloromethyl)-1,2,3-tris(dodecyloxy)benzene **59**¹³⁷



A solution of thionyl chloride **58** (0.803 mL, 10.89 mmol) was added dropwise to a solution of the benzyl alcohol (900 mg, 1.361 mmol) in CH_2Cl_2 (30 mL) and the reaction mixture was stirred for 18 h. The solvent was removed under reduced pressure and the reaction crude was sonicated in MeOH to afford the 5-(chloromethyl)-1,2,3-tris(dodecyloxy)benzene **59** (898 mg, 97 %) as a yellowish solid.

¹H-NMR (400MHz, CDCl_3): δ = 0.87-90 (m, 9 H; CH_3), 1.22-1.35 (m, 48 H; $(\text{CH}_2)_8\text{CH}_3$), 1.43-1.50 (m, 6 H; $\text{OCH}_2\text{CH}_2\text{CH}_2$), 1.70-1.83 (m, 6 H; $\text{OCH}_2\text{CH}_2\text{CH}_2$), 3.92-3.99 (m, 6 H; OCH_2CH_2), 4.51 (s, 2 H; $\text{H}_2\text{NCH}_2\text{Ar}$), 6.57 (s, 2 H, ArH).

Synthesis of 2-(3,4,5-tris(dodecyloxy)benzyl)isoindoline-1,3-dione **61**¹³⁸



A solution of 5-(chloromethyl)-1,2,3-tris(dodecyloxy)benzene **59** (1.233 g, 1.814 mmol) and phthalimide potassium salt (420 mg, 2.268 mmol) in DMF (100 ml) was heated at 90 °C overnight. The reaction mixture was cooled down to r.t and the solvent was

¹³⁷ Middel, O.; Verboom, W.; Reinhoudt, D. N. *Eur. J. Org. Chem.* **2002**, 2587.

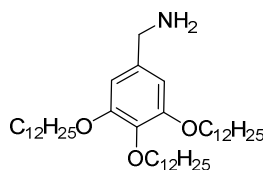
¹³⁸ Zhu, K.; Zhang, M.; Wang, F.; Li, N.; Li, S.; Huang, F. *New J. Chem.* **2008**, 32, 1827.

11. Experimental Part II

evaporated under reduced pressure. The residue was redissolved in CH_2Cl_2 and was washed with water, brine and dried over MgSO_4 . The solvent was removed under reduced pressure to afford the 2-(3,4,5-tris(dodecyloxy)benzyl)isoindoline-1,3-dione **61** (1.420, 99 %) that was used on the next step without further purification.

$^1\text{H-NMR}$ (400MHz, CDCl_3): δ = 0.86-89 (m, 9H; CH_3), 1.22-1.34 (m, 48 H; $(\text{CH}_2)_8\text{CH}_3$), 1.39-1.49 (m, 6 H; $\text{OCH}_2\text{CH}_2\text{CH}_2$), 1.67-1.80 (m, 6 H; $\text{OCH}_2\text{CH}_2\text{CH}_2$), 3.89 (t, 2 H; $^3J(\text{H,H}) = 6.66$ Hz, *para*- OCH_2), 3.95 (t, 4 H; $^3J(\text{H,H}) = 6.47$ Hz, *meta*- OCH_2), 4.72 (s, 2 H; $\text{H}_2\text{NCH}_2\text{Ar}$), 6.66 (s, 2 H, H_1), 7.69-7.71 (m, 2 H; *ArH*), 7.83-7.85 (m, 2 H; *ArH*).

Synthesis of (3,4,5-tris(dodecyloxy)phenyl)methanamine **54**¹³⁸



A solution of 2-(3,4,5-tris(dodecyloxy)benzyl)isoindoline-1,3-dione **60** (1.96 g, 2.48 mmol), hydrazine monohydrate (1.044 mL, 21.08 mmol) in methanol (150 mL) was refluxed for 18 h. The reaction was cooled down and the solvent was removed under reduced pressure. The reaction crude was taken up in CH_2Cl_2 and the organic extracts were washed with water, brine and dried over MgSO_4 . The solvent was removed under reduced pressure to afford the benzylic amine (817 mg, 50 %) as a white solid.

$^1\text{H-NMR}$ (400MHz, CDCl_3): δ = 0.88 (t, 9 H; $^3J(\text{H,H}) = 6.90$ Hz, CH_3), 1.22-1.38 (m, 48 H; $(\text{CH}_2)_8\text{CH}_3$), 1.41-1.51 (m, 6 H; $\text{OCH}_2\text{CH}_2\text{CH}_2$), 1.70-1.82 (m, 6 H; OCH_2CH_2), 3.63 (bs, 2 H; $\text{H}_2\text{NCH}_2\text{Ar}$), 3.92 (t, 2 H; $^3J(\text{H,H}) = 6.67$ Hz, *para*- OCH_2CH_2), 3.97 (t, 4 H; $^3J(\text{H,H}) = 6.54$ Hz, *meta*- OCH_2CH_2), 6.50 (s, 2 H, *ArH*).

11. Experimental Part II

(CH₂(CH₂)₉CH₃), 29.66 ((CH₂)₈CH₃), 29.69 ((CH₂)₈CH₃), 29.70 ((CH₂)₈CH₃), 29.72 ((CH₂)₈CH₃), 29.74 ((CH₂)₈CH₃), 29.77 ((CH₂)₈CH₃), 29.78 ((CH₂)₈CH₃), 31.94 ((CH₂)₈CH₃), 31.95 ((CH₂)₈CH₃), 36.40 (C-H_aH_b), 38.91 (OCH₂CH₂CH₂N), 44.75 (OCH₂CH₂CH₂N), 56.07 (OCH₃), 68.64 (C-H₅H₆), 69.09 (OCH₂(CH₂)₁₀CH₃), 73.49 (OCH₂(CH₂)₁₀CH₃), 100.00 (C), 105.88 (C-H₅), 113.56 (C-H₁), 115.00 (C-H₂), 132.04 (C), 132.39 (C), 134.77 (C), 137.01 (C), 146.68 (C), 147.96 (C), 158.30 (C).

IR (ATR): $\tilde{\nu}$ = 3325, 2918, 2850, 2108, 1623, 1576, 1509, 1467, 1437, 1384, 1331, 1260, 1225, 1194, 1119, 1092, 1015, 869, 853, 806, 743, 721, 648, 624, 550, 510, 453, 414 cm⁻¹.

HR-FT-MALDI-MS *m/z*: calculated for C₁₆₅H₂₈₆N₆O₁₈Na⁺: 2664.1574; found: 2659.1859 ([MNa]⁺).

M.p. 140-146 °C

11. Experimental Part II

General Conclusions

Regarding the first part of the thesis, a series of trimeric porphyrin-based receptors have been prepared and the interaction with a series of fullerenes studied.

The acyclic tweezer-like receptor **1** that combines two different fullerene recognition motifs as well as the cyclic porphyrin trimer **2**, its flexible analogue **3**, the sterically unhindered receptor **5** and the extensive porphyrin trimer **7** were successfully synthesized and characterized.

The formation of inclusion complexes with C_{60} , C_{70} , C_{84} and Sc_3NC_{80} was monitored by means of UV-Vis absorption and fluorescence emission spectroscopic techniques, 1H -NMR spectroscopy and mass spectrometry. Preliminary complexation experiments were as well carried out with the CTV-porphyrin **1** and the cyclic trimer **7** and the *bucky onion* sample. The interaction between trimer **5** with SWCNT was preliminary studied.

Receptor **1** was able to target a wide range of fullerene sizes. It successfully formed host-guest interactions with C_{60} , C_{70} , C_{84} and Sc_3NC_{80} . A clear trend is observed throughout the fullerenes. CTV-porphyrin receptor **1** shows greater affinity to bigger sized fullerene. The association constants for the encapsulation of C_{70} , C_{84} and Sc_3NC_{80} were quantified in toluene from both the UV-Vis absorption and the fluorescence emission titration experiments. Preliminary complexation studies with the *bucky onion* sample indicated interaction with the CNOs.

Receptor **2** failed to form complexes with most of the guests. Interaction was observed only with C_{70} . No interaction was observed with C_{60} , C_{78} and C_{84} . The flexible receptor **3** was able to successfully encapsulate C_{70} , C_{84} and $ScN_3@C_{80}$ at a receptor concentration of 10^{-6} M. No interaction was observed with the major fullerene (C_{60}) at that concentration.

General Conclusions

Interaction between receptor **5** was observed for C_{70} , C_{84} and $ScN_3@C_{80}$ at a receptor concentration of 10^{-6} M in toluene. No interaction was observed with the major fullerene (C_{60}) at that concentration. Trimer **5** showed the strongest interaction towards the endohedral fullerene $Sc_3N@C_{80}$. Preliminary complexation studies were performed with both the *bucky onion* sample and the SWCNT. The association with these guests was monitored by UV-Vis absorption spectroscopy.

Preliminary complexation studies were performed between receptor **7** and carbon *onion* sample. The changes observed on the UV-Vis absorption receptor spectra indicated interaction with the *bucky onion* sample in DMF.

Regarding the second part of the thesis, synthetic attempts to prepare CTV-monomer **35** were not successful. The CTV-monomer **36** was synthesized and characterized. The aggregation of the CTV-monomers was monitored by means of 1H -NMR experiments. The formation of a columnar aggregate could not be confirmed.

“Majority Rules” chiral amplification studies were performed in DCM, no chirality transfer was observed. It was observed that a minimum ee of 0.3 was required for the sample to express chirality. This could indicate formation of columnar aggregates above that ratio.

The mesomorphic behavior was also investigated by DSC and POM. A phase transition around 62-67 °C was identified when cooling down from the melted sample within the cooling thermograms. Birefringent textures were observed under crossed polarized light at the transition temperatures. Unfortunately, no typical patterns could be identified.

UNIVERSITAT ROVIRA I VIRGILI

CYCLOTRIVERATRYLENE AND PORPHYRIN SCAFFOLDS FOR MOLECULAR RECOGNITION AND SELF-ASSEMBLY

Berta Camafort Blanco

Dipòsit Legal: T 677-2015

UNIVERSITAT ROVIRA I VIRGILI

CYCLOTRIVERATRYLENE AND PORPHYRIN SCAFFOLDS FOR MOLECULAR RECOGNITION AND SELF-ASSEMBLY

Berta Camafort Blanco

Dipòsit Legal: T 677-2015